The Effects of Oxidative Stress on Synapse Development in *Drosophila*.

Valerie Milton

PhD
University of York
Department of Biology

September 2011

Abstract

Mutations in *spinster*, a late-endosomal/ lysosomal protein have been shown to cause overgrowth of the *Drosophila* neuromuscular junction, coupled with impaired synaptic transmission (Sweeney and Davies, 2002). Oxidative stress is implicated in many neurodegenerative disorders; however, its effects on development are still unclear.

In this thesis, it is shown that oxidative stress is implicated in the development of the *spinster* phenotype; overgrowth of the NMJ is rescued by over-expression of superoxide-dismutase (SOD) and catalase, components of the anti-oxidant defence system. Overgrowth can also be caused by oxidative stress in the absence of lysosomal dysfunction; synapse overgrowth is also observed in mutants defective for protection from ROS, and animals subjected to excessive ROS.

The data shown here also indicate that spinster and oxidative stress induced overgrowth requires ASK/JNK/AP-1 signalling pathways, attenuating ASK/JNK/AP-1 activity reduces overgrowth. Genes required for autophagy (Atg1 and Atg18) are also required for overgrowth, thus it is suggested that autophagy and JNK signalling are linked in NMJ development and dysregulated JNK/AP-1 signalling is involved in the generation of the neuronal phenotype observed in *spinster*.

spinster and oxidative stress mutants also have impaired physiology showing reduced crawling speed and impaired synaptic transmission. AMPK is also required for *spinster* overgrowth, suggesting an energy deficit, supported by the presence of aberrant mitochondria.

Table of Contents:

List of Figures: ..... **vii**

List of Tables: ..... **ix**

Acknowledgements ..... **x**

Declaration: ..... **xi**

1. Introduction **1**

1.1. Oxidative Stress **1**

1.1.1. Reactive Oxygen Species 1

1.1.2. Generation of ROS 2

1.1.3. ROS and Iron/Transition Metals 8

1.1.4. Oxidative Stress 8

1.1.5. Oxidative Damage 9

1.1.6. Reactive Nitrogen Species 11

1.1.7. Cellular Anti-oxidant Systems 12

1.2. Autophagy **19**

1.2.1. What is autophagy? 19

1.2.2. The Regulation of Autophagy 20

1.2.3. Molecular mechanism of autophagy 22

1.3. Autophagy, lysosomes and oxidative stress in neurodegenerative diseases **25**

1.3.1. Lysosomal Storage Disorders 25

1.3.2. Autophagy and Neurodegeneration 26

1.3.3. Oxidative Stress, Ageing and Neurodegenerative Diseases 27

1.3.4. Using *Drosophila* to study LSDs 28

1.4. Neurotransmission **30**

1.4.1. Action Potential 30

1.4.2. Synaptic Transmission 30

1.5. *Drosophila* neuromuscular junction as a model of synapse development 32
1.5.1. *Drosophila* as a model organism 32
1.5.2. The *Drosophila* 3rd instar larval neuromuscular junction..... 33
1.5.3. Anatomy of the larval neuromuscular junction..... 34
1.5.4. Development of the *Drosophila* NMJ..... 36
1.6. Oxidative Stress Autophagy and Synapse Development 40
1.6.1. Oxidative Stress and Synapse Development 40
1.6.2. Oxidative Stress and Synaptic Function..... 43
1.7. Aims..... 46

2. Materials and Methods 47
2.1. *Drosophila* Husbandry and Techniques 47
2.1.1. *Drosophila* Stocks..... 47
2.1.2. *Drosophila* Husbandry 47
Table 2.1: *Drosophila* stocks used in this investigation 52
2.1.3. Crossing Schemes..... 52
2.2. Immunohistochemistry and Imaging..... 53
2.2.1. Third Instar Larval Dissection 53
2.2.2. Larval Fixation and Immunohistochemistry 53
Table 2.2: Antibodies used in this investigation.. 54
2.2.3. Microscopy and Analysis 55
2.3. Adult Head Sectioning and Electron Microscopy 56
2.3.1. Embedding of *Drosophila* Adult Heads in Spurr's Resin 56
2.3.2. Head Sectioning 57
2.3.3. Transmission Electron Microscopy (TEM) and Image Analysis 57
2.4. Molecular Biology 58
2.4.1. Polymerase Chain Reaction (PCR) and DNA Agarose Gel Electrophoresis..... 58
2.4.2. Genomic DNA extraction 59
2.4.3. Gel Extraction 59

2.4.4. DNA Sequencing 59
2.5. Biochemical Analysis 60
2.5.1. Bradford Assay 60
2.5.2. Quantification of Oxidative Stress 60
2.6. Physiological Analysis of Larvae 61
2.6.1. Crawling Speed Analysis 61
2.6.2. Intramuscular Recordings 61

3. Oxidative Stress Contributes to Synaptic Overgrowth in *spinster*, a Model of a Lysosomal Storage Disorder 63
3.1. Introduction 63
3.2. Results 65
3.2.1. *spin* carries an oxidative stress burden 65
3.2.2. Neuromuscular junction morphology is perturbed in *spinster* 69
3.2.3. Relieving oxidative stress reduces overgrowth of the neuromuscular junction in *spinster* 73
3.2.4. Oxidative stress contributes to overgrowth in *highwire* 79
3.3. Discussion 83

4. Oxidative Stress Causes Overgrowth of the *Drosophila* Neuromuscular Junction 87
4.1. Introduction 87
4.2. Results 88
4.2.1. Oxidative stress alters bouton number and muscle surface area 88
4.2.2. Oxidative stress causes changes in synaptic branching 93
4.2.3. Oxidative stress causes changes in bouton size 95
4.2.4. Growth of the neuromuscular junction in animals carrying an oxidative burden is reduced by expressed anti-oxidant transgenes. 99
4.3. Discussion 105

5. JNK/AP-1 Signalling and Autophagy are Required for Overgrowth of the Neuromuscular Junction 109

5.1. Introduction 109
5.2. Results 111
5.2.1. Oxidative stress and *spinster* overgrowth share the same genetic pathway; *spinster* and *sod1* induced overgrowth act synergistically 111
5.2.2. JNK signalling is upregulated in *spinster* 112
5.2.3. Components of AP-1 modify synapse development 113
5.2.4. Reducing JNK/AP-1 signalling rescues *spinster* induced overgrowth 116
5.2.5. Fos is required both pre- and post- synaptically for *spinster* induced overgrowth 119
5.2.6. JNK signalling is upregulated by paraquat 120
5.2.7. Reducing ASK/JNK/AP-1 signalling reduces paraquat induced overgrowth 122
5.2.8. Reducing JNK/AP-1 signalling in *sod* mutants reduces synaptic overgrowth 127
5.2.9. Autophagy gene function affects synapse development 135
5.2.10. Autophagy is required for *spinster* induced overgrowth 138
5.2.11. Autophagy is required pre- and post- synaptically for *spinster* induced overgrowth 139
5.2.12. Autophagy is required for paraquat induced overgrowth 139
5.3. Discussion 143
5.3.1. ASK/JNK signalling is required for oxidative stress induced overgrowth 143
5.3.2. Fos/Jun involvement in synaptic growth is context dependent 144
5.3.3. Autophagy and Synapse Development 146
5.3.4. Muscular and Neuronal Input 147
6. *Spinster* and Oxidative Stress Mutants have Impaired Physiology 149
6.1. Introduction 149
6.2. Results 153
6.2.1. Mutations with overgrown larval NMJs have impaired physiology . 153

6.2.2. Reduction in *spinster* crawling speed is not rescued through expression of anti-oxidants 154
6.2.3. Reduction in *highwire* crawling speed is not rescued by expression of *hSOD1* pre- and post-synaptically 155
6.2.4. Reduction in crawling speed in *sod1* mutants is not rescued by expression of *hSOD1* 155
6.2.5. The effects of *sod1*, *sod2* and *spinster* on synaptic transmission .. 159
6.2.6. Normal and aberrant mitochondria are seen to be present in the *spinster* mutant. 164
6.2.7. AMPK is required for *spinster* induced overgrowth 166
6.2.8. Increased activation of AMPK is required pre- and post- synaptically to drive synapse growth 168
6.2.9. AMPK activity is required for crawling 170
6.3. Discussion 172
6.3.1. Mutations causing oxidative stress can impair motor function 172
6.3.2. Increased AMPK activity can cause synaptic overgrowth and is required for *spinster* induced overgrowth 175
7. Discussion and Future Research 176
7.1. Introduction 176
7.2. *spinster* as a model of a lysosomal storage disorder 176
7.2.1. Oxidative stress causes synaptic overgrowth 177
7.3. ASK/JNK/AP-1 signalling is required for oxidative stress induced synaptic overgrowth 181
7.3.1. AP-1 activity is differentially required for oxidative stress induced growth 181
7.3.2. Fos is required both in the nerve and the muscle for synaptic overgrowth in *spinster* and *sod2* 182
7.4. Autophagy is required for synaptic overgrowth 183
7.4.1. Autophagy is required for synaptic overgrowth 183
7.4.2. Autophagy is required in the muscle for *spinster* overgrowth 184

7.4.3. It is not known whether JNK is upstream of or downstream of autophagy in *spinster* and paraquat induced overgrowth 184
7.5. AMPK is implicated in synaptic growth 185
7.5.1. AMPK can drive synaptic overgrowth 185
7.5.2. AMPK is required for *spinster* induced overgrowth 185
7.5.3. Mitochondrial defects in *spinster* 187
7.6. Physiological output is more sensitive to oxidative stress than morphology of the neuromuscular junction 188
7.7. Summary 189
Appendix 1: Bouton Numbers and MSA 190
Appendix 2: Branch Number and Normalisation 195
Appendix 3: Bouton Width 195
Abbreviations: 196
References: 200

List of Figures:

	TITLE	Page No.
Fig. 1.1	The addition of electrons to oxygen……..	2
Fig. 1.2	The mitochondrial respiratory chain……..	4
Fig. 1.3	The mitochondrial respiratory chain can leak electrons to create superoxide anions……	6
Fig. 1.4	Sources of ROS, primary cellular defences and signalling responses…….....	9
Fig. 1.5	The regulation of autophagy……..	21
Fig. 3.1	*spinster* mutants have increased levels of peroxidated lipids. This is reduced by expressing an anti-oxidant transgene……..	66
Fig. 3.2	The oxidative stress response is activated in spinster……...	68
Fig. 3.3	*spinster* has increased bouton number with no change in muscle surface area……	70
Fig. 3.4	*spinster* mutants have increased branch number proportional to increase in bouton number……	71
Fig. 3.5	*spinster* has smaller boutons than wildtype and a greater proportion of smaller boutons……	72
Fig. 3.6	*spinster* has increased branching due to oxidative stress…….	75
Fig. 3.7	Relieving the oxidative stress burden in *spinster* through expressing anti-oxidant transgenes reduces synaptic overgrowth……	76
Fig. 3.8	Expression of UAS*hSOD1* reduces synaptic overgrowth in *spinster* when expressed in either the nerve the muscle or both……	78
Fig. 3.9	Reducing oxidative stress through expression of UAS*hSOD1* rescues synaptic overgrowth in *highwire*……..	80
Fig. 3.10	Reducing oxidative stress through expression of UAS*cat* fails to rescue synaptic overgrowth in *highwire*……	82
Fig. 4.1	Paraquat causes synaptic overgrowth relative to muscle surface area…….....	89
Fig. 4.2	Rotenone impairs synaptic growth with no change in muscle surface……	90
Fig. 4.3	Mutations that cause oxidative stress tend to cause synaptic overgrowth……	92
Fig. 4.4	10mM paraquat causes an increase in branch number…….	94
Fig. 4.5	Mutations in sod1 and sod2 cause different effects in branch	94

	number……..	
Fig. 4.6	Paraquat causes changes in bouton size…….	97
Fig. 4.7	Mutations in sod cause changes in bouton size……..	98
Fig. 4.8	Paraquat induced synaptic growth, but not reduced muscle surface area, is rescued by antioxidants …….	100
Fig. 4.9	Synaptic overgrowth and reduced muscle surface area in sod1 mutants is rescued by antioxidants……..	102
Fig. 4.10	Change in branch number in sod1 mutants is rescued by antioxidants…….	103
Fig. 4.11	Synaptic overgrowth in *sod2* mutants is rescued by antioxidants…….	104
Fig. 4.12	Reduced branching in *sod2* mutants is rescued by antioxidants…….	105
Fig. 5.1	Mutations in *sod1* and *spinster* act synergistically to cause synaptic overgrowth…….	111
Fig. 5.2	*puckered* is upregulated in *spinster*……..	113
Fig. 5.3	Fos and Jun can alter synapse growth…….	115
Fig. 5.4	ASK/JNK/AP-1 signalling is required for *spinster* overgrowth…	117
Fig. 5.5	JNK/Fos signalling is required for spinster-induced overgrowth…….	119
Fig. 5.6	Fos signalling is required pre- and post- synaptically for *spinster* induced synapse overgrowth……..	120
Fig. 5.7	*puckered* is upregulated in paraquat-fed animals……..	121
Fig.5.8	ASK/JNK/AP-1 signalling is required for paraquat-induced growth…….	123
Fig. 5.9	JNK signalling is required for paraquat-induced overgrowth….	125
Fig. 5.10	AP-1 signalling is required for *sod1*-induced overgrowth…….	127
Fig. 5.11	AP-1 signalling is required for changes in branching in *sod1* mutants……..	129
Fig.5.12	JNK/AP-1 signalling is required for *sod2*-induced overgrowth…	130
Fig. 5.13	Changes in branch number in *sod2* mutants require JNK/AP-1 signalling…….	132
Fig. 5.14	Fos signalling is required either from the muscle or the nerve for *sod2* induced overgrowth……..	133
Fig. 5.15	Changing levels of autophagy alters synaptic size…….	135

Fig. 5.16	*spinster* induced overgrowth requires autophagy genes……	139
Fig. 5.17	Autophagy genes are required both in the nerve and the muscle for *spinster*-induced overgrowth……..	140
Fig. 5.18	paraquat induced overgrowth requires autophagy genes	141
Fig. 6.1	Mutations in *spinster*, *highwire*, *sod1* and *sod2* result in reduced crawling speed……..	153
Fig. 6.2	Reducing ROS in *spinster* does not rescue crawling speed….	155
Fig. 6.3	Reducing ROS in *highwire* does not rescue crawling speed….	156
Fig. 6.4	Reducing ROS in *sod1* does not rescue crawling speed……..	157
Fig. 6.5	*spinster* has a normal resting membrane potential, *sod1* and *sod2* have increased resting membrane potentials……	159
Fig. 6.6	*spinster* and *sod2* have normal EJPs whereas *sod1* have increased EJP amplitude……	160
Fig. 6.7	*spinster* and *sod2* have normal EJPs for the resting membrane potential, whereas *sod1* have higher EJP amplitude than expected……	162
Fig. 6.8	Aberrant mitochondria are present in *spinster*……	164
Fig. 6.9	*Spinster* induced overgrowth requires AMPK……..	166
Fig. 6.10	Increased AMPK activity pre- and post- synaptically results in synaptic overgrowth……	168
Fig. 6.11	AMPK is involved in determining crawling speed……	170

List of Tables:

	TITLE	Page
Table 1.1	Components of the JNK signalling cascade……	17
Table 2.1	*Drosophila* stocks used in this investigation……	48
Table 2.2	Antibodies used in this investigation……	54

Acknowledgements

I would like to begin by thanking my supervisor Sean Sweeney for putting up with me throughout the course of my PhD. I extend my thanks to other members of the Sweeney and Elliott lab past and present, including Laura Briggs, Matt Oswald, Sam Hindle and Amanda Vincent. For the helpful thoughts and advice I thank the members of my TAP committee, Chris Elliott and Henry Leese.

I am grateful to our collaborators in Plymouth, Iain Robinson and Helen Jarrett, for their tireless work and corrections of the manuscript.

I would like to thank all my friends in York for their support and advice: Samik Datta, Lucy Goulding, Kate O'Hara, Jenny Fosten, Matt Beacham, Mark Eslick, Laura Blackmore, Dan Horsfall and my biology filth, Zeenat Nordally, Illaria Zanardi, Jen Lucey, Andy Suggitt and Ben Owens. I would also like to thank my friends from further afield for reminding me of a life beyond a thesis.

Finally I would like to thank my family, who predisposed me to science, and have always been there to check my work, hear my grumbles and make me food. Included in the family is Percy, our lovely dog. I also thank my sister for generally being a legend. Further gratitude has to go to my parents for proof-reading my thesis.

Declaration:

I hereby declare that the work presented in this thesis is my own work except where stated in the text or figures.

Data from chapters 3, 4 and 5 have been incorporated into a paper entitled ‘Oxidative stress induces overgrowth of the *Drosophila* neuromuscular junction’, which was published in PNAS (2011).

Parts of the introduction were published in a review article entitled ‘Oxidative stress in synapse development and function’ in Developmental Neurobiology (2011)

1. Introduction

The main aim of this investigation is to elucidate the effects of oxidative stress on synapse development. Oxidative stress can be broadly defined as an imbalance between the oxidant and reductive capacity of the cell, in favour of pro-oxidants. Oxidative stress occurs when generation of reaction oxygen species (ROS) overcome the reductive capacity of the cell (Sies, 1997). This leads to increased cellular damage and activation of the cellular stress response. This is an interesting area for research as little is currently known about how oxidative stress impinges on neuronal development. ROS are important signalling molecules throughout physiology, and are used to signal developmental changes (Vieira *et al.*, 2011) and are important in immune responses (E.g. Tennenberg *et al*., 1993) and long term potentiation (Klann *et al.*, 1998); they are also implicated in a vast number of pathologies, most notably in neurodegenerative diseases (Buhmann *et al.*, 2004). This means that when ROS levels are increased they can act as highly potent signalling molecules leading to aberrant activation of signalling pathways, in addition to cellular damage. ROS are potent and far-reaching in their damaging effects and require close regulation, consequently there is a well-characterised stress response mounted by the cell upon detection of pathological levels of ROS.

1.1. Oxidative Stress

1.1.1. Reactive Oxygen Species

There are a number of ROS that are produced within the cell, including the principal ROS, superoxide anions ($O_2^{-\cdot}$), hydrogen peroxide (H_2O_2), hydroxyl radicals ($OH^{\cdot}$) and hydroxyl anions ($OH^{-\cdot}$). Generally, ROS formation begins with the generation of superoxide anions. These are formed by the addition of an electron to molecular oxygen. They are highly unstable molecules and rapidly dismutate to form hydrogen peroxide. This reaction is catalysed by superoxide

dismutase (SOD) (McCord and Fridovich, 1968 and 1969a and b), which allows this reaction to occur 10000x faster than in the absence of the enzyme. Hydrogen peroxide is not a radical although it is still highly reactive and in the presence of superoxide anions accepts electrons from transition metals to produce hydroxyl radicals ($^{\cdot}OH$) and hydroxyl anions (OH^-), a process termed the Fenton reaction ($Fe^{2+} + H_2O_2 \rightarrow Fe^{3+} + OH^{\cdot} + OH^-$).

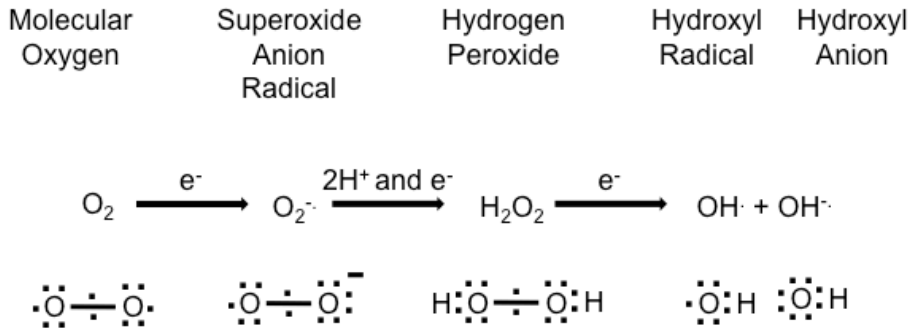

Figure 1.1. The addition of electrons to oxygen
Molecular oxygen O_2 is reduced to superoxide anions $O_2^{-\cdot}$. Addition of a further electron in the presence of hydrogen produces hydrogen peroxide (H_2O_2). This is further reduced to form hydroxyl radicals and hydroxyl anions ($OH^{\cdot}$ and $OH^{\cdot -}$ respectively).

1.1.2. Generation of ROS

ROS are a natural by-product of normal cellular metabolism; the most notable source is believed to be mitochondrial respiration. There are also many other sources of ROS within the cell (reviewed by Brown and Borutaite, 2011) including peroxisomes, the endoplasmic reticulum, nicotinamide adenine dinucleotide phosphate (NADPHs) (McNally *et al.*, 2003; reviewed in Bedard *et al.*, 2007) and xanthine oxidase (Gonzalez-Mateos *et al.*, 2004). Some ROS are generated as a by-product but they are also produced as signalling molecules.

1.1.2.1. Mitochondrial Generation of ROS

Mitochondria are oval shaped organelles approximately 1-2μm long and 0.5-1μm wide, with inner and outer membranes that form two compartments; firstly the intercristal space, between the outer and inner membrane, otherwise known as the intermembrane space and secondly the matrix, enclosed by the inner membrane; the matrix is also known as the intermembrane space (Palade, 1953). During mitochondrial respiration electrons are donated from electron donors such as nicotinamide adenine nucleotide (NADH) and $FADH_2$ and are transferred along the mitochondrial electron transport chain (ETC) between electron carriers, complexes I-IV, located in the inner membrane. The final electron acceptor is O_2, the most electronegative acceptor in the chain. Transfer of electrons along the ETC releases energy and these exergenic steps are coupled with the transport of protons into the intermembrane space to create a proton gradient. The flow of protons down the concentration gradient, back into the matrix provides the free energy for the production of ATP from ADP, through the actions of ATP synthase, otherwise known as complex V (Lehninger Chap 19)(Fig. 1.2). Electrons can leak prematurely from the electron transport chain to bind to O_2 to form $O_2^{-\cdot}$ (Fig 1.3) (Boveris and Chance, 1973).

Ordinarily, the electron carrier NADH donates electrons to complex I, NADH dehydrogenase, which transfers the electrons to the lipophilic electron shuttling molecule coenzyme Q (ubiquinone). This process is coupled to transport of H^+ into the intermembrane space. Conenzyme Q also receives electrons from complex II, succinate dehydrogenase, which oxidises succinate via FAD. Succinate is a Kreb's/ citric acid cycle intermediate. This process is not coupled to the movement of H^+. Therefore, e^- entering the ETC at this point yields less free energy. Coenzyme Q is freely diffusible within the membrane and transports electrons to complex III, coenzyme QH_2-cytochrome *c* reductase. Electron transfer is coupled to proton movement into the intermembrane space.

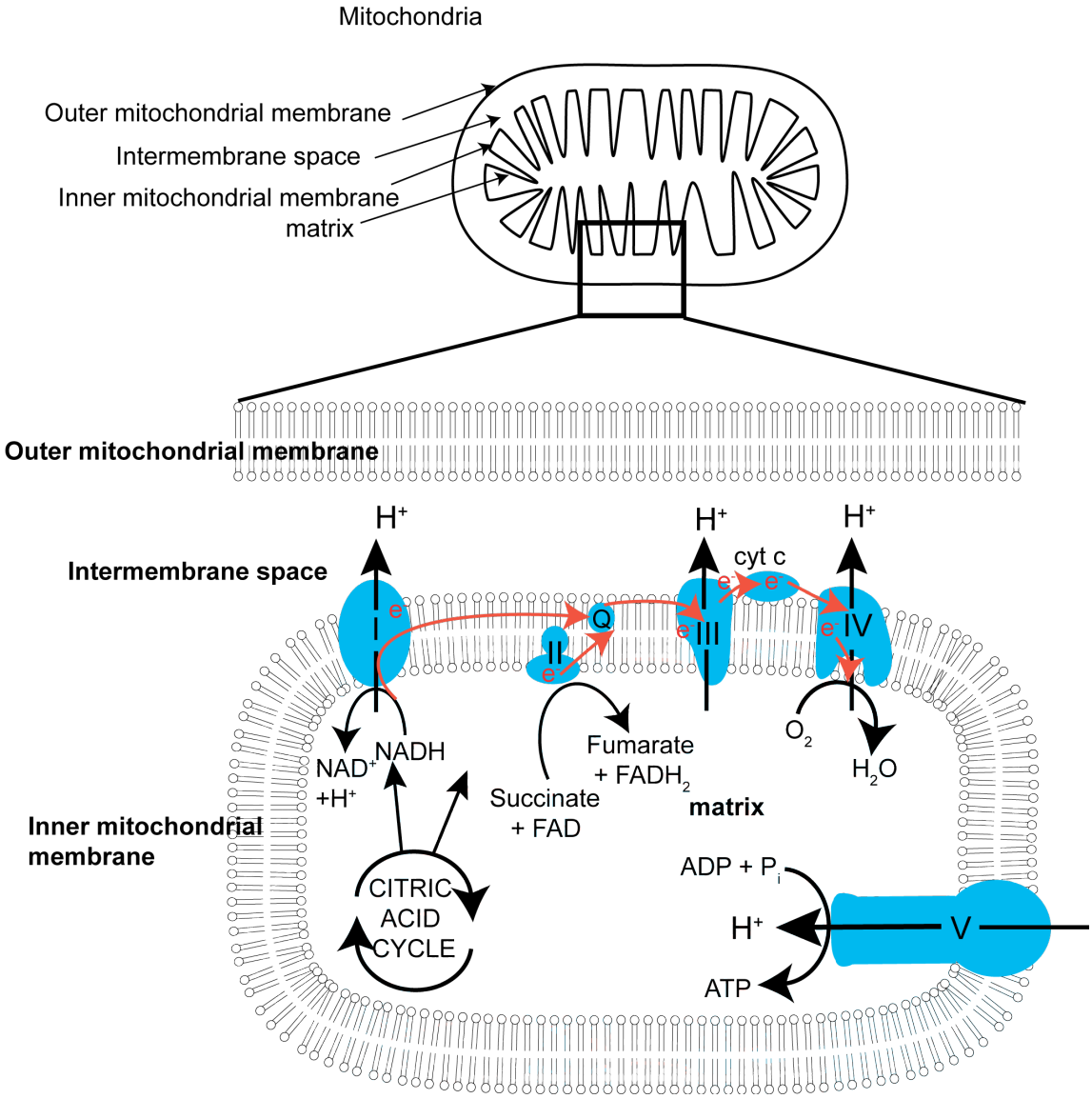

Figure 1.2 The mitochondrial respiratory chain
Electrons are transported along the electron transport chain, protons are transported across the inner mitochondrial membrane into the intermembrane space creating a proton gradient. Protons are transported back across the membrane through complex V of the mitochondrial transport chain, ATPase, converting ADP to ATP.

At complex III electrons are transferred from coenzyme Q to cytochrome *c*, another electron shuttling molecule, which binds to the outer face of the inner membrane and transports electrons to complex IV, cytochrome oxidase. Complex IV, cytochrome *c* oxidase transfers electrons to O_2, which together with

H^+ results in the formation of water; once more this transfer of electron coincides with the movement of protons into the intermembrane space. The electrochemical gradient is harnessed by ATP synthase, which comprises two components F_0 and F_1. F_0 acts as a proton channel, through which protons flow from the intermembrane space to the matrix, down the electrochemical gradient. This drives the rotation of F_1 which catalyses the synthesis of ADP from ATP. This process is termed oxidative phosphorylation.

ROS are produced when electron transfer to oxygen results in the generation of superoxide anions ($O_2^{-\cdot}$). Traditionally it is reported that 1-2% oxygen molecules used in mitochondria are converted to superoxide anions (Boveris and Chance 1973), however this is most likely an overestimation as, this figure was derived from isolated mitochondria in the presence of a complex III toxin (antimycin) with saturated levels of substrate and oxygen. More recent estimations put the figure at 0.15% oxygen being converted to superoxide anions (St-Pierre *et al.*, 2002). ROS formation was originally identified at two points of the electron transport chain; in an unknown site of complex I and conenzyme Q at complex III (Turrens and Boveris, 1980; Turrens *et al.*, 1985, Cadenas *et al.*, 1977). Subsequently, more sites of ROS generation have been identified, although none are fully characterised, and the relative contribution of each site is likely to be tissue and species specific. There is evidence to support the presence of two ROS producing sites in complex I, the ubiquinone binding site and the flavin mononucleotide group (FMN) (Liu *et al.*, 2002). Succinate linked ROS generation is inhibited by rotenone, a complex I inhibitor, suggesting ROS production actually occurs via reversed electron transfer between succinate and NAD+ to form NADH (Liu *et al.*, 2002), however there is still much debate concerning ROS production at complex I (reviewed by Andreyev *et al.*, 2005).

.

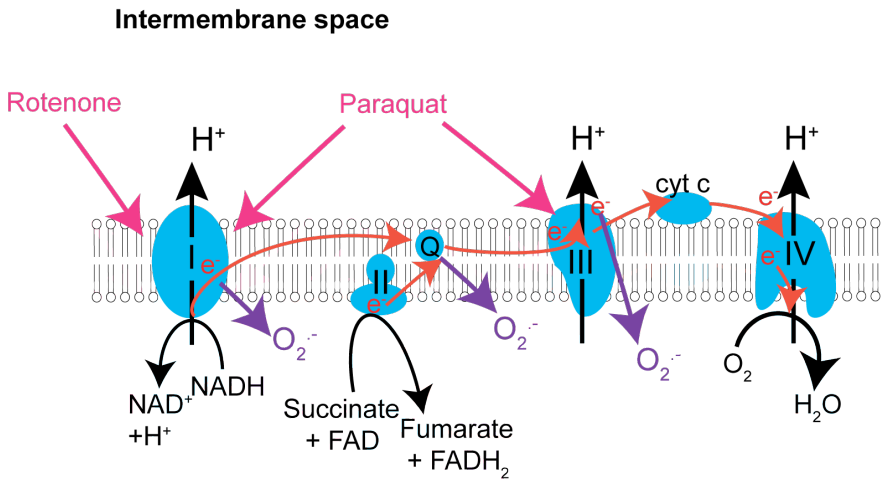

Figure 1.3 The mitochondrial respiratory chain can leak electrons to create superoxide anions.
As electrons are transported along the electron transport chain, leaking can occur resulting in the formation of superoxide anions. Rotenone and paraquat are two electrotoxins that increase the rate of superoxide anion formation. Rotenone acts at complex I whereas paraquat acts at complex I and complex III.

1.1.2.2. Non-mitochondrial sources of ROS

Although mitochondria are commonly accepted to be the greatest producers of ROS within the cell it has also been suggested that non-mitochondrial sources of ROS could contribute more to ROS production than previously thought, dependent on cell type (Brown and Borutaite, 2011). There are many non-mitochondrial sources of ROS, for example the endoplasmic reticulum (ER) (Liu *et al.*, 2004; Park *et al.*, 2010), peroxisomes, cytosolic enzymes and plasma membrane bound enzymes. In the ER the main sources of ROS are p450 (Bondy and Naderi, 1994) enzymes and ERO1 (Tu *et al.*, 2002). Cytochrome p450 enzymes are heme-thiolate enzymes that form part of the membrane-bound microsomal monooxygenase system (MMO), located in the ER, where lipophillic substrates are oxidised (Capedevila *et al.*, 1981; for review see Zanger *et al.*, 2004). Superoxide anions are formed when the electrons are transferred to oxygen rather than the substrate, and it has been indicated that this route may contribute to ROS generation in *vivo* (Kuthan and Ullrich, 1982).

Furthermore the ER requires an oxidising environment to allow the formation of disulphide bonds (Hwang *et al.*, 1992; reviewed Gaut and Hendershot, 1993). ERO1, a thiol oxidase enzyme catalyses the formation of disulphide bonds in the ER (Tu *et al.*, 2002). Electrons are transferred from dithiols to molecular oxygen yielding hydrogen peroxide (Gross *et al.*, 2006).

Peroxisomes, single membrane bound organelles, are an important site of ROS generation (Boveris *et al.*, 1972). Peroxisomes break down long chain fatty acids, whereby β-oxidation of fatty acids occurs resulting in the shortening of fatty acids and conversion to acetyl CoA, to enter the citric acid cycle and provide energy for the cell. Therefore in the peroxisome hydrogen peroxide is produced as organic substrates are oxidised:

$RH_2 + O_2 \rightarrow R + H_2O_2$

Peroxidation of subsequent substrates occurs, through the actions of catalase, as it uses hydrogen peroxide to oxidise further substrates, in the process, turning reactive hydrogen peroxide into less harmful water:

$H_2O_2 + R'H_2 \rightarrow R' + H_2O$

Excess hydrogen peroxide is broken down by catalase to produce oxygen and water (Albert *et al.*, 2008).

Membrane-bound NADPH oxidases, such as nitric oxide synthase, catalyse the formation of superoxides. NADPH oxidases are activated through assembly in the membrane in the respiratory burst (otherwise termed oxidative burst), where superoxides are released from immune cells to kill bacteria or fungi (Bokock and Knaus, 2003).

Xanthine oxidases (XO) are another source of ROS within the cell (Gonzalez-Mateos *et al.*, 2001). Xanthine oxidases catalyse the oxidation of hypoxanthine

to xanthine and thence to uric acid: hypoxanthine + H_2O + O_2 → xanthine + H_2O_2 and xanthine + H_2O + O_2 →uric acid + H_2O_2.

1.1.3. ROS and Iron/Transition Metals

Transition metals are essential for most forms of aerobic life, but they are also dangerous pro-oxidants, especially iron. The role of iron in oxidative stress is an important one (Missirlis *et al.*, 2003; Kurz *et al.*, 2008a and b) as iron is the most abundant transition metal in the body and is essential for the function of many enzymes. Iron can undergo the Fenton reaction with hydrogen peroxide to generate hydroxyl anions and hydroxyl radicals:

$Fe^{2+} + H_2O_2 \rightarrow Fe^{3+} + HO^{\cdot} + OH^{-}$

Furthermore, iron can potentiate lipid peroxidation (Gutteridge, 1982) and catechols such as dopamine can be converted to highly reactive semiquinones (Schipper, 2004a and b). Iron concentration has been shown to increase with age in rats, humans and mice (Cook and Yu, 1998; Sohal *et al.*, 1999; Donahue *et al.*, 2006). Hydrogen peroxide can induce activity of heme-oxygenase-1 (HO-1) increasing degradation of heme thereby liberating more free iron, potentially inducing a vicious cycle. Therefore levels of iron are tightly regulated. Dysregulation of iron metabolism is an important contributor to Alzheimer's Disease (AD) pathology through the generation of oxidative stress (for review see Puntarulo, 2005).

1.1.4. Oxidative Stress

Oxidative stress has been implicated in the aetiology of numerous pathologies, including many neurodegenerative disorders such as Alzheimer's disease (Papolla *et al.*, 1992), Parkinson's disease (Castellani *et al.*, 1996, Buhmann *et al*., 2004), Creutzfeldt–Jakob Disease (Arlt *et al.*, 2002) and lysosomal storage disorders (Deganuto *et al.*, 2007, Fu *et al.*, 2010). ROS are natural by-products of many cellular processes, most notably mitochondrial respiration (Loschen *et*

al., 1971; Boveris *et al.*, 1972). Low levels of ROS are required as cell-signalling molecules in many processes including long-term potentiation (LTP), the biological correlate of learning and memory (Bindokas *et al.*, 1996; Klann *et al.*, 1998), differentiation (Vieira *et al.*, 2011) and cytokine secretion (Kina *et al.*, 2009). ROS are involved in neutrophil recruitment and lymphocyte activation, key to the immune response (Smith and Ford, 1983; Marriott *et al.*, 2008; Reth *et al.*, 2002). ROS have also been implicated in autoimmune conditions including inflammatory bowel diseases (Leiper *et al.*, 2001). ROS are normally maintained at these low physiological levels by a system of ROS scavengers, otherwise termed anti-oxidants. The balance between the generation and neutralisation of ROS is normally tightly regulated; oxidative stress occurs when the generation of ROS overpowers the antioxidant defence system. Oxidative stress can be caused either by increased generation of ROS or impaired neutralisation of ROS. The consequences of oxidative stress comprise two main facets: random cellular damage and the activation of the cellular stress response signalling pathways. Firstly, oxidative stress involves random cellular damage as chain reactions occur causing lipid peroxidation, DNA and protein damage. Secondly, oxidative stress entails the organised cell stress response that can lead to the many different outcomes, such as proliferation, growth arrest or cell death (For review see Barnham *et al.*, 2004).

1.1.5. Oxidative Damage

ROS cause random cellular damage through chain reactions, resulting in the further formation of ROS. Oxidative damage can be defined as “the biomolecular damage caused by attack of reactive species upon the constituents on living organism” (Halliwell and Whiteman, 2004). ROS cause addition of double bonds to DNA bases, with the removal of a hydrogen atom from thymine and deoxyribose. ROS can also cause strand breaks and base and nucleotide modifications, as well as changes in DNA conformation that may cause inaccurate replications. Furthermore, ROS can alter methylation status

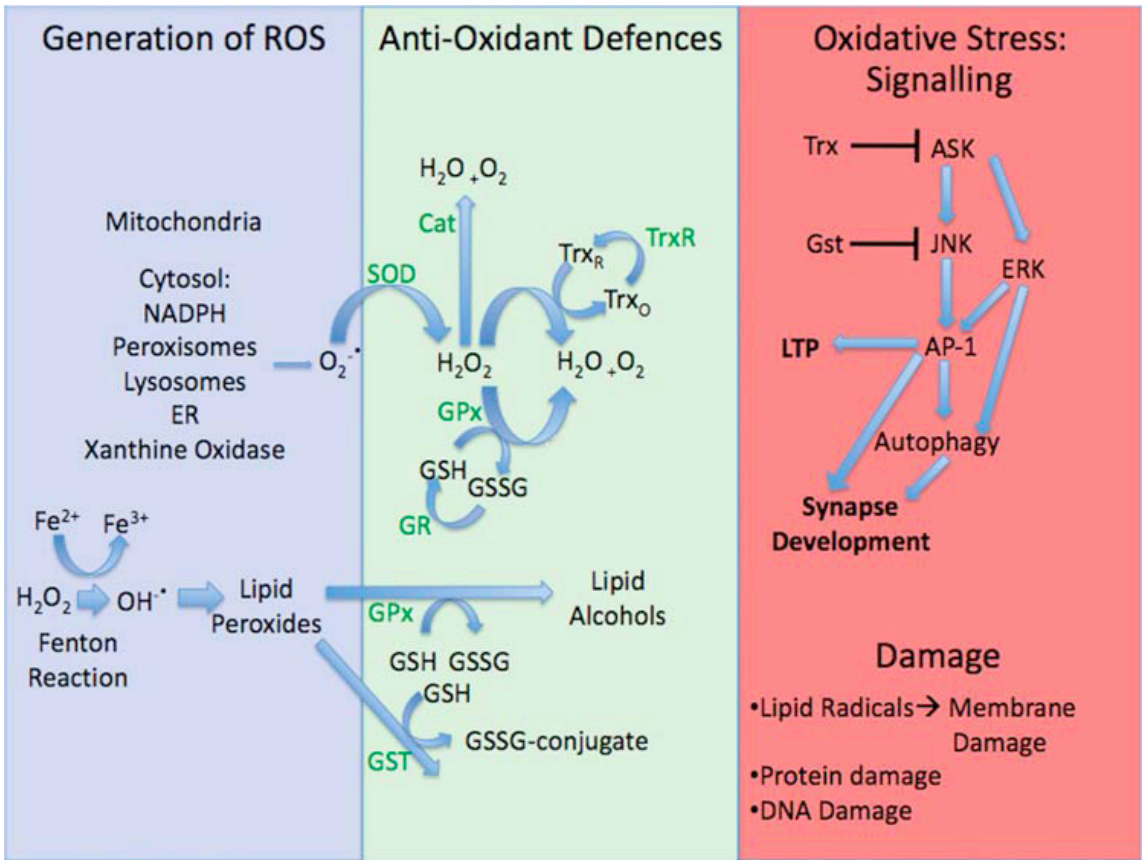

Figure 1.4: Sources of ROS, primary cellular defences, and signalling responses. Reactive oxygen species (ROS) can be generated from various sources in the cytosol or mitochondria. The cell is protected from ROS by superoxide dismutase (SOD), catalase (Cat), thioredoxin reductase (TrxR), glutathione peroxidase (GPx), and Glutathione S-transferase (GST). GSH represents monomeric glutathione, and GSSG represents glutathione disulfide, GSSG is reduced to GSH by glutathione reductase (GR). The cellular response to excessive ROS, via the activation of the ASK/JNK/AP-1 pathway, is autophagy. ASK and JNK are inhibited by reduced thioredoxin and glutathione, respectively, demonstrating that their activation state is directly affected by redox status. JNK/AP-1 activation is known to regulate synaptic responses. ERK is also activated in response to oxidative stress while also known to regulate synapse development through AP-1 and autophagy gene activation. AP-1 has also been implicated in the generation and maintenance of LTP.

resulting in changed gene expression levels (Weitzman *et al*., 1994). ROS are known to alter protein activity in a number of ways. The presence of ROS can result in changes in oxidation state of transfer metals, vital to protein function. An example of this is aconitase, a constituent of the citric acid cycle, which

contains $[Fe_4S_4]^{2+}$, required for catalytic activity. In the presence of superoxide anions this is converted to $[Fe_4S_4]^{+}$, rendering it inactive (Gardner and Fridovich, 1991b). OH^{-} ions cause H^{+} abstraction, for example of tyrosine, forming tyrosyl radicals, resulting in dityrosine linkages, altering protein structure and activity. Cysteine and methionine are particularly susceptible to oxidation due to their sulphur content, resulting in disulphide cross-linking. This is reversible through the actions of reductases; a built in ROS scavenger mechanism (Berlett and Stadtman, 1997).

ROS also oxidatively degrade fatty acids, they react with double bonds of unsaturated fatty acids. This is termed lipid peroxidation and results in the formation of lipid peroxyl radicals, or lipid peroxides. Formation of these species begins a chain reaction resulting in the breakdown of these peroxides resulting in the formation of end products such as 4-hydroxy-2,3-nonenal (HNE) and malondialdehyde (MDA), acrolein and F_2-isoprostanes. These breakdown products can cause further problems, by interacting with DNA (Marnett, 1999).

The initial cause of oxidative stress is often hard to determine due to the positive feedback loop, as the presence of ROS increase their generation. ROS impair mitochondrial function thereby further increasing levels of ROS. ROS also act to destabilise the lysosomal membrane, which can cause lysosomal dysfunction leading to increased ROS generation from the lysosomes, releasing iron from this iron-rich environment (Seehafer and Pearce, 2006; Terman and Brunk, 2006).

1.1.6. Reactive Nitrogen Species

Reactive nitrogen species (RNS) are also another causative component of cellular stress, the stress generated by ROS and RNS together is termed 'nitrosative stress' (Reviewed in Knott and Bossy-Wetzel, 2009). Nitric oxide ($NO^{\cdot}$) is a biological messenger, important in neuronal transmission and inflammatory responses (Lipton *et al.*, 1993). It is produced by nitric oxide

synthase (NOS), which catalyses the formation of NO from arginine and NADPH (Palmer and Johns, 1998). NO acts as a good transient messenger, as it is highly reactive and only persists for a few seconds. It can react with superoxide to form peroxynitrite ($ONOO^-$). This can react with proteins that require transition metal centres, resulting in protein modification. In mammalian systems there are three NOS isoforms, neuronal nNOS, inducible iNOS and endothelial eNOS (Nelson *et al.*, 2003). In *Drosophila* there is only one NOS isoform, which is expressed both in the nervous system and elsewhere. NO has been implicated in long term potentiation (Maffei *et al.*, 2003; Hopper *et al.*, 2006), but also in neurodegeneration (Ferrante *et al.*, 1997), showing again how signalling pathways can become pathological in certain situations if activation is not suitably regulated. It is unclear how this signalling system is compartmentalised and controlled to prevent cellular damage

1.1.7. Cellular Anti-oxidant Systems

In light of the damage ROS can cause it is not surprising that there is a system in place to keep ROS at low physiological levels; the cell's anti-oxidant defence system. The cell has direct and indirect defences against oxidative stress. Direct defences combat oxidative stress through dissipating reactive oxygen species. The indirect defences constitute cellular signalling responses to increased levels of ROS. There are a number of cellular redox sensors that detect increased levels of ROS and activate intimately coupled anti-oxidant defences. The source and level of the ROS detected determine the response elicited. *Drosophila* are highly useful for studying these pathways as the mammalian systems are complicated and involve a certain level of redundancy, whereas the system in *Drosophila* is simpler and therefore easier to study though can still elucidate mechanisms conserved in mammals. Coupled with the short generation time and powerful genetic armoury this makes *Drosophila* a highly useful tool.

1.1.7.1. Cellular Anti-Oxidants: Endogenous and Derived

Constitutive anti-oxidant defences are employed to maintain low levels of ROS. These comprise a battery of anti-oxidants to convert harmful reactive oxygen species into relatively harmless products. Halliwell and Gutteridge (1989) defined an anti-oxidant as "any substance that, when present at low concentrations compared with that of an oxidizable substrate, significantly delays or inhibits oxidation of that substrate". There are a number of ways in which anti-oxidants can be categorised, for example chemical or enzymatic, hydrophilic vs. hydrophobic, whether they are synthesised *de novo* or absorbed from the diet/atmosphere. They can also be categorised by their method of action, these being prevention, enzymatic diversion/ neutralisation, scavenging and quenching. The actions of the anti-oxidant system is complex and must be tightly regulated; as well as low levels being required to prevent harm, ROS are also important signalling molecules, and therefore levels of ROS must be closely monitored and controlled. The main anti-oxidants are superoxide dismutase, which converts superoxide anions to hydrogen peroxide and catalase, thioredoxin and glutathione, which are involved in the conversion of hydrogen peroxide to oxygen and water (Fig. 1.4).

Superoxide dismutase (SOD) is an enzyme that begins the channelling of ROS into relatively harmless products. It catalyses the conversion of superoxide anions, which are highly unstable to the more stable, but diffusible and longer-lived hydrogen peroxide (H_2O_2) (McCord and Fridovich, 1968 and 1969). There are three main families of SOD depending on the metal ion used as a cofactor in the conversion of superoxide to hydrogen peroxide. In *Drosophila* there are only two SOD isoforms. SOD1, otherwise known as SOD [Cu-Zn] is predominantly cytosolic, but also found in the mitochondrial intermembrane space, the mitochondrial periplasm (Missirlis *et al.*, 2003). It functions as a homodimer (Kirkland and Phillips, 1987). SOD2, otherwise known as SOD [Mn], acts predominantly in the mitochondria in eukaryotes. SOD2 is found as

homotetramers in the mitochondrial matrix, where each subunit is bound to its cofactor Mn (Duttaroy *et al.*, 1994 and 1997). In higher animals there is a third SOD orthologue, SOD3, otherwise known as EcSOD, due to its extracellular localisation. Unlike the other SOD isoforms, which are ubiquitously expressed, SOD3 shows specific-tissue localisation (Fattman *et al.*, 2003).

Hydrogen peroxide, produced by the action of SOD, is then enzymatically degraded to, relatively harmless, oxygen (O_2) and water (H_2O) through the actions of catalase (May, 1901). Catalase contains an Fe^{3+} at its active site, as do many peroxidases. The reaction occurs in two steps that are dependent on Fe^{3+}. One molecule of hydrogen peroxide binds and is split apart, water is released and oxygen is bound to Fe^{3+} to combine with a second hydrogen peroxide molecule to form another water molecule and oxygen gas. Hydrogen peroxide can also be degraded by the thiol-reducing systems involving either thioredoxin or glutathione. Thiols are compounds that contain a carbon-bonded sulphydryl, this acts as a reducing agent, which can be reversibly oxidised and reduced (Sies, 1997). Thioredoxin is oxidised during the degradation of hydrogen peroxide and is then reduced by thioredoxin reductase, using electrons donated from NADPH. Breakdown of hydrogen peroxide using glutathione requires the actions of glutathione peroxidase (Mills, 1957). Oxidised glutathione is then reduced by glutathione reductase, to regenerate reduced glutathione, once again using NADPH as an electron donor. Glutathione *S*-transferases are also important in anti-oxidant defence, they catalyse the conjugation of lipophilic substrates with reduced glutathione (Sheehan *et al.*, 2001); the conjugates are more easily excreted.

In addition to this directed enzymatically driven degradation of ROS, there are many molecules that act in a similar way to glutathione and theioredoxin, collectively termed ROS scavengers. There are many non-enzymatic ROS scavengers some obtained from the diet and some are synthesised. Examples of these include α-tocopherol (vitamin E), ascorbic acid (vitamin C), β-carotene,

uric acid and melatonin. α-tocopherol is the most widely studied vitamin E, and is a very important lipid-soluble antioxidant. Tocopherol reacts with lipid radicals preventing the propagation of further radicals; it can then be recycled by being reduced by other anti-oxidants, such as ascorbic acid (Brigelius-Flohe and Traber, 1999). Ascorbic acid is a redox catalyst, it is oxidised by free-radicals and consequently becomes a free radical itself, however the ascorbyl radical formed is relatively stable and unreactive. Upon the loss of another electron dehydroascorbic acid is formed, both ascorbyl radical and dehydroascorbic acid can be reduced or metabolised (Reviewed in Paddayatty *et al.*, 2003). Another antioxidant is melatonin, which cannot undergo redox cycling, and has hence been termed a terminal anti-oxidant; upon oxidation it forms stable products. There exists an orchestration to this multifaceted protection system. Expression of SOD alone would generate a burden of hydrogen peroxide. The balance of antioxidants must therefore be tightly regulated if efficient protection from oxidative stress is to be achieved. Upon increased levels of ROS these responses need to be upregulated and this is performed by cellular signalling pathways indirectly combating oxidative stress by upregulating the direct defences and can lead to a vast array of cellular outcomes, including apoptosis, proliferation, growth arrest etc.

1.1.7.2. Cellular Signalling in Response to Oxidative Stress

ROS activate the cell's stress response mechanism, that is to say there are sensors in place to detect increased levels of ROS, which, in turn, activate the cellular stress response. These responses entail the activation of MAPK signalling pathways including extracellular signal regulated kinase (ERK), p38 mitogen activated kinase (p38MAPK) c-Jun N-terminal kinase (JNK) signalling cascades (Reviewed in Davis, 2000; Paul *et al.*, 1997).

JNK was originally identified as a stress activated kinase (Hibi *et al.*, 1993; Derijard *et al.*, 1994). It forms the central point of an important signalling cascade, allowing the cell to respond to a variety of intracellular and extracellular

cues; and one that will form a main focus of this investigation. It has been shown to be activated in response to ROS and differentially been shown to both promote (Tournier *et al.*, 2000) and prevent (Minamino *et al.*, 1999) apoptosis. JNK contains a Thr-Pro-Tyr motif, when JNK is activated it undergoes dual phosphorylation of threonine and tyrosine. This phosphorylation level is controlled by upstream kinase activity (See table 1). Directly upstream of JNK are two JNKK, hemipterous (hep)/MKK7 and MKK4 (Tournier *et al.*, 1999). MKK7 has been implicated in oxidative stress responses in both *Drosophila* and mammals. Overexpression of MKK7 in *Drosophila* neurons confers increased resistance to paraquat toxicity (Wang *et al.*, 2003). In addition to this, mutations in JNK or MKK7 result in increased sensitivity to paraquat, an electrotoxin used to generate oxidative stress in animal models, further indicative of their protective role. There is a further expansion in the number of molecules at the level upstream of this; there are at least 6 JNKKKs in *Drosophila* and mammals. Apoptosis signal regulating kinase (ASK) is a JNKKK (*Drosophila* orthologue also termed Pk92B) that is activated in response to oxidative stress to drive apoptosis (Wassarman *et al.*, 1996; Kuranaga *et al.*, 2002; Cha *et al.*, 2005). Wallenda has been implicated in regeneration following axonal injury although a role in the oxidative stress response has not been confirmed (Xiong *et al.*, 2010). Upstream of these many JNKKK is the JNKKKK, termed misshapen in *Drosophila*. The mammalian orthologues are MINK, NIK/HGK, and TNIK.

JNK activity is tightly regulated by its upstream signalling components, though the components through which specificity is maintained are not fully understood. In addition to this JNK has a vast number of targets including activator protein-1 (AP-1). This is a dileucine zipper transcription factor formed of dimers of Fos and Jun (kayak and jun-related-antigen respectively in *Drosophila*). Upon phosphorylation of AP-1 its activity is upregulated leading to increased tranascription of targets of AP-1 such as sulfiredoxin (Wei *et al.*, 2008b). Biochemical and genetic data both suggest that, although in mammals only Jun

can homodimerise, Fos can homodimerise as well in *Drosophila* (Perkins *et al.*, 1990; O'Shea *et al.*, 1992). JNK-derived AP-1 activity is crucial for the stress response (Yang *et al.*, 1997).

Activity	*Drosophila* Gene	Mammalian Orthologue
JNKKKK	misshapen (msn)	MINK, NIK/HGK, TNIK
JNKKK	Pk92B	ASK
	Tak1	TAK
	Tak12	TAK
	slipper (slpr)	MLK
	wallenda (wnd)	DLK, ZPK
	Mekk1	MEKK1-4
JNKK	hemipterous (hep)	MKK7
	mkk4	MKK4
JNK	basket (bsk)	JNK
Transcription Factor	jra	JUN
	kayak (kay)	FOS

Table 1. Components of the JNK signalling cascade

There are a number of ways in which JNK signalling pathway activity is determined by redox state using redox regulatory proteins such as thioredoxin (Trx). Trx has redox-sensitive cysteine residues within its active centre. Reduced Trx binds to, and inhibits, ASK-1, thus limiting activation of downstream MAPKs. Oxidative stress, hence the oxidation of Trx, results in the dissociation of this complex, activating ASK-1 (Saitoh *et al*., 1998).

The activation of JNK under conditions of oxidative stress is also enhanced by reducing the interaction between JNK and glutathione S-transferase (GSTp). When reduced GSHp monomers inhibit JNK, whereas under cellular stress dimers and multimers can form, which are no longer capable of binding JNK; thus oxidative stress results in the disinhibition of JNK (Adler *et al*., 1999). Although originally identified as a stress response, JNK signalling has been shown to be crucial in learning and memory, and furthermore a role in the

development of the nervous system (Sanyal *et al.*, 2002 and 2003). AP-1 activity is also modified directly depending on redox potential, depending on the oxidation state of certain cysteine residues. Upon oxidation AP-1 is no longer able to bind DNA, and thus can no longer act as a transcription factor. There are, however, mechanisms in place to preserve AP-1 activity by maintaining its reduced state and thus its ability to bind DNA. Firstly, multiprotein bridging factor-1 (MBF1) prevents oxidation by interacting with the basic region of Jun and inhibiting S-cystenal cystenylation (Jindra *et al.*, 2004). Secondly, the nuclear protein redox factor 1 (Ref-1), originally identified as DNA base pair exision repair and so-called apurinic/apyramidic endonuclease (APE-1) reduces oxidised AP-1 thus reactivating it. Ref-1 levels are changed in response to oxidative stress; reducing ROS production causes a decrease in Ref-1 levels, which is reversed by the application of hydrogen peroxide (Ando *et al*., 2008). Furthermore it has also been suggested that Ref-1 itself is regulated by its redox state (Walker *et al*., 1993).

ERK has been widely shown to be activated in response to oxidative stress (Garg and Chang, 2003,; Yamane *et al.*, 2009). Upon activation, ERK phosphorylates p66schA, at ser36. Knocking out p66schA in mice increases longevity and resistance to oxidative stress (Migliaccio *et al.*, 1999), with ser36 being vital to the pro-apoptotic effects of pp66schA. p66schA in turn acts on downstream signalling molecules such as the phosphorylation/inactivation of Foxo3A. Hence in p66schA knock-outs, Foxo3A activity is increased leading to increased transcription of ROS scavengers (Nemoto and Finkel, 2002), and has been shown to be neuroprotective in models of motor neuron disease (Mojsilovic-Petrovic *et al.*, 2009).

The nuclear factor eyrthroid 2-related factor 2 (NRF2)/Kelch-like ECH-associated protein 1 (KEAP-1) pathway is also involved in adaptation to oxidative stress. Nrf2 is a cap'n'collar transcription factor that regulates the transcription of a number of anti-oxidant transgenes such as heme-oxygenase I

and periredoxin (Ishii *et al.*, 2000) and glutathione S-transferase (Hayes *et al.*, 2000). Activity of Nrf2 is regulated by KEAP-1, which is a cytoplasmic actin binding protein that binds Nrf2 and promotes its proteosomal degradation hence preventing translocation to the nucleus to act as a transcription factor (Motohashi and Yamamoto, 2004). ROS and electrophiles stimulate the dissociation of Nrf2 and KeAP-1 allowing Nrf2 to translocate to the nucleus to bind to the anti-oxidant response element (ARE) to promote the transcription of antioxidant stress proteins and detoxifying enzymes. Cap'n'collar transcription factors, like other bZip transcription factors function as dimers. Potential binding partners include Maf (Motohashi *et al.*, 2002) proteins and Jun (Venugopal and Jaiswal, 1998; Jeyapaul and Jaiswal, 2000) as the ARE sequence has high homology with the AP-1 binding consensus. Putatively as a consequence of Jun/Nrf2 binding, Fos can inhibit Nrf2 directed transcription (Venugopal and Jaiswal, 1996). This indicates how complex these pathways are and how output from oxidative stress responses can be so varied depending on the relative levels of activation of various components of the signalling pathways.

1.2. Autophagy

1.2.1. What is autophagy?

Autophagy literally means self-eating, and can be described as a stress induced catabolic process through which, components of the cell can be degraded and recycled, following fusion with the lysosome. Autophagy is generally non-specific but can be selective as well for example the degradation of mitochondria known as mitophagy. Primarily, autophagy occurs to protect cells against stress, hence autophagy genes are upregulated by AP-1 and NRF2, stress response genes (Jegga *et al.*, 2011). In addition to its primary role in the stress response, autophagy is involved in development, aging and immunity. Autophagy can promote longevity; conversely, overactivation of autophagic degradation can lead to autophagic cell death, otherwise known as type II programmed cell death

(PCD). Genes involved in autophagy (atg genes) were identified in a screen in yeast (Tsukada and Ohsumi, 1993; Thumm *et al.*, 1994, Klionsky *et al.*, 2003), and orthologues have been found and characterised in a variety of higher organisms. These studies are indicative of the conserved molecular machinery between species. There are three different types of autophagy: micro-autophagy, macro-autophagy and chaperone mediated autophagy. Henceforth autophagy will refer to macroautophagy (unless otherwise stated). Autophagy involves the formation of double-membrane vesicles around the components to undergo autophagy. These vesicles are called autophagosomes and ultimately fuse with lysosomes to allow the contents of the autophagosome to be degraded by acid hydrolases contained in the lysosome.

1.2.2. The Regulation of Autophagy

The regulation of autophagy is highly complex (Fig. 1.5), and context dependent. It occurs normally at a basal level to degrade long-lived proteins and old or superfluous organelles. Autophagy has shown to be activated in response to starvation; cellular components that are deemed unnecessary are recycled to compensate for limited nutrition (For Review see Chen and Klionsky, 2011). TOR is a major regulator of autophagy. TOR activity inhibits autophagy. TOR is a protein kinase that is activated in nutrient-rich conditions, to inhibit autophagy. When TOR is inhibited, for example through starvation or rapamycin treatment autophagy is induced. Many signalling pathways that regulate autophagy converge to control TOR. TOR, in fact, functions as part of two complexes termed TOR complex 1 and 2 (TORC1 and 2). Only TORC1 is inhibited by rapamycin and it also regulates translation through phosphorylation of S6K (RSK). One upstream regulator or TOR is Rheb. Rheb is a GTPase that binds to and activates TOR (Patel *et al.*, 2003). Rheb activity is, in turn, controlled by the tumour sclerosis complexes 1 and 2 (TSC1/2), which act as dimer to negatively regulate Rheb (Inoki *et al.*, 2003) (Fig. 1.5) TSC1/2 is activated by AMPK, which can directly inhibit TOR (Gwinn *et al.*, 2008). AMPK is activated by increased

AMP:ATP (Hardie and Carling, 1997) and increased ROS (Han *et al.*,

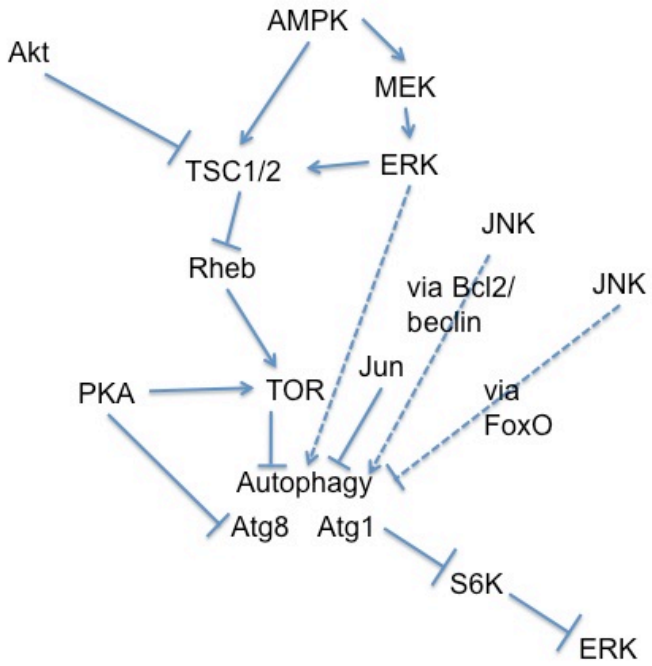

Fig. 1.5: The regulation of autophagy: *Normal arrows (→) denote direct activation; perpendicular lines denote direct inhibition (—|); dashed lines denote indirect regulation.*

2010). Activity of TSC1/2 is also regulated by Akt, which is a mediator of insulin signalling that negatively regulates TSC1/2 (Potter *et al.*, 2003). Protein Kinase A also acts to inhibit autophagy, either directly through phosphorylation of Atg8 (Cherra *et al.*, 2010), or indirectly through phosphorylation of TOR (Mavrakis *et al.*, 2006). S6 kinase is another protein that is regulated by TOR. S6K is increased by TOR activity, as S6K is inhibited by atg1 (Lee *et al.*, 2007), which is inhibited by TOR. S6K decreases ERK activation. ERK however, is also able to activate autophagy (Pattingre *et al.*, 2003), showing the complex integration of many signalling pathways involved in the regulation of autophagy. MEK/ERK signalling has also been implicated as an intermediate step between AMPK and TSC (Wang *et al.*, 2009). As discussed earlier JNK also regulates autophagy.

JNK signalling activates transcription of autophagy genes in response to oxidative stress (Wu *et al.*, 2009). JNK also phosphorylates bcl2, which is known to bind to and thereby inhibit, beclin (atg6). Therefore, upon JNK phosphorylation Bcl2 and beclin dissociate leading to increased autophagy (Wei et al., 2008c). However, the regulation of autophagy by this pathway has also been shown to act in other ways. Jun can inhibit autophagy in mammals (Yogev and Shaulian, 2010; Yogev *et al.*, 2010). JNK also negatively regulates FoxO dependent autophagy in neurons (Xu *et al.*, 2011). The regulation of autophagy is normally tightly controlled due to the integration of many signalling pathways activated in response to many cellular factors and components.

1.2.3. Molecular mechanism of autophagy

A lot has been learnt about autophagy by studying an analogue of autophagy in yeast known as 'cytoplasm to vacuole transport' (cvt). This is how cellular components are targeted to the vacuole, the equivalent of the lysosome in yeast. The cvt pathway shows high homology to degradative autophagy (Harding *et al.*, 1996; Scott *et al.*, 1996). Starvation induced autophagy also occurs in yeast so the presence of both these pathways has helped to elucidate the mechanisms involved as there is a high level of conservation between both the molecules and mechanisms used in yeast and higher organisms such as *Drosophila* and mammals.

The process of autophagy can be broken down into phases (Klionsky, 2005):
(I) Induction and cargo selection
(II) Isolation membrane and membrane nucleation
(III) Vesicle elongation
(IV) Retrieval
(V) Vesicle docking and fusion
(VI) Vesicle breakdown and degradation

Induction of autophagy is controlled by ATG1, ATG13 and ATG17. Only ATG1 and ATG13 are present in *Drosophila* where ATG1 and ATG13 are phosphorylated by TOR in nutrient rich environments, thus phosphorylation decreases during starvation, or TOR inactivation. However, during starvation and hence initiation of autophagy TOR no longer phosphorylates ATG1 or ATG13, and ATG13 is phosphorylated by ATG1 (Suzuki *et al.*, 2001). The precise mechanims varies across species although the prevailing feature across all species is that autophagy is inhibited in nutrient-rich environments when TOR is activated and directly phosphorylates ATG13 (Scott *et al.*, 2000). Accordingly, TOR inactivation leading to the induction of autophagy changes the phosphorylation state of ATG13. In yeast and mammals ATG13 is hyperphosphorylated in nutrient rich conditions and therefore less phosphorylated during the induction of autophagy. Starvation increases affinity of ATG13 for ATG1. During induction of autophagy in *Drosophila* ATG1 phosphorylates ATG13, resulting in hyperphosphorylation (Kamada *et al.*, 2000). Following initiation of autophagy the phagophore, also known as the isolation membrane, engulfs the cytoplasmic material that is to undergo autophagy to form an autophagosome; whereby a double membrane is formed around the material (membrane nucleation). Mechanisms and molecular components involved in nucleation are not fully understood, however, in yeast it has been shown to involve formation of a complex between class III phosphatidylinositol kinase (PI3K)/Vps34, beclin/ATG6/Vps30, ATG14 and Vps15. Atg 7 and Atg8 are also involved (Axe *et al.*, 2008). In mammals, additional components and regulators of this complex have also been identified, but how the PI3K complex forms in *Drosophila* is unclear. This PI3K complex recruits other proteins required for autophagy and promotes their localisation to the phagophore, such as the Atg2-Atg18 complex; Atg9 is also recruited (Obara *et al.*, 2008; Stromhaug *et al.*, 2004; Xie and Klionsky, 2008). Elongation of the vesicle occurs in two ways, both using ubiquitination-like conjugation systems. The first system involves the conjugation of Atg5 and Atg12, through the catalytic activity

of Atg7, which has E1 like activity, hence activating the process. Atg10 then continues the ubiquitination-like process, catalysing the conjugation step, similar to an E2. No E3 like component has yet been identified in this system. The second elongation system involves the conjugation of Atg8 to phosphatidyl-ethanolamine (PE). Atg4 cleaves Atg8 allowing it to be activated by Atg7 (E1-like), and transferred to Atg3 (E2-like) to be conjugated to PE (Glick *et al.*, 2010). In this manner it is effectively inserted into the autophagosomal membrane. In many degradative pathways, retrieval of selected components occurs to allow recycling. Of all the proteins involved in vesicle formation and elongation, only Atg19 and Atg8PE are present in the completed vesicle. The mechanisms of retrieval are not well understood although the retrieval at Atg9 is known to involve and Atg18, 2 and PI(3)P. The completed autophagosome then undergoes maturation by docking and fusion with the lysosome (vacuole in yeast) for vesicle breakdown and degradation. This process, as with other vesicle fusion processes involves activity of SNARE proteins (Darsow *et al.*, 2007) and Rabs, notably Rab7 (Jager *et al.*, 2004), members of the HOPS complex have also been implicated (Lindmo *et al.*, 2006; Pulipparacharuvil *et al.*, 2005). LAMP1 and LAMP2 have been shown to be required for autophagosome-lysosome fusion (Gozalez-Polo *et al.*, 2005).

Increased lysosomal storage can result in impaired autophagic delivery to the lysosome leading to accumulation of autophagosomes, thereby identifying lysosomal storage disorders as having a block in autophagy leading to build up of polyubiquitinated proteins and dysfunctional mitochondria, the putative mediators of cell death in these disorders.

1.3. Autophagy, lysosomes and oxidative stress in neurodegenerative diseases

1.3.1. Lysosomal Storage Disorders

Lysosomal storage disorders (LSDs) are a collection of around 45 metabolic disorders, with a collective occurrence of approximately 1 in 8000 live births (Meikle *et al.*, 1999). LSDs are characterised by enlargement and proliferation of lysosomes, with the identity of the stored material being determined by the trafficking pathway/protein that is causing the pathology. LSDs have far reaching implications, and are multi-systemic, resulting in childhood neurodegeneration and severe heart and lung problems (Futerman and van Meer, 2004).

As material is degraded it is moved to lysosomes either through autophagic or endocytic pathways. The build up that occurs naturally during aging, of things that cannot be further degraded in the lysosome is termed lipofuscin. This is otherwise known as 'aging pigment' and has been implicated in a number of neurodegenerative disorders, although how it impacts on neuronal function is not completely understood. Build up of a similar nature is a classical hallmark of LSDs. This lipopigment is termed ceroid, when present in pathological states (Kurz *et al.*, 2008b).

1.3.1.1. Lysosomal storage disorders and oxidative stress

LSDs have been shown to involve oxidative stress, similar to many other neurodegenerative disorders. Lysosomes are sensitive to oxidative stress, which can enhance the formation of hydroxyl radicals leading to permeabilisation of the lysosomal membrane leading to a vicious cycle between the generation of ceroid and the generation of ROS.

Hydrogen peroxide diffuses into the lysosome, which does not contain catalase or glutathione peroxidase to break it down. Furthermore, lysosomes have a low

pH and a high concentration of iron, making them susceptible to further generation of ROS/oxidative stress due to the conditions being conducive to the Fenton Reaction:

$Fe^{2+} + H_2O_2 \rightarrow Fe^{3+} + HO^{\cdot} + OH^{-}$

Moreover, oxidative stress can cause peroxidation of the lysosomal membrane, and hence destabilisation. This can cause the lysosome to leak and releases the acid hydrolases into the cytosol. It has also been suggested that if lysosomal function is impaired organelles will not be adequately recycled and hence old mitochondria may build up, and hydrolases released from the lysosomes may attack the mitochondria, both though activation of phospholipases and activation of cytochrome c release, thus further adding to the generation of ROS. Lysosomal permeabilsation has been shown to induce apoptosis (Nylandsted *et al.*, 2004) although more severe rupture may cause necrosis, showing the potential role in neurodegenerative conditions. However the importance of lysosomal function and how it is affected by ROS and oxidative stress in synaptic development is an area less well understood.

1.3.2. Autophagy and Neurodegeneration

Autophagy is generally considered cytoprotective, as aging cellular components are recycled (Arsham and Neufeld, 2009). It is activated through JNK signalling, which improves tolerance to oxidative stress (Wu *et al.*, 2009; Wang *et al.*, 2003). Increasing basal levels of autophagy in the nervous system has in fact been shown to increase longevity in addition to improved resistance to oxidative stress (Simonsen *et al.*, 2008). Inducing autophagy through rapamycin or lithium is protective in a model of Huntington's disease, as it upregulates the clearance of the disease causing aggregations (Sarkar *et al.*, 2009). Inhibition of autophagy can lead to build up of old mitochondria and other damaged or old organelles and proteins. However, the situation is a complex one. In a model of ischaemia inhibiting autophagy and lysosomal function reduced neural cell death

(Kubota *et al.*, 2010). Furthermore, inhibiting autophagy in a model of frontotemporal dementia that is caused by mutations in the endosomal sorting complex is protective against neural cell death (Lee and Gao, 2009). The role of autophagy in neurodegeneration is somewhat paradoxical because impairing autophagy can mimic LSD but can also rescue/ reduce an LSD phenotype because it prevents build up of autophagosomes and lysosomes, which lead to further generation of ROS. The effects of changing levels of autophagy in neurodegeneration depends somewhat on whether autophagy leads to the build up or degradation of the primary pathological component of the disease.

1.3.3. Oxidative Stress, Ageing and Neurodegenerative Diseases

Harman proposed the 'free radical theory' of ageing, and pathological degeneration of a similar kind to ageing (Harman 1956), first suggesting that constitutively produced ROS interact with cellular components exhibiting a deleterious effect that results in ageing. It had already been noted for a long time that animals that have higher metabolic rates tend to have shorter lives, leading to the 'rate of living' hypothesis, although how metabolism and the ageing process were linked remained unknown. Long-lived cells are particularly susceptible to oxidative stress, meaning the nervous system is prone to oxidative damage. The inability of most neurons to divide means that as they die they are not replaced so neuronal death leads to neurodegeneration. Neurons have been suggested as the 'weak link' in defence against ROS as overexpressing SOD1 only in motor neurons significantly increases longevity (Parkes *et al.*, 2008). Moreover, antioxidants are found at lower levels in the nervous system than other tissues (Halliwell, 1992; Halliwell, 2006). ROS have been implicated in Alzheimer's, Parkinson's, Huntington's, Gaucher's (Deganuto *et al.*, 2007) diseases, Friedrich's ataxia and Amyotrophic lateral sclerosis. In fact amyloid-beta (Aβ), the protein involved in the pathology of AD, has been shown to interact directly with catalase (Milton, 1999) and inhibition of catalase

worsens Aβ-toxicity (Milton, 2001). In addition NADPH oxidase production of ROS has been strongly implicated in the pathology of Alzheimer's disease (Park *et al.*, 2008) due to Aβ-induction of ROS generation by NADPH oxidase (McDonald *et al.*, 1997). ROS generation can occur as a result of normal signalling pathways being hijacked pathologically, often resulting in the generation of a vicious cycle. For example, NADPH oxidase derived ROS are vital for CLIC1, a Cl-channel, activation, but Aβ induced ROS generation is dependent on CLIC1 activation (Milton *et al.*, 2008). ROS have been clearly implicated in cognitive decline and there is a large body of research into how ROS affect neuronal function to cause cognitive decline (Dröge and Schipper, 2007; Guidi *et al.*, 2006). However, the role of ROS in developmental pathologies has not been widely investigated, furthermore, neurodegenerative diseases as a result of pathological development is becoming an increasingly likely possibility. The role of ROS in normal physiology, as opposed to pathological states, is less well understood. Increasingly ROS are being highlighted as signalling molecules in embryonic development (Viera *et al.*, 2011; Le Belle *et al.*, 2011; Kim and Wong, 2009) and synaptic plasticity. ROS are important signalling molecules in long-term potentiation (LTP), the biological correlate of learning and memory (Bindokas *et al.*, 1996; Klann *et al*., 1998). Hence the situation is complex; ROS are vital to learning and memory, yet also result in physiological decline with ageing.

1.3.4. Using *Drosophila* to study LSDs

Drosophila are very useful for studying lysosomal storage disorders, as mutations and transgenes are relatively easily produced. The powerful genetic toolbox coupled with the short generation time make the study of these disorders in *Drosophila* highly insightful, efficient and economical. A number of specific LSDs have been modelled in *Drosophila* including Juvenile Batten Disease, modelled through changing expression of the gene CLN3 (Tuxworth *et al.*, 2009 and 2011), mucolipidosis type IV (Venkatachalam *et al,*. 2008) and

Niemann Pick type C (Huang *et al.*, 2005). Generally, autosomal recessive LSDs are caused by compound heterozygote mutations, meaning that the mutations in the two alleles are different (E.g. Tylki-Szymańska *et al.*, 2007). Coupled with other genetic and epigenetic differences means that there is great variation between development and progression of symptoms. However some clinical manifestations are highly characteristic. Even though present only in more severe cases neurological/neuronopathic symptoms are common to LSD. Therefore understanding how lysosomal dysfunction impacts on neuronal development and function could help elucidate general disease mechanisms.

1.3.4.1. A model of lysosomal storage disorder: *spinster*

The *Drosophila* mutant *spinster* was originally identified during a screen for mating phenotypes, where the female was identified as being reluctant to mate (Yamamoto and Nakano, 1999). In addition to this phenotype it was also noted that *spinster*, otherwise known as *benchwarmer*, have reduced longevity, impaired programmed cell death, neural degeneration and accumulation of aurofluorescent pigment in the neurons; all characteristic of LSDs (Nakano *et al.*, 2001). Subsequently it was identified in a screen for synaptic growth (Sweeney and Davis, 2002). Further support for *spinster* as a model of a LSD was provided when Sweeney and Davis showed that *spinster* is localised to the late endosome/lysosome (Sweeney and Davis, 2002). Spinster encodes a 12 transmembrane transporter that localises to the late endosome/ lysosome and is expressed both pre- and post- synaptically during synapse growth and development. The neuronal phenotype of spinster is an increase in synapse size and bouton number coupled with impaired synaptic transmission (Sweeney and Davis, 2002). Mutations in *spinster* lead to dysregulated TGFβ that is required for the overgrowth phenotype. Ectopic nerve growth has been demonstrated in models of LSDs (March *et al.*, 1995), and the aim of this study is to identify other pathogenically activated signalling cascades that might be involved in the generation of overgrowth phenotypes. Endocytic defects were confirmed by

Dermaut et al., (2005), with possible tau toxicity. Both studies show mulitlamellar inclusions and accumulation of lysosomes (Nakano *et al.*, 2001; Dermaut *et al.*, 2005)

1.4. Neurotransmission

1.4.1. Action Potential

Neuronal activity was first shown to be electrical when Galvani (1791) observed contraction in the hind legs of frogs when a metal hooked attached to an iron railing was attached to the medulla (reviewed by Cowan and Kandell, 2003). Action potentials occur in excitable cells and are simply defined as when the electrical membrane potential of a cell rapidly rises and falls due to movement of ions across the membrane. These nerve impulses are termed spikes, and the temporal sequence in which these occur is termed a spike train. Voltage gated ion channels (VGICs), are channels that are shut when the cell is at resting potential (~-65mV) until threshold potential is reached (~-55mV), Na^+ ions flow in increasing the membrane potential, and all the VGICs open and Na^+ flow in until the membrane polarity is reversed, at which point the Na^+ channels are inactivated, and hence close. This results in Na^+ ions being transported out of the cell, K^+ channels are activated so K^+ floods out of the cell; this results in a negative shift, otherwise termed afterhyperpolarisation (for review see Nachmansohn, 1971; Ginsborg, 1973).

1.4.2. Synaptic Transmission

Neurons communicate with other neurons and cells through synaptic transmission. Synaptic transmission briefly entails the release of chemicals, neurotransmitters, from the pre-synaptic terminal to act on receptors on the post-synaptic terminal.

When the action potential reaches the presynaptic terminal depolarisation results in the opening of Ca^{2+} channels, leading to increased Ca^{2+} in the neuron.

Vesicles containing neurotransmitter are linked to calcium-sensitive proteins, upon calcium binding these proteins change protein conformation, thereby resulting in exocytosis, where the vesicle fuses with the plasma membrane releasing the neurotransmitter into the synaptic cleft. The neurotransmitter released binds to ligand gated ion channels (LGICs), resulting in an Na^+ influx and K^+ efflux. Due to the permeability of the membrane more Na^+ moves in than K^+ out, resulting in local depolarisation. Synaptic potentials are the local depolarisations, with measurable delay following synaptic input, linking the presynaptic terminal and the effects it has on the post-synaptic terminal. The synaptic potential is distinct from action potentials in that they are graded responses rather than the all-in-one action potential. The depolarisation spreads along the muscle fibre into transverse tubules, causing release of Ca^{2+} from the sarcolemma, consequently the muscle contracts (reviewed by Cowan and Kandell, 2003).

1.4.2.1. Neurotransmitter release

Clathrin coated vesicles are endocytosed and then recycled, and that each vesicular fusion is equivalent to one quantal release (Heuse and Rease, 1973 as reviewed by Cowan and Kandell, 2003). The presynaptic density is a specialised area in the presynaptic process, directly apposed to the postsynaptic density. The presynaptic density has a thicker denser membrane that the rest of the presynaptic terminal, with a presynaptic vesicular grid with pyramidal projections that extend into the synaptic processes. Between these projections vesicles align prior to release, this led to the hypothesis of ‘docking sites’, these areas are now know as ‘active zones’ (Couteaux and Pecot-Dechavassine, 1970). Boutons are swellings in the presynaptic terminal containing bundles of intermediate or neuro-filaments, these filaments can also be clustered around mitochondria and other organelles and contain active zones.

1.4.2.2. Post-synaptic responses

Neurotransmitter release is quantal in nature, this was first shown by Fatt and Katz (Fatt and Katz, 1951) established the quantal hypothesis when they observed spontaneous depolarising potentials, even in the absence of stimulation. These are termed mini EPPs (mEPPs). Drugs that enhance the action of the neurotransmitter cause prolonged potentials whereas drugs that inhibit the actions of the neurotransmitter abolish these mEPPs. Depolarising the presynaptic terminal increases the frequency of mEPPs whereas, abolishing neuronal input causes mEPPs to disappear, indicative of mEPPs being presynaptic in origin. mEPPs are Na^+ dependent, but do not require Ca^{2+}. They were suggested to be caused by individual quanta being released from the pre-synaptic terminal. EPPs were shown to be whole integer duplicates of mEPPs. Release of quanta is probabilistic and an action potential increases the probability of neurotransmitter release. This hypothesis was greatly supported when Palay and Palade (1955) and de Robertis and Bennett (1955) showed the presence of synaptic vesicles with the first high-quality EM of the synapse. This led to the Ca^{2+} hypothesis (Katz and Miledi 1965), they subsequently showed that APs cause Ca^{2+} conductance to increase, but neurotransmitter release does not depend on Na^+ or K^+ (reviewed by Cowan and Kandell, 2003).

1.5. *Drosophila* neuromuscular junction as a model of synapse development

1.5.1. *Drosophila* as a model organism

Drosophila melanogaster, the common fruit fly, has been used as a model for many years, since pioneering work by Thomas Hunt Morgan at Columbia University. Using *Drosophila* has elucidated many developmental and disease processes both at the cellular and molecular level. The short life cycle and high numbers of progeny make *Drosophila* a relatively cheap model animal.

1.5.1.1. Genetic Tools

Drosophila are highly amenable to genetic manipulations and lend themselves to genetic investigation, as the males do not undergo recombination. Further to this, balancer chromosomes can be used to prevent recombination in females (Rubin and Lewis, 2000). Balancer chromosomes also carry markers, so mutations can be tracked. Mutations can readily generated in a number of ways such as P-elements whereby a large transposon can be inserted into the genomic DNA, impairing transcription and EMS, which produces point mutations. Transposon-mediated transformation can be used to generate transgenic flies (Takeuchi *et al.*, 2007). This allows the implementation of the Gal4/UAS system, a tissue specific expression system, whereby specific transgenes can be expressed in different tissues through the use of two different transgenic strains of *Drosophila* (Brand and Perrimon 1993). Use of this system involves the generation of two lines of flies, the driver and the responder. The driver contains a Gal4 promoter, whereby the promoter element of a gene is linked to Gal4 expression. Therefore, Gal4 is co-expressed in the same localisation as promoter to which it is linked. The responder transgenic line contains an upstream activating sequence linked to the gene to be expressed. Gal4 is a yeast transcription factor that binds to UAS and activates transcription. A more recent development in the field of *Drosophila* genetics is the introduction of RNAi lines (Dietzl *et al.*, 2007), to knock down gene expression by sequence-specific gene silencing (For review see Paddison *et al.*, 2002a and b).

1.5.2. The *Drosophila* 3rd instar larval neuromuscular junction

Each abdominal hemisegment of the larva contains 30 syncytial muscles that receive innervation by two motor neurons. The dorsal muscles receive innervation from the anterior intersegmental nerve (ISN), and the ventral from the posterior segmental nerve (SN). The transverse nerve (TN) innervates the lateral muscles of each hemisegment. Axons leave these nerves to form highly characterised NMJs at each muscle. A number of the neurons in each

hemisegment are well characterised, muscle 6/7 in hemisegment A3 is innervated by RP3, one of the RP neurons RP1-5. RP1-5 send their axons out to the periphery through the anterior root of the anterior fascicle (Keshishian *et al.*, 1996).

There are two broad classes of NMJ in *Drosophila*. Type I NMJs have short terminal branches and large boutons where as type II NMJs have long thin branches with very many small boutons. Type I axons have thick axonal processes and the presynaptic portion of the NMJ is enveloped by the subsynaptic reticulum (SSR), a junctional membrane produced by the muscle. Type I NMJs innervate all body wall muscle and are predominantly glutamatergic and comprise 2 types of boutons, differentiated most notably by size, into type Ib (big) and type Is (small). In addition to differences in size, type Is have less SSR and are generally further away from the branch. Type II NMJs determine excitation state, and transmit octopamine and glutamate. There are generally two motor neurons of this type per hemisegment, which innervate all but 8 muscles per segment, and do not have an SSR (Broadie and Bate, 1993; Keshishian *et al.*, 1996). This study focuses on type I NMJ development.

1.5.3. Anatomy of the larval neuromuscular junction

Prior to synaptic contact, between the synapse and the muscle, development of the two components in independent; neurons in twist mutants, which do not have body wall muscles, target correctly and presynaptic zones form normally to begin with. Synapse formation begins approximately 13 hours after egg-laying (AEL), when the growth cone of the extending axons contacts the myopodia of the developing muscle; subsequent NMJ development requires input from both the muscle and the nerve (Broadie and Bate, 1993). Varicosities develop in the presynaptic terminal, after they become confined to the synaptic area. Synaptic boutons, containing T-bars and active zones are visible three hours after the first contact. Active zones are areas of the bouton that are neurotransmitter release sites; vesicles cluster here and then fuse with the membrane during synaptic

transmission. T-bars are a morphology seen in some active zones, which are electron dense T-shaped areas thought to promote vesicle fusion. Mutations in an active zone protein bruchpilot (BRP) result in T-bars not formed, although normal apposition between the pre- and post-synaptic membrane is maintained. The absence of T-bars is accompanied by impaired synaptic transmission (Kittel *et al.*, 2006a and b; Wagh *et al.*, 2006), showing that this protein is vital for active zone assembly and normal synaptic transmission. Active zone clustering is dependent from feedback from the muscle. In mef2 mutants, where the myoblasts are unable to fuse, active zones do not cluster correctly, and remain evenly distributed along the presynaptic area.

Following release from the pre-synaptic terminal glutamate binds to glutamate receptors GluRs in the post-synaptic membrane. Muscular glutamate receptors in *Drosophila* are homologous to AMPA and kainite receptors in vertebrates (Featherstone *et al.*, 2005; Marrus *et al*., 2004). They are ionotropic receptors that is to say there are receptor-gated ion pores composed of four subunits. Currently 6 subunits have been identified in *Drosophila*; DGluRIIA and B have distinct physiological properties and either is required for the localisation of DGluRIII. Receptor composition is determined by afferent input (Marrus and DiAntonio, 2005).

Release of glutamate causes receptors to cluster in the post-synaptic membrane apposed to the presynaptic processes, and without this neuronal input the second increase in glutamate receptors does not occur and they remain homogeneously expressed throughout the muscle. The need for synaptic transmission shows how dependent the two synaptic components are on each other for correct synaptic development. One hour after initial contact synaptic currents can be detected, followed by muscle contractions two hours after first contact, thus 16-17 hours AEL the first functional NMJ is formed (reviewed by Featherstone and Broadie, 2000; and Keshishian et al.,1996).

1.5.4. Development of the *Drosophila* NMJ

As with all developmental processes, growth of the synapse is dependent on the integration of many complex signalling pathways. Development is controlled through bi-directional signalling between the presynaptic nerve-terminal and the post-synaptic muscle. The larval NMJ is a dynamic system that changes throughout development. The development of the muscle and the nervous components of the NMJ occur in tandem. That is to say, expansion of the NMJ parallels the exponential muscle growth occurring during larval development. From 1st instar to 3rd instar the muscle grows 100x, and concurrently the presynaptic area expands as well (Atwood *et al.*; 1993, Schuster *et al.*, 1996a Keshishian *et al.*, 1993; Gorczyca *et al.*, 1993). Muscle development, in terms of size and formation occurs relatively normally even in the absence of innervation, although receptor clustering is dependent on glutamate.

Discs-large (dlg) is an important determinant of synaptic development in *Drosophila*. It forms part of the post-synaptic density, and is involved in the clustering and stabilising of GluRIIB containing receptors (Chen and Featherstone, 2005). In type I NMJs its expression is firstly pre-synaptic and then shifts to the post-synaptic side. It is highly important in synapse development and is involved in the clustering of K+ channels (shaker) (Tejedor *et al.*, 1997). Mutations in dlg have reduced formation of the SSR and an increase in bouton size and with an increase in the number of active zones per bouton (Lahey *et al.*, 1994). Dlg colocalises with FasII, which is believed to aid bouton formation through a bidirectional signal between the muscle and the nerve (Thomas *et al.*, 1997). Null mutants have normal synaptogenesis but then the boutons retract and the larvae die at 1st instar. FasII regulates synaptic growth in a dose dependent manner. It is required both pre- and post-synaptically to prevent synapse elimination. In hypomorphs containing less than 10% normal FasII levels bouton number is decreased but bouton size in increased and the number of active zones per bouton is increased. *FasII*

hypomorphs with 50% normal expression have increased bouton number, with increased synaptic sprouting (Schuster *et al.*, 1996a). In *shaker* and *dunce* mutants, which show a similar overgrowth to *FasII* hypomorphs, increased cAMP activity lead to a 50% decrease in FasII levels, required for this overgrowth phenotype (Schuster *et al.*, 1996b). While FasII reduction accounts for structural changes, *FasII* hypomorphs do not show the hyperexcitability phenotypes. The electrophysiological changes in *dunce* are due to cAMP dependent increases in CREB (Davis *et al.*, 1996). This shows how signalling pathways can diverge and converge resulting in a variety of phenotypes that share some commonality but differ in characteristics. Reduced levels of FasII have also been implicated in increased bouton number in *hangover* mutants (Schwenkert *et al.*, 2008). There is no change in neuronal transmission in these mutants, again showing that mechanisms governing function do not always correlate with those determining growth.

1.5.4.1. Morphogenic Signalling

Two well characterised signalling pathways involved in synapse development are Wingless and TGFβ signalling. Wingless is secreted by the motor neuron (Packard *et al.*, 2002), thus an anterograde signal. Signalling is mediated by the postsynaptic receptor DFrizzled2 (DFz2). Upon activation DFz2 undergoes cleavage whereby the C-terminal domain translocates to the nucleus to modify gene transcription (Mathew *et al.*, 2005); it is as yet unknown which genes are regulated by this pathway. Concurrently during synapse development, retrograde signalling is mediated by Gbb released from the muscle (Marques, 2005). This activates TGF-β signalling, through the activation and dimerisation of a type I TGF-β receptors encoded by Thick Veins (Tkv) and saxophone (Sax) with type II TGF-β receptors, encoded by wishful thinking (Wit). Ligand binding and activation of these receptors effects the phosphorylation of MAD. Activated MAD putatively interacts with MED (Medea, a coSMAD), translocates to the

nucleus, determining gene transcription (McCabe *et al.*, 2003; Sanyal *et al.*, 2003).

1.5.4.2. MAPK signalling

AP-1 has previously been shown to be important in the regulation of synapse size and strength during development (Sanyal *et al.*, 2002 and 2003). AP-1 is a transcription factor composed of homo- and hetero-dimers of Fos and Jun, basic leucine zipper proteins, that controls the transcription of numerous genes. AP-1 can be activated by Jun N-Terminal Kinase (JNK). JNK is a serine/threonine kinase, traditionally known as a stress activated protein kinase (SAPK) due to its role in the cellular stress response. The activity of this pathway is under the control of a negative feedback loop; one of the target genes of AP-1 is puckered, a phosphotase which inhibits JNK. During synapse development AP-1 positively regulates synaptic strength and size; such that increased expression of Fos and Jun in the neurons but not the muscle increases bouton number (Sanyal *et al.*, 2002).

The importance of the AP-1 pathway in synaptic development has been highlighted by studies on a number of mutants. Highwire, an E3 ubiquitin ligase, localises to the presynaptic terminal. Loss of Highwire results in synaptic overgrowth, thus highwire is believed to restrain synaptic overgrowth through downregulation of a growth-promoting signal. Highwire is believed to bind to DFsn to suppress synaptic overgrowth (Wu *et al.*, 2007). The overgrowth seen in *highwire* and *DFsn* can be suppressed by removing a MAPKKK known as wallenda, confirming the role of MAPK signalling in the regulation of growth. Furthermore, removing JNK or Fos also suppressed synaptic overgrowth in *highwire*, thus it is proposed that Highwire downregulates Wallenda consequently attenuating JNK/Fos signalling (Collins *et al*., 2006). Thus the model proposed is that under normal physiological conditions Highwire inhibits MAPK signalling cascades involving wallenda/JNK/Fos consequently restraining synaptic growth. In the absence of highwire this inhibition is released and the

overactivity of the JNK/Fos pathway results in synaptic overgrowth (Collins *et al*., 2006).

ERK has also been shown to be involved in synapse development in the control of active zone density (Wairkar *et al*., 2009). During synapse development ERK activity is inhibited by atg1 (unc-51). When ERK activity is disinhibited, increased activity leads to decreased functional synapse formation with synapses forming without active zones, vital for neurotransmitter release (Wairkar *et al*., 2009). Accordingly, with mutations in S6K where there is decreased ERK activity leading to increased bouton number as S6K negatively regulates bouton number through ERK signalling (Fischer *et al*., 2009). Focal adhesion kinase (Fak56) also restricts ERK signalling, suppressing NMJ growth. When this restriction is released, such as in Fak66 mutants the synapses overgrow, and have increased branching (Tsai *et al*., 2008). ERK can modulate synaptic growth through regulation of the adhesion molecule FasII; levels of ERK and FasII are inversely correlated (Koh *et al*., 2002)

1.5.4.3. Autophagy and synaptic growth

Autophagy has been implicated in the control of synapse development, due to autophagic regulation of highwire (Shen and Ganetzky, 2009). Defects in autophagy lead to a build up of highwire, increasing the level of inhibition on wallenda/JNK/Fos signalling resulting in decreased synaptic growth. Accordingly, increased autophagy leads to potentiation of synaptic growth (Shen and Ganetzky, 2009). Other regulators of autophagy have also been implicated in synapse development, although the data from different studies are somewhat paradoxical. Increasing Rheb activity in the nerve results in synaptic overgrowth, however increased Rheb increases TOR activity reducing induction of autophagy. Conversely expression of Rheb in the muscle causes a slight reduction in synaptic growth. Supporting the role for Rheb as a potentiator of synaptic growth, mutations in *rheb* have significantly smaller NMJs than wildtype (Knox *et al.*, 2007). The finding that inhibiting TOR with rapamycin increases

bouton number is consistent between these studies. The observation that rapamycin does not inhibit Rheb-mediated synaptic growth suggests that TORC1/S6K is not involved in the generation of this overgrowth, thus they suggest overgrowth is mediated by TORC2 (Knox *et al.*, 2007). In addition Fischer *et al.* (2009) found that mutations in S6K result in potentiated synaptic growth through inhibition of ERK signalling (Fischer *et al.*, 2009), suggesting that S6K negatively regulates bouton number.

1.6. Oxidative Stress Autophagy and Synapse Development

1.6.1. Oxidative Stress and Synapse Development

In addition to its role in the stress response, JNK signalling has been shown to positively regulate synapse size and strength (Sanyal *et al.*, 2002). Furthermore, presynaptic JNK signalling has been shown to be dysregulated in *hiw* mutants resulting in synapse overgrowth (Collins *et al.*, 2006). Synapses are areas of high energy demand thus have high numbers of mitochondria making them susceptible to oxidative stress. Furthermore the fact that nerves are post-mitotic and do not generally degenerate meaning that degraded material builds up overtime, leading to the presence of ceroid in aged neurons and diseased neurons where degradation in impaired, such as lysosomal storage disorders (LSDs). Furthermore there is great commonality between the pathways that are activated in oxidative stress and those involved in synapse development. JNK has been shown to activate bouton number (Sanyal *et al.*, 2002), and has also been shown to be activated in response to oxidative stress. Furthermore autophagy is transcriptionally activated during oxidative stress, and autophagy drives synapse growth. JNK signalling activates autophagy and hiw has been shown to be degraded by autophagy, thus resulting in increased activity of JNK signalling with defective autophagy, thus there is a feedback loop, indicative of the complexity of signalling involved in control of synapse

development. Autophagy has recently been shown to drive synapse growth (Shen and Ganetzky, 2009). Driving autophagy increases synapse size; this was shown to require JNK signalling. There is, however conflicting data on the role of regulators of autophagy in the control of synapse development. Knox *et al*. (2007) showed that driving Rheb activity resulted in increased bouton number, which was not inhibited by rapamycin suggesting that Rheb is controlling synapse development through other mechanisms.

Recently further indirect research into the effects of oxidative stress on synapse development has been investigated through analysis of NMJ development in a model of Parkinson's disease caused by LRRK2 mutations, where synaptic overgrowth can be seen at the Drosophila NMJ. In addition overexpression of LRRK2 causes undergrowth of the NMJ, these phenotypes have been shown to be due to specific interactions with both the pre- and post- synaptic machinery, resulting in dysregulation of protein synthesis and perturbed microtubule formation (Lee *et al.*, 2010b). However the investigators did not investigate if oxidative stress had a causative role in the generation of these phenotypes.

Mutations in SOD1 in a mouse model of amyotrophic lateral sclerosis (ALS) have been investigated and it has been put forward that SOD1 mutations could result in problems in maturation of motor neurons and networks (Durand *et al.*, 2006), with problems in axonal transport detectable well before the onset of symptoms (Williamson and Cleveland, 1999). Amendola *et al.* (2004) found motor deficits very early on, in mice only 1 week old, which could be indicative of developmental abnormalities. In addition to pathologies caused by loss of SOD1 function, overexpression of SOD1 has also been implicated in neuronal pathology (Avraham *et al.*, 1988). In Down's syndrome there are 3 copies of chromosome 21 present, which is where the gene for SOD1 is located. By transgenically overexpressing SOD1, it is possible to dissect which aspects of DS pathology might be caused by the increased gene dosage of SOD1, as increased SOD could lead to increased levels of hydrogen peroxide. It has been

shown that rat cells with increased SOD1 show decreased levels of neurotransmitter uptake (Elroy-Stein and Groner, 1988). Mice with elevated levels of human SOD1 were noticed to have terminal axon degeneration in the NMJ of the tongue, coupled with changes in the endplate (Avraham *et al.*, 1988). The role of increased SOD1 is complex, highlighting the anti-oxidant paradox: Increased levels of SOD1 cause increased levels of peroxidated lipids, indicative of oxidative damage yet also increased resistance to paraquat (Elroy-Stein *et al.*, 1986). Mutations in *sod2* in *Drosophila* also cause reduced longevity and movement however these phenotypes affect the muscle prior to neuronal dysfunction (Godenshwege *et al.*, 2009). In addition longevity is improved when SOD2 function is restored in the muscle but not the nerve. Conversely, reduced longevity in *sod1* mutants was rescued by motor neuron expression of SOD1 (Parkes *et al.*, 1998) and therefore it is necessary to dissect neuronal and muscular components of effects of increased ROS on synapse development and function. This demonstrates how the source of ROS is important to the generation of the phenotype it produces, not just the identity of the species and its level. *sod1* mutations seem to affect neurons more whereas *sod2* mutations have more severe and earlier effects in the muscle.

In a model of encephalopathy, caused by mutations in *succinate dehydrogenase A* (*sdhA*) ROS have also been shown to cause synapse loss in a study of synapse development. (Mast *et al.*, 2008). Synapse loss is rescued by tocopherol (vitamin E, an anti-oxidant) indicative of oxidative stress having a causative role in synapse loss.

More recently Fos signalling has also been implicated in the synaptic overgrowth seen in the mutant *spinster*, a model of lysosomal storage disorder that shows aberrant TGFβ signalling (Bowers and Sweeney, personal communication). In addition to synaptic overgrowth spinster has an accumulation of ceroid lipopigment (lipofuscin) in lysosomes throughout the nervous system (Nakano *et al.*, 2001), this is indicative of the generation of ROS, and used as a marker of

oxidative stress and ageing. From this, it is postulated that spinster is suffering from oxidative stress.

1.6.2. Oxidative Stress and Synaptic Function

Components of the molecular machinery involved in synaptic transmission are affected by oxidative stress. Hydrogen peroxide has been shown to have dual action at the frog NMJ depending on the concentration. At micromolar concentrations H_2O_2, EPPs were increased but at higher concentrations EPPs were inhibited. The facilitation seen at lower concentrations was not affected by the presence of Fe^{2+}, a pro-oxidant species, conversely the presence of increased of Fe^{2+} did increase the inhibition of transmission caused at higher concentrations, this is indicative of the involvement of hydroxyl radicals in this inhibition (Giniatullin and Giniatullin, 2003). Both evoked and spontaneous quantal release are reduced through the reactions between ROS and SNAP25, a component of the SNARE complex required for membrane fusion (Giniatullin *et al.*, 2006). During high levels of activity in skeletal muscle ATP and ROS, generated intracellularly, can be released. Extracellular ATP has been shown to cause pre-synaptic inhibition, which can be reduced by the presence of anti-oxidants, such as extracellular catalase. NO was also shown to prevent synaptic transmission however, inhibiting NO production did not prevent ATP-dependent depression, whereas preventing P2 activation reduced ROS production (Giniatullin *et al*., 2005). The role of PKC in the effects of ROS on synaptic transmission has been shown as PKC inhibitors prevent both the facilitation and the depression caused by H_2O_2. Conversely, overactivation of PKC using PMA also prevents the facilitation but has no effect on the depression (Giniatullin and Giniatullin, 2003).

LTP is purported to be the biological correlate of learning and memory and it is a form of synaptic plasticity that is defined as ‘long-lasting increase in the efficacy of synaptic transmission’ (Bliss and Lomo, 1973). ROS are becoming increasingly seen as important signalling molecules in many biological

processes, with an important function in central synapses in the generation of LTP (Klann, 1998; Klann *et al.*, 1998). The general principle of both hippocampal and spinal cord LTP are similar, repeated activity leads to increased responsiveness dependant on NMDA receptors. Application of ROS induces LTP and while NMDA receptor activity is required for the induction but not the maintenance of LTP, depleting ROS through the application of ROS scavengers inhibited both the induction and maintenance of LTP. These data suggest that high frequency stimulation of neurons leads to NMDA receptor activation resulting in increases in endogenous ROS (Lee *et al.*, 2010a). Activation of NMDA receptors results in generation of superoxide anions (Bindokas *et al.*, 1996) furthermore, LTP is blocked by superoxide scavengers (Klann *et al.*, 1998). The effector of superoxide in LTP is most likely PKC, which is activated due to oxidation of a cysteine rich area, a cofactor binding area of PKC; oxidation causes zinc to be released from the zinc finger domain (Knapp and Klann, 2002), furthermore the presence of superoxide scavengers that prevent LTP accordingly prevent superoxide induced rises in PKC activity. Increasing the level of superoxide anions by the X/XO system in hippocampal slices increases PKC activity (Knapp and Klann, 2000). Superoxide induced LTP, although still dependent on increased [Ca^{2+}], does not require Ca^{2+} influx through NMDA-Rs, superoxide anions activate type 3 ryanodine receptors and L-type Ca2+ channels. ERK signalling is also required for superoxide induced LTP (Huddleston *et al.*, 2008).

Conversely H_2O_2 prevents normal LTP (Pellmar *et al.*, 1991; Auerbach and Segal 1997), the reduction in LTP caused by SOD (Halliwell *et al.*, 1992b) may be due to the increased levels of H2O2, as this reduction is partially rescued by catalase, which converts H_2O_2 to water and oxygen (Knapp and Klann, 2002). Thus it seems the relative balance and localisation of action of different ROS may be the key to understanding the role of ROS in LTP. The effects of ROS on synaptic transmission are varied suggesting a high level of context dependence,

determining the signalling pathways and effectors involved. The *Drosophila* NMJ, as a glutamatergic synapse, could be highly useful to elucidate the effects of ROS on synaptic transmission and how pathogenic activation of signalling pathways involved in the control of synaptic development and function, such as JNK/AP-1 can be affected during oxidative stress. This could help to understand both developmental and neurodegenerative conditions.

1.7. Aims

- To establish whether *spinster* is incurring oxidative stress and determine whether oxidative stress is contributing to the synaptic overgrowth phenotype.
- Can oxidative stress cause synaptic overgrowth independently of lysosomal dysfunction?
- Are ASK/JNK/AP-1 activation and autophagy required for synaptic growth observed under conditions of oxidative stress?
- Oxidative stress is known to impair mitochondrial function. Does oxidative stress/ *spinster* cause an energy deficit resulting in impaired physiological output? If this is the case, are compensatory metabolic pathways induced in spinster?

2. Materials and Methods

2.1. *Drosophila* Husbandry and Techniques

2.1.1. *Drosophila* Stocks

Drosophila stocks used in this research were obtained from the Bloomington Stock Centre (Indiana University: http://flystocks.bio), donated from other labs or created using stocks already contained within the lab. A full list of stocks used in this investigation is shown in table 2.1.

2.1.2. *Drosophila* Husbandry

Drosophila were maintained in 25cm^3 plastic vials containing 7-8ml standard yeast-sugar-agar media composed of 25g/l sugar, 3.75g/l agar, 0.125 $CaCl_2$, 0.125g/l $FeSO_4$, 0.125g/l MnCl, 0.125g/l NaCl 2g/l potassium-sodium tatrate, 0.0015g/l Bavistine and 0.2g/l p-hydroxybenzoic acid methyl ester (Nipagin) (Carpenter, 1950). Apple juice agar plates (16g/l agar, 40g/l sucrose and 200ml apple juice per litre) were used for egg collection, using a cage, and moved from this to instant fly food using forceps. Formula 4-24 (Carolina Biological Supplies) instant fly food was prepared by mixing equal volumes of fly food and water (containing any pharmacological agents as required) with a pinch of yeast per vial. Vials were topped with cotton wool to allow air-flow and prevent escape.

Stocks were maintained at 18^{0}C, where they were 'turned over' into new vials every 4 weeks, or at 25^{0}C, where they are turned over every week. Flies at 25^{0}C used for experimental crosses to obtain larvae were turned over every 2-3 days to increase the number of progeny and prevent overcrowding of larvae. To allow selection of flies they were anaesthetised with CO_2 via a porous pad connected to a compressed gas cylinder (Dutscher Scientific, UK) and using a dissection microscope (Zeiss Stemi 2000 Dissection Microscope).

STOCK	Chromosome	Description	Source
WILDTYPE			
w^{-1118}	N/A	Wildtype (white eyes)	Sweeney lab stock
Canton S	N/A	Wildtype (red eyes)	Sweeney lab stock
BALANCER STOCKS			
FM6-GFP/-	First	First Chromosome Balancer	Sweeney lab stock
CyOGFP/Sco	Second	Second Chromosome Balancer	Sweeney lab stock
CyOGFP/If; TM6b/MKRS	Second and third	Second and Third Chromosome Balancer	Sweeney lab stock
CyOtubGAL80/If; TM6b/MKRS	Second and third	Second and Third Chromosome Balancer with GAL80	Sweeney lab stock (unpublished)
GAL4 DRIVERS			
*spin*GAL4/TM6b	Third	Spinster promoter: Pre- and post-synaptic driver (low level ubiquitous)	Nakano *et al.* (2001)
*MHC*GAL4/TM6b	Third	Myosin heavy chain promoter: Muscle specific driver	Corey Goodman lab stock (donation)
*elav*GAL4/TM6b	Third	Embryonic lethal abnormal vision promoter: Pan neuronal driver	Corey Goodman lab stock (donation)
*tub*GAL4/TM6b	Third	Tubulin promoter: Global driver	Lee and Luo (2001)

UAS STOCKS

UAS-*fos*	Second	Wildtype Fos	Bloomington Stock Centre
UAS-*fos-RNAi*/TM6b	Third	RNAi to reduce Fos expression	Vienna *Drosophila* Resource Centre
UAS-fos^{DN}	Second and Third	Impaired transcription activity	Eresh *et al.* (1997)
UAS-jun^{DN}	Second and Third	Impaired transcription activity	Eresh *et al.* (1997)
UAS-*jun*RNAi/FM6-GFP	First	RNAi to reduce Jun expression	Vienna *Drosophila* Resource Centre
UAS-jnk^{DN}	Second and Third	JNK without kinase activity (K53R)	Weber *et al.* (2000)
UAS-ask^{DN}	Second	ASK without kinase activity	Kuranaga *et al.* (2002)
UAS-$AMPK^{T184D}$	Third	Pseudo-phosphorylated AMPK	Jay Brennan
UAS-*AMPK-RNAi(1827)*	Third	RNAi to reduce AMPK subunit-α expression	Vienna *Drosophila* Resource Centre
UAS-*AMPK-RNAi(106200)*	Third	RNAi to reduce AMPK subunit-α expression	Vienna *Drosophila* Resource Centre
UAS-*hSOD1*	Second	Human SOD1	Parkes *et al.* (1998)
UAS-*cat*	Second	Wildtype Catalase	Missirlis *et al.,* (2001)
UAS-$trxR1^{CYTO}$	Third	Wildtype cytoplasmic thioredoxin reductase	Missirlis *et al.,* (2002)

UAS-*trxR1*^{MITO}	Third	Wildtype mitochondrial thioredoxin reductase	Fannis Missirlis
UAS-*gst*^{81A}	Second	Wildtype glutathione	Whitworth *et al.* (2005)
UAS-*atg1*^{68}	Third	Wildtype ATG1	Neufeld
UAS-*atg1*^{CG}	Third	Wildtype ATG1	Neufeld
UAS-*atg5-RNAi*	First	RNAi to reduce atg5 expression	Vienna *Drosophila* Resource Centre
UAS-*spin*	Third	Wildtype spinster	Sweeney lab stock
MUTANT STOCKS			
spin^{4}/CyOGFP	Second	Loss of function of spinster due to P-element excision	Nakano *et al.* (2001)
spin^{5}/CyOGFP	Second	Loss of function of spinster due to P-element excision	Nakano *et al.* (2001)
spin$^{\Delta 58}$/CyOGFP	Second	Loss of function of spinster	Bloomington Stock Centre
sod1^{n1}/TM6b	Third	Loss of function of sod1 EMS point mutation	Parkes *et al.* (1998)
sod1^{n64}/TM6b	Third	Loss of function of sod1 EMS point mutation	Parkes *et al.* (1998)
sod2^{DELTA}/CyOGFP	Second	Loss of function of sod2 due to P element	Zheng *et al.* (2009)
sod2$^{\Delta 02}$/CyOGFP	Second	Loss of function of sod2 due to P element	Zheng *et al.* (2009)

sdhB^{EY}/CyOGFP	Second	Loss of function of succinate dehydrogenase B (P element insertion)	Walker *et al.* (2006) Bellen *et al.* (2004)
sesB^{9ED1}/FM7GFP	First	Stress sensitive B loss of function (mitochondrial nucleotide transporter) EMS point mutation	Janca *et al.* (1986)
cat^{1}/TM6b	Third	Catalase loss of function EMS point mutation	Mackay *et al.* (1989)
atg1^{DG}/TM6b	Third	*atg1*$^{[DG23110]}$ ATG1 loss of function (P-element)	Bloomington Stock Centre
atg1^{PZ}/TM6b	Third	*atg1*$^{[00305]}$ ATG1 loss of function (P-element)	Bloomington Stock Centre
atg18^{KG}/TM6b	Third	*atg18*$^{[KG03090]}$ ATG18 loss of function (P-element)	Bloomington Stock Centre
puc^{E69}/TM6b	Third	puckered LACZ reporter as heterozygote (P-element)	Ring and Martinez Arias (1993)
loe/TM6b	Third	Loss of one isoform of AMPK γ subunit function unit	Deak *et al.* (1997)
OTHER TRANSGENES			
gst-D-GFP/CyOGFP	Second	GFP reporter of glutathione expression using cap'n'collar (Nrf2/KeAP-1) transcription factor	Skyotis and Bohmann (2008)

Table 2.1: *Drosophila* stocks used in this investigation

2.1.3. Crossing Schemes

2.1.3.1. Crosses

Crosses were set up by combining virgin females and males of the required genotypes, in the same vial. Virgin females were selected based on the well-regarded observation that females reject courtship for the first 8 hours after eclosion. Young female flies were selected in two ways: firstly, for two hours following eclosion the meconium can be seen through the abdominal cuticle, as well as being light in pigment and still having unexpanded wings; secondly, once a vial was emptied of adults, 8 hours later any females collected will be virgins. Once probable virgins were collected they were kept isolated from males and their virginity confirmed by observing that any eggs they laid did not hatch.

2.1.3.2. Balancer Chromosomes

Mutant alleles in *Drosophila* can be easily tracked through the use of balancer chromosomes. These are chromosomes that carry dominant phenotypic markers with large chromosomal insertions that prevent recombination. The balancer stocks used in this investigation were *FM6*, on the first chromosome (with or without GFP), which presents a bar eye phenotype; *CyO* (with or without GFP) on the 2nd chromosome which has curly wings; *TM6b* on the 3rd chromosome which has 'humoral' as its dominant marker in adults, which can be seen as increased hairs on the 'shoulders' of the adult and 'tubby' in larvae, a significantly shortened and fattened and *TM3* on the 3rd, identified by 'stubble', a shortening of the hairs on the thorax. When expressed in the same animal *TM3* and *TM6b* (*TM3*/*TM6b*) show the 'ebony' phenotype, a blackening of the whole fly. Markers are also used when double balancing *Drosophila* stocks, *Sco* on

the second, which can be identified by a lack of hair on the scutellum and *MKRS* on the third, which also shows stubble.

2.1.3.3. Recombination

To obtain a fly with two required genetic components on the same chromosome were created by allowing recombination to occur in the female. This was achieved by mating the parent stocks with each other and selecting the females that carried both genetic components. These were then crossed to the balancer stock for the relevant chromosome, and potential recombinants selected based on eye colour when possible. The presence of each mutation or transgene was then confirmed by PCR when necessary.

2.2. Immunohistochemistry and Imaging

2.2.1. Third Instar Larval Dissection

Wandering 3rd instar larvae were taken, once they had crawled out of the food and up the side of the vial, and selected based on genotype. The required larvae were transferred to a Sylgard dish (Silicone elastromere kit, Dow Corning), and dissected in either PBS or haemolymph-like buffer (HL3: (70mM NaCl,5mM KCl, 1mM CaCl2.2H2O, 10mM NaHCO3, 5mM trehalose, 115mM sucrose and 5mM BES)) (Stewart et al., 1994). The anterior and posterior ends of the larvae were pinned down with minuten pins (Austerlitz Insect Pins 0.1mm diameter, Fine Science Tools), scissors were used to cut laterally at the posterior and dorsal end of the larvae, and a cut made up the dorsal side. The gut, fat bodies, salivary glands and internal organs were removed using forceps, and the muscle wall pinned back.

2.2.2. Larval Fixation and Immunohistochemistry

Larvae were fixed either for 7 minutes in 3.7% formaldehyde in PBS, or 2 minutes in Bouin's solution, the pins removed and the larvae transferred to 1.5ml

eppendorf tubes and washed 3 times in PBS-T (0.1% Triton X-100 in PBS). Antibody incubations were carried out in the desired concentration in of antibody, see table 2.2.2.2 in PBS-T, at 4^0C overnight on a rocker, or for two hours at room temperature. 3 x 5 minute washes were performed at room temperature before application of the secondary antibody, for 1 hour at room temperature, before washing 3 times for 5 minutes. Preparations were then transferred to 70% glycerol in PBS to eradicate air from the larval preparations. Following 2 hours in this solution the larvae were mounted onto microscope slides in Vectashield (Vector Laboratories). Coverslips were placed on top of the preparations and sealed with nail varnish.

ANTIBODY	STAINS	CONC	HOST SPECIES	SOURCE
Anti-Horseradish-peroxidase-Cy3 (HRP-Cy3)	Neuronal Tissue	1:200	Goat	Jackson Laboratories
Anti-synaptotagmin (Anti-SYT)	Synaptic Boutons	1:1000	Rabbit	Sweeney Lab
Anti-Bruchpilot	Active Zones	1:50	Mouse	Developmental Studies Hybridoma Bank (DSHB), Iowa, US

Table 2.2: Antibodies used in this investigation.

2.2.3. Microscopy and Analysis

2.2.3.1. Bouton Counts Normalisation to Muscle Surface Area, and Imaging

Bouton number was analysed by counting each singular spherical structure stained with anti-synaptotagmin at the NMJ, using a Leica DMLA fluorescence microscope with a 40x objective lens. Muscle surface area (MSA) was calculated by imaging hemisegment A3 with a 10x objective, in phase mode and a Leica DC500 digital camera. Images were analysed using 'imageJ', by measuring the length and width of the muscle in pixels. This measurement was then converted to μm using an image taken of a haemocytometer to measure the number of pixels in 1μm. The mean muscle surface area of wildtype was then used for normalisation; the bouton number being normalised was divided by its MSA and multiplied by the mean wildtype MSA. This in effect gives the number of boutons at the NMJ if it were a wildtype size (Lnenicka and Keshishian, 2000; Schuster *et al.*, 1996a).

NMJs were imaged using a Zeiss Axioplan 2 confocal microscope (Technology Facility, Biology Department, The University of York); taking z-stacks using 63x objective (oil immersion lens). Generally, two z-stacks were needed due to the size of the NMJ, these were merged using Adobe Photoshop (Adode Systems Uxbridge, UK)

2.2.3.2. Bouton size analysis

Confocal images were taken as described in 2.2.3.1 and opened in imageJ and measured across the widest part. The measurement was converted from pixels to μm by multiplying by the number of pixels in a μm.

2.2.3.3. Analysis of GFP Transgene Expression (Confocal)

Adult flies were dipped briefly in ethanol to reduce surface tension, and pinned dorsal side down through the abdomen. Dissections were performed in 4% paraformaldehyde/PBS and incubated in this solution with primary antibodies

overnight in the dark, washed for 3 hours then incubated in secondary antibody overnight, and mounted in Vectashield.

2.3. Adult Head Sectioning and Electron Microscopy

2.3.1. Embedding of *Drosophila* Adult Heads in Spurr's Resin

Flies were submerged in 30% EtOH to reduce surface tension and transferred to fixative (4%PFA, 1% gluteraldehyde in 0.1M sodium phosphate buffer, pH 7.4). The proboscis and air sacs were removed as much as possible and the dissected heads transferred to glass vials containing the fixative. The remaining air sacs and cuticle were removed as much as possible by applying vacuum pressure to the vials. The preparations were transferred to 1.5ml eppendorf tubes containing 500μl fresh fixative. Submersion of the preparations was ensured by trapping them in the bottom of the tube; using a slimline cigarette filter tip (Swan) held in position with a 0.2ml PCR tube with the bottom cut off. Preparations were incubated in fixative overnight at 4^0C on a 360^0 rotator. 3x 10 minute washes with 0.1M sodium phosphate buffer were performed to remove excess fixative from the preparations. Preparations were incubated in 250μl 1% osmium tetroxide (OsO_4) on 0.1M sodium phosphate buffer for 1 hour, and washed 3x 10 minutes in 0.1M sodium phosphate buffer and 3x 10 minute washes in distilled water. Incubations in increasing concentrations of acetone (30, 50, 70 and 90%) for 20 minutes each and 3 x 30 minute incubations in 100% acetone (dehydrated using a molecular sieve) were performed to dehydrate the preparations. The preparations were incubated in increasing concentrations of Spurr's resin in acetone; 25, 50, 75, 90 and 3x 100% resin for 45 minutes with rotation (Spurr, 1969; 5g vinylcyclohexene dioxide, 3g diglycidyl ether of polypropylene glycol, 13g nonenyl succinic anhydride, 0.25ml 2-dimethylaminoethanol. Incubations in 100% resin were performed at 37^0C to reduce viscosity. The head preparations were embedded in moulds (Silastic J Kit, Dow, USA) half-filled with resin, semi-polymerised by incubation at 70^0C for

3.5-4 hours. Heads were orientated as required (dorsal end against one end of the well) and covered with unpolymerised resin to fill the well, and polymerisation completed by incubation at 70^0C for 24 hours. Resin blocks were left to cool and removed from the moulds once cooled.

2.3.2. Head Sectioning

Blocks were trimmed to near the preparation using a fine-bladed hacksaw. Blocks were then secured in chuck and trimmed using a razor blade to expose the cuticle. The block was then trimmed around the head to reduce cutting area, leaving a truncated pyramid containing the head. 1μm sections were cut on the microtome (Leica Ultracut UCT) using glass knives. Sections were placed on microscope slides in drops of water, dried on a hot plate at 80^0C and stained (0.6 toluidine blue in 0.3% sodium carbonate) for ~5seconds, rinsed in distilled water and dried. Sections were imaged using Zeiss Axiocam HRm camera and Zeiss Axiovert 200 microscope to locate regions to section for TEM.

2.3.3. Transmission Electron Microscopy (TEM) and Image Analysis

Once the area to investigate using EM was reached in thick sections, thin sections (60-70nm) were made (carried out by Meg Stark, Technology Facility, York). Sections were incubated in uranyl acetate in 50% ethanol in 10 minutes and then submerged in distilled water. Sections were stained for 10 minutes in lead citrate with sodium hydroxide pellets, and then washed in distilled water. Images were taken using a TECNAI G^2 (version 2.18) TEM (120kV) using analySIS software.

2.4. Molecular Biology

2.4.1. Polymerase Chain Reaction (PCR) and DNA Agarose Gel Electrophoresis

2x PCR mastermix (Promega, UK) was used in a 20μl reaction volume containing (final concentrations) 1μM primers and <250ng DNA template. Primers were either designed manually or using Primer Designer, Net Primer. The melting temperature (T_m) calculated using NetPrimer or Primer3 software or {4(N^o Guanine and Cytosine)+2(N^o of Adenine and Thymine)}. The elongation time for a particular fragment is calculated based on the knowledge that *taq* polymerase produced 1kb DNA a minute. Standard PCR cycling conditions were: initial denaturation at 94^0C for 10 minutes; cycles of 94^0C for 30secs, T_m for 60secs, 72^0C for elongation; cycles were followed with a final elongation period at 72^0C for 5 minutes. Reactions were then cooled to 4^0C to prevent DNA decomposition. Analysis of PCR products was analysed using agarose gel electrophoresis. Appropriate volumes of PCR product and 6x loading dye (Promega, UK) were mixed and loaded onto a 1% agarose gel in TAE buffer (Tris-Acetate and 0.05M EDTA) with 0.1% SyberSafe and leaving to polymerise in the gel tank, once polymerised the gel is submerged in TAE. 1kb or 100kb ladder (Invitrogen or Promega) was also loaded onto the gel to allow determination of the size of the PCR product. The gel was run for 45 minutes at a potential difference of 100v. For visualisation of DNA the gel was transferred to a blue-light box and imaged.

Oligos:
SOD1_F:catcccgtccacagagc
SOD1_R:ggtgcgtccgatgatgct
GAL4_F:gcagcgtaccacaacaggtccc
GAL4_R:ggcgtgactgagcgatgcga

2.4.2. Genomic DNA extraction

Single flies were ruptured in squishing buffer (10mM Tris pH 8.2, 1mM EDTA, 25mM NaCl, 200μg/ml proteinase K) using a pipette tip, and incubated at 37^0C for 1 hour, followed by a 2 minute incubation at 95^0C. The preparation can be stored at -20^0C until needed, when 1μl is used as DNA template for PCR.

2.4.3. Gel Extraction

DNA extraction from excised gel bands were carried out using QIAquick gel extraction kit (Qiagen) according to the manufacturer's protocol. The gel fragment was dissolved in 3x volume of buffer QG (100mg gel ≅ 100μl buffer) at 50^0C, 1 volume of isopropanal added and transferred to QIAquick spin column and centrifuged for 1 minute at 13000*g* to bind the DNA to the column. To remove the excess agarose the column was washed with 500μl buffer QG and then with 750μl buffer PE to remove salts. Residual ethanol was removed by centrifugation and the DNA eluted with 30μl nucleotide free water. DNA concentration and quality was determined with an ND-1000 spectrophotometer (NanoDrop; Thermo Scientific, DE, USA).

2.4.4. DNA Sequencing

DNA sequencing was used to confirm the presence of mutations in potential recombinants. The area including the mutation was amplified using PCR and the product purified through gel extraction. Sequencing reactions were sent to Technology Facility, University of York. 3-10ng/μl of PCR product and 3.2μM primer were required. Sequencing results were analysed using Chromas (Version 1.45, Conor McCarthy, Australia) and NCBI bl2seq software.

2.5. Biochemical Analysis

2.5.1. Bradford Assay

Protein concentration was determined by measuring absorbance at 595nm in the presence of Bradford reagent which contains Coomassie; this changes absorbance upon its binding with protein. 30μl protein solution was added to 900μl Bradford reagent (Sigma), left for 15 minutes and the absorbance recorded.

2.5.2. Quantification of Oxidative Stress

2.5.2.1. Lipid Peroxidation Assay

Levels of peroxidated lipids were analysed using Bioxytech LPO-586 (OxisResearch, Oxis International, California, USA) according to the manufacturer's instructions. Standards were made up of 0-20μM 1,1,3,3-tetramethoxypropane (TMOP), which is hydrolysed in the assay to produce standards of 0-4μM malondialdehyde (MDA) (final concentration). 30 flies of each genotype were ruptured/ homogenised (on ice) in 750μl 5mM butylated hydroxytoluene in 20mM PBS pH 7.4 and centrifuged at 3000*g* for 10 minutes at 4^0C, using 3x 200μl aliquots of the supernatant for the assay. A Bradford assay was carried out to ensure equal protein concentrations. 650μl diluted reagent R1 (N-methyl-2-phenylindole in acetonitrile diluted with ferric iron in methanol) was added to each tube including the standards and vortexed. 150μl reagent R2 (methanesulphonic acid) was added and the preparations incubated to 45^0C for 60 minutes. The samples were centrifuged (15000*g* for 10 minutes) and the supernatant absorbance measured at 586nm.

2.5.2.2. Quantification of *gst-D-GFP* Expression (Fluorimetry)

10 flies of each genotype were ruptured/ homogenised in 100μl lysis buffer (150mM NaCl, 20mM Tris-HCl pH8.0, 2mM EDTA, 0.5% (v/v) Igepal and 1 mini

protease inhibitor cocktail tablet (Roche)). Preparations were incubated on ice for 20 minutes, centrifuged at 13000*g* for 10 minutes, the supernatant transferred into a new tube and centrifuged again for 10 minutes at 13000*g*. The supernatant was removed, 300μl PBS added and the fluorescence quantified by measuring emission at 490-600nm (following excitation at 480nm) using a Fluoromax4 (Horiba Scientific) and the accompanying software Fluorescence V3.

2.6. Physiological Analysis of Larvae

2.6.1. Crawling Speed Analysis

Larvae were selected based on genotype and transferred to HL3 saline. Larvae were transferred, using a paintbrush, to 90mm diameter petri-dishes containing agar, and left to recover on the agar plate until they started to move. Larvae were recorded for 45s (CAMERA and VirtualDub). The videos were decompressed, and analysed using ImageJ. The speed of each larval recording was calculated using median and thresh track plug-ins for ImageJ, to give the x and y changes in the video, this was then converted to a larval speed based using Excel (based on the fact that 226 frames were recorded in 45 seconds and using conversion of pixels:mm).

2.6.2. Intramuscular Recordings

Larvae were dissected in HL3 solution as described in section 2.2.1, except only the middle of the ventral sides are pulled out, using one pin in each side (rather than 2 which facilitates imaging). Glass electrodes were pulled from 1mm borsosilicate glass to form a sharp pipette (resistance 10-20mOhms) (Flaming Brown micropipette puller model P-97, Sutter Instrument Co) with the following settings: P=200, heat=240-260, pull=100, vel=100, time=132. Electrodes were loaded with 3M Potassium Acetate, and the recording taken from muscle 6/7 in hemisegment in A3. Recordings were taken in DasyLab and the resting

membrane potential calculated by subtracting the initial recording before entry into the muscle and post entry to the muscle. Mean EJPs were calculated by overlaying 5-6 EJPs and taking the mean values for each animal.

3. Oxidative Stress Contributes to Synaptic Overgrowth in *spinster*, a Model of a Lysosomal Storage Disorder

3.1. Introduction

Oxidative stress, as discussed earlier is caused by an imbalance between the generation and dissipation of ROS. There is a high correlation between oxidative stress and neurodegeneration; oxidative stress is believed to be partially causative to neurodegeneration and is also a consequence of neurodegenerative disease processes (Patten *et al*., 2010).

Lysosomal storage disorders, as described earlier (1.3.1) are a group of 40-50 metabolic disorders caused by impaired turnover of cellular constituents, as a result of lysosomal dysfunction. Most LSDs have a neurodegenerative component amongst many other cellular and multi-systemic symptoms. However, it is unclear how lysosomal dysfunction leads to neurodegeneration but lysosomal storage disorders have recently been shown to exhibit markers of oxidative stress (Deganuto *et al.*, 2007; Fu *et al.*, 2010; Wei *et al.*, 2008a; Filippon *et al.*, 2011).

Firstly oxidative stress has been implicated in Niemann Pick type C, an autosomal recessive LSD caused by abnormal function of NPC1 or 2, which leads to the build up of unesterifed cholesterol and glycosphingolipids (Zampieri *et al.*, 2009; Fu *et al.*, 2010). Secondly, Gaucher's disease (Deganuto *et al.*, 2007), one of the most common LSDs, which is caused by a build up of glucocerebroside, due to defective glucocerebrosidase, has an oxidative component. Fibroblasts from patients with Gaucher's disease have impaired redox status and are sensitive to oxidative stress as they are unable to mount an appropriate response to oxidative insults. Thirdly, oxidative stress has been

implicated in juvenile neuronal ceroid lipofuscinosis (JNCL). Mutations in *CLN3*, the gene known to cause JNCL, result in hypersensitivity to oxidative stress and the protein has been shown to interact with stress signalling pathways (Tuxworth *et al.*, 2011).

In addition LSDs have been shown to cause ectopic synaptic growth (Purpura and Suzuki 1976; Walkley *et al.*, 1985 and 1988a and b). Swainsonine is a plant-derived product that inhibits alpha-mannosidase, a lysosomal hydrolase, and can be used to model mannosidase disorders, a type of LSD (Dorling *et al.*, 1980, Hartley *et al.*, 1971). This model was shown to cause ectopic axon Hillock neurite outgrowth in the cortical pyramidal and multipolar cells of the amygdala in cats (*Walkley et al.*, 1985 and 1988a and b). However, it is not known whether this ectopic growth is caused by a direct effect of lysosomal dysfunction or due to downstream signalling of the oxidative stress generated by lysosomal dysfunction.

Spinster is a protein with 12 transmembrane domains that localises to the lysosome and shows high homology to sugar transporters. Mutations in *spinster* provide a good model of a lysosomal storage disorder, with increased numbers of enlarged endosomal/lysosomal compartments, coupled with neurodegeneration and synaptic overgrowth (Nakano *et al.*, 2001; Dermaut *et al.*, 2005; Sweeney and Davis, 2002). Mutations in *spinster* have previously shown to cause 100% overgrowth of the neuromuscular junction (Sweeney and Davies, 2002). However, the presence of increased reactive oxygen species/ oxidative stress has not been determined, nor the relationship between oxidative stress and synaptic overgrowth.

Here, increased levels of oxidative cellular damage and activation of the cellular stress response are identified in *spinster*. In addition, it is shown that relieving oxidative stress, through the expression of anti-oxidant transgenes, partially rescues the level of synaptic overgrowth. Moreover, another overgrowth

phenotype, *highwire*, is rescued by expression of antioxidants suggesting that the relationship between oxidative stress and synaptic overgrowth is causative not just correlative.

3.2. Results

3.2.1. *spin* carries an oxidative stress burden

Increased levels of reactive oxygen species lead to a number of forms of oxidative damage. One of the most common markers of oxidative stress is increased levels of peroxidated lipids. This can be determined by measuring the levels of certain aldehydes, such as malondialdehyde (MDA), that are the end products of lipid peroxidation. The *spinster* mutants previously indentified as having synaptic overgrowth (Sweeney and Davies, 2002) are transheterozygotes (the allelic combination $spin^{4}/spin^{5}$) that rarely survive to adulthood. Consequently for analysis of lipid peroxidation levels, where a large number of flies are needed, transheterozygotes of $spin^{\Delta 58}/spin^{4}$ and $spin^{\Delta 58}/spin^{5}$ were used, an allelic combination that survives regularly to adulthood, but with a shortened lifespan (Nakano *et al.*, 2001; Dermaut *et al.*, 2005). In *spinster* mutants the level of peroxidated lipid end product is increased by 83% compared to wildtype ($p<0.001$, ANOVA) (Fig. 3.1) whereas the level of peroxidated lipids is significantly reduced by expression of the human form of superoxide dismutase (UAS*hSOD1*), the enzyme that converts highly reactive superoxide anions to hydrogen peroxide, under the control of *spin*GAL4 ($p<0.001$, ANOVA). This suggests that *spinster* mutants incur increased levels of oxidative damage that are reduced by increasing the level of anti-oxidant defence. Expression of this transgene in a non-mutant background did not change the levels of peroxidated lipids, suggesting that any increase in

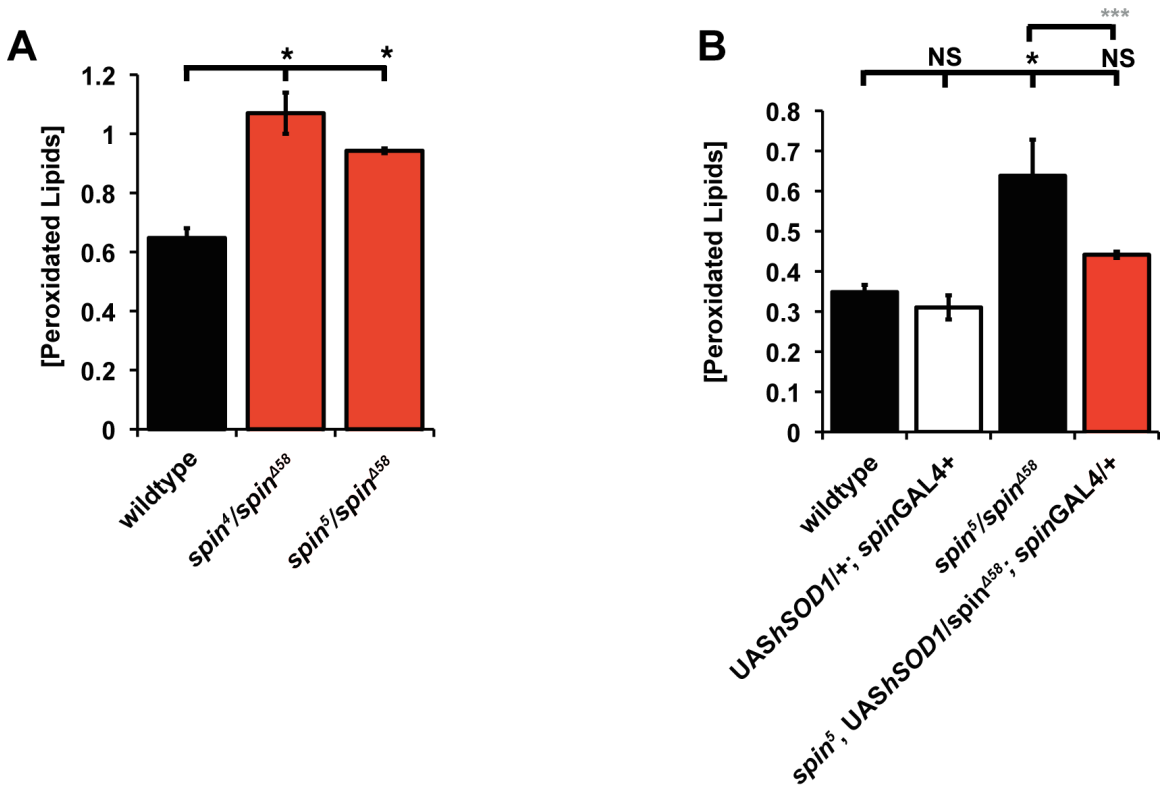

Figure 3.1 *spinster* mutants have increased levels of peroxidated lipids. This is reduced by expressing an antioxidant transgene. (A) Two different spinster mutant combinations both have significantly increased levels of peroxidated lipids compared to wildtype flies. Levels are increased from 0.65±0.033μM TMOP to 1.1±0.07μM and 0.94±0.01μM TMOP in *spin*^{4}*/spin*In $^{\Delta 58}$ and *spin*^{5}*/spin*$^{\Delta 58}$ respectively ($p<0.05$, ANOVA). (B) Wildtype flies show a mean level of MDA equivalent to 0.34±0.02μM TMOP. In *spinster* mutants (*spin*^{5}*/spin*$^{\Delta 58}$) the level of peroxidated lipid end product increases by 83% to 0.64±0.1μM ($p<0.05$, ANOVA). Expression of UAS*hSOD1* under the control of *spin*GAL4 reduces the level of peroxidated lipids to 0.44±0.01μM significantly reduced compared to *spinster* ($p<0.001$, Student's *t*-test). It is no longer statistically different to wildtype ($p>0.05$, Student's *t*-test and ANOVA). Expression of this transgene in a non-mutant background did not cause any change in the levels of peroxidated lipids compared to wildtype: 0.31±0.03μM TMOP ($p>0.05$, ANOVA and Student's *t*-test).

hydrogen peroxide levels caused by increased SOD1 activity was maintained within normal limits by the actions of other anti-oxidant enzymes, that break down hydrogen peroxide. The level of damage incurred suggests that ROS are increased in *spinster* and cause cellular damage due to insufficient levels of antioxidants to deal with the increased levels of ROS. In addition, augmented

ROS levels activate the cellular stress response, leading to increased transcription of anti-oxidants such as glutathione S-transferase-D (gst-D). Transcription of this gene is regulated by KeAP-1/Nrf2 signalling (Sykiotis and Bohmann, 2008). Nrf2 is a cap'n'collar transcription factor that regulates the transcription of a number of anti-oxidant transgenes such as heme-oxygenase I, peroxiredoxin (Ishii *et al.*, 2000) and glutathione S-transferases (Hayes *et al.*, 2000). Activity of Nrf2 is regulated by KEAP-1, a cytoplasmic actin binding protein that binds Nrf2 and promotes its proteosomal degradation hence preventing translocation to the nucleus to act as a transcription factor (Motohashi and Yamamoto, 2004). ROS and electrophiles stimulate the dissociation of Nrf2 and KeAP-1 allowing Nrf2 to translocate to the nucleus to bind to the anti-oxidant response element (ARE) to promote the transcription of antioxidant stress proteins and detoxifying enzymes. Therefore, upon oxidative stress gstD is upregulated and, by means of a reporter construct *gstD*-GFP, whereby the gstD promoter is fused to a GFP open reading frame, levels of *gst-D*-GFP can be monitored. Hence, when the breakdown of Nrf2 is decreased by reduced activity of KEAP-1, less Nrf2 is broken down and the increased Nrf2 translocates to the nucleus where it binds to the ARE increasing transcription. In this way, it also binds to the promoter fused to GFP and can therefore identify increased activation of the cellular stress response.

Here, fluorimetry and confocal imaging were used to investigate increased transcription of this transgene in *spinster*. Five day old flies were used and the level of GFP analysed. The genotypes tested were *gst-D*-GFP in a wildtype background (*gst-D*-GFP/+), which was compared to *gst-D*-GFP levels in *spinster* ($spin^{5}$, *gst-D*-GFP/ $spin^{\Delta 58}$). The levels of GFP are significantly increased in *spinster* compared to wildtype ($p<0.001$, ANOVA). This was shown by both fluorimetry and confocal microscopy (Fig. 3.2A and B respectively). A different *spinster* mutant combination was also investigated; ($spin^{5}$, *gst-D*-GFP/ $spin^{4}$)

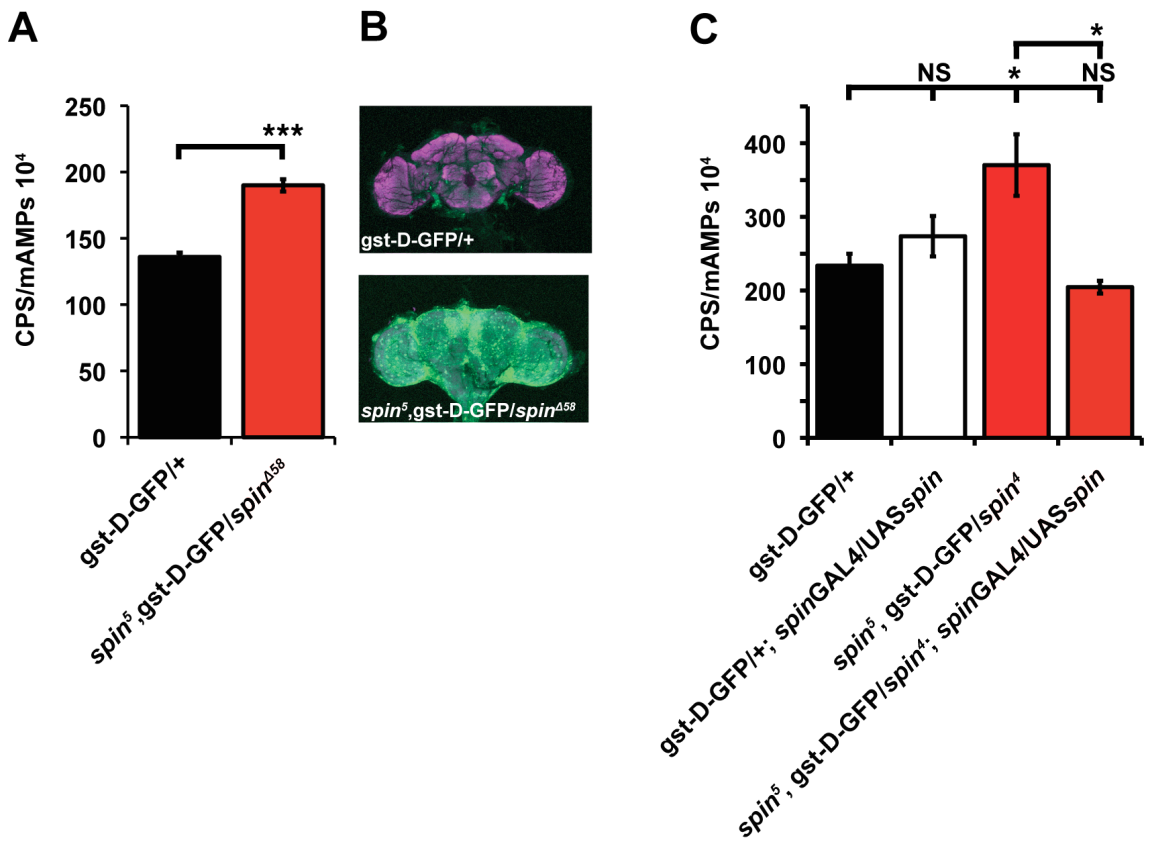

Figure 3.2: The oxidative stress response is activated in *spinster*. (A) *spin* mutants (*spin*^{5}/*spin*$^{\Delta 58}$) have increased levels of gst-D-GFP ($p<0.001$, Student's *t*-test) indicating activation of the stress response. Increased GFP is shown through fluorimetry, the graph shows emission at the peak amplitude of GFP emission, error bars show SEM (n=3). (B) Increased GFP can also be seen in z-stacks of adult heads (neuropil shown in magenta). (C) A different spinster mutant combination *spin*^{4}/*spin*^{5} also caused significant upregulation of gst-D-GFP. Expression of spin under the control of *spin*GAL4 rescues this phenotype.

which is also shown to have significantly increased levels of GFP (Fig. 3.2C). The presence of this phenotype in two different *spinster* genotypes suggests it is caused by *spinster* mutations directly and not by other mutations that have arisen in the *spinster* lines.

To confirm that this phenotype is caused by loss of function in *spinster,* and not by background mutations, expression of a wildtype *spinster* cDNA under the

UAS- mediated control of *spin*GAL4 was used. This completely rescues the increased levels of *gst-D*-GFP in a *spinster* mutant background demonstrating that the increased level of *gst-D*-GFP is in fact caused by loss of *spinster.* Although the level of ROS has not been directly assayed in *spinster*, taken together, the data suggest that ROS are present in *spinster*, since both main facets of oxidative stress have been demonstrated. The presence of increased cellular damage and activation of the cellular stress response demonstrates an imbalance between the generation and breakdown of ROS, indicative of oxidative stress. However this association does not indicate the direction of causation with respect to the phenotypes seen in *spinster*. To test this, the next step is to determine whether relieving oxidative stress rescues the neuromuscular junction phenotypes previously identified in *spinster*.

3.2.2. Neuromuscular junction morphology is perturbed in *spinster*

Mutations in *spinster* cause an increase in bouton number as identified by Sweeney and Davies (2002) indicating a synaptic overgrowth. Some of the mutant allele combinations used in this study were different to those published. It was therefore necessary to confirm that these less severe combinations also cause overgrowth of the neuromuscular junction. Sweeney and Davis used 7 different allelic combinations and all showed a significant overgrowth. Both mutant combinations that are viable through to adulthood show a significant increase in bouton number (Fig. 3.3A). The muscle surface area of the larvae is not significantly affected by these mutations (Fig. 3.3B). Consequently, a similar trend can be seen in bouton number prior to and following normalisation (Fig. 3.3C). The normalisation step is carried out as increases in

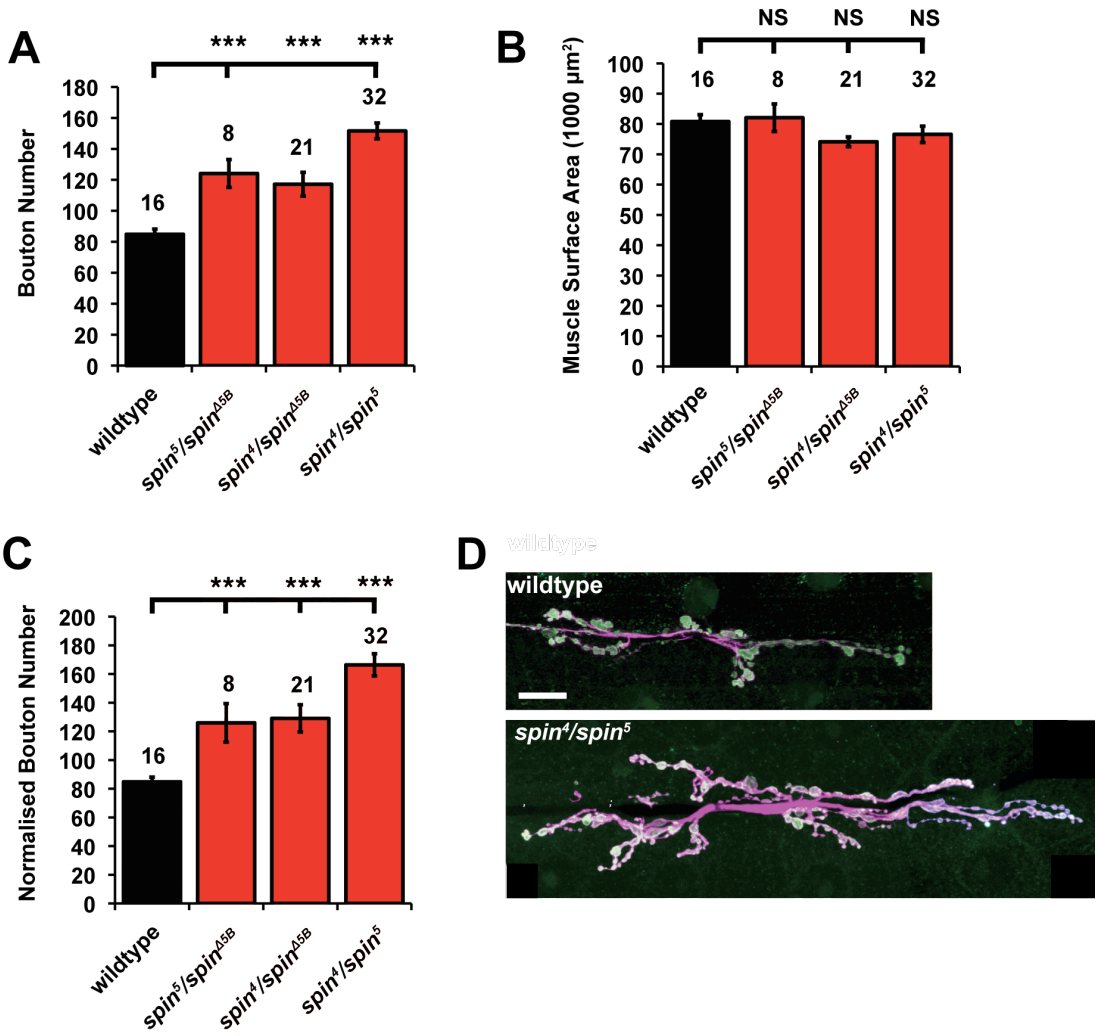

Figure 3.3. *spinster* has increased bouton number with no change in muscle surface area. (A) Bouton numbers are wildtype of 85±3.3 (n=16) to 124±9.0 (n=8), 117±7.7 (n=21) and 152±5.1 (n=32) for the mutant combinations $spin^5/spin^{\Delta 58}$, $spin^4/spin^{\Delta 58}$ and $spin^4/spin^5$ respectively ($p<0.001$; ANOVA). (B) The surface area of muscle 6/7 in segment A3 is 80801±2265µm^2, and in *spinster* mutations it is 82068±4538, 74129±1635 and 76580±2716µm^2 for the combinations $spin^5/spin^{\Delta 58}$, $spin^4/spin^{\Delta 58}$ and $spin^4/spin^5$ respectively ($p>0.05$; ANOVA). (C) When normalised to muscle surface area the bouton number for $spin^5/spin^{\Delta 58}$, $spin^4/spin^{\Delta 58}$ and $spin^4/spin^5$ is 126±13.4, 129±9.5 and 166±7.8 respectively. (D) Representative images of wildtype and *spinster* NMJs at muscle 6/7 segment A3. Nerves shown in magenta through α-HRP staining. Synaptic boutons visualised in green by α-synaptotagmin staining. Scale bar = 20µm.

bouton number during synaptic growth are proportional to muscle surface area (Schuster *et al.*, 1996a). The trend seen is as expected: $spin^4/spin^{\Delta 58}$ and

spin^{5}/*spin*$^{\Delta 58}$ both show increased bouton number compared to wildtype but less of an overgrowth than the more severe mutant combination *spin*^{4}/*spin*^{5}.

The remainder of the analysis of neuromuscular junction analysis was carried out in *spin*^{4}/*spin*^{5}, the most severe overgrowth phenotype and the genotype most extensively described in Sweeney and Davis (2002).

The branch number was also analysed in *spinster* mutants and is significantly increased in *spin*^{4}/*spin*^{5} compared to wildtype ($p<0.001$; ANOVA) (Fig. 3.4A). This is consistent with many other overgrowth phenotypes where branching tends to increase with bouton number showing *spinster* growth is consistent with a normal pattern of growth.

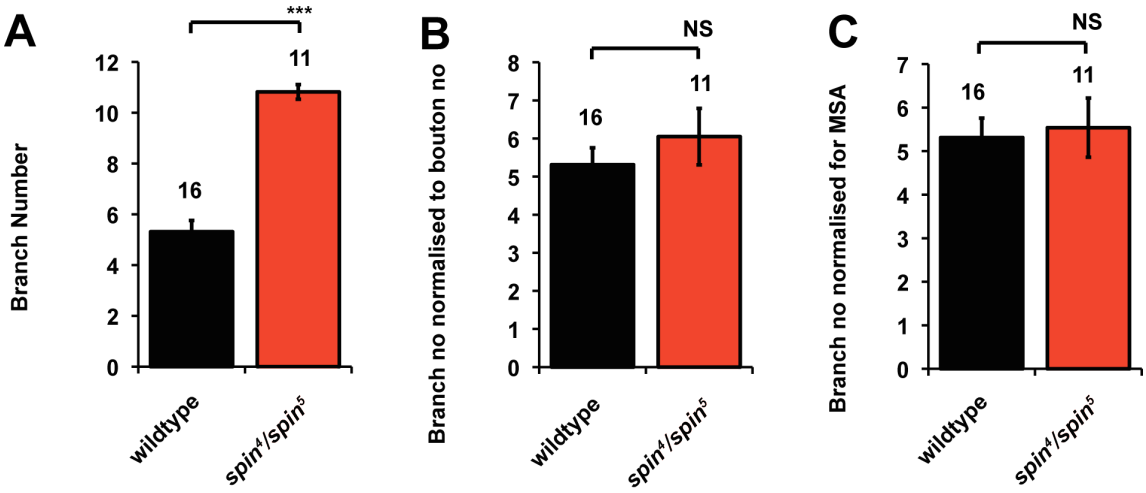

Figure 3.4 *Spinster* mutants have increased branch number proportional to increase in bouton number. (A) Wildtype larvae have a mean branch number of 5.31±0.44 (n=16). This is significantly increased in *spinster* to 10.82±1.33 (n=11; $p<0.001$ Student's *t*-test). (B) When normalised to bouton number there is no significant difference between branch number in wildtype and *spinster*, which has a mean normalised branch number of 6.05±0.74 (n=11; $p>>0.05$ Student's *t*-test). (C) When normalised to account for muscle surface area and bouton number when *spinster* has a mean branch number of 5.54±0.68 (n=11; $p>>0.05$ Student's *t*-test).

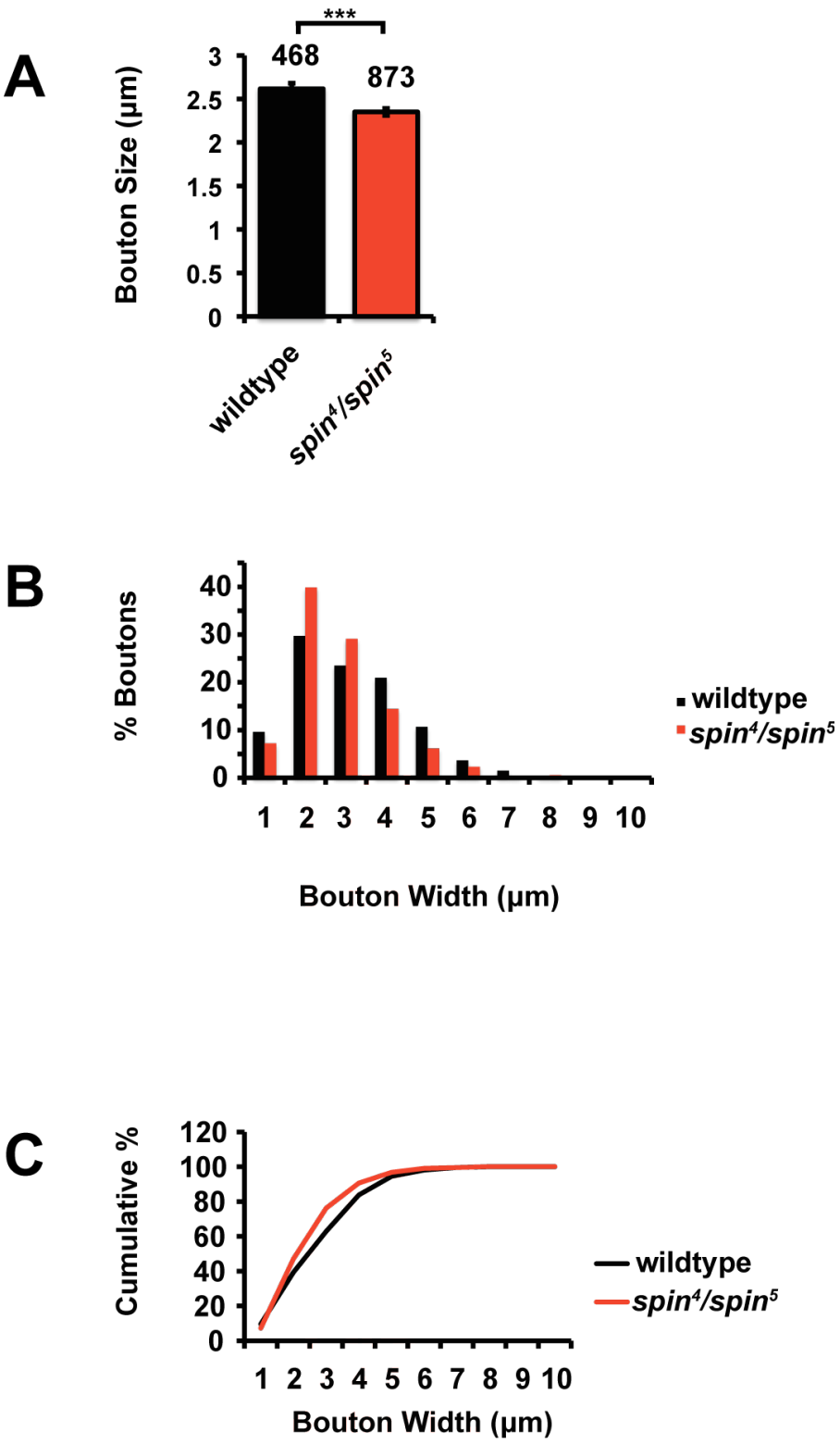
A
***
468
873
Bouton Size (µm)
3
2.5
2
1.5
1
0.5
0
wildtype
spin4/spin5
B
% Boutons
40
30
20
10
0
1 2 3 4 5 6 7 8 9 10
Bouton Width (µm)
wildtype
spin4/spin5
C
Cumulative %
120
100
80
60
40
20
0
1 2 3 4 5 6 7 8 9 10
Bouton Width (µm)
wildtype
spin4/spin5

Figure 3.5 *spinster* has reduced mean bouton width and a greater proportion of smaller boutons. (A) Mean bouton width in wildtype and *spinster* is 2.6±0.06 (n=468) and 2.35±0.04 (n=873) ($p<0.001$, Student's *t*-test) respectively. (B) Bouton size in *spinster* is also displayed as % boutons at each μm width, the distribution of bouton size is significantly different, with *spinster* showing a higher proportion of smaller boutons. ($p<0.001$, Kolmogorov-Smirnov). (C) Cumulative % bouton numbers at each μm width in wildtype and *spinster* showing the difference in distribution.

Branch number increases proportionately with bouton number as when branch number is normalised to wildtype bouton number there is no significant change between *spinster* and wildtype (Fig. 3.4B). As in *spinster* there is no significant change in muscle surface area the same trend is seen when muscle surface area is accounted for (Fig. 3.4C).

During analysis of bouton number in a variety of phenotypes a difference in bouton size was indicated. Another overgrowth phenotype *highwire* (*hiw*) has been shown to have significantly reduced bouton size in comparison to wildtype (Collins *et al.*, 2006). Mutations in *spinster* results in reduced mean bouton width compared to wildtype (Fig. 3.5A). However, due to the presence of different bouton populations at muscle 6/7 it is useful to look at the proportion of smaller boutons, (type1s) and larger boutons (type1b), although classification of these based on size varies greatly in different studies. They are clearly defined by innervation and morphology but for the purposes of this study size was investigated in μm increments to establish the distribution on bouton width. Bouton size was found to exhibit a different distribution of width between wildtype and *spinster* ($p<0.001$; Kolmogorov-Smirnoff) with a greater proportion of smaller boutons in *spinster* mutants (Fig. 3.5B and C). Nonetheless, the spinster mutants have consistently overgrown synapses compared to wildtype.

3.2.3. Relieving oxidative stress reduces overgrowth of the neuromuscular junction in *spinster*

Increased levels of oxidative damage and activation of the cellular stress response in *spinster* are indicative of increased levels of ROS. Normally ROS

are maintained at physiological levels through a tightly regulated balance between their generation and a complex system of anti-oxidants. Given the indication that *spinster* is carrying an oxidative stress burden, it is proposed that such oxidative stress might be a causative factor in the generation of overgrowth at the neuromuscular junction. To test this hypothesis anti-oxidant transgenes were expressed under the control of *spin*GAL4. Thus, transgenes were expressed concurrently pre- and post- synaptically, in the nerve and muscle. Expression of the anti-oxidant transgene UAS*trx*^{CYTO} relieves oxidative stress and prevents the increase in branch number seen in *spinster*, showing that oxidative stress causes increased branching in *spinster* (Fig. 3.6).

Bouton number was investigated through the expression of four different antioxidant transgenes, UAS*hSOD1*, UAS*cat*, UAS*trxR*^{CYTO} and UAS*trxR*^{MITO} These were expressed concurrently pre- and post-synaptically and all significantly rescue synaptic overgrowth (Fig. 3.7; $p<0.001$, ANOVA).

Expression of UAS*hSOD1* will promote the generation of hydrogen peroxide from superoxide anions. This is the cytoplasmic and mitochondrial periplasm form of the enzyme (Missirlis *et al.*, 2003). The other three anti-oxidant transgenes are involved in the conversion of hydrogen peroxide to water and oxygen, or neutralisation of other ROS, not superoxide anions; only SOD acts on superoxide produce hydrogen peroxide. Catalase acts directly to convert hydrogen peroxide to water (May, 1901), whereas thioredoxin reductase (TrxR) acts to reduce oxidised thioredoxin, allowing it to be used again in the breakdown of hydrogen peroxide. This process is coupled to the oxidation and

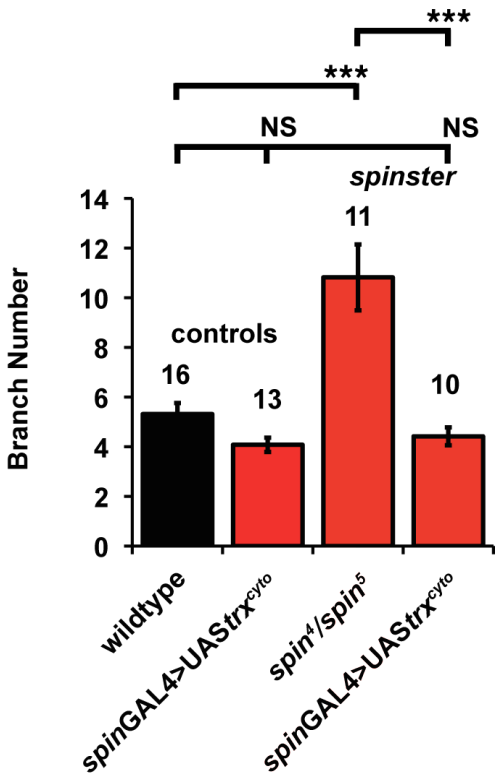

Figure 3.6 *spinster* has increased branching due to oxidative stress. The mean number of branches per neuromuscular junction was increased from 4.54 (n=11) in wildtype to 10.8 (n=11) in *spinster* (Fig. 3.4). Expressing the anti-oxidant transgene UAS*trx*^{CYTO} significantly reduces branch number to 4.4±0.35 (n=12, p<0.001, ANOVA) back to wildtype levels. Expression of this transgene in a wildtype background does not cause any significant change in branch number 4.07±0.29 (p>>0.05 compared to wildtype, ANOVA).

3. Oxidative Stress Contributes to Synaptic Overgrowth in spinster, a Model of a Lysosomal Storage Disorder

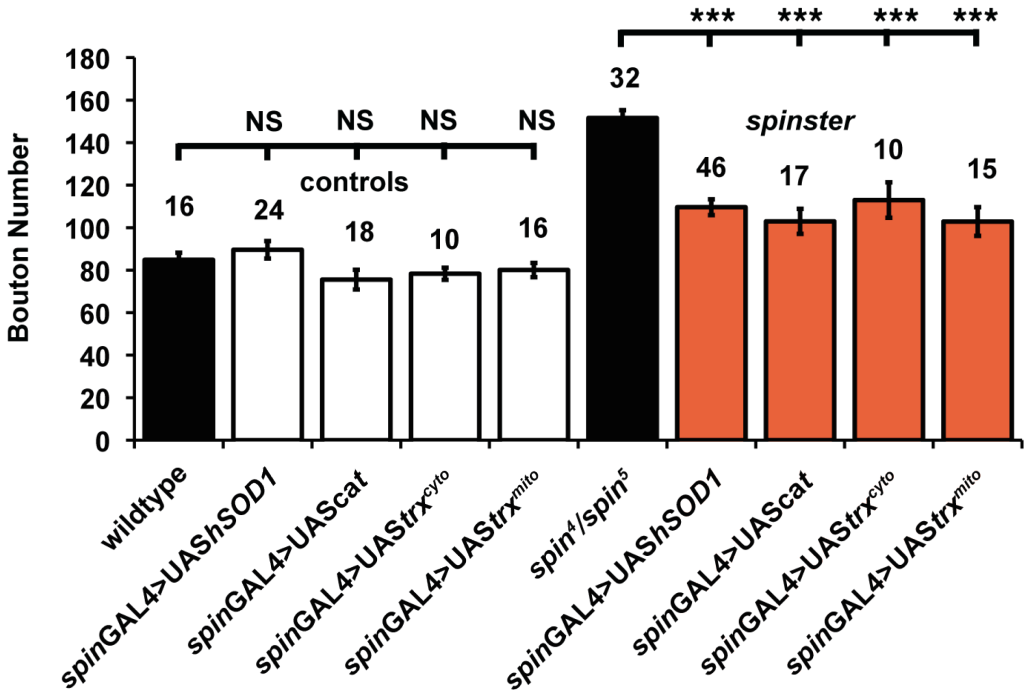

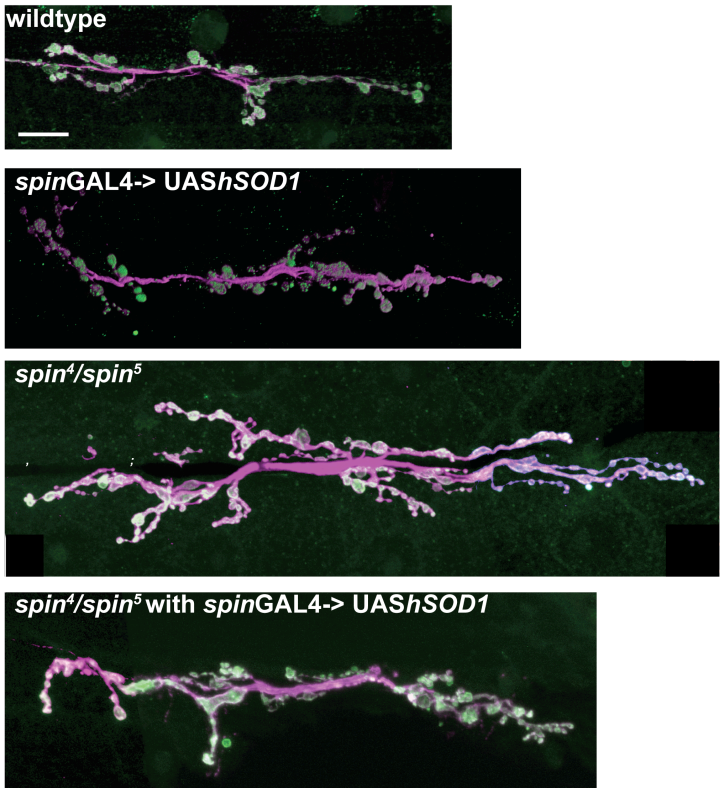

Figure 3.7 Relieving the oxidative stress burden in spinster through expressing anti-oxidant transgenes reduces synaptic overgrowth. Expression of UAS*hSOD1*, UAS*cat*, UAS*trx*^{CYTO}, UAS*trx*^{MITO}, did not cause any significant change in bouton number in a wildtype background, with bouton numbers of 90±4.1 (n=24), 76±4.6 (n=18), 78±2.9 (n=10) and 80±3.3 (n=16), Expression of these transgenes in *spinster* resulted in a reduction of bouton number from *spinster* with a bouton number of 152 (n=32). Bouton number is significantly reduced to 110±3.7 (n=46) by the expression of UAS*hSOD1*, to 103±5.9 (n=17) by UAS*cat*, 113±8.3 (n=10) by UAS*trx*^{CYTO} and to 103±6.8 by UAS*trx*^{MITO} ($p<0.001$; ANOVA) respectively. Representative images of NMJs at muscle 6/7 segment A3 with nerves shown in magenta through α-HRP staining. Synaptic boutons visualised in green by α-synaptotagmin staining. Scale bars denote 20μm.

reduction of NADPH (Holmgren, 1989). Two UAS*trx-R* transgenes were used in this experiment; one that acts in the cytoplasm and one in the mitochondria (Missirlis *et al.*, 2002).

The similar effects of different anti-oxidants suggests that it is the level of oxidative stress that is significant in causing the overgrowth rather than the cellular localisation, or the proportion of superoxide anions in relation to hydrogen peroxide. This assumption is arrived at because it is immaterial to the level of rescue afforded, which ROS are acted upon; all the anti-oxidant enzymes expressed increase the breakdown of ROS and rescue synaptic overgrowth. These data also indicate that the sub-cellular localisation of the anti-oxidant is of no consequence to the level of rescue provided, since expressing cytoplasmic or mitochondrial anti-oxidant transgenes afforded the same level of rescue, although as overexpression was used there may also be expression outside its normal localisation. Unfortunately, this could not be further confirmed by comparing the effects of expression of UAS*sod2* in *spinster* as it was not possible to recombine this transgene with the *spinster* mutants, suggesting they are close together on the 2nd chromosome. Although reducing oxidative stress rescues branch number and bouton number it is not known whether bouton size is also rescued by expression of these transgenes.

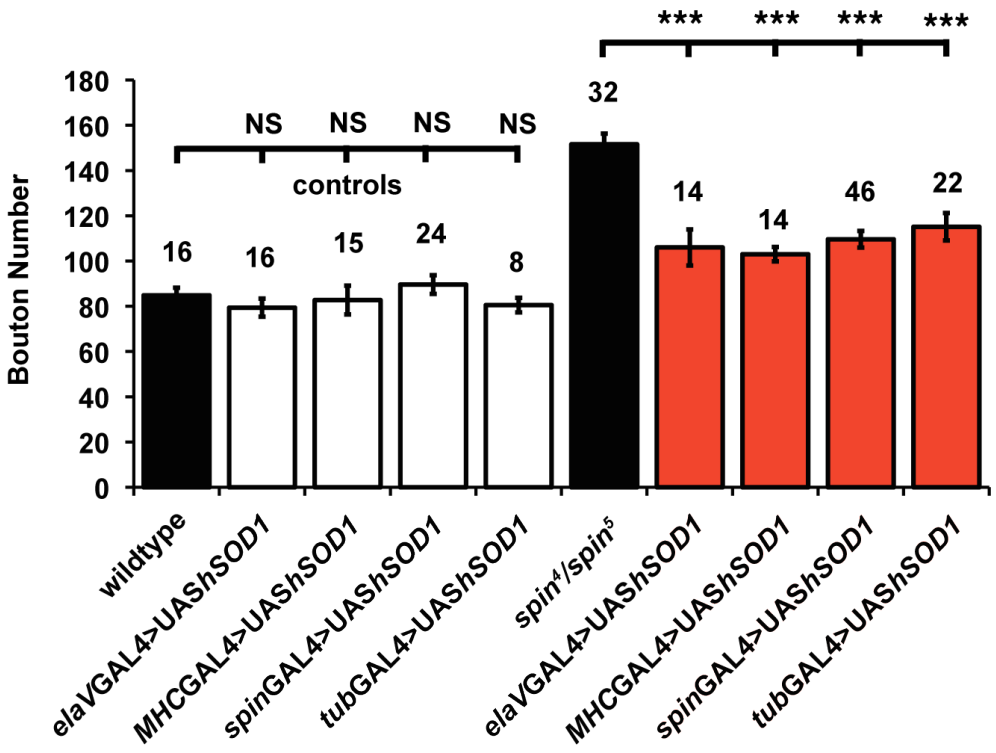

Figure 3.8 Expression of UAS*hSOD1* reduces synaptic overgrowth in *spinster* when expressed in either the nerve the muscle or both. Expression of UAS*hSOD1* under the control of *elaV*GAL4, *MHC*GAL4, *spin*GAL4 and *tub*GAL4 in a wildtype background did not cause any change in bouton number from wildtype, 85±3.3 (n=16) to 79±4.0 (n=16), 83±6.4 (n=15), 90±4.1 (n=24) and 81±3.2 (n=8), respectively. Expression of *hSOD1,* under control of these GAL4 drivers significantly rescues synaptic overgrowth. Expression in the nerve reduces bouton number to 106±8.0 (n=14), in the muscle 103±3.2 (n=14). As already shown concurrent expression in the nerve and muscle, by *spin*GAL4, reduces bouton number to 110±3.7 (n=46) *tub*GAL4 driven expression of UAS*hSOD1* in *spinster* rescued bouton number to 115±6.0 (n=22).

Having established that relieving the oxidative burden pre- and post-synaptically, through the *spin*GAL4 driver, rescues synaptic overgrowth it was decided to determine whether input from the pre- and post- synaptic compartments alone can rescue bouton number. As spin cDNA expression is required both in the nerve and the muscle to fully rescue overgrowth in the *spinster* mutant. This will elucidate whether oxidative stress and resultant signalling from both the nerve and the muscle contributes to synaptic overgrowth in *spinster*. To do this UAS*hSOD1* was expressed either pre- or post-

synaptically by *elaV*GAL4 or *MHC*GAL4 respectively. UAS*hSOD1* was also expressed at high levels globally under the control of *tub*GAL4. Expression of UAS*hSOD1* under the control of *elaV*GAL4, *MHC*GAL4, *spin*GAL4 and *tub*GAL4 in a wildtype background did not change in bouton number from wildtype (Fig. 3.8). However, expression of *hSOD1,* under control of these GAL4 drivers significantly rescues synaptic overgrowth in a spinster mutant background. Expression in the nerve, muscle or both concurrently provided the same level of rescue. Global high level expression also afforded a similar level of rescue. This suggests that there is a limit to the level of rescue *hSOD1* can provide, possibly due the breakdown of hydrogen peroxide becoming the rate-limiting step in the anti-oxidant pathway. These data are consistent with Sweeney and Davis (2002), who showed that *spinster* induced overgrowth is caused by contribution from both the pre- and post- synaptic compartments of the neuromuscular junction.

3.2.4. Oxidative stress contributes to overgrowth in *highwire*

Highwire is an E3 ubiquitin ligase that regulates the development of the neuromuscular junction by limiting JNK signalling (Collins *et al.*, 2006). Mutations in *hiw* result in overactivation of this pathway leading to Fos-dependent synaptic overgrowth. This occurs as highwire is required for the ubiquitination, and hence breakdown, of wallenda, a JNKKK. In highwire mutants, the level of wallenda is left unchecked and is increased leading to heightened activity in the downstream pathway. Depleting wallenda, JNK or Fos signalling in *highwire* mutants prevents this overgrowth, as the increased activity in this pathway is impeded. It is interesting to note that Jun was not involved suggesting that, as postulated, Fos can act independently of Jun in *Drosophila* (Perkins *et al.*, 1990, O'Shea *et al.*, 1992). Highwire is regulated by autophagy, suggesting one mechanism through which autophagy promotes synapse growth

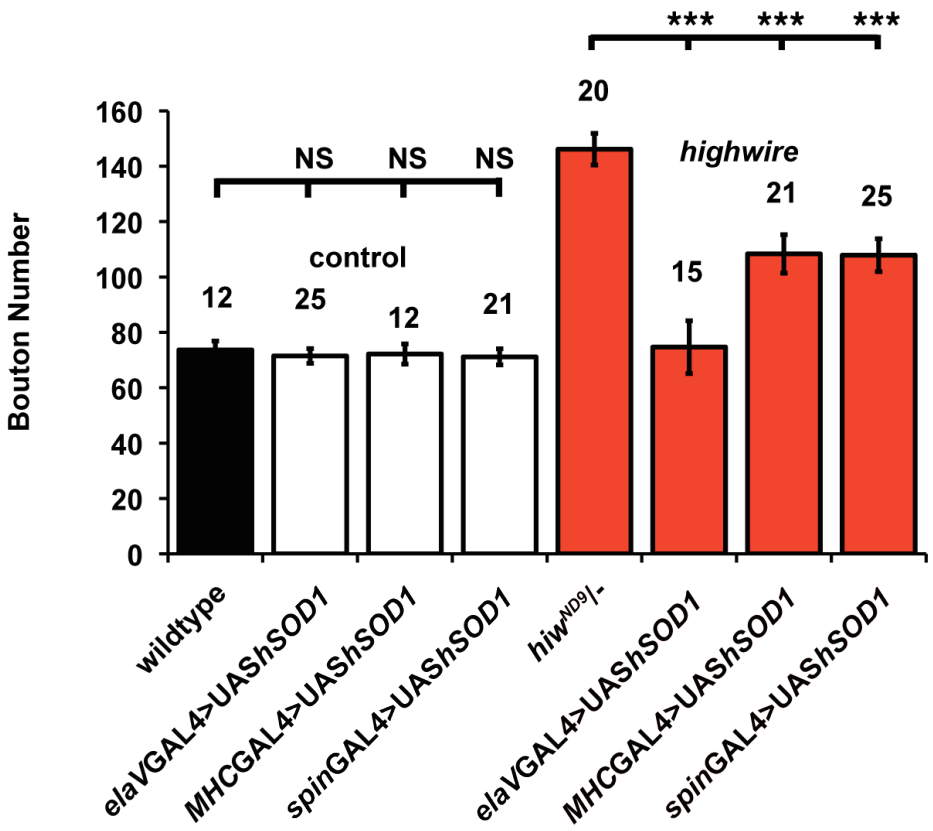
***
***
***
20
160
140
120
100
80
60
40
20
0
NS
NS
NS
highwire
21
25
control
15
12
25
12
21
Bouton Number
wildtype
elaVGAL4>UAShSOD1
MHCGAL4>UAShSOD1
spinGAL4>UAShSOD1
hiwND9/-
elaVGAL4>UAShSOD1
MHCGAL4>UAShSOD1
spinGAL4>UAShSOD1

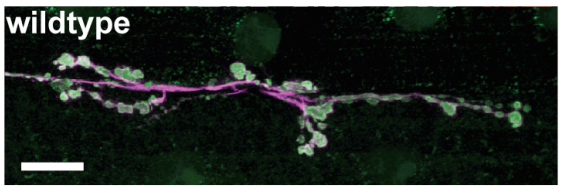
wildtype

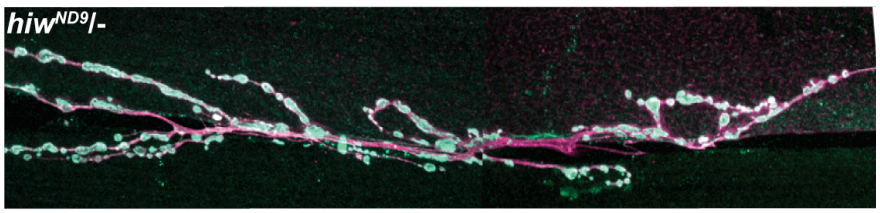
hiwND9/-

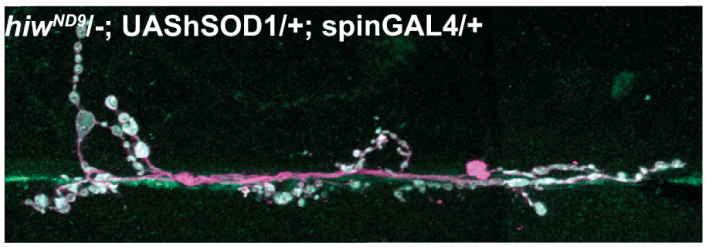
hiwND9/-; UAShSOD1/+; spinGAL4/+

Figure 3.9 Expression of UAS*hSOD1* rescues synaptic overgrowth in *highwire.* Wildtype males have a mean bouton number of 74±3.2 (n=12). *hiw* mutants have a bouton number of 146±5.7 (n=20). *hSOD1* did not cause any change in bouton number in a wildtype background; *elaV*GAL4, *MHC*GAL4 and *spin*GAL4 driving *hSOD1* having bouton numbers of 71±2.6 (n=25), 72±3.6 (n=12), and 71±2.9 (n=21) respectively. When these transgenes were expressed in *hiw* mutants a significant rescue of bouton number was seen. Neuronal expression of *hSOD1* affords complete rescue of NMJ overgrowth to 75±9.5 (n=15), whereas expression of *hSOD1* under control of *MHC*GAL4 and *spin*GAL4 both reduced bouton number to 108±7.0 (n=21) and 108±6.0 (n=25) respectively. Representative images of NMJs at muscle 6/7 segment A3 with nerves shown in magenta through α-HRP staining. Synaptic boutons visualised in green by α-synaptotagmin staining. Scale bars denote 20μm.

(Shen and Ganetzky, 2009). In addition, JNK has been shown to activate autophagy transcriptionally (Wu *et al.*, 2009) so the cyclical nature of this pathway is evident. Mutations in degradative pathways have been implicated in a number of neurodegenerative disorders and have been cited as a source of ROS. One of the genetic determinants of Parkinson's disease is *parkin* an E3 ubiquitin ligase, however it is now known whether the loss of ubiquitination that causes PD with this mutation, furthermore *parkin* is involved in regulation of JNK signalling (Cha *et al.*, 2005). It was therefore decided to investigate whether oxidative stress causes any of the overgrowth seen in *hiw*. As oxidative stress can lead to the increased activity of JNK signalling and could contribute to synaptic overgrowth. The anti-oxidant transgenes UAS*cat* and UAS*hSOD1* were expressed in the nerve using *elaV*GAL4, in the muscle using *MHC*GAL4 and concurrently in the nerve and muscle using *spin*GAL4 (Fig. 3.9 and 10). Analysis of NMJs in *hiw* was carried out in males, which are approximately 10% smaller than females and consequently have a lower number of boutons. As in the females, any expression ofUAS*hSOD1,* whether in the nerves, muscles or both did not cause any change in bouton number in a wildtype background. However, when these transgenes were expressed in *hiw* mutants a significant rescue of bouton number was seen. Neuronal expression of *hSOD1* affords complete rescue of NMJ overgrowth whereas expression of *hSOD1* under

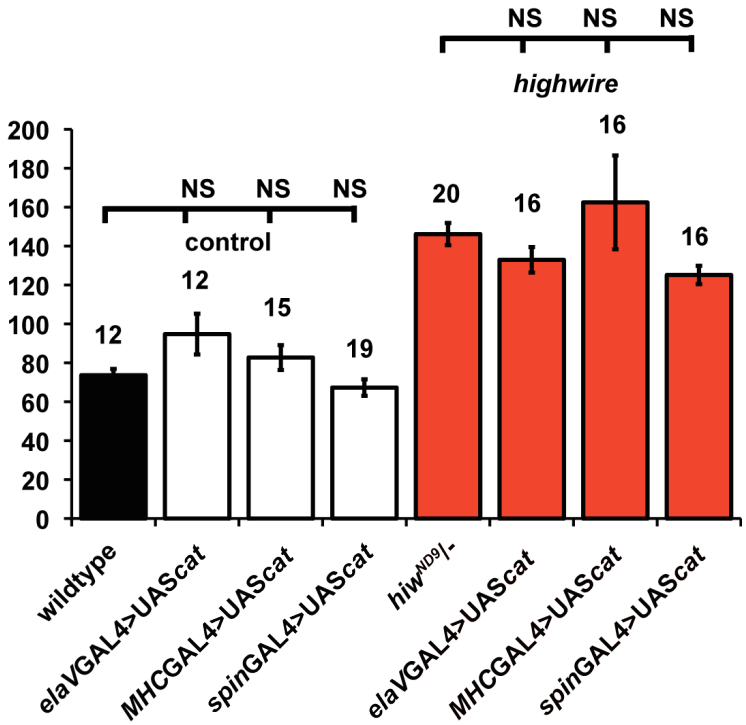

Figure 3.10 Reducing oxidative stress through expression of UAS*cat* fails to rescue synaptic overgrowth in *highwire*. UAS*cat* did not cause any change in bouton number in a wildtype background. *elaV*GAL4, *MHC*GAL4 and *spin*GAL4 driving UAS*cat* having bouton numbers of 95±10 (n=12), 83±6.3 (n=15), and 67±4.3 (n=19) respectively .Expression of UAS*cat* pre-synaptically in *highwire* caused a bouton number of 133±6.5 (n=16). Expression in the muscle did not significantly affect bouton number 162±24.1 (n=16), and expression concurrently in the muscle and nerve under control of *spin*GAL4 resulted in a bouton number of 125±4.7 (n=16). These are not significantly different to bouton numbers in *highwire* (p>0.05, ANOVA).

control of *MHC*GAL4 and *spin*GAL4 both significantly reduced bouton number, but only a partial rescue, not back to wildtype levels (Fig. 3.9). Previously *highwire* overgrowth was thought to be controlled entirely through the pre-synaptic compartment. This is somewhat inconsistent with the data shown here, although ROS can diffuse freely between cells and it therefore non-autonomous, unlike activity in some signalling pathways. The same GAL4 drivers were used to ascertain the effects of increasing levels of catalase using UAS*cat*. Once again (Fig. 3.10), similar to the females, expression of UAS*cat* pre- (elaV) or

post (MHC) synaptically or both (spin) does not cause any significant change in bouton number in wildtype males. Expression of UAS*cat* in these tissues did not cause any significant change in bouton number in *highwire* ($p>0.05$ ANOVA). The observation that increasing the breakdown of hydrogen peroxide does not alter alleviate *highwire* induced overgrowth, suggests that the level of hydrogen peroxide is not contributing to the overgrowth phenotype. However, relieving the superoxide burden completely rescues the overgrowth phenotype suggesting that a misregulated component in the *highwire* mutants is sensitive to activation by superoxide specifically rather than other ROS.

3.3. Discussion

Mutations in *spinster* have been shown to cause aberrant carbohydrate storage in the lysosomes and accumulation of multilamellar membrane components. Endocytic defects and neurodegeneration are also observed (Dermaut et al., 2005). Oxidative stress has been implicated in a number of neurodegenerative conditions including a number of lysosomal storage disorders, so it was investigated whether *spinster* is carrying an oxidative stress burden. The data here demonstrate that mutations in *spinster,* a transmembrane lysosomal protein, result in oxidative stress. Increased levels of peroxidated lipids and increased transcription of *gst-D-GFP* show that *spinster* incurs oxidative damage and activation of the cellular stress response. Increased levels of malondialdehyde were found in the blood of mucopolysaccharidosis type II patients, and this was found to be reduced following 6 months of enzyme replacement therapy (Fillipon *et al.*, 2011), again suggesting the causative role of lysosomal dysfunction in the generation of oxidative stress. This is likely to be a result of the presence of lipofuscin, which is caused by and goes on to cause oxidative stress and is a common characteristic of LSDs (Yamamoto *et al.*, 1999).

In addition to the presence of oxidative stress the morphology of the neuromuscular junction was also analysed, and it is found that spinster mutants have increased branch number, coupled to increased bouton number. Bouton size shows a different distribution in *spinster* compared to wildtype. There are more smaller boutons in *spinster* compared to wildtype; this is akin to but not as severe as the bouton size phenotype seen in *highwire* mutants. Having shown the presence of oxidative stress in *spinster* the question of whether oxidative stress is causative to the synaptic overgrowth phenotype remained. The regulation of synapse growth is a complex process involving the integration of many signalling pathways that act both anterogradely and retrogradely, thus signalling between the nerve and the muscle and the reverse is required for normal development (For review see Collins and DiAntonio, 2007). By expressing an anti-oxidant transgene *UAS-hSOD1* the level of oxidative damage in *spinster* is reduced suggesting that ROS is impinging upon one of these growth pathways.

All the anti-oxidants transgenes when expressed pre- and post-synaptically using *spin*GAL4 in *spinster* mutants cause a significant reduction in bouton number, but none provide a full rescue. These data suggest that there is a only certain level of rescue that can be obtained by reducing oxidative stress; there are other causative factors in *spinster* that are contributing to the overgrowth and further relieving oxidative stress is unable to combat these other causative factors. For this to be confirmed a number of anti-oxidants would have to be expressed concurrently both pre- and post synaptically. To deal with the level of oxidative stress a number of different anti-oxidant might need to be expressed together to effectively convert superoxide anions to hydrogen peroxide and then degraded further to water and oxygen. For example expressing SOD will increase the levels of hydrogen peroxide while dissipating the superoxide anions. Conversely, all the other anti-oxidant transgenes expressed work by converting hydrogen peroxide to water and oxygen. However it has not been

investigated whether the change in bouton size is rescued by relieving the oxidative burden.

Mutations in *spinster* have previously been shown to cause overgrowth of the *Drosophila* neuromuscular junction due to dysregulation of TGFβ signalling (Sweeney and Davies, 2002). The data shown here is consistent with TGF-beta being permissive for synapse growth. Tissue specific expression of *spinster* cDNA showed that *spinster* is required both pre- and post- synaptically for normal synaptic development, there is 50% synaptic overgrowth contributed from each compartment (Sweeney and Davies, 2002). Here, it is shown that pre- or post- synaptic expression of UAS*hSOD1* afford a similar level of rescue, which is the same as obtained by concurrent expression pre- and post-synaptically with *spinGAL4* or *tubGAL4*. Once again a battery of anti-oxidants may be required to fully rescue this severe overgrowth phenotype, alternatively full rescue of overgrowth might not be possible with anti-oxidants alone due to the persistent increased presence of signalling molecules, normally down-regulated through lysosomal systems.

The involvement of oxidative stress in generating overgrowth of the neuromuscular junction was also investigated in *highwire*; differential involvement was found in *spinster* and *highwire*. Reducing oxidative stress through the expression of UAS*hSOD1* reduces synaptic overgrowth most efficiently when expressed pre-synaptically in *highwire.* Conversely there is no difference between the level of rescue seen in *spinster* between pre- and post-synaptic expression of UAS*hSOD1*. This is in keeping with published data that highwire and its downstream effector wallenda is expressed in the nerve (Wan *et al.*, 2000) and that depleting presynaptic signalling is sufficient to rescue synaptic overgrowth (Collins *et al.*, 2006), whereas in *spinster* mutants pre- and post-synaptic expression of UAS*spin* was required to rescue the overgrowth phenotype (Sweeney and Davies, 2002). However post-synaptic involvement in

highwire-induced overgrowth been investigated, although there is an electrophysiological phenotype in *highwire* mutants (Wan *et al.*, 2000).

The data here also suggest that superoxide anions and hydrogen peroxide contribute to synaptic overgrowth in *spinster* but only superoxide anions contribute to overgrowth in *highwire* as overexpression of catalase to breakdown hydrogen peroxide did not change *highwire*-induced overgrowth. Although dendritogenesis and syanptogenesis have previously been identified in models of lysosomal storage disorders, the causes of increased synapse formation had not previously been identified. The data shown here clearly indicate that oxidative stress is having a causative role in increased synaptic growth in *spinster,* a model of a lysosomal storage disorder.

4. Oxidative Stress Causes Overgrowth of the *Drosophila* Neuromuscular Junction

4.1. Introduction

In chapter 3, it was shown that *spinster* is carrying an oxidative burden leading to increased oxidative damage and activation of stress response pathways. It was also observed that expressing antioxidant transgenes could prevent synaptic overgrowth in both *spinster* and *highwire*. This suggests that oxidative stress is causative of the synaptic overgrowth phenotype seen in these mutants. Due to these effects of oxidative stress on synapse development in these mutants it is postulated that oxidative stress can cause synaptic overgrowth. Consequently, to test this hypothesis it was investigated whether it is possible to recapitulate this overgrowth phenotype through the generation of oxidative stress independent of the lysosomal dysfunction arising in *spinster*. This would allow dissection of this phenotype and could elucidate what is caused as a result of oxidative stress and what is a direct result of lysosomal dysfunction. The effects of oxidative stress on synapse development were investigated by inducing oxidative stress in the developing larvae in a number of ways. Firstly, larvae were exposed to toxins known to cause oxidative stress, namely paraquat and rotenone. Secondly, mutations known to cause oxidative stress were used, there being two ways in which mutations can generate oxidative stress. Stress can be induced either by increasing the generation of ROS such as *sesB* or by reducing the animals capacity to breakdown ROS, through mutations in the anti-oxidant defence system, such as *sod1*.

Mutations in *spinster* were also shown to cause other changes in synaptic morphology, such as increased branch number and increased proportion of smaller boutons. To determine whether oxidative stress or other aspects of

spinster induce these changes these phenotypes were investigated in animals carrying an oxidative burden.

4.2. Results

4.2.1. Oxidative stress alters bouton number and muscle surface area

4.2.1.1. Paraquat causes overgrowth of the neuromuscular junction

Paraquat is an electrotoxin that impairs mitochondrial function and undergoes redox cycling within the cell (Bus *et al.*, 1976a and b). Exposure to this toxin has been known to cause Parkinson's disease in farm workers exposed to this pesticide (Tanner *et al.*, 2011). It is also commonly used to cause oxidative stress in experimental systems. Paraquat undergoes redox cycling in the cell and also impairs mitochondrial function through acting at complex I or complex III (Fukushima *et al.*, 1994 and 2002; Richardson *et al.*, 2005; Ramachandiran *et al.*, 2007). By feeding larvae paraquat through the larval stages of development, paraquat is seen to cause no change in bouton number, at 1mM, 5mM or 10mM, prior to muscle normalisation (Fig. 4.1A). Lower concentrations of paraquat do not cause any change in muscle surface. However, 10mM paraquat causes a significant reduction in muscle surface area (Fig. 4.1B). Given the observation that muscle size and bouton number share a proportional relationship (Schuster *et al.*, 1996a; Lnenicka and Keshishian, 2000) it is common to normalise bouton number to muscle surface area. Consequently, when bouton number is normalised to account for these changes in muscle surface area 1mM and 5mM do not cause any change in bouton number whereas 10mM paraquat causes a significant increase in bouton number relative to muscle surface area (FIG 4.1C), suggesting that oxidative stress, as a result of paraquat exposure, causes synaptic overgrowth.

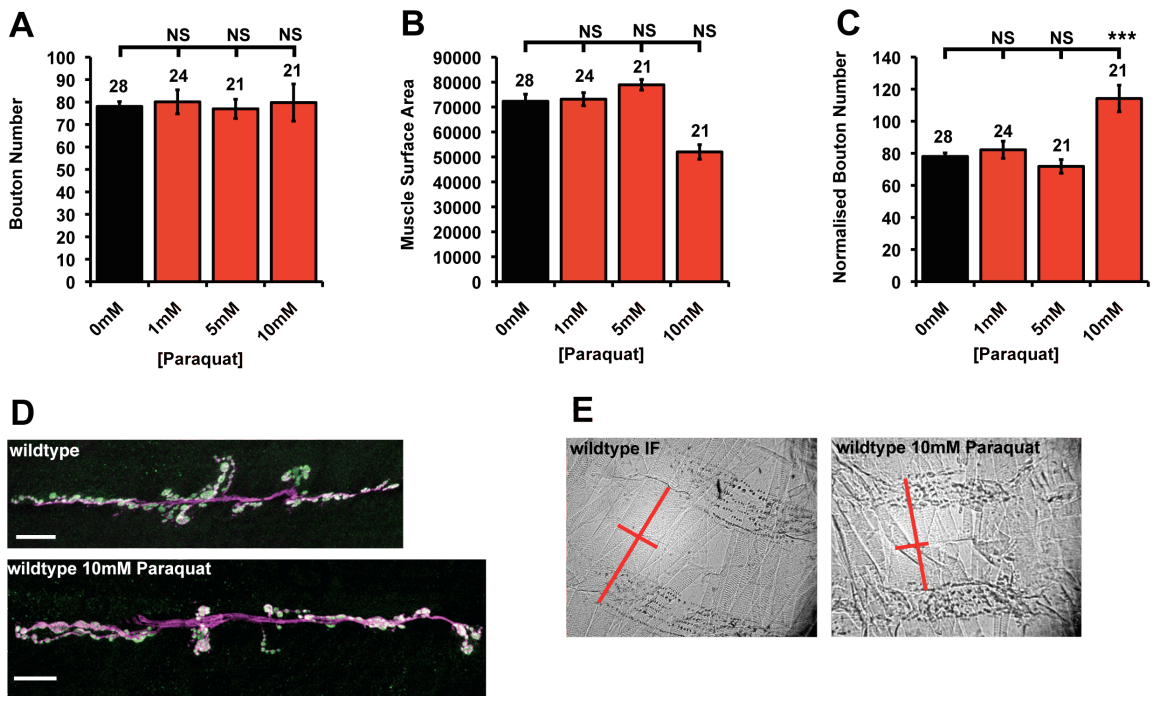

Figure 4.1 Paraquat causes synaptic overgrowth relative to muscle surface area. (A) On instant food in the absence of paraquat wildtype larvae have a mean bouton number of 78±2.1 (n=28). When fed on 1, 5 and 10mM paraquat this is not significantly changed with mean bouton numbers of 80±3.5 (n=24), 77±3.5 (n=21) and 80±6.6 (n=41) ($p>0.05$, ANOVA). (B) On instant food wildtype larvae have a mean muscle surface area of 72313±2837μm^2. 1mM and 5mM paraquat cause no change with muscle surface areas of 73162±2665 μm^2 and 78917±2120μm^2 respectively ($p>0.05$, ANOVA). 10mM paraquat caused a significant reduction in muscle surface area to 52003±2922μm^2. ($p<0.001$, ANOVA). (C) When normalised to muscle surface area 1 and 5mM paraquat do not cause any change in bouton number; 82±5.3 and 72±4.3 respectively ($p>0.05$ ANOVA). 10mM causes a significant increase in normalised bouton number to 114±8.3 ($p<0.001$). (D) Representative images of wildtype NMJs at muscle 6/7 segment A3 in normal instant food and in 10mM paraquat. Nerves shown in magenta through α-HRP staining. Synaptic boutons visualised in green by α-synaptotagmin staining. Scale bar = 20μm (E) Representative images of muscles showing length and width (red lines).

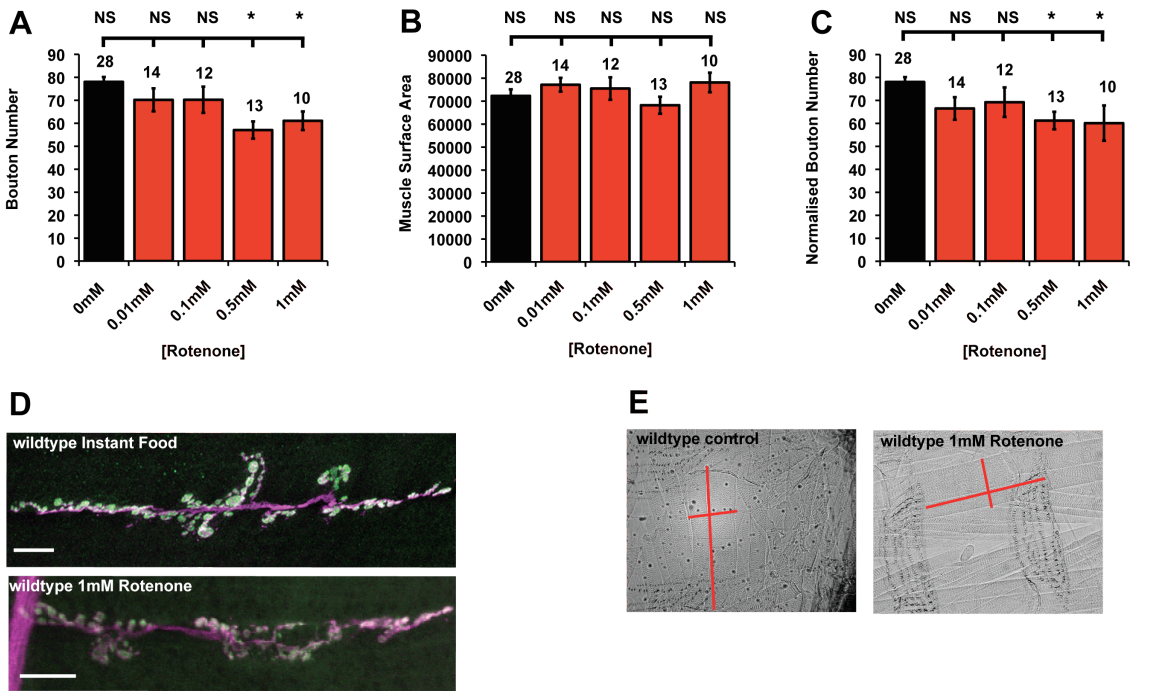

Figure 4.2. Rotenone reduces synaptic growth with no change in muscle surface area. (A) 0.01mM and 0.1mM Rotenone did not cause any change in bouton number; 70±5.01 (n=14), 70±5.69 (n=12) no significantly different from wildtype: 78±2.1 (n=28), ($p>0.05$, ANOVA). 0.5mM and 1mM rotenone cause a significant reduction in bouton number with 57±3.74 (n=13) and 61±4.04 (n=13), ($p<0.05$, ANOVA). (B) 0.01mM, 0.1mM, 0.5mM and 1mM rotenone have muscle surface areas of 77142±2994μm^2, 75513±4880μm^2, 68243±3700μm^2 and 78154±4262µm, respectively. (C) Following normalisation the bouton numbers shown the same trend as prior to normalisation as the muscle surface areas were not significantly altered; 67±4.92, 69±6.43, 61±8.2 and 60±7.7 for 0.01, 0.1, 0.5 and 1mM rotenone. Normalised bouton numbers in larvae exposed to 0.5 and 1mM rotenone were significantly reduced compared to wildtype ($p<0.05$). (D) Representative images of wildtype NMJs without rotenone and in 1mM rotenone at muscle 6/7 segment A3. Nerves shown in magenta through α-HRP staining. Synaptic boutons visualised in green by α-synaptotagmin staining Scale bar = 20μm. (E) Representative images of muscles showing length and width (red lines).

4.2.1.2. Rotenone causes undergrowth of the neuromuscular junction

Rotenone is also known to cause oxidative stress and is commonly used as a model of Parkinson's disease (Betarbet *et al.*, 2000; Sherer *et al.*, 2003). It impairs mitochondrial complex I function (Sherer *et al.*, 2003). Low doses of rotenone (0.01mM, 0.1mM) did not cause any change in bouton number, however, higher doses of rotenone do cause changes at the neuromuscular

junction. 0.5mM and 1mM rotenone cause a significant reduction in bouton number ($p<0.05$, ANOVA) (Fig. 4.2A). No change in muscle surface area is seen at any concentration of rotenone ($p>0.05$, ANOVA) (Fig. 4.2B). Following normalisation, a similar pattern of changes in bouton number persists as prior to normalisation; higher concentrations of rotenone cause a significant reduction in bouton number, even relative to muscle surface area (FIG. 4.2C).

4.2.1.3. Mutations that increase generation of ROS or reduce protection from oxidative stress tend to cause overgrowth of the neuromuscular junction

In addition to the effects of environmental causes of oxidative stress, the effects of oxidative stress on synapse development were investigated further through the use of mutations that cause oxidative stress. Three mutants in the anti-oxidant defence system were analysed: *sod1*, *sod2* and *cat*. Additionally, two mutants known to cause hypersensitivity to oxidative stress, through increased generation of ROS were analysed: *succinate dehydrogenase B (sdhB)* and *stress sensitive B (sesB*). SdhB is a component of complex II of the mitochondrial respiratory chain, mutations in this protein result in hypersensitivity to ROS and reduced longevity (Walker *et al*., 2006). *sesB* encodes a mitochondrial adenosine nucleotide transporter. Mutations in this gene cause increased sensitivity to oxidative stress and increased bouton number (Trotta *et al.*, 2004). The morphology of the neuromuscular junction in these mutants was examined and it was found that *sdhB* causes a reduction in bouton number prior to normalisation Mutations in *sesB* cause an increase in bouton number ($p<0.05$, ANOVA). Mutations in the anti-oxidant defence system were also analysed. *cat* mutants, which have a reduced capacity to break down hydrogen peroxide, and thus are prone to oxidative stress have a normal bouton number prior to

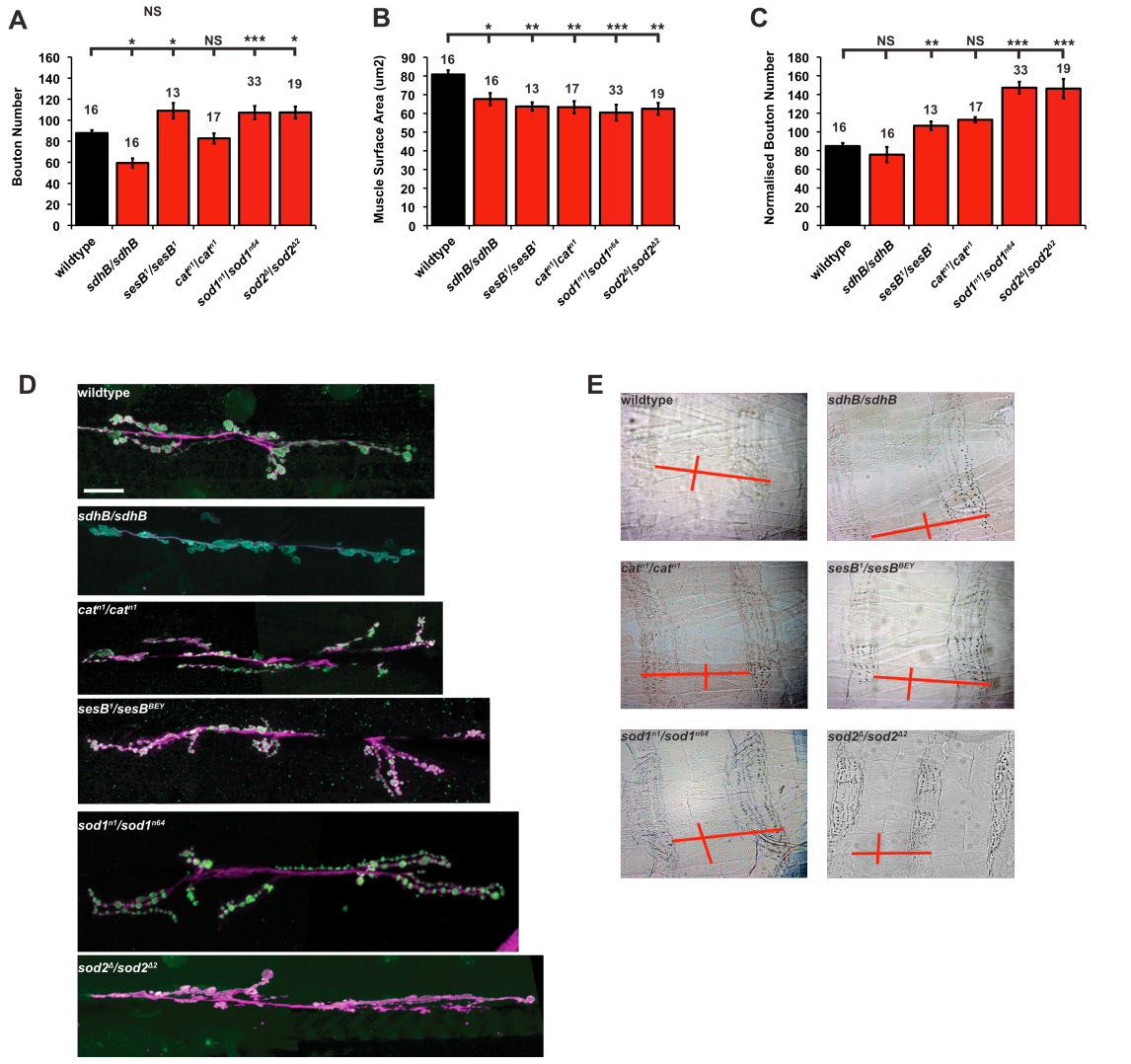

Figure 4.3. Mutations that cause oxidative stress tend to cause synaptic overgrowth. (A) *sdhB* has a significant reduction in bouton number 59±4.4 (n=16), ($p<0.05$, ANOVA) whereas *sesB* has an overgrowth 109±4.0 (n=13), ($p<0.05$, ANOVA). *cat* does not cause any change in bouton number 83±4.8 (n=17), ($p>0.05$, ANOVA).*sod1* and *sod2* have significantly increased bouton numbers of 108±4.9 (n=33, $p<0.001$, ANOVA) and 107±5.9 (n=17, $p<0.05$,ANOVA) (B) All the mutations cause a significant reduction in muscle surface area, *sdhB, ses*B, *cat, sod1 and sod2 h*ave muscle surface areas of 67668±3238μm^2, 63699±2222μm^2, 63334±3229μm^2, 59272±2744μm^2 and 61909±3000μm^2 respectively. (*$p<0.05$, **$p<0.01$ and ***$p<0.001$, ANOVA). (C) Following normalisation to muscle surface area s*dhB and cat* show no significant change in bouton number ($p>0.05$, ANOVA), *sesB* has a significant increase in normalised bouton number 107±5.9 ($p<0.01$, ANOVA) and *sod1 and sod2* have an even greater increase in normalised bouton number 156±9.6 and 147±11.6

respectively. (D) Representative images of wildtype and oxidative stress mutants at muscle 6/7 segment A3. Nerves shown in magenta through α-HRP staining. Synaptic boutons visualised in green by α-synaptotagmin staining. (E) Representative images of muscles showing length and width (red lines).

normalisation. Conversely, mutations in superoxide dismutase, the enzyme that catalyses the conversion of superoxide anions to hydrogen peroxide, cause synaptic overgrowth. Both forms of the enzyme, *sod1* and *sod2*, cytoplasmic and mitochondrial have significantly increased bouton number ($p<0.001$ and $p<0.01$ ANOVA, respectively) (Fig. 4.3A). All of the mutations investigated cause a significant reduction in muscle surface area, with varying significances (Fig. 4.3B). Due to the changes in muscle surface area, bouton number was normalised for muscle surface area, as the relationship between muscle size and bouton number is well documented (Schuster *et al.*, 1996a). When muscle surface area is accounted for there is no change in normalised bouton number in *sdhB* and it is statistically similar to wildtype ($p>0.05$, ANOVA). *sesB* has an increased normalised bouton number compared to wildtype ($p<0.01$, ANOVA). Mutations in the anti-oxidant defence system also had different effects on bouton number. *cat* did not cause a significant difference in normalised bouton number ($p>0.05$, ANOVA). Whereas, *sod1* and *sod2* cause a significant increase in bouton number proportional to muscle surface area (Fig. 4.3C). However, when statistical analysis is performed without *sod* mutants the overgrowth seen in *cat* relative to muscle surface areas is significant ($p<0.05$, ANOVA).

4.2.2. Oxidative stress causes changes in synaptic branching

Synapse growth is most normally quantified in terms of addition of boutons. However branching is also used as a common read-out of neuromuscular junction development. Mutations in *spinster* were shown to have increased branching in proportion to increased bouton number (Fig. 3.4) so branching was

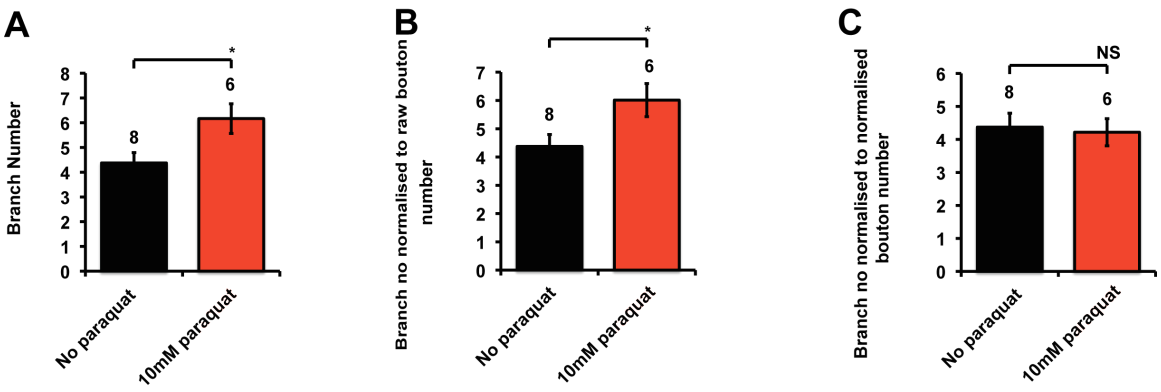

Figure 4.4. 10mM paraquat causes an increase in branch number. (A) Wildtype NMJs have a mean branch number of 4.38±0.42 (n=8). This is significantly increased in paraquat to 6.17±0.6 (n=6) ($p<0.05$, Student's *t*-test). (B) When normalised to bouton number 10mM paraquat has a mean branch no of 6.01±0.6 (n=6; $p<0.05$, Student's *t*-test). (C) When normalised to normalised bouton number and therefore accounting for muscle surface area, there is no change in branch number between no paraquat and 10mM paraquat: 4.22±0.4 ($p>0.05$ Student's *t*-test).

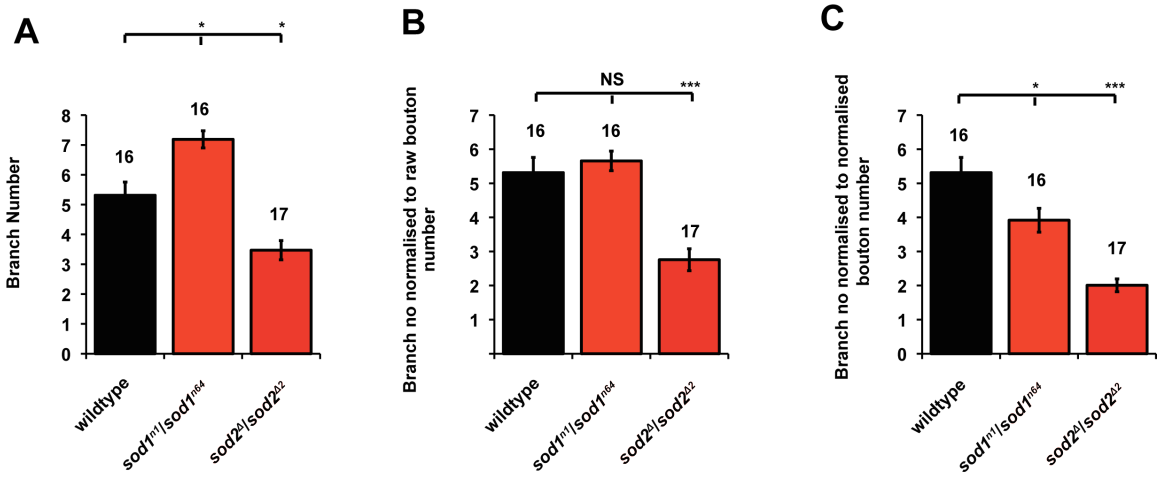

Figure 4.5. Mutations in *sod1* and *sod2* cause different effects in branch number. (A) *sod1* causes an increase in branch number from 5.3±0.44 (n=16) to 7.25±0.92 (n=7) ($p<0.05$, ANOVA). Conversely, mutations in *sod2* caused a significant reduction in branch number to 3.5±0.32 (n=17) ($p<0.05$, ANOVA). (B) When normalised to bouton number *sod1* mutants have statistically similar branch number to wildtype 5.66±0.5 (n=16; $p>0.05$, ANOVA) and *sod2* mutants have significantly reduced branch number relative to bouton number of 2.76±0.3 (n=17; $p<0.001$, ANOVA). (C) When taking into account muscle surface area and bouton number both *sod1* and *sod2* have significantly reduced branch numbers of 3.92±0.3 (n=16; $p<0.05$, ANOVA) and 2.01±0.2 (n=17; $p<0.001$, ANOVA).

investigated in the overgrowth phenotypes identified above. 10mM paraquat causes an increase in branching (Fig. 4.4A). When normalised to bouton number, 10mM paraquat also causes a significant increase in branch number (Fig. 4.4B) as raw bouton number is not increased by 10mM paraquat. However, when normalised to take account of muscle surface area there is no significant difference between no paraquat and 10mM paraquat (Fig. 4.4C). This suggests that the change in branching has more to do with muscle surface area than bouton number in paraquat fed animals. Mutations in *sod* also caused changes in branch number. *sod1* causes a significant increase in the number of branches where as *sod2* causes a significant reduction in the number of branches (Fig. 4.5A). When normalised for bouton number *sod1* shows similar branching in proportion to bouton number, whereas the reduction seen in *sod2* is made more severe when accounting for bouton number (Fig. 4.5B). Having taken account for muscle surface area by comparing branch number to normalised bouton number both *sod1* and *sod2* have a significant reduction in branch number (Fig. 4.5C). This suggests once again that ROS cause different effects depending on the cellular source of the ROS. This is because *sod1* would presumably lead to predominantly cytoplasmic derived ROS whereas *sod2* is more likely to lead to mitochondrial derived increases in ROS, thus differing effects can be seen on NMJ morphology depending on the source of the ROS. Although this does not entirely fit with paraquat, which purportedly acts to increase ROS generation by increasing superoxide generation by the mitochondria and leads to an increase in branch number, akin to that seen in *sod1*. However, the possibility of paraquat acting cytoplasmically as well cannot be overlooked.

4.2.3. Oxidative stress causes changes in bouton size

10mM paraquat causes a significant reduction in mean bouton size (Fig. 4.6A). However what can also be important is the proportion of type Ib and type Is boutons at the NMJ. Even though each type of bouton is clearly defined by their

innervation then are more loosely defined by their size however the range considered to be type Ib as compared to Is varies somewhat between studies. Therefore to compare bouton size the width of boutons in 1μm increments was analysed. Paraquat exposure results in increased proportion of smaller boutons compared to larger boutons (Fig. 4.6B). There are more boutons sized 0-2μm than in wildtype (Fig. 4.6B). The distribution of bouton size in paraquat fed animals is different to wildtype animals on normal food, with a higher proportion of smaller boutons in paraquat fed animals than in controls ($p<0.001$, Kolmogorov-Smirnov). *sod1* mutants have significantly reduced mean bouton size compared to wildtype ($p<0.001$, ANOVA) whereas *sod2* mutants have the same mean bouton width as wildtype (Fig. 4.7A). As mentioned for previous genotypes and phenotypes, it is not just the mean bouton width that is important to analyse but the frequency of different sized boutons and hence the distribution width. Both *sod1* and *sod2* mutants show different distributions of bouton size compared to wildtype. *sod1* mutants have more boutons sized 0-3μm, than in wildtype, whereas *sod2* mutants have an increased proportion of boutons sized 3-4μm (Fig. 4.7B). When plotted as cumulative percentages In addition when compared to each other *sod1* and *sod2* also show different distributions of bouton size ($p<0.001$, Kolmogorov-Smirnov) (Fig. 4.7C). *sod1* seems to cause a similar change in distribution to paraquat, with an increase in the proportion of smaller boutons ($p<0.001$, Kolmogorov-Smirnov). However, as mentioned earlier, *sod1* would probably result in predominantly cytoplasmic oxidative stress, where as paraquat has been suggested to be mainly mitochondrial oxidative stress. Conversely, mitochondrial increases in superoxide caused by *sod2* mutations causes different effects. This suggests that oxidative stress does not uniformly alter bouton size, and depends exactly on the form of the insult incurred, but does not correlate well with differential effects of mitochondrial and cytoplasmic sources of ROS.

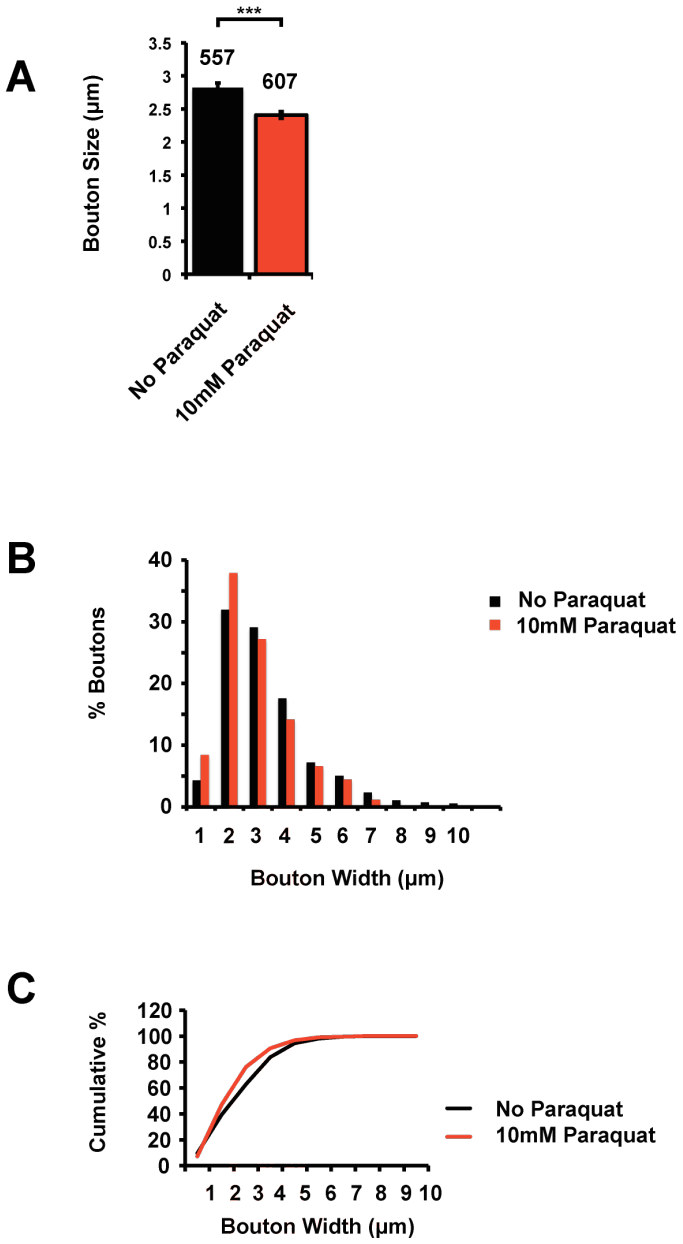

Figure 4.6. Paraquat causes changes in bouton size. Bouton widths were taken from 7 NMJs for each condition (A) Paraquat causes a significant reduction in mean bouton width from 2.82±0.068µm (n=557) to 2.41±0.052µm (n=607 ($p<0.001$, Student's *t*-test). (B) This shows the % of boutons in at each µm width, showing the increased proportion of smaller boutons in 10mM paraquat; this difference distribution is significant ($p<0.001$, Kolmogorov-Smirnov). (C) This shows the cumulative percentage of boutons in each µm width.

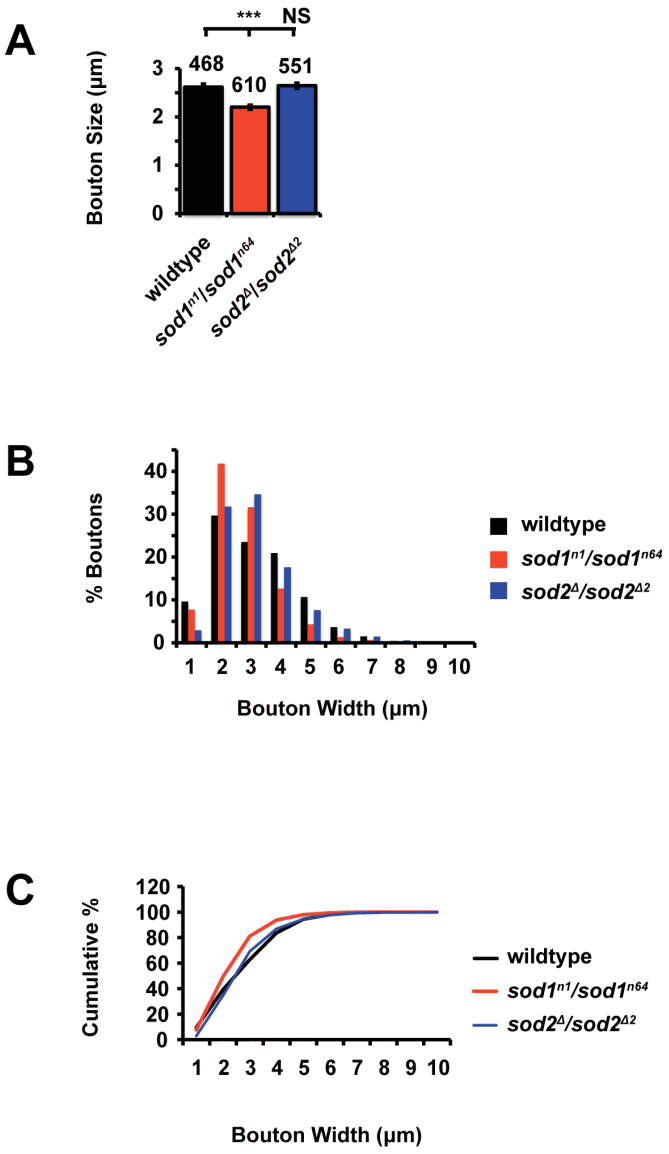

Figure 4.7. Mutations in *sod* cause changes in bouton size. Bouton widths were taken from 5 NMJs for wildtype and *sod2*, and 6 NMJs for *sod1* (A) *sod1* has a significantly reduced mean bouton width compared to wildtype; reduced from 2.62±0.064µm (n=468) in wildtype to 2.2±0.042µm (n=610) ($p<0.001$, ANOVA). *sod2* mutants have a mean bouton width of 2.65±0.053 µm, not statistically different to wildtype ($p>0.05$, ANOVA). (B) This shows the % of boutons in at each µm width, showing the increased proportion of smaller boutons in *sod1*; this difference distribution is significant ($p<0.001$, Kolmogorov-Smirnov). *sod2* mutants also show a difference in the distribution of bouton sizes ($p<0.001$, Kolmogorov-Smirnov) with an increased proportion of medium-sized boutons. (C) This shows the cumulative percentage of boutons in each µm width.

4.2.4. Growth of the neuromuscular junction in animals carrying an oxidative burden is reduced by expressed anti-oxidant transgenes.

The data above show that bouton number is significantly increased in proportion to muscle surface area in a number of conditions of oxidative stress introduced by a number of different methods. This is highly suggestive of oxidative stress driving synaptic growth. To confirm this, oxidative stress was relieved through the expression of anti-oxidant transgenes to see if this prevented the growth seen in these conditions. This was further to the results seen in the previous chapter where expression of anti-oxidant transgenes reduced the growth seen in *spinster* and *highwire* mutants.

4.2.4.1. Paraquat induced growth is reduced by expression of *hSOD1* concurrently pre- and post-synaptically

To establish whether the overgrowth caused by paraquat is due to oxidative stress, or other cellular effects of paraquat, an anti-oxidant transgene was expressed to reduce oxidative stress levels. *UAShSOD1* was expressed under the control of *spinGAL4*, so it was expressed concurrently pre- and post-synaptically. Expression of *spinGAL4>UAShSOD1* causes no change in bouton number (Fig. 4.8A) or muscle surface area (Fig. 4.8B) in the absence of paraquat. However, this transgene in the presence of 10mM paraquat causes a significant reduction in bouton number (Fig. 4.8A). This is significantly different from wildtype in the presence and absence of paraquat and the expression of the transgene in the absence of paraquat ($p<0.001$, ANOVA). No difference in muscle surface area is observed between wildtype and *UAShSOD1/+;spinGAL4/+* in the presence of 10mM paraquat (Fig. 4.8B). This suggests that oxidative stress is not involved in the reduced muscle surface area caused by paraquat. Accordingly, normalised bouton number is rescued back to

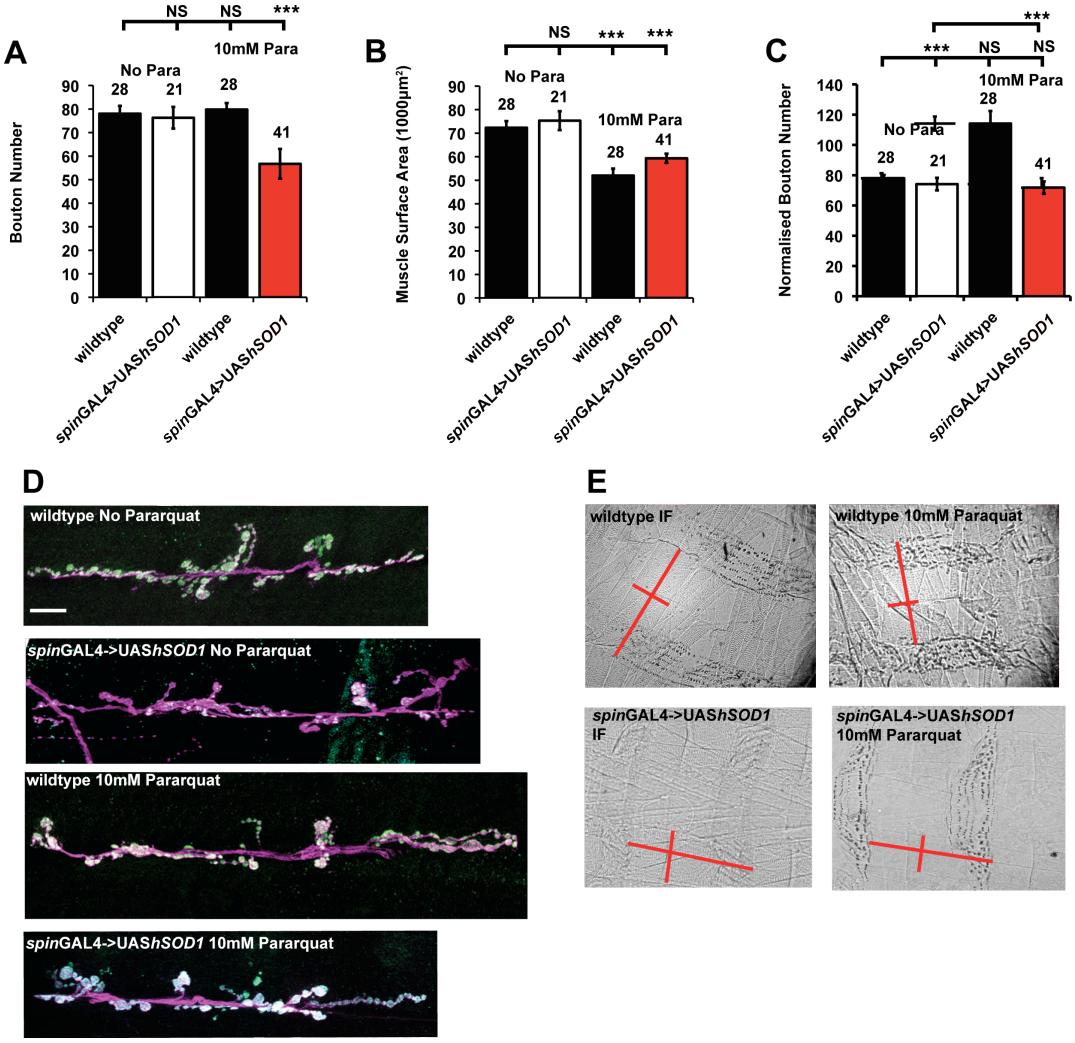

Figure 4.8. Paraquat induced synaptic growth, but not reduced muscle surface area, is rescued by antioxidants. (A) Expression of UAS*hSOD1* under control of *spinGA*L4 did not cause any change in bouton number 76±5.6 (n=21) compared to wildtype. However expression of this transgene combination in animals fed 10mM paraquat caused a significant reduction in bouton number 57±2.6 (n=41) compared to wildtype both with and without paraquat ($p<0.001$). (B) Expression of this transgene combination does not rescue the reduced muscle surface area caused by 10mM paraquat; with muscle surface areas of 52003±2922µm^2 in wildtype and 59332±1937µm^2 in *spin*GAL4>UAS*hSOD1* both fed on 10mM paraquat. Expression of *spin*GAL4>UAS*hSOD1* on normal food did not alter muscle surface area; 75308±3996µm^2 compared to 72313±2837µm^2 in wildtype. (C) Following normalisation, *spin*GAL4>UAS*hSOD1* doesn't cause any change in bouton number 74±4.1 compared to wildtype 78±2.14. Expression of *hSOD1* in 10mM paraquat prevents the increase in

normalised bouton number seen in wildtype, with a bouton number of 72±4.1 in the transgenic larvae ($p<0.001$ ANOVA compared to wildtype 10mM). (D) Representative images of wildtype and *spin*GAL4>UAS*hSOD1* NMJs at muscle 6/7 segment A3in normal instant food and in 10mM paraquat. Nerves shown in magenta through α-HRP staining. Synaptic boutons visualised in green by α-synaptotagmin staining. Scale Bar = 20μm. (E) Representative images of muscles showing length and width (red lines).

wildtype levels by the expression of this antioxidant transgene; this is not statistically different to wildtype in the absence of paraquat and *UAShSOD1/+; spinGAL4/+* in the absence of paraquat ($p>>0.05$, ANOVA), and significantly different to wildtype with 10mM paraquat ($p<0.001$, ANOVA) (Fig. 4.8C).

4.2.4.2. *sod* mutant induced growth is rescued by expression of anti-oxidant transgenes

Increased bouton number in *sod1* mutants is rescued by expressing either *hSOD1* or *cat* pre- and post-synaptically both in terms of raw bouton number (Fig. 4.9A) and normalised bouton number (Fig. 4.9C) ($p<0.001$, compared to *sod1* and $p>>0.05$ compared to wildtype, ANOVA). Expression of these transgenes did not cause any difference to bouton number (Fig. 4.9A) or muscle surface area in the wildtype (Fig. 4.9B). Expression of these transgenes significantly rescues the reduction in muscle surface area seen in *sod1* mutants (Fig. 4.9B). Expression of these transgenes also rescues the increased branching seen in *sod1* mutants (Fig. 4.10).

sod2 induced overgrowth is rescued by expression of UAS*trxR1*^{CYTO}, both in terms of raw bouton number (Fig. 4.11A) and when normalised to muscle surface area (Fig. 4.11C). In contrast to the data shown for *sod1* expression of an antioxidant did not rescue muscle surface area (Fig. 4.11B). As shown earlier (Fig. 4.5), *sod2* mutants have significantly reduced branching. With *spin*GAL4/UAS*trxR1*^{CYTO} the branch number is no longer significantly different from wildtype, this could be interpreted as a partial rescue (Fig. 4.12).

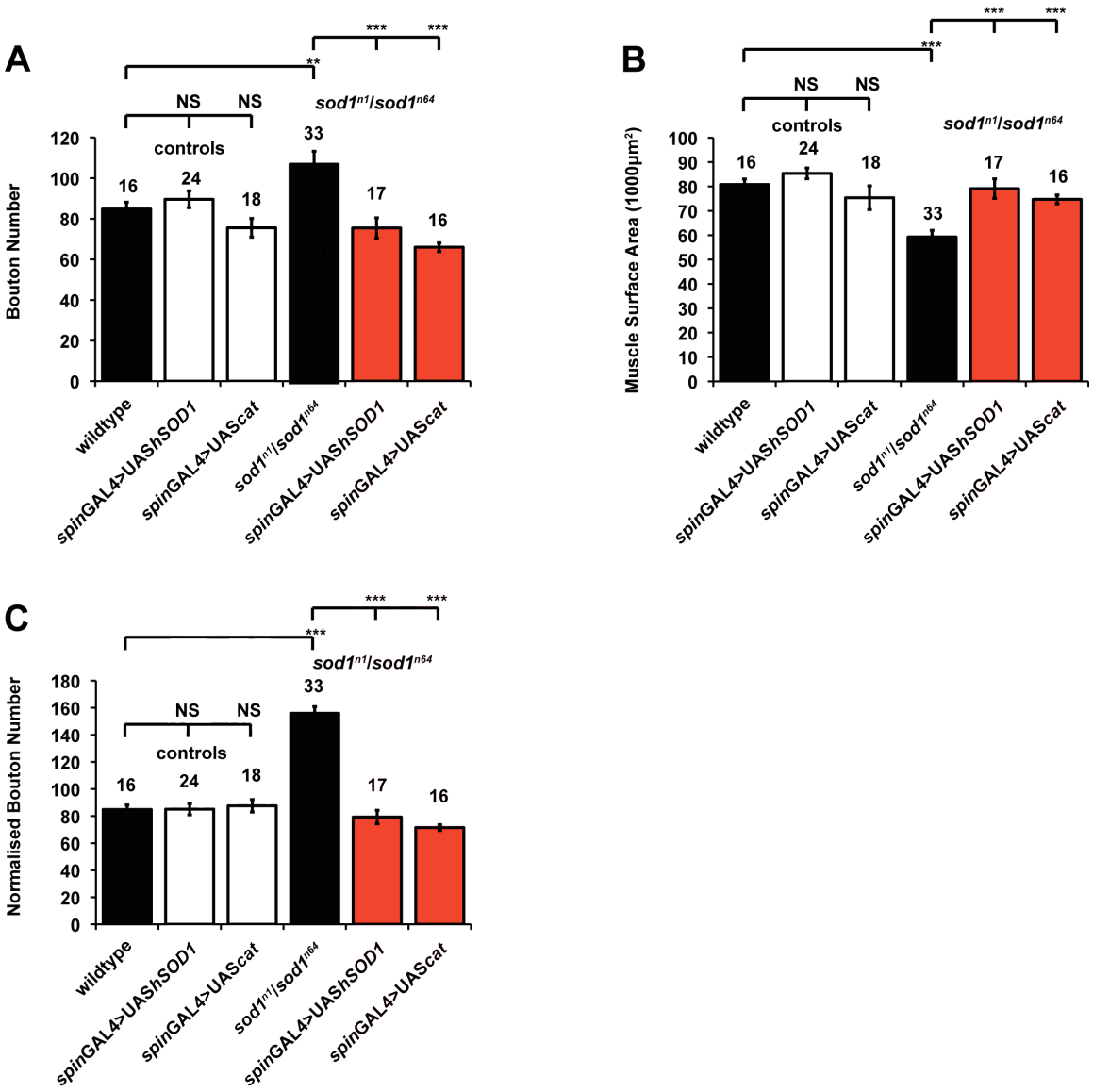

Figure 4.9. Synaptic overgrowth and reduced muscle surface area in *sod1* mutants is rescued by antioxidants. (A) *spin*GAL4>UAS*cat* and *spin*GAL4>UAS*hSOD1* have bouton numbers statistically similar to wildtype; 90±4.12 (n=24) and 76±4.6 (n=18) (p>0.05, ANOVA) respectively. Expression of these anti-oxidant transgenes in a *sod1* background fully rescues bouton number back to wildtype levels with expression of *hSOD1* and *cat* reducing bouton number to 75±5 (n=17) and 66±2.14 (n=16) respectively (p<0.001, ANOVA compared to *sod1* and p>0.05 compared to wildtype). (B) Expression of *hSOD1* and *cat* did not cause any change to muscle surface area in wildtype background; 85387±2237µm^2 and 75369±2744µm^2 respectively. Expression of these transgenes in *sod1* transheterozygotes rescues muscle surface area back to wildtype level; 79112±3990µm^2 and 74703±1805µm^2 for *hSOD1* and *cat* respectively (**p<0.01, ***p<0.001, ANOVA compared to *sod1*

transheterozygotes and p>0.05, ANOVA compared to wildtype). (C) Following normalisation expression of the anti-oxidants transgenes *hSOD1 and cat* does not cause any change in bouton number; 85±3.32 and 88±8.67. Expression of these transgenes in *sod1* transheterozygotes significantly reduces bouton number from 156±9.95 to 79±5.85 and 72±1.81 for *hSOD1* and *cat* respectively (p<0.001, ANOVA, compared to *sod1* mutants and p>0.05 ANOVA compared to wildtype).

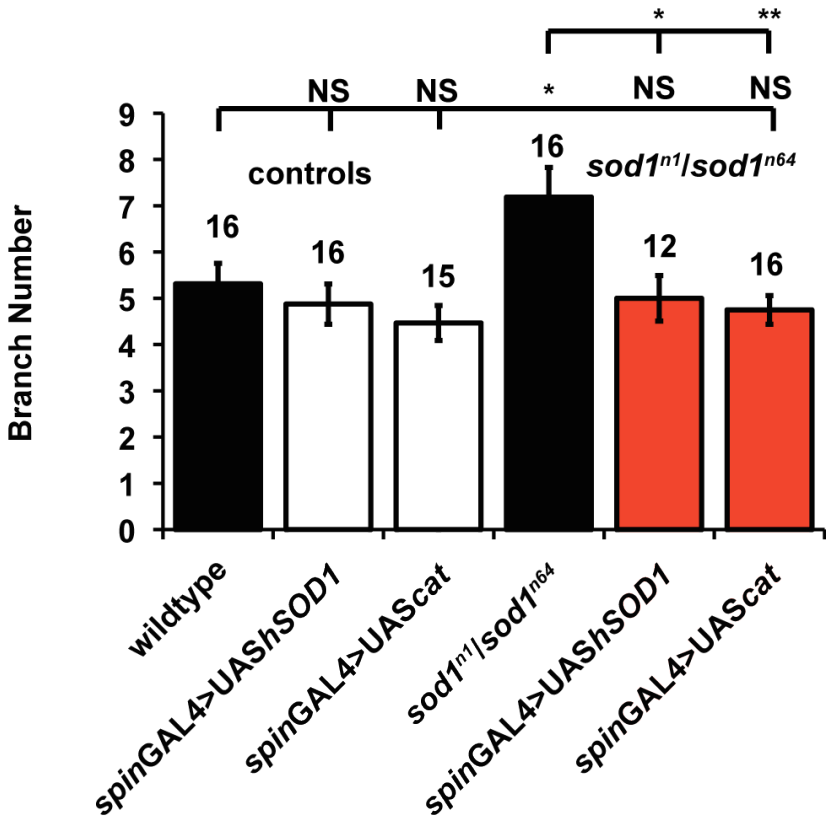

Figure 4.10. Change in branch number in *sod1* mutants is rescued by antioxidants (A) *spin*GAL4>UAS*cat* and *spin*GAL4>UAS*hSOD1* have branch numbers statistically similar to wildtype; 4.9±0.44 (n=16) and 4.7±0.38 (n=15) (p>0.05, ANOVA) respectively. sod1 mutants have increased branching with a mean of 7.2±0.64 (n=16) (p<0.05, ANOVA). Expression of these anti-oxidant transgenes in a *sod1* background fully rescues branch number back to wildtype levels with expression of *hSOD1* and *cat* reducing branch number to 5±0.49 (n=12) and 4.75±0.31 (n=16) respectively (p<0.05, p<0.01 ANOVA compared to *sod1* and p>0.05 compared to wildtype).

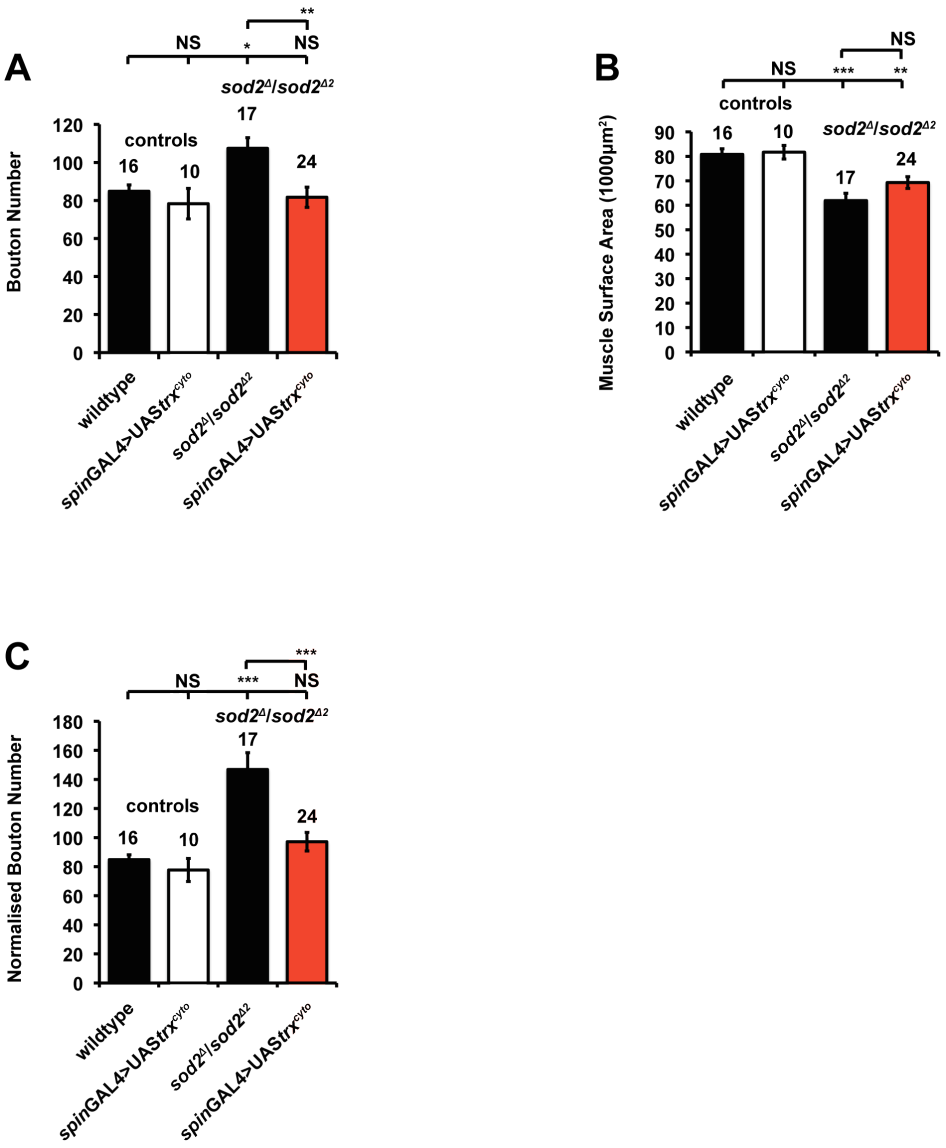

Figure 4.11. Synaptic overgrowth, but not reduced muscle surface area, in *sod2* mutants is rescued by antioxidants. (A) *spin*GAL4>UAS*TrxR*^{CYTO} doesn't cause any change in bouton 78±8.01 (n=10) in a reduction in bouton number from 107±5.59 (n=17) to 82±5.31 (n=24) ($p<0.01$); this rescue is significantly similar to wildtype ($p>0.05$, ANOVA). (B) *spin*GAL4>UAS*TrxR*^{CYTO} doesn't affect muscle surface area; 81684±2755 compared to wildtype 80801±2265µm^2 ($p>0.05$, ANOVA). *sod2* mutations result in decreased muscle surface area; 61909±3000µm^2 ($p<0.001$, ANOVA). This is not affected by *TrxR*^{CYTO} expression; 69271±2378µm^2 ($p>0.05$, ANOVA compared to *sod2* transheterozygotes). (C) Following normalisation *spin*GAL4>UAS*TrxR*^{CYTO} has a bouton number of 78±7.93, similar to wildtype 85±3.32 ($p>0.05$, ANOVA). Expression of *TrxR*^{CYTO} in *sod2* mutants reduced bouton number from 147±11.6 to 97±6.39 ($p<0.001$, ANOVA), this is not significantly different to wildtype ($p>0.05$, ANOVA).

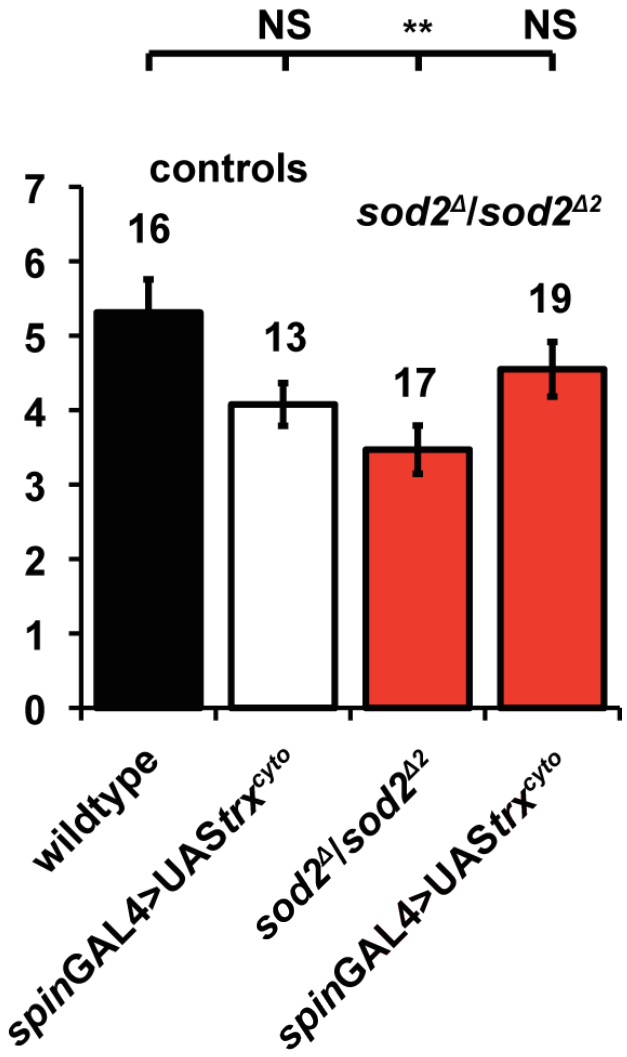

Figure 4.12: Reduced branching in *sod2* mutants is rescued by antioxidants. *spin*GAL4>UAS*TrxR*^{CYTO} doesn't cause any change in branch number (n=13) but does increase *sod2* branch number from 3.5±0.32 (n=17) ($p<0.01$, ANOVA compared to wildtype) to 4.55±0.39 (n=19) ($p>0.05$, ANOVA, compared to wildtype).

4.3. Discussion

The general trend of the data above is that oxidative stress causes an increase in bouton number coupled with a decrease in muscle surface area. Paraquat

causes overgrowth of the synapse, which is rescued by expressing *UAS-hSOD1* pre- and post-synaptically. This however does not rescue muscle surface area, suggesting that oxidative stress is the causative factor in synapse overgrowth whereas the reduction in muscle surface area is not relieved at all by expression of this transgene suggesting that it is an energy deficit, or some other cellular effect of the paraquat that results in the significant reduction of muscle surface area. Alternatively, the level of anti-oxidant expresision was not sufficient to rescue this phenotype, or the cells were suffering from increased levels of hydrogen peroxide, due to increased SOD activity. Expression using a stronger promoter such as *tubulin*GAL4 or expression of a battery of antioxidants could answer these questions. However, this was not investigated in this study as synaptic overgrowth is the focus of this investigation and this was fully rescued by expression of *spin*GAL4>UAS*hSOD1*.

All the mutations investigated that cause oxidative stress cause a significant reduction in muscle surface. However rotenone did not cause any reduction in muscle size. This could be due to a number of reasons, such as the dose of rotenone not causing the threshold level of oxidative stress required to result in impaired muscle development. It would be interesting to analyse the comparative levels of oxidative stress in the conditions studied here and investigate the correlation between oxidative damage, activation of stress response and synaptic phenotypes. Not all the mutations cause changes in bouton number, relative to the muscle surface area. This, taken together with the data shown above that rotenone, in fact, causes a significant decrease in normalised bouton number; suggest that oxidative stress does not always cause synaptic overgrowth. This shows that the effects of oxidative stress can vary greatly and depend on the level, source and species of ROS involved. There could be a number of reasons for the differential effects observed. Firstly activation of different cellular signalling pathways could cause the different effects. Another reason for rotenone causing synaptic undergrowth could be

through the effects of rotenone on microtubule formation. Rotenone impairs the formation and generation of microtubule networks (Brinkley *et al.*, 1974; Srivastava and Panda, 2007). Autophagy and many other cellular processes depend on normal microtubule function/form. Autophagy has been shown to drive synapse growth (Shen and Ganetzky, 2009), and normal synaptic formation can be impaired by cytoskeletal disruption (Koch *et al.*, 2008) hence this could explain the effects of rotenone on synapse development.

sod1 and *sod2* mutants show very similar muscle surface area and bouton number however the other phenotypes investigated differ greatly. As discussed earlier, *sod1* is predominantly cytoplasmic but also expressed in the inner mitochondrial membrane, whereas *sod2* is expressed in the mitochondria. This suggests that the bouton number and muscle surface area are determined by the general presence of oxidative stress in these mutants, while the bouton size and branch number may be determined by the origin of the oxidative stress. This could indicate that different pathways are involved in the generation of certain neuromuscular junction phenotypes. However mutations that are known to cause oxidative stress do not always cause synaptic overgrowth*, sdhB* and *cat* both cause oxidative stress but without any significant synaptic overgrowth, in fact *sdhB* shows a significant undergrowth prior to normalisation. The role of *cat* requires more investigation as it does cause a significant increase in bouton number relative to muscle surface area, when statistical analysis is carried out without *sod*. The consistent phenotype is the reduction in muscle surface area, but conclusions can also be drawn that oxidative stress can cause synaptic overgrowth as suggested by the data that show the effects of relieving oxidative stress in these mutations.

Mutations in SOD would lead to increased level of superoxide anions, and it is somewhat counter-intuitive that overgrowth in both *sod1* and *sod2* can be rescued by expressing anti-oxidants that catalyse the conversion of hydrogen

peroxide. However, this does suggest that it is the overall level of oxidative stress that drives synaptic growth. This however is somewhat paradoxical because as discussed earlier not all cases of increased ROS lead to synaptic overgrowth suggesting specificity dependent on ROS species and source. It might be significant to note that expressing predominantly cytoplasmic antioxidants in primarily mitochondrial forms of oxidative stress (paraquat and *sod2)* rescues bouton number but not muscle surface area. Perhaps indicative of the signalling caused by oxidative stress leading to increased bouton addition, whereas reduced muscle size could be due to energy deficit and metabolic defects caused by mitochondrial dysfunction, or due to differential activation of signalling pathways in response to cytoplasmic and mitochondrial derived ROS.

5. JNK/AP-1 Signalling and Autophagy are Required for Overgrowth of the Neuromuscular Junction

5.1. Introduction

JNK/AP-1 signalling is activated in response to oxidative stress (Klintworth *et al.*, 2007, Wang *et al.*, 2003); in fact JNK was originally identified as a stress activated protein kinase (SAPK). In addition this pathway has been seen to regulate synaptic development (Sanyal *et al.*, 2002 and 2003). Increased neuronal expression of Fos and Jun together as AP-1 increases bouton number, whereas depleting activity of either one in the neuron has been shown to reduce bouton number and synaptic strength (Sanyal *et al.*, 2002). Furthermore, neuronal expression of wallenda, a JNKKK, and its downstream effectors, JNK and Fos are necessary for synaptic overgrowth in *highwire* (Collins *et al.*, 2006). Given the commonality in the pathways involved in synaptic development and the oxidative stress response it was investigated whether JNK/AP-1 signalling is upregulated in *spinster* and other conditions involving oxidative stress and whether this is causing the synaptic overgrowth seen to be caused by oxidative stress. More recently, activation of autophagy has been shown to drive NMJ expansion (Shen and Ganetzky, 2009). Increased neuronal expression of Atg1, involved in the initiation of autophagy, drives synapse overgrowth, and neuronal expression of Atg1 rescues the reduction in bouton number seen in *atg1* mutants (Wairkar *et al.*, 2009; Shen and Ganetzky, 2009). Autophagy mutants are believed to cause a reduction in bouton number due to accumulation of *highwire*. As discussed earlier Highwire, is an E3 ubiquitin ligase that is involved in the breakdown of wallenda, a JNKKK (Collins *et al.*, 2006). Thus when autophagy is defective highwire builds up so there is an elevated level of

breakdown of wallenda leading to reduced activity in the downstream signalling pathway. This in turn reduces JNK signalling. Accordingly, with increased neuronal expression of atg1 there is an increased level of synaptic growth, as more highwire is broken down, disinhibiting wallenda and downstream signalling, promoting synaptic growth. Hence, wallenda and JNK are required for synaptic overgrowth in the presence of increased autophagy (Shen and Ganetzky, 2009). This suggests that wallenda and JNK are acting downstream of both autophagy and highwire to promote synapse growth. This is supported by the observation that autophagy is not required for *highwire* induced overgrowth, as mutations in autophagy do not prevent the *highwire* overgrowth phenotype. Although this is indicative of autophagy being upstream of JNK signalling, oxidative stress activates autophagy through JNK signalling (Wu *et al.*, 2009). Autophagy is activated in response to oxidative stress to protect the cell by degradation of damaged proteins, lipids and organelles (Li *et al.*, 2006; Ogata *et al.*, 2006; Arsham and Neufeld, 2009). Oxidative stress can also activate autophagic cell death (Higgins *et al.*, 2011; Chen *et al.*, 2008; Cheng *et al.*, 2009). This suggests that oxidative stress could be activating JNK signaling leading to synaptic overgrowth and it was reasoned that activation of autophagy would be critical to the process of synaptic overgrowth induced by oxidative stress. It is possible that activation of these pathways is cyclical as autophagy is known to act upstream of JNK signalling but also be activated by JNK signalling. Moreover, JNK activity directly regulates autophagy through regulation of Beclin; otherwise known as atg6 (Park *et al.*, 2009) and JNK regulates FoxO dependent autophagy (Pattingre *et al.*, 2006).

5.2. Results

5.2.1. Oxidative stress and *spinster* overgrowth share the same genetic pathway; *spinster* and *sod1* induced overgrowth act synergistically

Firstly, it was determined whether *spinster* and *sod1*-induced overgrowth were acting through the same genetic/signalling pathway**.** This was done analyzing heterozygote mutations of *sod1* and *spin*. Heterozygotes of two *spinster* mutants, $spin^4$/+ and $spin^5$/+ have bouton numbers similar to wildtype.

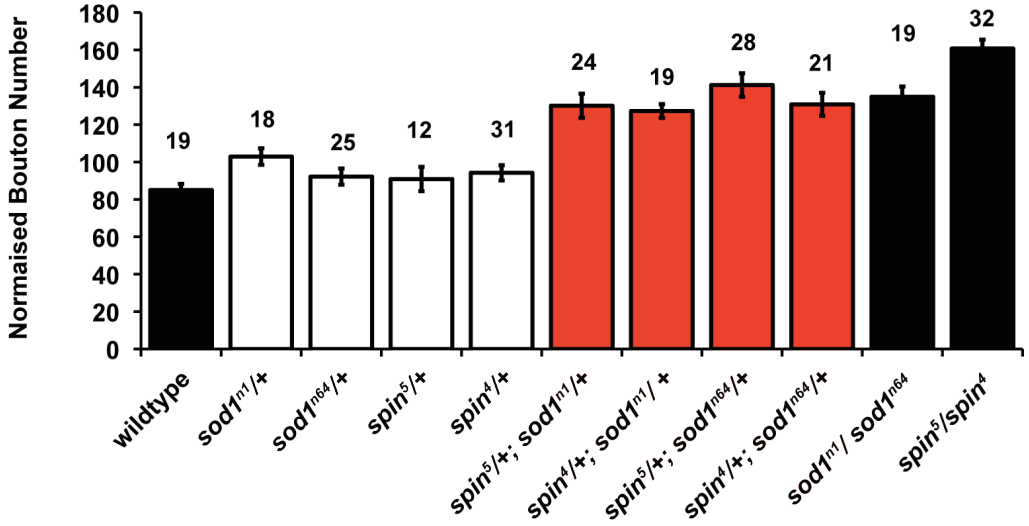

Figure 5.1: Mutations in sod1 and spin act synergistically to cause synaptic overgrowth. Larvae carrying heterozygous mutations for both sod1 and spin are significantly overgrown compared to the heterozygous mutations alone. Wildtype, sod1n1/+, sod1n64/+, spin4/+ and spin5/+ are not statistically significantly different (p>>0.05) with bouton numbers of 103±4.4 (n=18), 92±4.3 (n=92), 91±6.5 (n=12) and 94±4.1 (n=31) respectively. In all combinations, mutants of spin and sod1 are overgrown compared to wildtype or the constituent heterozygotes alone (p<0.001 ANOVA).

Similarly, *sod1* mutant heterozygotes ($sod1^{n1}$/+ and $sod1^{n64}$/+) do not lead to significant overgrowth (ANOVA p>0.05). However, combining these mutations in

a single animal by removing one functional copy of *spinster* and one copy of *sod1* so that each larva only has one wildtype copy and one mutant copy of each gene generates a significant increase in bouton number when compared to relevant heterozygotes (ANOVA $p<0.001$). Animals carrying heterozygous mutations in both *sod1* and *spinster* have a synaptic overgrowth that resembles the *spin* or *sod1* full mutant phenotypes suggesting a shared genetic pathway (Fig. 5.1). Having established that *spinster* and *sod1* act synergistically, with mutations in both causing a certain threshold to be reached at which synaptic overgrowth occurs, the next step was to determine which signalling pathways are activated in *spinster* and oxidative stress to contribute to synapse overgrowth.

5.2.2. JNK signalling is upregulated in *spinster*

JNK/AP-1 is a pathway widely known to be activated by oxidative stress (Wang *et al.*, 2003); it is also a known regulator of synaptic growth (Sanyal *et al.*, 2002). To test whether the JNK signalling pathway has been activated in *spinster* a puckered LacZ enhancer trap was used. Activation of the AP-1 pathway is known to directly transcriptionally activate *puckered*, a phosphatase inhibitor of JNK that mediates a feedback loop to regulate JNK signalling (Martin-Blanco *et al.*, 1998). Larval muscles in *spinster* were examined for the activation of the AP-1 pathway using the puc^{E69} enhancer trap by comparing β-galactosidase (ß-gal) expression to ascertain the relative activation of JNK/AP-1 signalling.

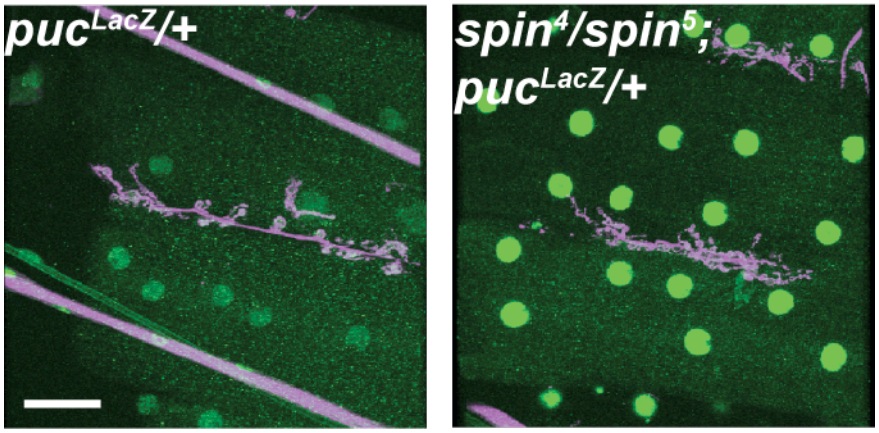

Figure 5.2: *puckered* is upregulated in *spinster*: Expression of *puc*^{LacZ}, an enhancer trap reporter of JNK/AP-1 activation, is increased in the muscle in spin compared with wildtype, nerves shown in magenta, LacZ in green. Scale bar = 40µm.

Greatly increased expression of ß-gal is seen in *spinster* compared to wildtype this was observed by immunofluorescence (keeping the settings the same for both genotypes) indicating an activation of the AP-1 pathway in muscles of *spinster* (Fig. 5.2). Having established that JNK/AP-1 signalling is upregulated in *spinster* the next line of investigation was to establish whether over activity of this pathway is causative in the generation of synapse overgrowth in *spinster*.

5.2.3. Components of AP-1 modify synapse development

To establish how AP-1 regulates synapse growth and the GAL4/UAS system was used to overexpress Jun and Fos either separately or together as AP-1 in the nerve, muscle or both. The presynaptic functions of Fos and JNK are relatively well documented. It has previously been shown that neuronal overexpression, of both Jun and Fos leads to increased growth (Sanyal *et al.*, 2002), and depletion of either through expression of a dominant negative reduces bouton number, suggesting they are acting as a heterodimer. Overexpression of AP-1 in the muscle was not shown to increase bouton number (Sanyal *et al.*, 2003). However, only Fos is implicated in *highwire*-

induced overgrowth, suggesting that Fos is able to act as a homodimer in a model of synapse overgrowth (Collins *et al.*, 2006).

The data shown here (Fig. 5.3) are somewhat at odds with this previously published data. Fig. 5.3 shows that expression of Jun or Fos in the neuron or the muscle alone does not alter bouton number significantly compared to wildtype, in agreement with Sanyal *et al.* (2002). However, expression of Jun simultaneously in the nerve and muscle with *spin*GAL4 causes a 26% increase in bouton number ($p<0.05$, ANOVA). This is the only significant difference when all the values shown in the graph are compared using ANOVA. However, more differences can be seen when comparing only one driver or one UAS construct. When expression of UAS*Fos* under control of the *MHC*GAL4, *elaV*GAL4 and *spin*GAL4 are compared alone, simultaneous expression of Fos in the muscle and nerve results in a significant reduction in bouton number ($p<0.05$, ANOVA). Expression of Fos and Jun, together as AP-1, does not cause any change in bouton number with any of these GAL4 drivers. This is at odds with the published data but correlates with Jun providing an overgrowth and Fos an undergrowth with *spin*GAL4. Expression of these transgenes in any combination does not significantly affect muscle surface area (Fig. 5.3B). However, when normalised for muscle surface area there is a slight change in the level of significance of overgrowth caused by overexpression of Jun. Following normalisation, neuronal expression still does not significantly affect bouton number, however both muscular and simultaneous expression in the nerve and muscle cause a significant overgrowth ($p<0.05$, ANOVA). Expression of Fos or AP-1 controlled by these three drivers does not significantly affect normalised bouton number (Fig, 5.3C).

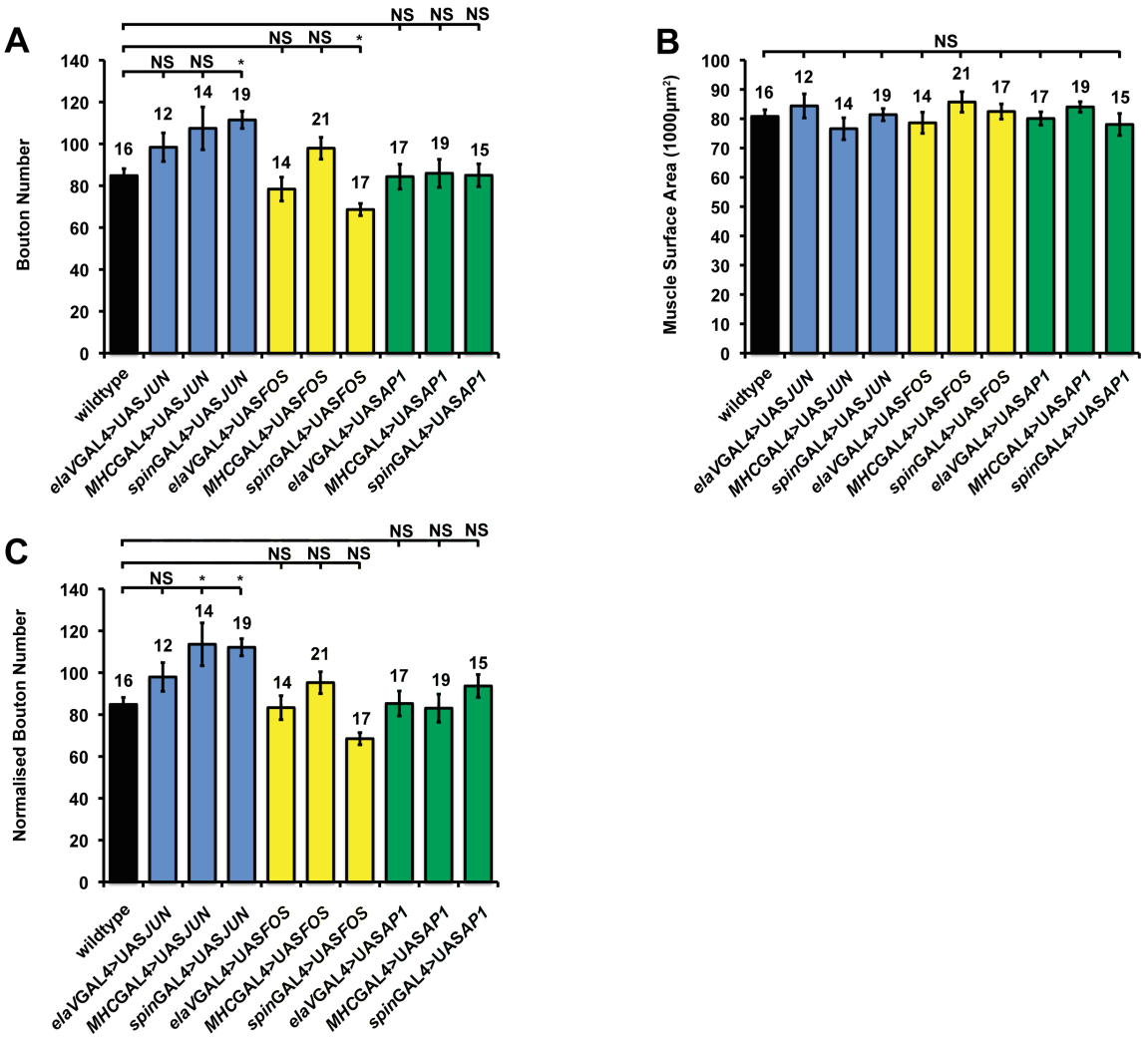

Figure 5.3: Fos and Jun can alter synapse growth. (A) Neuronal or muscular overexpression of JUN does not alter bouton number; 98±6.8 (n=12) and 107±10.2 (n=14). Concurrent expression with s*pin*GAL4 causes significant overgrowth 111±4.1(n=19) ($p<0.05$, ANOVA). Neuronal or muscular expression of FOS did not cause any change in bouton number, 78±5.7 (n=15) and 98±5.2 (n=14). Expression pre- and post-synaptically causes a reduction in bouton number to 69±2.9 (n=21, $p<0.05$, ANOVA). Expression of AP-1 in either the muscle or the nerve or both causes no change in bouton number, 84±5.9 (n =17). (B) Expression of any of these transgenes causes no change in muscle surface area ($p>>0.05$, ANOVA). (C) Following normalisation for muscle surface area, neuronal expression did not significantly change bouton number: 98±9.0 (n=12) whereas *MHC*GAL4>JUN or *spinG*AL4>J*UN* have significantly increased bouton numbers of 114±10.1 (n=14) and 112±5.3 (n=19), respectively. Expression of FOS pre- or post-synaptically or both causes no change in normalised bouton number: 83±7.1 (n=15), 95±7.6 (n=14) and 68±3.4 (n=21) respectively ($p>0.05$, ANOVA). Expression of FOS and JUN together also causes no

change in normalised bouton number when expressed pre- or post-synaptically or both with normalised bouton numbers of 85±5.5 (n=17), 83±6.5 (n=18) and 94±9.2 (n=15) ($p>0.05$, ANOVA).

5.2.4. Reducing JNK/AP-1 signalling rescues *spinster* induced overgrowth

Once again the GAL4/UAS system was employed, this time to dissect the signalling pathway involved in the generation of synaptic overgrowth. Dominant negative transgenes for components of ASK/JNK/AP-1 signalling were expressed simultaneously pre- and post- synaptically (using *spin*GAL4). These dominant negative transgenes act to reduce normal activity through competing with the endogenously produced protein. The ASK dominant negative transgene is UAS-*ask*^{K618M} and is kinase dead and can therefore not activate its downstream signalling partners through phosphorylation (Kuranaga *et al.*, 2002). UAS-*jnk*^{K53R} is also a kinase dead form of the enzyme (Madhani *et al.*, 1997; Weber *et al.*, 2000). The Jun and Fos dominant negatives act in a different manner. Jun and Fos are B-Zip domain transcription factors, this family of TFs act as dimers and they contain a B-Zip domain that comprises a sequence specific DNA binding domain and a leucine zipper domain that is needed for the dimerisation of two DNA binding domains. The dominant negative transgenes of Jun and Fos, originally known as Jbz and Fbz respectively, only contain a bZIP fragment which means they act in a dominant negative fashion as they are able to bind DNA but unable to initiate transcription (Bohmann *et al.*, 1994; Eresh *et al.*, 1997).

As discussed earlier, ASK is a JNKKK that has been identified for its role in the stress response, however it has not previously been identified as having a role in synapse development. The role of ASK in the synaptic phenotypes identified was investigated due to its important role in regulating the stress response.

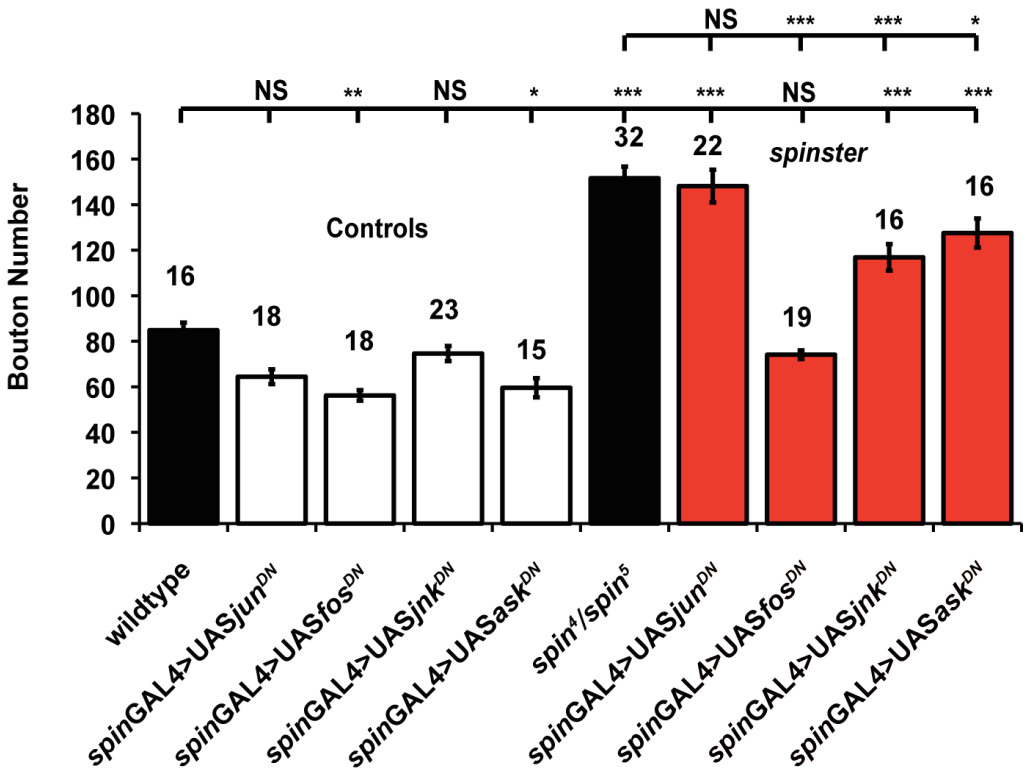

Figure 5.4: ASK/JNK/AP-1 signalling is required for *spinster* overgrowth. Expression of *spin*GAL4>UAS*jun*^{DN}or UAS*jnk*^{DN} in a wildtype background did not cause any change in bouton number compared to wildtype with bouton numbers of 64±3.24 (n=18) and 75±3.31 (n=23). *spin*GAL4>UAS*fos*^{DN} or UAS*ask*^{DN} cause a significant reduction in bouton number from 85 in wildtype to 56±2.3 (n=18) and 60±4.18 (n=15) respectively. Expression of *jun*^{DN} in a *spinster* background does not rescue overgrowth with a bouton number of 148±7.19 (n=22), not significantly different to *spinster* 152±5.1 (n=32) ($p>0.05$, ANOVA). Expression of *fos*^{DN} reduces *spinster*-induced overgrowth to 74±1.92 (n=19) ($p<0.001$, ANOVA) back to wildtype levels ($p>0.05$, ANOVA, compared to wildtype). Whereas *jnk*^{DN} and *ask*^{DN} only partially rescue bouton number to 117±5.79 (n=16) and 128±6.37 (n=16) ($p<0.001$ and 0.05, ANOVA) respectively, both significantly different to wildtype ($p<0.001$, ANOVA). Bouton counts of *spinster* with *jun*^{DN} *and fos*^{DN} carried out by Kate Gowers.

ASK, JNK, Fos and Jun dominant negative transgenes were expressed in *spinster* to establish which components of this signalling cascade are involved in the generation of synaptic overgrowth in *spinster*. As a control the dominant negative transgenes were expressed in a wildtype background. Expression of *jun*^{DN} and *jnk*^{DN} did not significantly affect bouton number, whereas expression

of *fos*^{DN} or *ask*^{DN} result in reduced bouton number. This is the first time that ASK has been suggested to have a role in synapse development in *Drosophila*.

The data here show that synaptic overgrowth in *spinster* is significantly reduced by depleting Fos, JNK and ASK signalling while reducing Jun activity did not reduce overgrowth. Reducing JNK or ASK signalling only provided a partial rescue, with the bouton numbers still significantly different to wildtype (Fig.5.4).

Conversely, reducing Fos signalling in *spinster* mutants gives a bouton number not statistically different to wildtype; a full rescue. To reaffirm these results JNK/Fos signalling was depleted in a different manner, namely, by expressing RNAi lines to reduce transcription of the target genes (Fig. 5.5). In a wildtype background expression of *Fos*RNAi does not reduce bouton number like expression of the dominant negative transgene does. Depleting JNK signalling through expression of RNAi in a wildtype background showed a significant reduction in bouton number, disparate to the effect of reducing signalling with the dominant negative. Expressing FosRNAi and JNKRNAi in a *spinster* mutant background similarly reduced bouton number consistent with the reduction observed using the dominant negative constructs. However the rescue observed with UAS*fosRNAi* was not as strong as the rescue with UAS*fos*^{DN}, suggesting that the reduction in the level of Fos signalling is not as much with RNAi. This is supported by the observation above that *Fos*^{DN} causes a significant reduction in bouton number where as *FosRNAi* does not. This would be expected as it is well known that some RNAi constructs deplete their cognate targets with variable preference (Dietzl *et al.*, 2007) and reduction of target mRNA is rarely total.

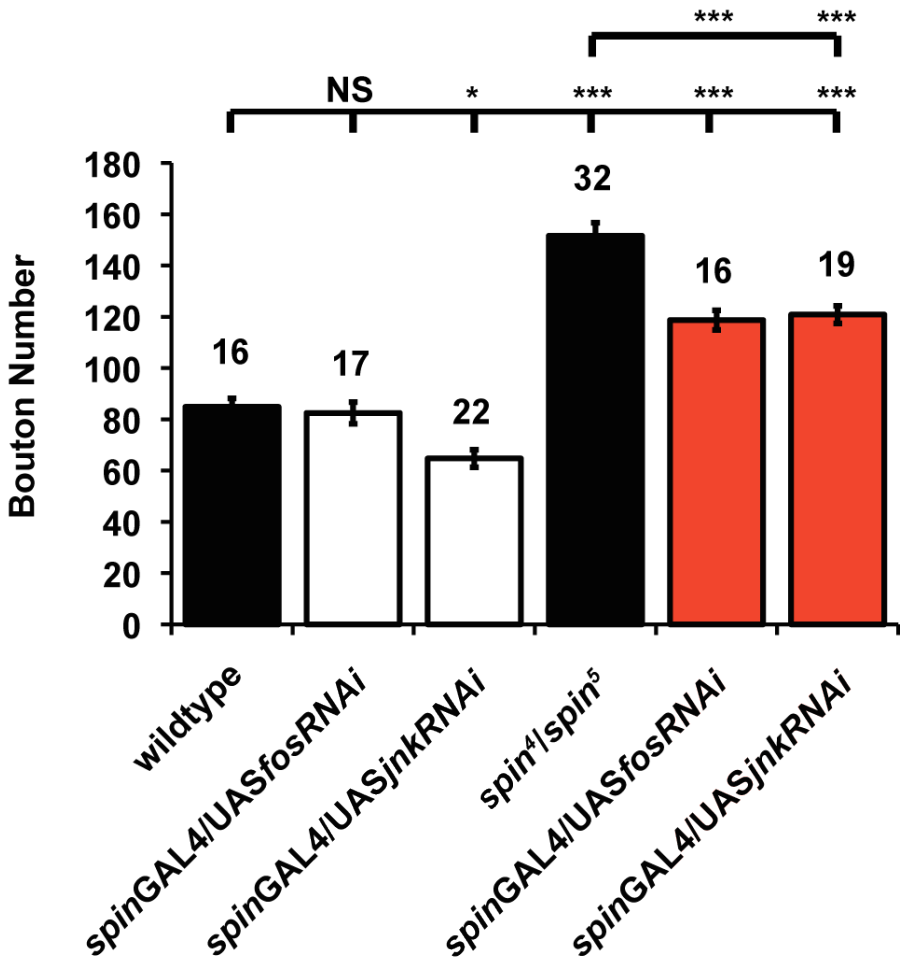

Figure 5.5: JNK/Fos signalling is required for *spinster-induced* overgrowth. *spin*GAL4>UAS*fosRNAi* causes no change in bouton number 82±4.24 (n=17). Expression of *jnk*RNAi causes a significant reduction in bouton number to 65±3.44 (n=22). Expression of these transgenes in *spinster* causes a reduction in bouton number from 152±5.06 to 119±3.81 (n=16) and 121±3.45 (n=19) ($p<0.001$, ANOVA).

5.2.5. Fos is required both pre- and post- synaptically for *spinster* induced overgrowth

As discussed earlier, expression of fos^{DN} simultaneously pre- and post-synaptically under the control of *spin*GAL4 provides a full rescue of *spinster*-induced overgrowth. Expression either pre- or post- synaptically using either *elaV*GAL4 or *MHC*GAL4 respectively affords partial rescue, with a bouton number between that of the mutant and simultaneous expression (Fig. 5.6). This

suggests that signalling is required both from the muscle and the nerve and that overactivation of Fos signalling in both leads to overgrowth seen in *spinster*.

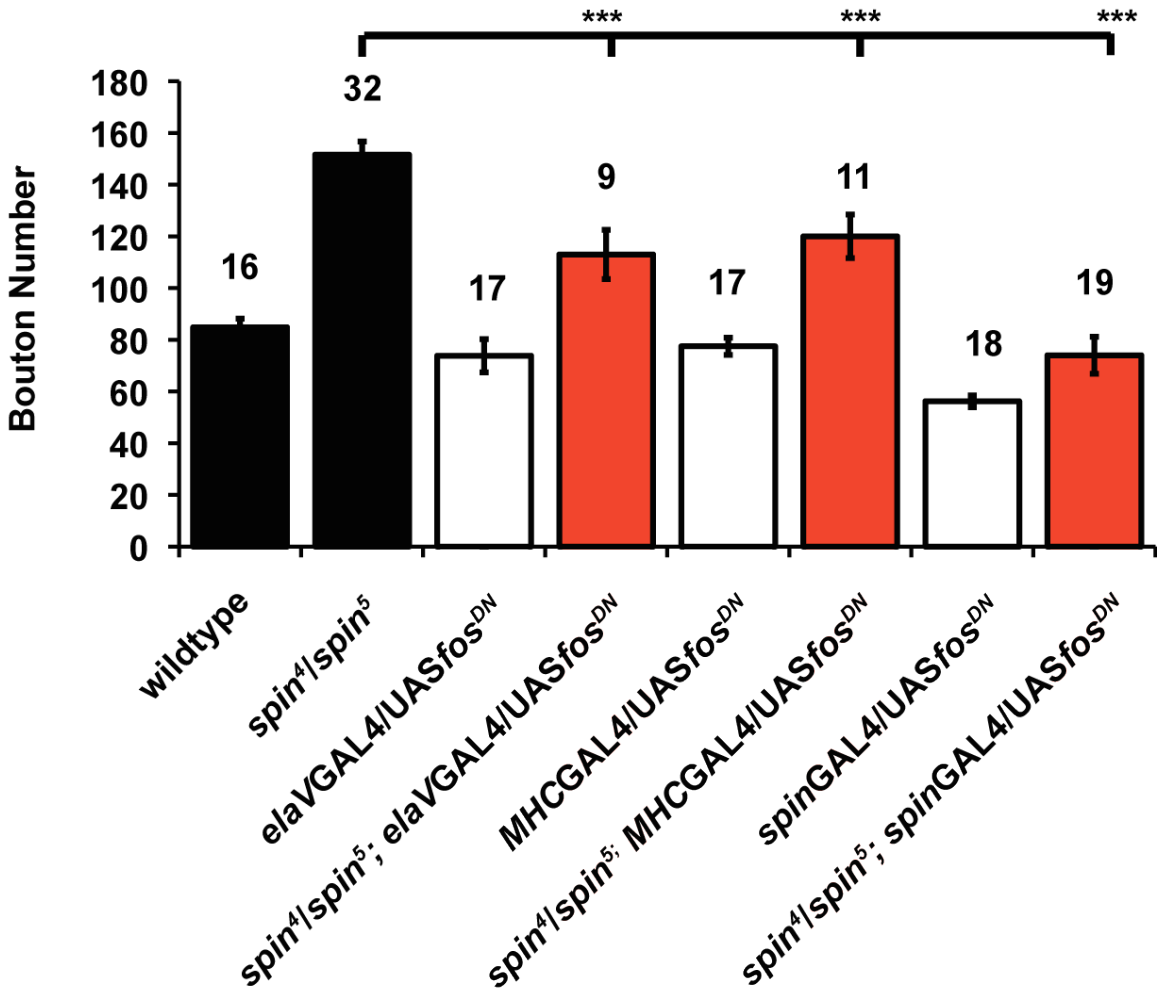

Fig. 5.6: Fos signalling is required pre- and post- synaptically for *spinster* induced synapse overgrowth. Expression of fos^{DN} pre-synaptically and post-synaptically causes no change in bouton number in a wildtype background 68±3.3 (n=20) and 79±3.68 (n=22). Expression in *spinster* reduces synaptic overgrowth to 113±9.49 (n=9) and 120±8.42 (n=11) respectively ($p<0.001$, ANOVA). Bouton counts in *spinster* with dominant negative transgenes performed by Kate Bowers

5.2.6. JNK signalling is upregulated by paraquat

The transgene puc^{E69} was used to investigate *puckered* transcript levels in paraquat fed animals. There is an upregulation compared to wildtype; indicative

of increased JNK/AP-1 activity (Fig. 5.7). This suggests that similar pathways are involved in the generation of synaptic growth caused in paraquat, as those shown to be involved in *spinster* induced overgrowth.

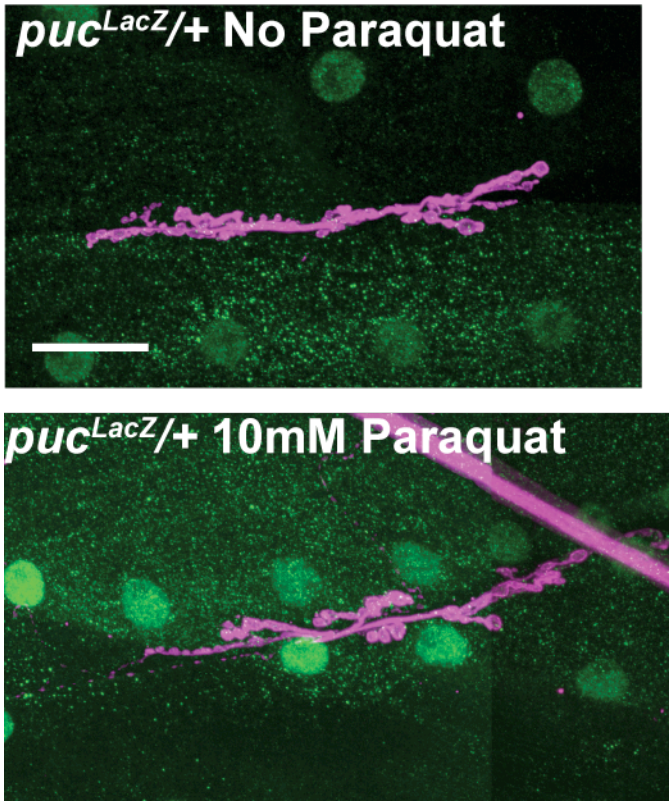

Figure 5.7: *puckered* is upregulated in paraquat-fed animals: Expression of puc^{LacZ}, an enhancer trap reporter of JNK/AP-1 activation, is increased in the muscle paraquat fed animals compared with controls, nerves shown in magenta, LacZ in green. Scale bar = 40μm.

5.2.7. Reducing ASK/JNK/AP-1 signalling reduces paraquat induced overgrowth

The same transgenes used in the *spinster* experiments were also used to dissect the signalling pathways involved in synaptic growth in paraquat fed animals. All components of the signalling pathway investigated, jun, fos, JNK and ASK, were found to be required for the synaptic growth induced by this treatment.

In the absence of paraquat, prior to normalisation fos^{DN} and ask^{DN} cause a significant reduction in bouton number expressed simultaneously pre- and post-synaptically under the control of *spin*GAL4. This indicates that Fos and ASK are important in normal synaptic development. Depleting *Jun* or *JNK* signalling in the absence of paraquat does not alter bouton number (Fig. 5.8A). Expression of any of these transgenes doesn't alter muscle surface area in the absence of paraquat (Fig. 5.8B). Following normalisation only *spin*GAL4>UASask^{DN} has a significantly reduced bouton number in the absence of paraquat. (Fig. 5.8C).

In the presence of 10mM paraquat, prior to normalisation for muscle surface area, depletion of Jun or Fos significantly reduces bouton number. Expression of jnk^{DN} or ask^{DN} with exposure to 10mM paraquat results in a bouton number not significantly different to wildtype in the presence of 10mM paraquat (Fig. 5.8A). *spin*GAL4>UASjun^{DN} partially rescues the reduction in muscle surface area caused by 10mM paraquat, so that it is significantly different to the muscle surface area of wildtype in 10mM paraquat. However, the muscle surface areas of *spin*GAL4>UASjnk^{DN} and UASask^{DN} in 10mM paraquat are not significantly reduced compared to wildtype (Fig. 5.8B). Having accounted for changes in muscle surface area through normalisation expression of all any of these transgenes significantly rescues paraquat induced growth, so it is not significantly different to wildtype in the absence of paraquat (Fig. 5.8C).

This data is recapitulated through expression of *jnkRNAi*. Expression of this transgene causes no reduction in bouton number or muscle surface (Fig. 5.9Aand B) area but does reduce paraquat-induced growth ($p<0.01$, ANOVA) back to wildtype levels ($p>0.05$, ANOVA) (Fig. 5.9C). The above data clearly show that ASK, JNK/AP-1 signaliing is required for paraquat-induced growth. The involvement is similar to that seen in *spinster,* in that ASK/JNK/AP-1 are required for both *spinster* and paraquat-induced growth. However, there is differential involvement of Fos and Jun; depletion of Jun signalling does not prevent synaptic overgrowth in *spinster* whereas Jun is required for paraquat induced growth.

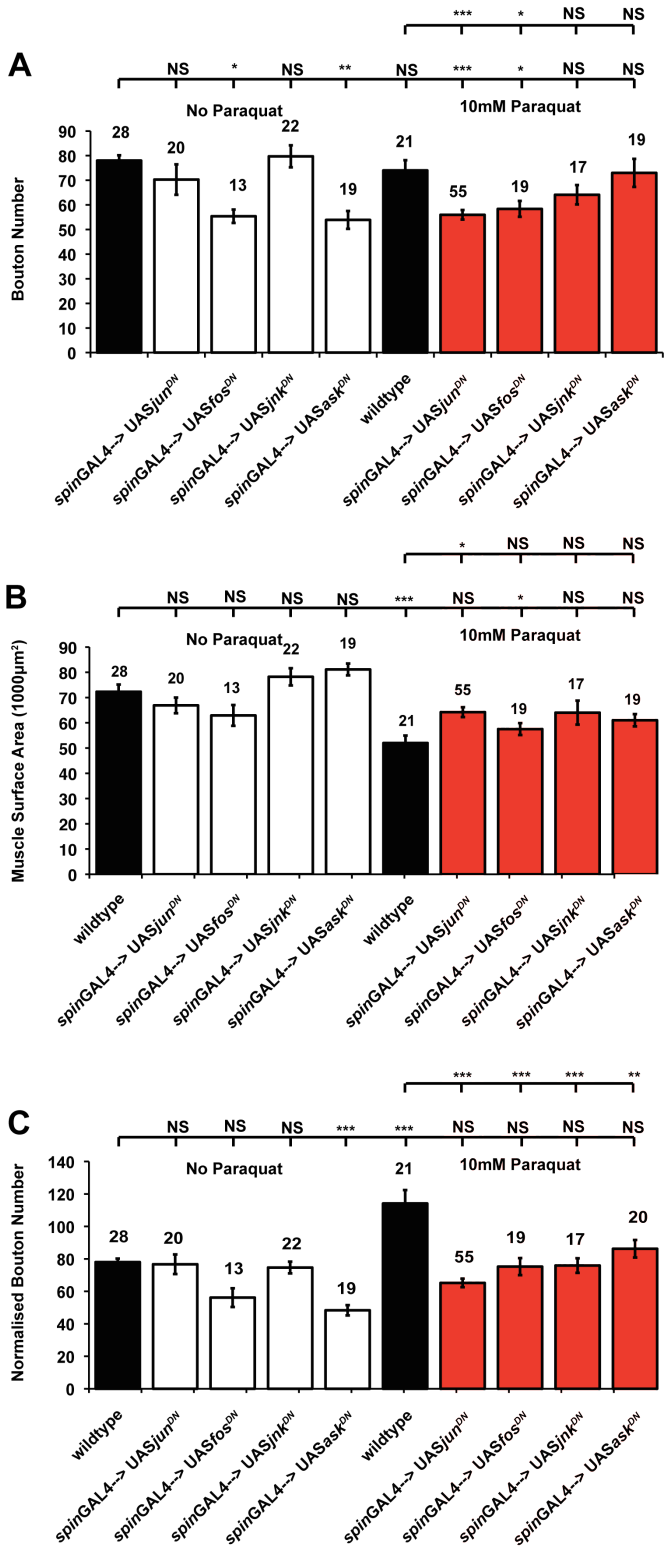
A
No Paraquat
10mM Paraquat
Bouton Number
B
Muscle Surface Area (1000μm²)
C
Normalised Bouton Number
wildtype
spinGAL4--> UASjun^DN
spinGAL4--> UASfos^DN
spinGAL4--> UASjnk^DN
spinGAL4--> UASask^DN

Figure 5.8: ASK/JNK/AP-1 signalling is required for paraquat-induced growth. (A) Prior to normalisation *spin*GAL4>UAS*fos*^{DN} and s*pin*GAL4>UAS*ask*^{DN} cause a significant reduction in bouton number with mean bouton numbers of 55±2.7 (n=13) ($p<0.05$, ANOVA) and 54±3.64 (n=19) ($p<0.001$, ANOVA). *spin*GAL4>UAS*jun*^{DN} *and* *spin*GAL4>UAS*jnk*^{DN} cause no change in bouton number 70±6.2 (n=20) and 80±3.64 (n=19). As shown earlier 10mM paraquat causes no change in bouton number: 74±4.1 (n=21). *spin*GAL4>UAS*jun*^{DN} and *spin*GAL4>UAS*fos*^{DN} cause a significant reduction in bouton number in 10mM paraquat; 56±1.93 (n=55) ($p<0.001$) and 59±3.23 (n=19) ($p<0.05$) respectively. *spin*GAL4>UAS*jnk*^{DN} and s*pin*GAL4>UAS*ask*^{DN} don't cause any change in bouton number in 10mM paraquat 64±3.92 (n=17) and 73±8.29 (n=20) respectively ($p>0.05$, ANOVA).
(B)Expression of *jun*^{DN}, *fos*^{DN}*, jnk*^{DN} and *ask*^{DN} doesn't cause any change in muscle surface area: 66897±3089 μm^2, 62919±4114 μm^2, 78220±3408 μm^2 and μm^2 81124±2992μm^2 respectively ($p>0.05$, ANOVA). As stated earlier 10mM paraquat causes a significant reduction in muscle surface area. Expression of *jun*^{DN}*,* causes a significant increase in muscle surface area in 10mM paraquat to 64243±1950μm^2 ($p<0.05$). This is not significantly different to wildtype in the absence of paraquat ($p>0.05$, ANOVA). *fos*^{DN}*, jnk*^{DN} and *ask*^{DN} cause no significant change in muscle surface area compared to wildtype in 10mM paraquat: 57525±2346 μm^2, 64027±4759 μm^2, 61032±2433μm^2 respectively ($p>0.05$, ANOVA). Only *spin*GAL4>UAS*fos*^{DN} in 10mM paraquat has a muscle surface area significantly different to wildtype in the absence of paraquat ($p<0.05$, ANOVA).
(C)change in normalised bouton number; 77±6.05, 56±5.77 and 75±3.59 respectively ($p>0.05$, ANOVA). *spin*GAL4>UAS*ask*^{DN} causes a significant reduction in normalised bouton number 48±3.2 (n=19) ($p<0.001$, ANOVA). The overgrowth caused by 10mM paraquat is significantly reduced by expression of *jun*^{DN} to 65±2.64 ($p<0.001$, ANOVA), by *fos*^{DN} to 75±5.26 ($p<0.001$, ANOVA), by *jnk*^{DN} to 76±4.49 ($p<0.001$, ANOVA) and by *ask*^{DN} to 86±5.4 ($p<0.01$, ANOVA). These are not significantly different to wildtype in the absence of paraquat ($p>0.05$, ANOVA).

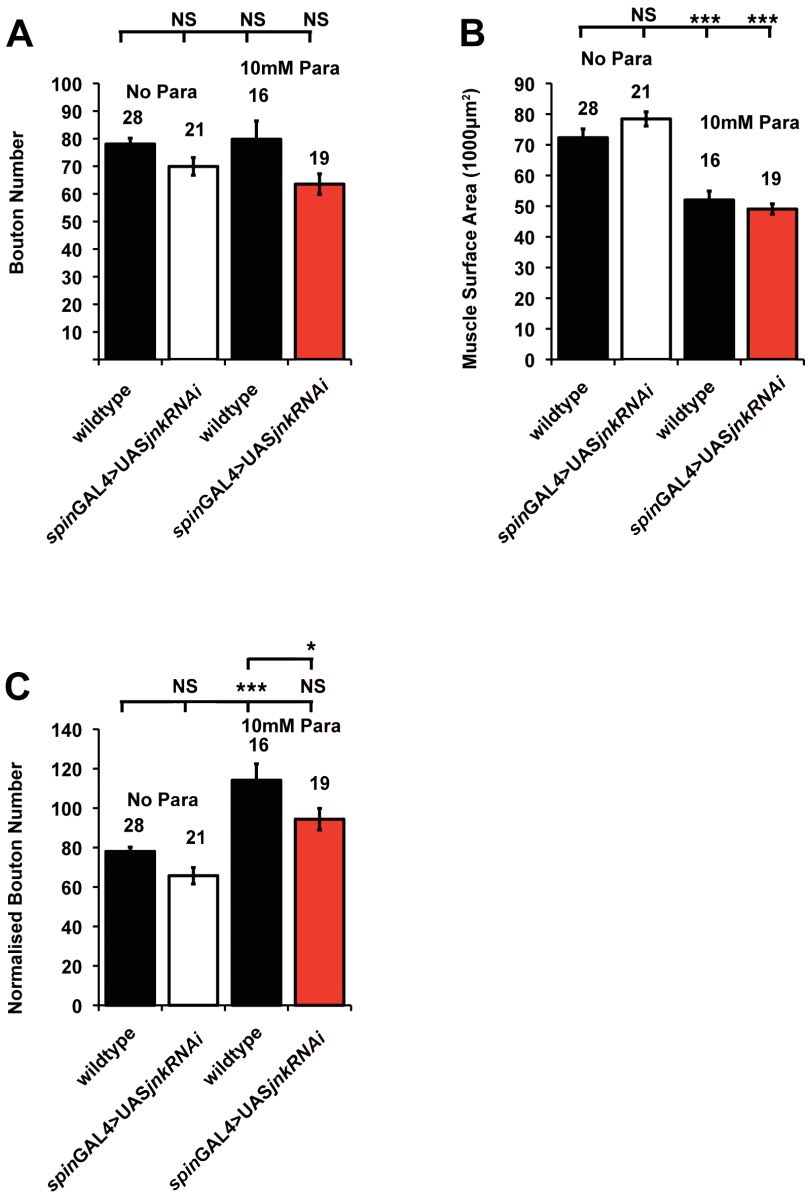

Figure 5.9: JNK signalling is required for paraquat-induced overgrowth.
(A)Expression of *jnkRNAi* causes no change in bouton number either in the absence or presence of paraquat with bouton numbers of 70±3.20 (n=21) and 64±3.73 (n=19) (p>0.05, ANOVA). (B)Expression of *jnkRNAi* causes no change in muscle surface area in the absence of paraquat: 78429±2837µm^2; not significantly different to wildtype (p>0.05, ANOVA). *jnkRNAi* does not rescue muscle surface area compared to wildtype in 10mM paraquat (p>0.05, ANOVA). (C)*spin*GAL4>UAS*jnkRNAi* causes no change in normalised bouton number 66±4.2 compared to wildtype (p>0.05, ANOVA). Expression of *jnkRNAi* significantly reduces overgrowth in 10mM paraquat (p<0.05, ANOVA), this is not significantly different to wildtype in the absence of paraquat (p>0.05, ANOVA).

5.2.8. Reducing JNK/AP-1 signalling in *sod* mutants reduces synaptic overgrowth

Prior to normalisation *spin*GAL4>UASjun^{DN} or UASfos^{DN} causes a significant reduction in bouton number compared to wildtype ($p<0.01$ and 0.001, ANOVA, respectively). Expression of jun^{DN} does not cause any change in bouton number in a *sod1* mutant background, whereas fos^{DN} reduces bouton number in *sod1* ($p<0.001$, ANOVA) so that it is not significantly different to wildtype ($p>0.05$, ANOVA) (Fig. 5.10A). That is to say only depleting Fos signalling not Jun rescues the increase in bouton number. Expression of both these transgenes in *sod1* significantly rescues muscle surface area ($p<0.001$, ANOVA) (Fig. 5.10B). As a result of this change in muscle surface area, when normalised for muscle surface area bouton number in *sod1* mutants is significantly reduced by expression of jun^{DN} and fully rescued back to wildtype levels by expression of fos^{DN} (Fig. 5.10C). Changes in branch number seen in *sod1* are also rescued by expression of jun^{DN} and fos^{DN} under the control of *spin*GAL4. Depleting Jun signalling does rescue as much as depleting Fos signalling, following a similar pattern to the rescue in bouton number.

In *sod2* mutants, jun^{DN}, fos^{DN} and jnk^{DN} significantly rescue bouton number prior to normalisation ($p<0.001$, 0.001 and 0.01,respectively ANOVA) (Fig. 5.12A). jun^{DN} does not rescue muscle surface area whereas fos^{DN} completely rescues muscle surface area and jnk^{DN} does not have a muscle surface area significantly different to *sod2* however, it is no longer significantly different to wildtype muscle surface area(Fig. 5.12B). In terms of normalised bouton number, expression of any of these transgenes significantly rescues normalised bouton number back to wildtype levels (Fig. 5.12C). Expression of any of these transgenes rescues the

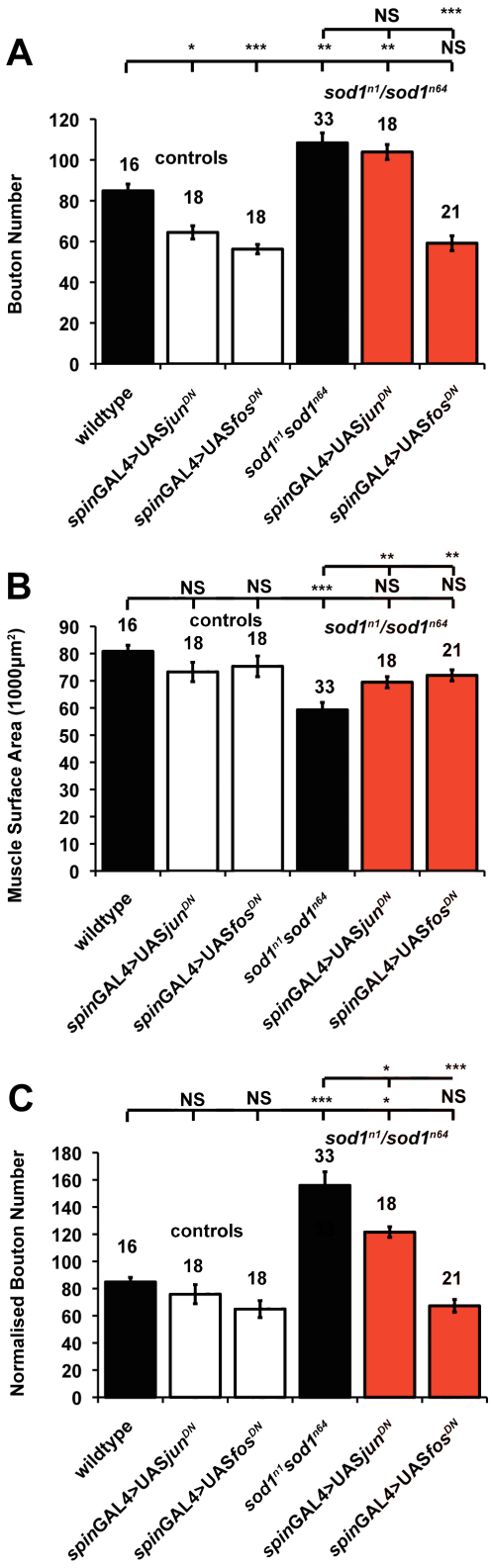
A
NS
***
*
***
**
**
NS
sod1n1/sod1n64
Bouton Number
120
100
80
60
40
20
0
16
controls
18
18
33
18
21
wildtype
spinGAL4>UASjunDN
spinGAL4>UASfosDN
sod1n1sod1n64
spinGAL4>UASjunDN
spinGAL4>UASfosDN
B
**
**
NS
NS
***
NS
NS
sod1n1/sod1n64
Muscle Surface Area (1000µm²)
90
80
70
60
50
40
30
20
10
0
16
controls
18
18
33
18
21
wildtype
spinGAL4>UASjunDN
spinGAL4>UASfosDN
sod1n1sod1n64
spinGAL4>UASjunDN
spinGAL4>UASfosDN
C
*
***
NS
NS
***
*
NS
sod1n1/sod1n64
Normalised Bouton Number
180
160
140
120
100
80
60
40
20
0
16
controls
18
18
33
18
21
wildtype
spinGAL4>UASjunDN
spinGAL4>UASfosDN
sod1n1sod1n64
spinGAL4>UASjunDN
spinGAL4>UASfosDN

Figure 5.10. AP-1 signalling is required for *sod1*-induced overgrowth.
(A)Prior to normalisation s*pin*GAL4>UAS*jun*^{DN} *spin*GAL4>UAS*fos*^{DN} and cause a significant reduction in bouton number with mean bouton numbers of 64±3.24(n=18) ($p<0.05$, ANOVA) and 56±2.29 (n=18) ($p<0.001$, ANOVA) respectively. Expression of *jun*^{DN} in a *sod1* background does not rescue bouton number 104±3.69 (n=18), ($p>0.05$ compared to *sod1;* $p<0.01$ compared to wildtype, ANOVA) whereas *fos*^{DN} expression significantly reduces *sod1* overgrowth to 59±3.7 (n=21), back to wildtype levels ($p<0.001$ compared to *sod1*; $p>0.05$ compared to wildtype). (B) Expression of *jun*^{DN} or *fos*^{DN} doesn't cause any change in muscle surface area: 73243±3578 and 75297±3820μm^2 respectively ($p>0.05$, ANOVA). As stated earlier *sod1* mutants show a significant reduction in muscle surface area. Expression of *jun*^{DN} or *fos*^{DN} causes a significant increase in muscle surface area in *sod1* mutants to 69466±2060 and 71978±2063μm^2 ($p<0.01$, ANOVA). These are not significantly different to wildtype ($p>0.05$, ANOVA). (C) Following normalisation, expression of *jun*^{DN}*or fos*^{DN} does not cause any change in normalised bouton number; 76±7.02 and 65±6.25 respectively. Expression of these transgenes in a *sod1* mutant background causes a significant reduction in normalised bouton number 122±3.88 ($p<0.05$, ANOVA) and 67±4.62 ($p<0.001$) respectively. *fos*^{DN} expression in a *sod1* background is not significantly different to wildtype bouton number ($p>0.05$), where as *jun*^{DN} in a *sod1* background is still significantly different to wildtype ($p<0.05$, ANOVA).

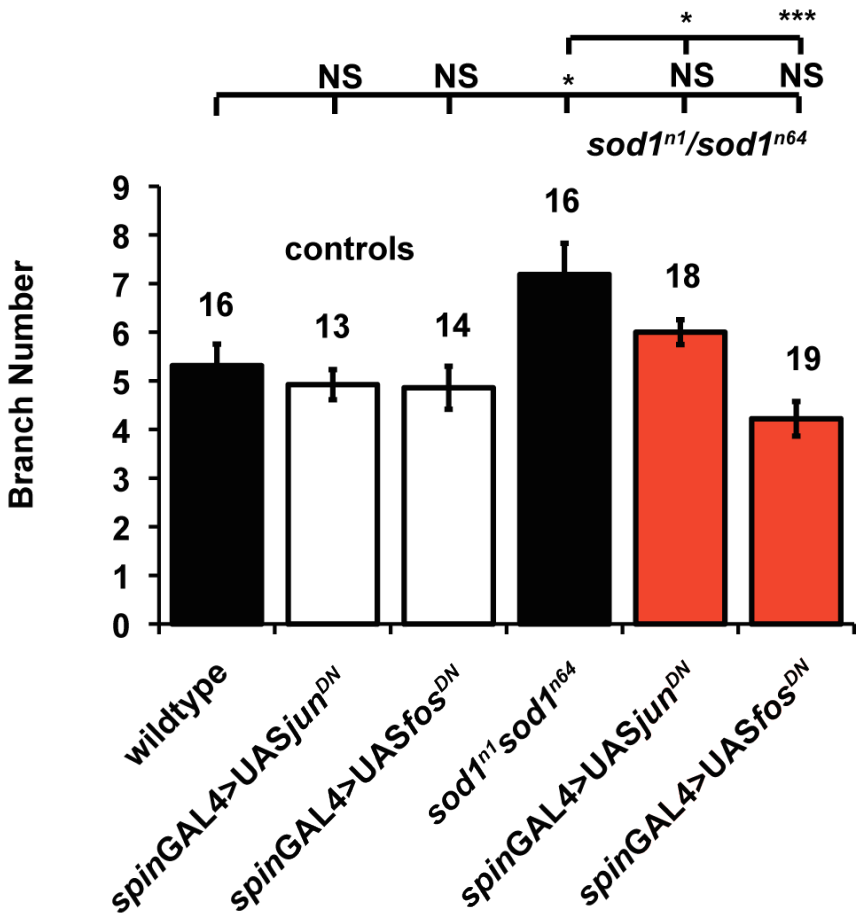

Figure 5.11. AP-1 signalling is required for changes in branching in *sod1* mutants. Expression of Jun^{DN} and Fos^{DN} caused no change in branch number both having branch numbers of 4.9±0.31 and 4.9±0.44 and (n=13 and 14 respectively, $p>0.05$, ANOVA). Expression of these transgenes in a *sod1* background significantly reduces branch number to 6±0.26 (n=18, $p<0.05$, ANOVA) and 4.20±.36 (n=19, $p<0.001$) respectively. These are not significantly different to wildtype ($p>0.05$, ANOVA).

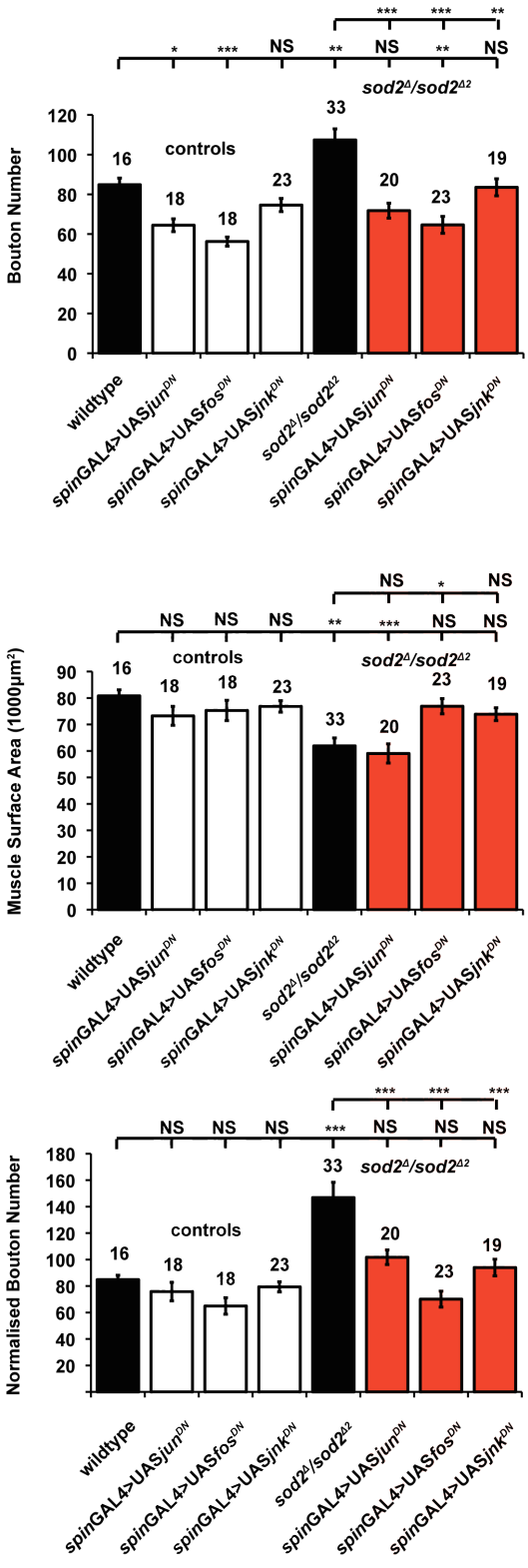
Bouton Number
Muscle Surface Area (1000µm²)
Normalised Bouton Number
controls
sod2Δ/sod2Δ2
wildtype
spinGAL4>UASjunDN
spinGAL4>UASfosDN
spinGAL4>UASjnkDN
sod2Δ/sod2Δ2
spinGAL4>UASjunDN
spinGAL4>UASfosDN
spinGAL4>UASjnkDN

Figure 5.12: JNK/AP-1 signalling is required for *sod2*-induced overgrowth.
(A)As shown previously, prior to normalisation s*pin*GAL4>UAS*jun*^{DN} *spin*GAL4>UAS*fos*^{DN} and cause a significant reduction in bouton number with mean bouton numbers of 64±3.24(n=18) ($p<0.05$, ANOVA) and 56±2.29 (n=18) ($p<0.001$, ANOVA) respectively *spin*GAL4>UAS*jnk*^{DN} causes no change in bouton number 75±3.31 (n=23) ($p>0.05$, ANOVA). Expression of these transgenes, *jun*^{DN}, *fos*^{DN} or *jnk*^{DN} in a *sod2* mutant background significantly reduces overgrowth to 72±3.77 (n=20) ($p<0.001$, ANOVA), 65±4.25 (n=23) ($p<0.001$, ANOVA) and 84±4.28 (n=19) ($p<0.01$, ANOVA). (B)Expression of *jun*^{DN}, *fos*^{DN} or *jnk*^{DN} doesn't cause any change in muscle surface area: 73243±3578, 75297±3820 and 76823±2153μm^2 respectively ($p>0.05$, ANOVA). As stated earlier *sod2* mutants show a significant reduction in muscle surface area. Expression of *jun*^{DN} in a sod2 background did not significantly change surface area of the mutant 59037±3609μm^2 whereas *fos*^{DN} causes a significant increase in muscle surface area in *sod2* mutants to 76877±2881μm^2 ($p<0.01$, ANOVA compared to *sod2*). Expression of *jnk*^{DN} in a *sod2* background resulted in a muscle surface area of 73878±2423μm^2 ($p>0.05$, ANOVA; compared to both wildtype and *sod2*). (C)Following normalisation, expression of *jun*^{DN}*or fos*^{DN} does not cause any change in normalised bouton number; 76±7.02 and 65±6.25 respectively. Expression of these transgenes in a *sod1* mutant background causes a significant reduction in normalised bouton number 122±3.88 ($p<0.05$, ANOVA) and 67±4.62 ($p<0.001$) respectively. *fos*^{DN} expression in a *sod1* background is not significantly different to wildtype bouton number ($p>0.05$), where as *jun*^{DN} in a *sod1* background is still significantly different to wildtype ($p<0.05$, ANOVA).

reduction in branch number seen in *sod2* mutants, so that they are not significantly different to wildtype (Fig. 5.13).

The data above show that there is slightly different pathway activation depending on the source or specific level of increased superoxide, as there is different involvement of AP-1 seen in *sod1* and *sod2* mutants. There is different involvement in the generation of both bouton number and muscle surface area as well as branch number. However this could be due to the effects of oxidative stress other than oxidative stress induced signalling, such as energy deficits.

Having established that *sod* mutants have Fos dependent overgrowth, in a fashion similar to *spinster* it was investigated whether Fos signalling was required from both the nerve and muscle, as with *spinster* (Fig. 5.6). To test this Fos signalling was depleted in either the nerve or the muscle using *elav*GAL4 or

*MHC*GAL4 to drive UAS*fos*^{DN}. Reducing Fos signalling in either the nerve or the muscle was enough to completely rescue *sod2*-induced overgrowth (Fig. 5.14A). This is at odds with the data seen in *spinster* where depletion of Fos is required both in the nerve and the muscle, i.e. under the control of *spin*GAL4 for

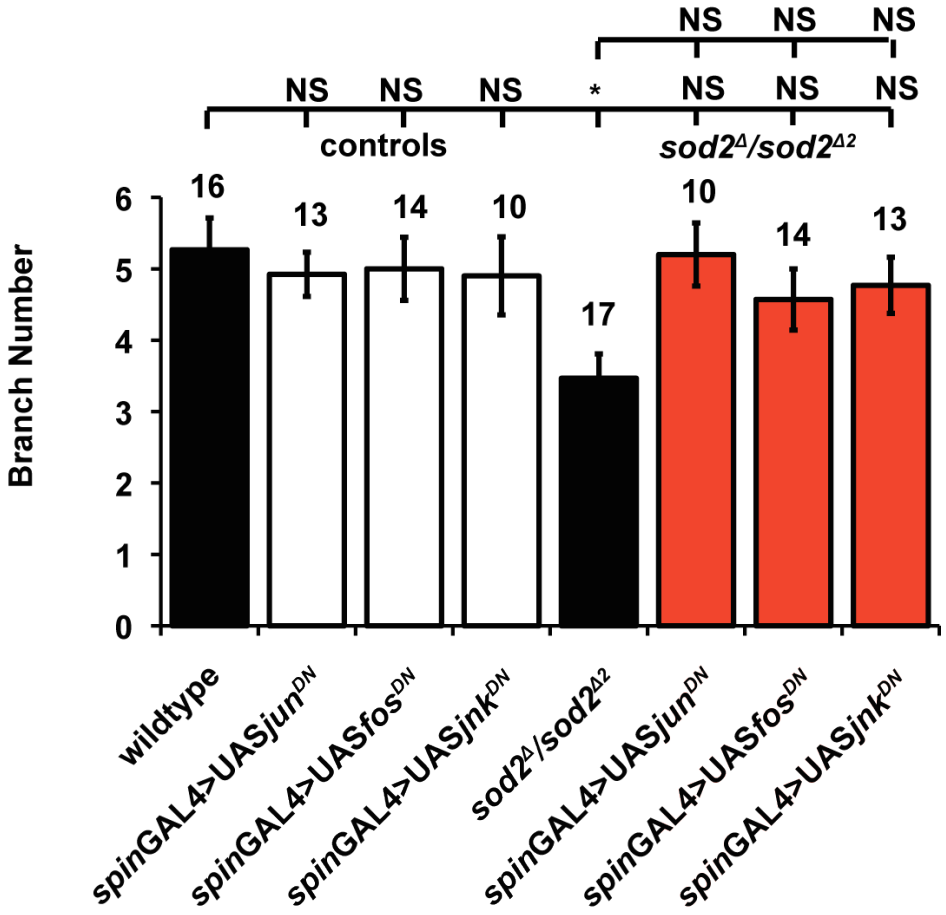

Figure 5.13: Changes in branch number in *sod2* mutants require JNK/AP-1 signalling. As shown above *spin*GAL4>UAS*jun*^{DN} or *fos*^{DN} does not change branch number, nor does *spin*GAL4>UAS*jnk*^{DN}, with a branch number of 4.9±0.55 (n=10). The reduction of branch number in *sod2* mutants to 3.5±0.24 (n=17, $p<0.05$, ANOVA) is rescued by the expression of *jun*^{DN}, *fos*^{DN} and *jnk*^{DN} have branch numbers of 5.2±0.44 (n=10), 4.8±0.43 (n=14) and 4.8±0.40 (n=13) so that it is no longer significantly different to wildtype ($p>0.05$, ANOVA).

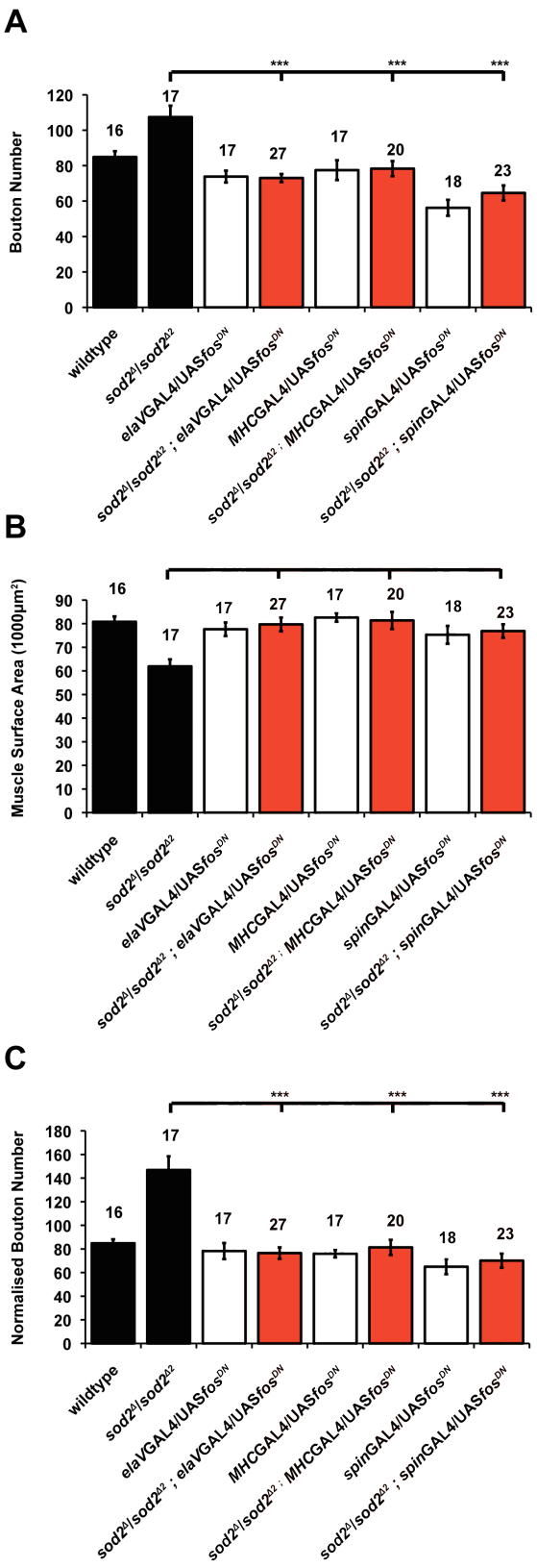
A
Bouton Number
120
100
80
60
40
20
0
***
***
***
16
17
17
27
17
20
18
23
wildtype
sod2Δ/sod2Δ2
elaVGAL4/UASfosDN
sod2Δ/sod2Δ2 ; elaVGAL4/UASfosDN
MHCGAL4/UASfosDN
sod2Δ/sod2Δ2 ; MHCGAL4/UASfosDN
spinGAL4/UASfosDN
sod2Δ/sod2Δ2 ; spinGAL4/UASfosDN
B
Muscle Surface Area (1000µm²)
90
80
70
60
50
40
30
20
10
0
16
17
17
27
17
20
18
23
C
Normalised Bouton Number
180
160
140
120
100
80
60
40
20
0
***
***
***
16
17
17
27
17
20
18
23

Figure 5.14: Fos signalling is required either from the muscle or the nerve for *sod2* induced overgrowth. (A) Expression of *fos*^{DN} in the nerve with *elaV*GAL4 causes no change in bouton number to 74±6.4 (n=17) but reduced *sod2* bouton number to 73±4.2 (n=27). Expression in the muscle with *MHC*GAL4>UAS*fos*^{DN} causes no change in bouton number 77±3.3 (n=17) but rescues *sod2* induced overgrowth to 78±4.5 (n=20) (B) As shown *sod2* has reduced muscle surface area expression of *fos*^{DN} in either the nerve or the muscle causes no change in muscle surface area with 77640±2888μm^2 and 82593±17712μm^2 respectively. Expression of these transgenes in a *sod2* mutant background results in muscle surface areas of 79692±2919μm^2 and 81371±3621μm^2, respectively, all statistically similar to wildtype (p>>.05, ANOVA) and significantly different to *sod2* (p<0.05, ANOVA). (C) When normalised to account for muscle surface area neuronal depletion of Fos signalling results in a bouton number of 78±6.9, and in *sod2* 77±4.9. Muscular expression of UAS*fos*^{DN} has a normalised bouton number of 76±3.1 whereas in *sod2* with muscular expression of UAS*fos*^{DN} has a normalised bouton number of 81±6.4, all statistically similar to wildtype (p>>0.05, ANOVA) and statistically different to *sod2* (p>0.05, ANOVA)

full suppression of overgrowth. However, the *sod2* overgrowth is not as severe as the overgrowth seen in *spinster* suggesting that Fos overactivation might not be as great therefore reducing signalling in only one synaptic compartment is enough to reduce synaptic overgrowth. Intriguingly, expression of f*os*^{DN} in either the muscle or the nerve or both fully reverses the reduction in muscle surface area seen in *sod2* mutants (Fig. 5.14B).

5.2.9. Autophagy gene function affects synapse development

Autophagy has previously been shown to regulate synapse development. Increasing levels of Rheb, one of the controllers of autophagy, in the neuron was shown to increase bouton number and EJP amplitude. Mutations in Rheb showed the opposite phenotype with decreased bouton number and EJPs (Knox *et al.*, 2007). Rheb acts upstream of TOR, which inhibits autophagy. Consequently, increased Rheb activity is proposed to decrease autophagy, through activation of TOR. However, inhibition of TOR through exposure to rapamycin does not prevent overgrowth. In addition, later studies have shown

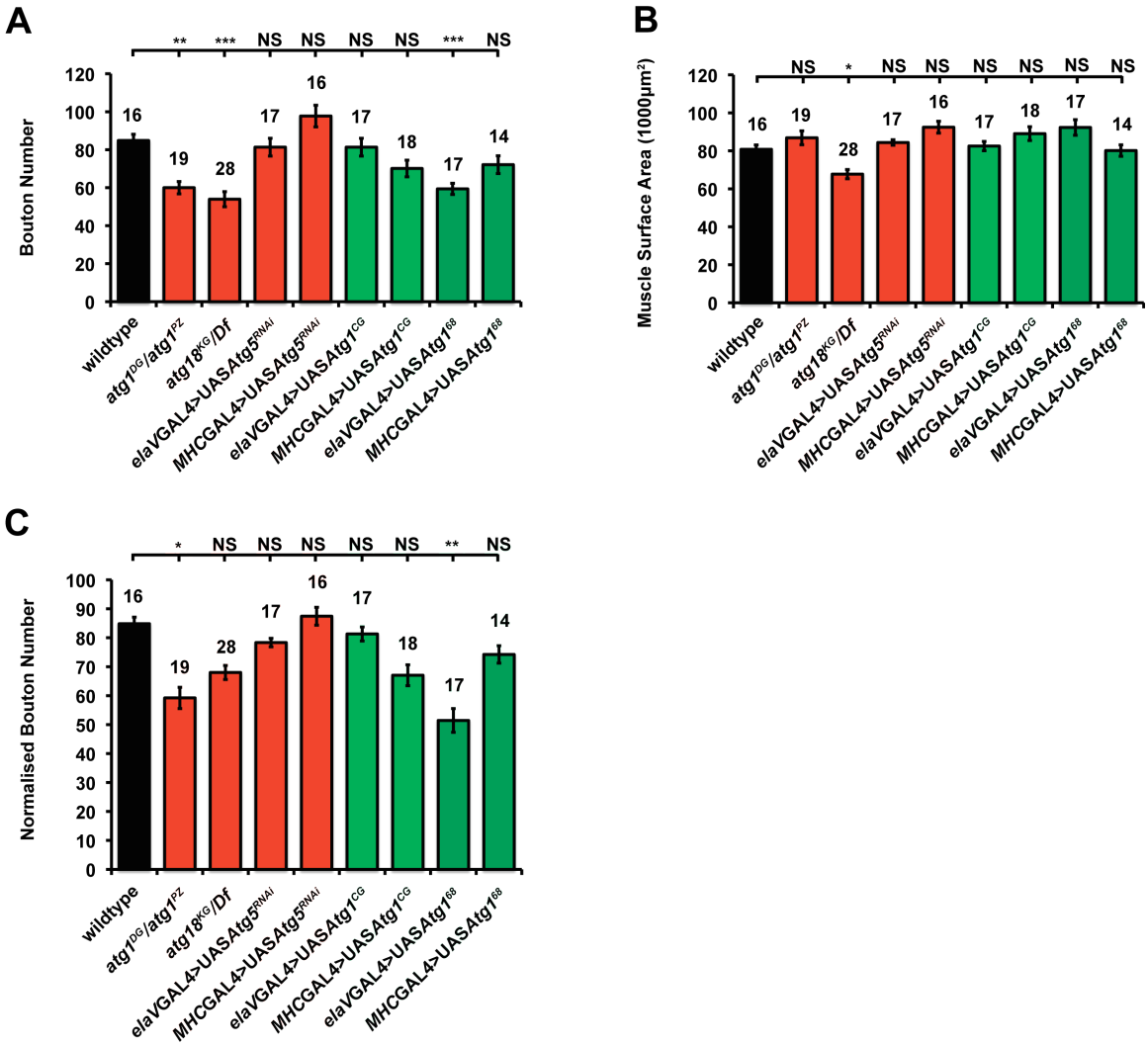

Figure 5.15: Changing levels of autophagy alters synaptic size. (A) Mutations in *atg1* and *atg18* cause significant reductions in bouton number: 60±3.2 (n=19, p<0.01, ANOVA) and 54±4.0 (n=28, p<0.001, ANOVA). Depleting atg5 in the muscle or the nerve with UAS*atg5RNAI* does not cause a significant change in bouton number; 81±4.7 (n=17) and 98±6.0 (n=16) respectively (p>0.05, ANOVA). Driving *atg1CG* in the nerve or muscle doesn't change bouton number significantly with bouton numbers of 81±4.7 (n=17) and 70±4.4 (n=17). Driving $atg1^{68}$ in the nerve causes a significant reduction in bouton number to 59±2.9 (n=29, p<0.001, ANOVA). Expression in the muscle causes no change in bouton number 72±4.7 (n=14, p>0.05, ANOVA). (B) atg1 mutants have statistically normal muscle surface area, 86857±3659 (n=19, p>0.05, ANOVA) mutants have significantly reduced muscle surface area 67737±2439 (n=28, p<0.05, ANOVA), other manipulations of atg genes shown here cause no change in muscle surface area. (C) When normalised for muscle surface area, *atg1* have

significantly reduced bouton number 59±5.8 (n=19), when *atg18* is normalised there is no significant change in bouton number 68±6.3 (n=28). *Atg5RNAi* in either the nerve or the muscle causes no change in normalised bouton number 78±4.8 (n=17) and 87±6.6 (n=17) ($p>0.05$, ANOVA). Driving atg1 activity in the nerve or muscle causes no change in bouton number with UAS$ATG1^{CG}$ 81±5.5 (n=17) and 67±5.0 (n=18), Using UAS$ATG1^{68}$ expression in the nerve causes a reduction in normalised bouton number, 51±4.3 (n=17, $p<0.01$, ANOVA), whereas expression in the muscle does not significantly alter bouton number 74±5.9 (n=14).

that rapamycin exposure results in increased bouton number (Shen and Ganetzky, 2009). This is consistent with the increase in bouton number caused by rapamycin as seen by Knox *et al.* (2007). However the mechanism suggested by Shen and Ganetzky (2009), whereby autophagy drives synapse growth is somewhat incompatible with other published data. As increased Rheb would lead to a decrease in autophagy but still leads to increased bouton number. Autophagy gene regulation of bouton number and how this compares to the previous data published was investigated. As, although driving Rheb in the muscle was shown to cause a slight reduction in bouton number the effect of driving atg1 in the muscle has not been fully investigated. This is because in the first study driving atg1 in muscle (Wairkar *et al.*, 2009) did not show any change in NMJ morphology. However, neuronal expression of this construct did not provide full rescue of the *atg1* mutant phenotype (Wairkar *et al.*, 2009), suggesting that it is not expressing highly enough to rescue the phenotype seen. Using a different UAS*atg1* construct Shen and Ganetzky fully rescue the *atg1* mutant phenotype with neuronal expression of this transgene. This suggests that their transgene is expressing more efficiently. It is this transgene that affords overgrowth when expressed neuronally in a wildtype background. However, this transgene has not been expressed in the muscle to determine any effects that this might have. The data in this area is, therefore, incomplete. It was investigated whether altered levels of autophagy in either the nerve, the muscle or both can impact on synapse development. Autophagy is occurring

globally in all cells. To this end, bouton number was compared between atg mutants that would presumably be defective for autophagy both pre- and post-synaptically. Autophagy function was also manipulated by employing a UAS-*atg5-RNAi* expression to allow comparison between mutants and RNAi depletion with UAS-*Atg1* expression, using two independently generated transgenes.

The data shown here (Fig. 5.15A) agree with published data that mutations in the autophagy genes *atg1* and *atg18* (Wairkar *et al.*, 2007; Shen and Ganetzky, 2009) show a significant deficit in synaptic growth, shown here by a reduction in bouton number compared to wildtype. *atg1* mutants show no significant change in muscle surface area, however *atg18* mutants have a significantly reduced muscle surface area (Fig. 5.15B). Consequently, when normalised for muscle surface area (Schuster *et al.*, 1996a), only *atg1* has significant undergrowth compared to wildtype (Fig. 5.15C). Depleting atg5 activity in either the nerve or the muscle using *elaV*GAL4 or *MHC*GAL4, respectively to drive UAS*atg5RNAi*, did not significantly affect bouton number, muscle surface area or normalised bouton number (Fig. 5.15A,B and C respectively). Overexpression of UAS$atg1^{+}$ has previously been shown to drive autophagy (Scott *et al.*, 2007; Shen and Ganetzky, 2009). The data shown here show contrary results to those published, where increased autophagy caused increased bouton numbers. Over-expression of $atg1^{CG}$ in the nerve or the muscle causes no change in bouton number. However, expression of UAS$atg1^{68}$ in the nerve with *elaV*GAL4 results in a significant reduction in bouton number whereas expression in the muscle with *MHC*GAL4 results in a bouton number statistically similar to wildtype. This trend is the same following normalisation (Fig. 5.15C) for muscle surface area as there is no change in muscle surface area (Fig. 5.15B).

5.2.10. Autophagy is required for *spinster* induced overgrowth

When introduced into a *spinster* mutant background, mutations in *atg1* or *atg18* rescue synapse overgrowth resulting in a significant reduction in bouton number.

Heterozygous combinations of *atg1* and *atg18* similarly restrict synaptic growth in *spinster* mutants (Fig. 5.16). Although a general decrease in branching in the *atg1* mutant combination (not quantified) was observed, the data demonstrate that an *atg* mutation can restrain *spinster* synapse overgrowth. In agreement with Shen and Ganetzky (2009) the data here suggest that autophagy functions to regulate synaptic growth and that this process is critical to synaptic overgrowth induced by oxidative stress.

5.2.11. Autophagy is required pre- and post- synaptically for *spinster* induced overgrowth

As shown earlier, functional autophagy is required for *spinster*-induced overgrowth. However, previously autophagy has only been shown to be involved presynaptically in synaptic development. To confirm this tissue specific inhibition of autophagy was used. Reducing autophagy through expression of UAS*atg5RNAi* in the nerve, using *elaV*GAL4, or in the muscle, using *MHC*GAL4 does not alter bouton number. However, expression of these transgenes in a *spinster* background reduces overgrowth significantly and equally (Fig. 5.17). This is the first time autophagy genes acting post-synaptically have been implicated in synaptic development.

5.2.12. Autophagy is required for paraquat induced overgrowth

Importantly, feeding of paraquat to *atg1* mutants failed to induce the expected synaptic overgrowth. Even prior to normalisation *atg1* mutants show a significant reduction in bouton number in 10mM paraquat (Fig. 5.18A). *atg1* mutants have a significantly increased muscle surface area but presence of this mutation in

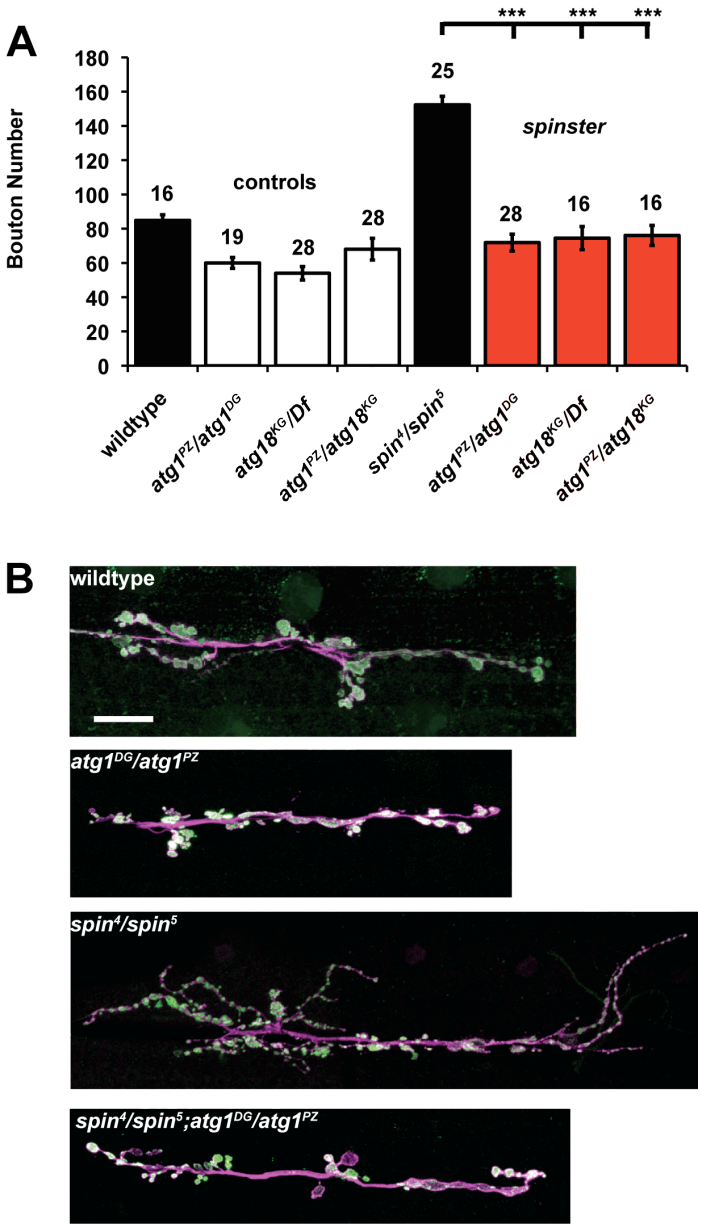

Figure 5.16: *spinster* induced overgrowth requires autophagy genes. (A)Autophagy is required for *spin*-induced synapse overgrowth. Mutants for autophagy genes Atg1 ($atg1^{PZ}/atg1^{DG}$) and Atg18 ($atg18^{KG}/Df$) and animals heterozygous for both alleles ($atg1^{PZ}/atg18^{KG}$) have a reduction in bouton number to 59±5.8 (n=19), 54±4.0 (n=28) and 68±6.3 (n=28). These mutations also reduce *spin*-induced overgrowth, to 72±4.9 (n=28), 75±6.7 (n=16) and 76±5.8 (n=15) respectively ($p>>0.05$ compared to wildtype and $atg1^{PZ}/atg1^{DG}$ ANOVA and $p<0.001$ compared to *spin*). (B) Representative images of NMJs at muscle 6/7 nerves shown in magenta with anti-HRP and boutons shown in green with anti-synaptotagmin. Scale bar =20μm

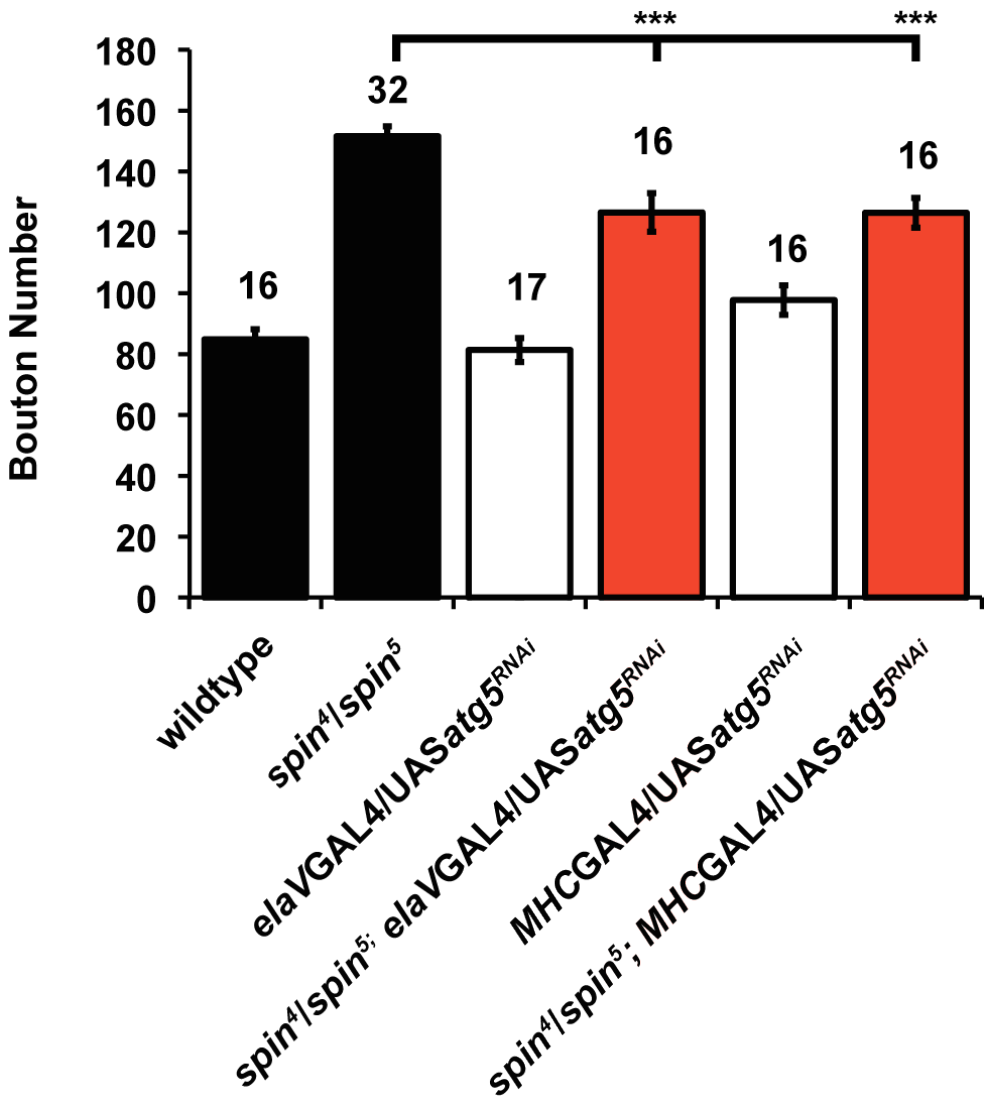

Figure 5.17: Autophagy genes are required both in the nerve and the muscle for *spinster*-induced overgrowth. Expression of *atg5IR* in the nerve or muscle partially rescues bouton number in *spinster* to 127±5.57 (n=16) and 126±6.51 (n=16) respectively ($p<0.001$ ANOVA).

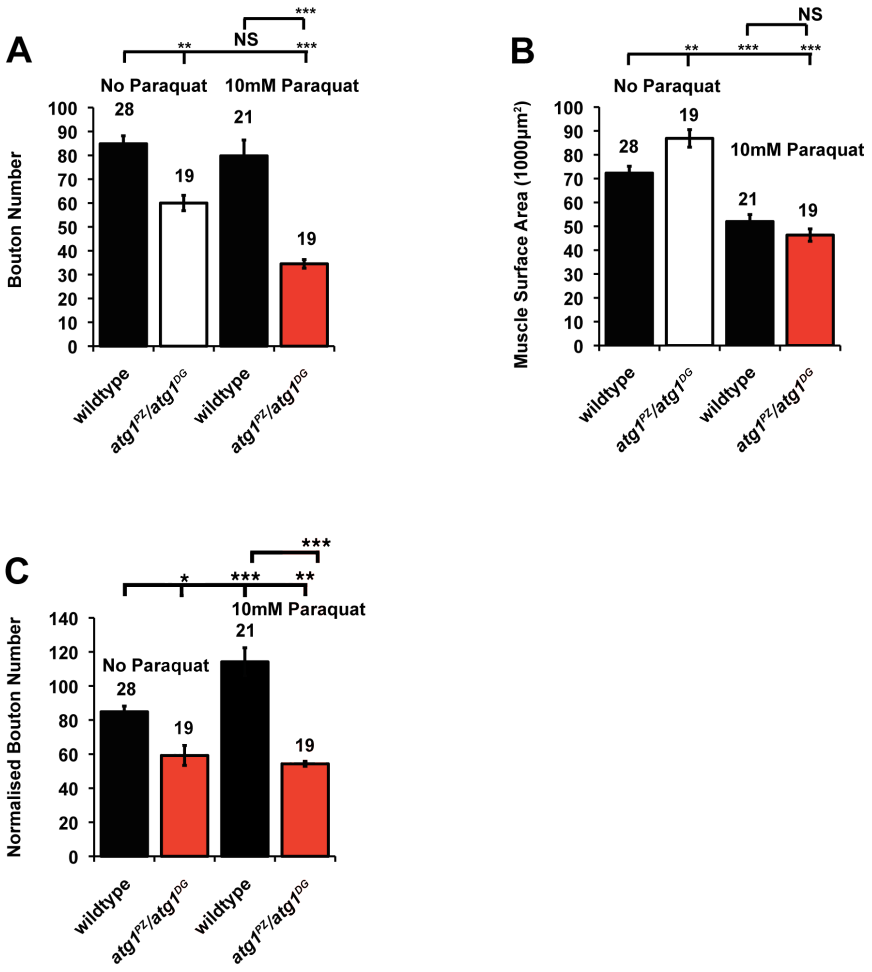

Figure 5.18: paraquat induced overgrowth requires autophagy genes. Mutations in *atg1* prevent paraquat-induced overgrowth. (A) *Atg1* mutants have significantly reduced bouton number compared to wildtype both in the absence and presence of 10mM paraquat. In the absence of paraquat *atg1* mutants have a bouton number of 60±3.2 (n=19, p<0.01, ANOVA). With 10mM paraquat these mutants have a bouton number of 35±1.8 (n=19, p<0.001, ANOVA compared to both wildtype with and without paraquat) (B) Paraquat induced reduction in muscle surface area still occurs in *atg1* mutants. There is no difference in muscle surface area in wildtype and *atg1* mutants in 10mM paraquat; 52003±2922 (n=21) and 46302±2580 (n=19) (p>0.05, ANOVA). Both are significantly reduced compared to wildtype without paraquat (p<0.001, ANOVA) (C) Mutations in *atg1* prevent paraquat induced increases in normalised bouton number. When normalised to muscle surface area *atg1* mutants in paraquat have a bouton number of 54±1.4 (n=19) significantly different to wildtype on 10mM paraquat (p<0.001, ANOVA).

10mM paraquat does not rescue muscle surface area(Fig. 5.18B). *atg1* mutants have a decreased normalised bouton number and also rescue overgrowth caused by 10mM paraquat (Fig. 5.18C).

5.3. Discussion

5.3.1. ASK/JNK signalling is required for oxidative stress induced overgrowth

The synergy seen between *spinster* and *sod1* heterozygotes to induce synapse overgrowth suggests a common signalling pathway. As JNK is known to be activated in response to oxidative stress this pathway was investigated for increased activity and found to be upregulated in both *spinster* and paraquat fed animals, as shown by increased expression of a *puckered* reporter. Depleting ASK and JNK signalling both rescue *spinster* and paraquat induced overgrowth. Activation of ASK occurs through the dissociation of thioredoxin under conditions of oxidative stress (Saitoh *et al.*, 1998) whereupon ASK is known to then activate JNK (Chen *et al.*, 2002; Cha *et al.*, 2005). JNK is also activated by oxidative stress as its activity is increased when glutathione is oxidized preventing its binding and inhibiting JNK. Thus in oxidative stress, the activity of this signalling pathway is upregulated both by direct activation and increased downstream activity due to phosphorylation. ASK has not been previously identified in having a role in synapse development. Here ASK is identified as having a role in normal synaptic development and the overgrowth caused by *spinster* and paraquat exposure (Fig.5.4 and 8 respectively) suggesting a role for ASK in the regulation of synaptic growth which may define responses to different cellular sources of oxidative stress. JNK has been shown to drive synapse development (Sanyal *et al.*, 2002) and is required for overgrowth in *highwire* mutants (Collins *et al.*, 2006) and in the presence of increased autophagy (Shen and Ganetzky, 2009). Here it is now shown that *spinster* (Fig.

5.4), *sod2* (Fig. 5.12) and paraquat (Fig. 5.8) induced overgrowth are all-dependent on functioning JNK. This was shown both by using a dominant negative transgene in all three conditions and confirmed using RNAi knockdown in *spinster* and paraquat treatment (Fig. 5.5 and 5.9 respectively). It remains to be investigated whether JNK is involved in *sod1*-induced overgrowth. However, even in the absence of this data it is clear that JNK activity is required for oxidative stress induced increases in bouton number.

5.3.2. Fos/Jun involvement in synaptic growth is context dependent

The requirement for Fos and Jun activity for overgrowth is found to be different between *spin* mutants, paraquat treated animals and *sod* mutants. This suggests differential activation of components of the AP-1 components in each condition. Depleting Jun signalling pre- and post- synaptically using *spin*GAL4>UASjun^{DN} does not affect *spinster* induced overgrowth (Fig. 5.4), however paraquat, *sod1* and *sod2* overgrowth are all rescued by depleting Jun signalling. It is interesting to note that *sod1* overgrowth is only rescued by jun^{DN} following normalisation, and then only partially compared to the full rescue seen with expression of fos^{DN}. In addition the rescue in branching seen by depleting Jun and Fos in *sod1* is more significant with Jun than Fos (Fig. 5.11). Where as the reduction in branching and the increase in bouton number seen in *sod2* is rescued by to the same extent by depleting Jun, Fos or JNK signalling. This is suggestive of differences between the relative levels of signalling of Jun and Fos depending on the source/type of ROS. Although in mammals only Jun can homodimerise, in *Drosophila*, Fos can also homodimerise and is known to act independently of Jun in synapse overgrowth in *hiw* mutants and conditions of cytoskeletal disruption (Collins *et al.*, 2006; Massaro *et al.*, 2009). Jun and Fos can also dimerise with other signalling components, such as Smad and Nrf2. Smads are important proteins in synapse development (Dudu *et al.*, 2006;

McCabe *et al.*, 2004; Rawson *et al.*, 2003; Sweeney and Davis, 2002); they are activated by phosphorylation in response to TGFβ signalling. In other contexts, Smad and AP-1 proteins are known to physically interact (Liberati *et al.*, 1999) and this signalling is known to converge at AP-1 sites to determine transcription activation (Zhang *et al.*, 1998; Liberati *et al.*, 1999). This links two important developmental pathways, AP-1 and TGFβ (Wong *et al.*, 1999). This provides an attractive explanation for the potentiation of synapse growth by AP-1 at the Drosophila NMJ. Only Fos, not Jun, has been implicated in the overgrowth seen in *highwire* although it is unknown as to whether Fos is homodimerising or acting with other binding partners. The mutations and treatments used in this study to produce oxidative stress lead to ROS generation from different subcellular sources. It is postulated that *spinster* and *sod1* produce ROS predominantly from non-mitochondrial compartments while paraquat treatment and *sod2* would generate ROS primarily from the mitochondria. *spinster,* paraquat and *sod* induced oxidative stress produce synapse growth via activation of JNK. However downstream of JNK there is differential involvement of Fos and Jun. The data shown here suggest that Fos is important for responses to both mitochondrial and non mitochondrial sources of ROS whereas Jun appears to be involved in the generation of overgrowth from predominantly mitochondrial sources of ROS. However, this distinction is currently only a hypothesis as it is hard to distinguish between different sources of ROS. Additionally, it is not known whether different abundances of RO species in each of the models used in this study. It is suggested that superoxide is the most potent activator of autophagic responses (Chen *et al.*, 2009) and this would be consistent with much of the data presented here. In *spinster* the source of ROS is probably predominantly non-mitochondrial, putatively deriving more from the lysosomes. However, mitochondrial recycling might be impaired leading to build up of old dysfunctional mitochondria resulting in increased levels of ROS being produced from the electron transport chain. In a similar manner, *sod1* is traditionally

thought of as the cytoplasmic form of SOD, however it is also expressed in the periplasm of the mitochondria, thus higher levels of ROS could also be derived from the mitochondria in this model. Activation of differential signalling modules by different sources and species of oxidative stress is therefore an attractive avenue of investigation for the future.

5.3.3. Autophagy and Synapse Development

Oxidative stress is a potent activator of autophagy. Recent work has shown that autophagy genes are directly activated by oxidative stress in a JNK dependent manner (Wu *et al.*, 2009). Activation of autophagy has been shown to drive synapse growth in *Drosophila* (Shen and Ganetzky, 2009) and the data in this study support this proposal. However, in the Shen and Ganetzky model, JNK was suggested to be downstream of activation of autophagy. This was proposed because the overgrowth in *highwire* mutants is not affected by mutations in autophagy genes. Autophagic downregulation of hiw protein (and subsequent activation of the JNKKK wallenda) has been proposed as a mechanism to regulate synaptic growth (Shen and Ganetzky, 2009). These data seem to be somewhat at odds with the observation that oxidative stress leads to upregulation of autophagy through the activation of JNK. Consistent with the findings of Wairkar (2007) and Shen and Ganetzky (2009) *atg1* and *atg18* function are required for oxidative stress and *spinster* induced synapse overgrowth. The experiments carried out to date are not targeted enough to suggest whether autophagy is acting upstream or downstream of JNK signalling in this instance. However, the findings here are different to Shen and Ganetzky (2009) insofar as overexpressing atg1 in the nerve does not cause synaptic overgrowth. In fact, it results in significant undergrowth. This leads to the suggestion that dysregulation of autophagy at the NMJ, whether up or down in the absence of oxidative stress results can result in synaptic undergrowth. Conversely, in the presence of oxidative stress and functioning autophagy there

is an increase in growth. It is also possible that there is a distinct output of ASK/JNK/AP-1 activity other than autophagy that leads to overgrowth. However as soon as autophagy is impaired there is an even greater undergrowth caused by the build up of *highwire* leading to inhibition of JNK signalling and hence fewer boutons. However, it has been shown that *spinster* overgrowth is due to loss of *spinster* in both the pre- and post- synaptic compartments, as shown by full rescue requiring transgene expression in both of these compartments. This is different to *highwire,* which was shown to be expressed only pre-synaptically. However *highwire* overgrowth has not been shown to be rescued by only presynaptic expression of wildtype highwire, as it was not possible to make a rescue construct at the time of the original paper (Wan *et al.*, 2000) although localisation data suggests that *highwire* is expressed presynaptically only.

5.3.4. Muscular and Neuronal Input

The hiw protein and its target wallenda (wnd) are both found presynaptically (Collins *et al.*, 2006) while JNK/AP-1 signalling and autophagy are contributing to synapse overgrowth in both the muscle and nerve. Furthermore, *spinster* overgrowth requires pre- and post-synaptic expression of the rescue construct to reverse the overgrowth, showing a clear role for the muscle in this phenotype. The observations of muscular involvement in *spinster* and *sod2* suggest a novel muscle derived JNK/AP-1 signal contributing to synapse growth that is likely to be independent of direct *hiw*/*wnd* regulation. Taken together, data from this study suggest that the highly conserved JNK/AP-1 signalling pathway, a well-known mediator of synaptic growth and function, acting both in the muscle and the nerve, can be activated by oxidative stress to induce synaptic overgrowth. In addition, autophagy is also required for *spinster* and oxidative stress induced growth, however it is now known whether this is upstream or downstream of JNK signalling in these conditions. Many neurodegenerative disorders generate an oxidative stress burden in affected neurons. Investigating the effects of

oxidative stress on synaptic development and function, as well as identifying signalling pathways, in such a disease context provides a potentially important insight into the pathology of a number of neurodegenerative diseases.

6. *Spinster* and Oxidative Stress Mutants have Impaired Physiology

6.1. Introduction

The *Drosophila* larval NMJ is an ideal system for studying synapse plasticity and morphological development in normal and diseased states. This preparation is also amenable to physiological analysis allowing a description of synaptic output to be generated in disease models. It is relatively straightforward to measure physiological output for the larval NMJ in a number of ways for example, larval crawling, muscle contraction and using recording electrodes in the muscle to measure synaptic transmission directly. The nervous system requires a great deal of energy, and therefore neuronal cells have high levels of mitochondria, making them more susceptible to oxidative stress. Moreover, neurons are long-lived cells that do not generally regenerate so old mitochondria can build up when degradation is impaired. In addition, ROS have been shown to affect synaptic transmission by a number of possible mechanisms (See 1.6.2). There are therefore, a number of aspects that remain to be investigated in *spinster* and *sod* mutants, such as the effects of these mutations on physiological output, and whether there is an energy deficit in *spinster*.

Synaptic overgrowth has been previously shown to be coupled to hyperexcitability, for example in *shaker* mutants, there is increased transmitter release at the NMJ (Ganetkzy and Wu, 1983; Wu *et al.*, 1983). Synaptic transmission defects have been previously observed in *highwire* and *spinster* mutants and in the preceding chapters synaptic overgrowth in these mutants have been shown to be partly due to oxidative stress. The next line of investigation was how oxidative stress affects physiological output and whether this is related to synaptic overgrowth.

Oxidative stress induces autophagy and autophagy is required for synaptic overgrowth. Another effect of oxidative stress is inefficiency in the electron coupling in mitochondria. This has the potential to reduce ATP production efficiency. A drop in ATP production is known to activate AMPK, a conserved pathway known to be activated when AMP:ATP ratio rises, inducing autophagy and metabolic pathways to generate more cellular energy. Decreased mitochondrial function leads to activation of a number of cell signalling pathways that can converge at a number of points, for example to regulate cell cycle transition (Owusu-Ansah *et al.*, 2008). In this case, increased ROS leads to the activation of ASK/JNK/Foxo ultimately arresting transition through the cell cycle. Concurrently reduced mitochondrial function results in increased AMP:ATP leading to the activation of AMPK, which leads to the activation of p53, again ultimately inhibiting cell cycle transition. This shows how loss of mitochondrial function generates activation of two distinct pathways that both have the same physiological output. Based on this it was postulated that the AMPK pathway could be responding to metabolic deficit and contributing to synaptic overgrowth, in a parallel to JNK/AP-1 signalling. It has been well documented that autophagy is activated in response to starvation and energy deprivation through AMPK. Consequently, it was investigated whether AMPK could be another upstream regulator of autophagy during synapse development. The previous data on this are conflicting as Knox *et al.*, (2007), suggested that autophagy negatively regulates synapse size as a downstream effector of Rheb, as oppsosed to autophagy positively regulting synapse development as shown by Shen and Ganetzky (2009). By driving Rheb in the motor neuron there is an increase in bouton number. Rheb activates TOR, which in turn inhibits autophagy through interactions with atg1. Therefore by increasing Rheb, TOR activity is increased reducing the level of autophagy. However, the mechanism put forward is somewhat unclear. Rapamycin causes an increase in bouton number, through inhibition of TOR leading to an increase in autophagy, somewhat at odds with the putative mechanism that Rheb decreases autophagy leading to overgrowth

(Knox *et al.*, 2007). Given the contradictory published data and the controversial results regarding increasing autophagy seen in the previous chapter the role AMPK in synapse development was investigated. This could potentially highlight how autophagy is regulated in *spinster*.

The previous results chapters have shown that oxidative stress can contribute to synaptic growth, through activation of JNK signalling and autophagy. However, how this affects synaptic function has not been determined. *Spinster* has been shown to have overgrown synapses coupled with impaired synaptic transmission (Sweeney and Davies, 2002). Quantal size, determined by measuring mini excitatory junction potentials (mEJPs) was shown to be normal. This means that the synaptic response to the release of neurotransmitter from a single synaptic vesicle was normal. However, quantal content, the number of effective vesicles released in response to a nerve impulse is reduced by 50% in *spinster,* as quantified by measuring the EJP and dividing it by the mEJP. This shows that fewer vesicles are released in response to an action potential. Mutations in *highwire* that cause synaptic overgrowth that is partially rescued by reducing ROS also cause physiological deficits. In addition to the reduced EJP amplitude and quantal content, *highwire* also displays reduced quantal size (Wan *et al.*, 2000). Quantal size is generally considered a measure of post-synaptic sensitivity to neurotransmitter rather than due to any change in the amount of neurotransmitter released in a single vesicle.

The effects of *sod* mutations on synaptic transmission at the *Drosophila* larva neuromuscular junction have not yet been investigated. Mutations in *sod2* result in reduced climbing ability in adults and the effects of mutations in *sod2* have been investigated at the giant fibre system (Godenschwege *et al.*, 2009). It was shown that amplitude of response to stimulation declined following eclosion but was completely rescued by muscular expression of UAS*sod2*, suggesting that *sod2* is required in the muscle for normal performance of the NMJ. Motor neuron output remained the same even after movement had ceased. However neuronal

output declined significantly compared to wildtype. Central circuitry was impaired but not as much as the defects seen at the NMJ, and changes in central circuitry occurred later. This suggests that muscle dysfunction is contributing more to the whole-organism phenotypes, such as impaired climbing, than neuronal dysfunction; neuronal dysfunction is severe but occurs later than muscle dysfunction. Hence neuronal function in adults is significantly impaired as a result of mutations in *sod2*. However, the effects of *sod1* or *sod2* mutations on synaptic transmission at the *Drosophila* larva NMJ are as yet unknown. Given that oxidative stress induces synapse overgrowth, the effects of oxidative stress on synaptic physiology were studied, by examining crawling behaviour and synaptic transmission.

As well as investigating the effects of these mutations in physiological output the effects of other upstream regulators of autophagy and metabolism on synaptic size in *spinster* were examined. Previous data in the Sweeney laboratory has shown that AMPK is involved in synaptic growth in *spinster*. Mutations in *löchrig* (*löe),* an isoform of the gamma-subunit of AMPK (Tschäpe *et al.*, 2002), prevent *spinster*-induced overgrowth. This mutation affects one isoform of one of the regulatory subunits of AMPK, which is involved in the regulation of autophagy. AMPK is known to be protective against neurodegeneration (Spasić *et al.*, 2008); in fact mutations in *löe* cause neurodegeneration (Tschäpe *et al.*, 2002). AMPK has a wide variety of effectors, generally stimulating lipid carbohydrate and protein metabolism to provide fuel to rectify the energy deficit. AMPK can also putatively inhibit protein synthesis through activation of certain PI3 Kinases. AMPK can differentially affect cell growth and apoptosis depending on the level of activation and effectors involved (Reviewed in Jansen *et al.*, 2009).

6.2. Results

6.2.1. Mutations with overgrown larval NMJs have impaired physiology

Drosophila larvae move around their environment in search of food or to escape predators by crawling (Mueller *et al.*, 2005). Larval crawling is a rhythmical, cyclic set of movements. The muscles of the larvae contract peristaltically, as muscle contractions propagate from one end of the body to another, and as this occurs the larva is able to move along the surface (Wang *et al.*, 1997). This is a complex physiological process involving central and peripheral synapses and effective muscle contraction (Song *et al.*, 2007). It involves central control and appropriate communication between the CNS, PNS and muscles. Crawling speed is therefore used as in indicator of physiological function. Mutations in *spinster*, *highwire*, *sod1* and *sod2* all cause significantly reduced crawling speeds compared to wildtype. All mutants are reduced to a similar extent; with *sod2* showing slightly further reduced crawling speed (Fig. 6.1). In addition to this, *sdhB* mutants were also investigated but only two larvae could be recorded crawling as such as a very high percentage of these larvae do not crawl. The reduction on crawling speed does not correlate with the level of overgrowth seen in these mutants. Due to the role of oxidative stress in *spinster* induced overgrowth it was examine whether this physiological phenotype is caused by oxidative stress. *spinster* has been shown to carry an oxidative stress burden, and the overgrowth phenotype is rescued by expression of antioxidant transgenes. *highwire* and *sod1* overgrowth is also reduced by expression of antioxidant transgenes. Since relieving oxidative stress reduces synaptic growth phenotypes in these mutants it was investigated whether expressing antioxidant transgenes reduces the crawling (physiological) phenotype, seen consistently in these mutants.

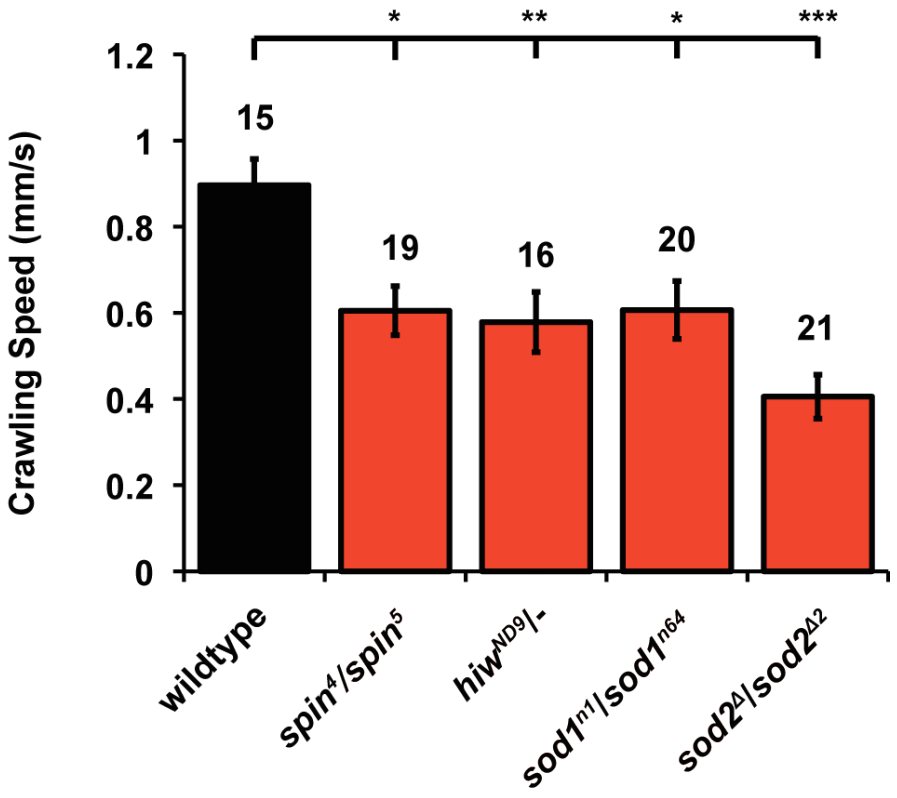

Figure 6.1: Mutations in *spinster*, *highwire*, *sod1* and *sod2* result in reduced crawling speed. Wildtype larvae have a crawling speed of 0.90±0.06mm/s (n=15), this is significantly reduced to 0.60±0.06mm/s (n=19) in *spinster* ($p<0.05$, ANOVA). The crawling speed of *highwire* mutants is 0.58±0.07mm/s (n=16), significantly reduced relative to wildtype ($p<0.01$, ANOVA). Mutations in SOD also cause significant reduction in crawling speed to 0.61±0.07mm/s (n=20, $p<0.05$, ANOVA) and 0.41±0.05mm/s (n=21, $p<0.001$, ANOVA) for *sod1* and *sod2*, the cytoplasmic and mitochondrial forms, respectively.

6.2.2. Reduction in *spinster* crawling speed is not rescued through expression of anti-oxidants

Expression of *spin*GAL4>UAS*hSOD1* does not significantly affect crawling speed, whereas expression of UAS*cat* pre- and post-synaptically caused a significant reduction in crawling speed. This seems an anomalous result and is at odds with data from the Elliott lab (York) who find that global and higher levels

of overexpression of *cat* using *act*GAL4>UAS*cat* has a normal crawling speed, not statistically different to wildtype (Vincent *et al.*, 2012). However, even when repeated, in case contaminated food had caused any problems, *spin*GAL4>UAS*cat* had significantly reduced crawling speed; the result was the same. Expression of *cat* pre- and post synaptically results in a reduction in crawling speed that is actually reduced to a level comparable to *spinster*. Expression of *h*SOD1 did not rescue the reduction in crawling speed seen in *spinster* suggesting that it is not only the level of oxidative stress causing the reduction in crawling speed, or the reduction in oxidative stress afforded by spinGAL4>UAS*hSOD1* is not sufficient to restore physiological function. Expression of *spin*GAL4>UAS*cat* in a *spinster* background further reduces crawling speed (Fig. 6.2). Expression of these antioxidants both showed an ameliorative effect on bouton number in *spinster* suggesting that the effects of ROS on growth are different from those affecting physiological function depending on the ROS species present.

6.2.3. Reduction in *highwire* crawling speed is not rescued by expression of *hSOD1* pre- and post-synaptically

As discussed earlier, expression of *hSOD1* pre- and post-synaptically does not significantly affect crawling speed. Nor does it rescue the reduction in crawling speed seen in *highwire* mutants. This suggests that the reduction of crawling speed in *highwire* is either not caused by increased levels of reactive oxygen species or caused by more ROS than are dissipated by *spin*GAL4>UAS*hSOD1* (Fig. 6.3).

6.2.4. Reduction in crawling speed in *sod1* mutants is not rescued by expression of *hSOD1*

The reduction in crawling speed seen in *sod1* mutants is not ameliorated by *spin*GAL4>UAS*hSOD1*. Expression of *hSOD1* fully rescued the increase in

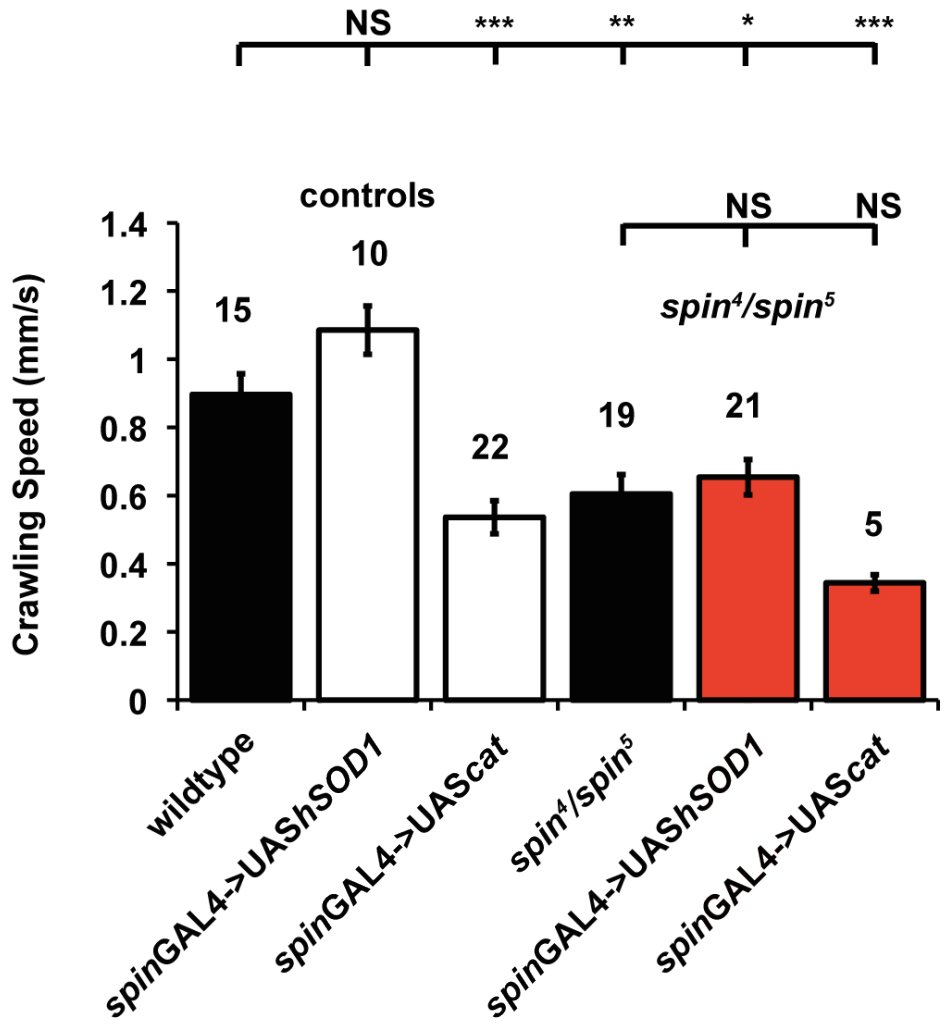

Figure 6.2 Reducing ROS in *spinster* does not rescue crawling speed. As shown earlier *spinster* causes a reduction in crawling speed from 0.90±0.06mm/s (n=15) for wildtype to 0.61±0.06mm/s (n=19) ($p<0.01$, ANOVA). Expression if *hSOD1* doesn't change crawling speed, 1.1±0.07mm/s (n=10, $p<<0.05$, ANOVA), whereas *spin*GAL4>UAS*cat* has a significantly reduced crawling speed of 0.54±0.06 (n=17, $p<0.001$, ANOVA). Expression of these transgenes in *spinster* does not significantly rescue crawling speed with speeds of 0.65±0.05mm/s (n=21) and 0.34±0.02mm/s (n=5).

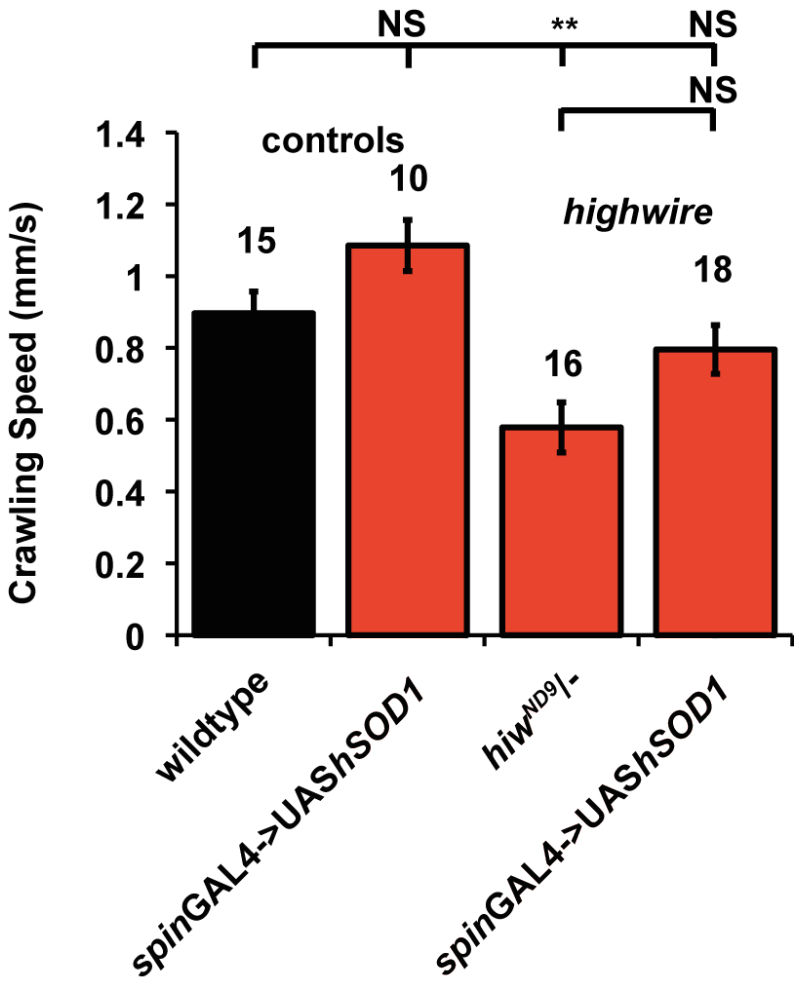

Figure 6.3: Reducing ROS in *highwire* does not rescue crawling speed. As shown earlier *highwire* causes a reduction in crawling speed from 0.90±0.06mm/s (n=15) for wildtype to 0.58±0.07mm/s (n=16, $p<0.01$, ANOVA). Expression of *hSOD1* does not change crawling speed, 1.1±0.07mm/s (n=10, $p<<0.05$, ANOVA), and expression of *hSOD1* in *highwire* does not significantly rescue crawling speed 0.80±0.07 mm/s (n=18) compared to *highwire* however, it is no longer significantly different to wildtype ($p>0.05$, ANOVA).

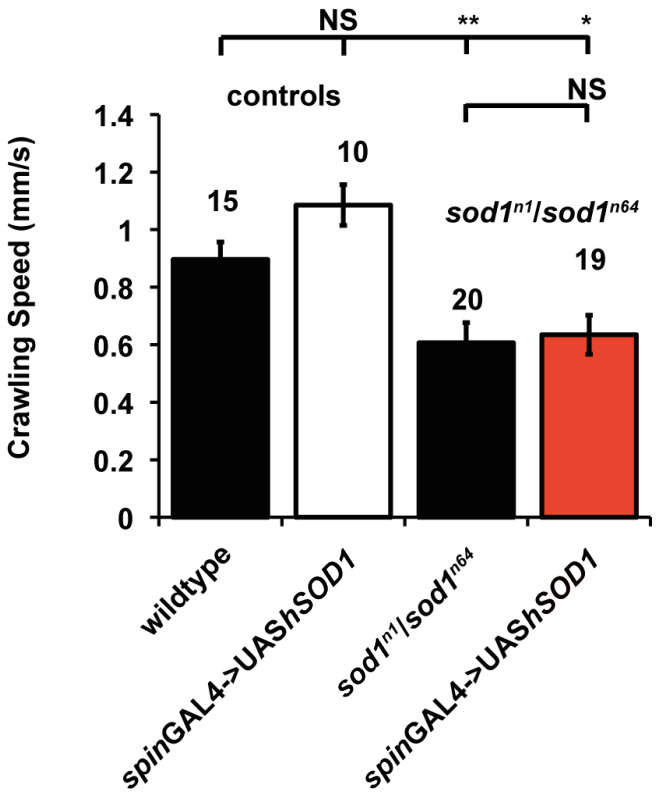

Figure 6.4: Reducing ROS in *sod1* does not rescue crawling speed. As shown earlier *sod1* causes a reduction in crawling speed from 0.90±0.06mm/s (n=15) for wildtype to 0.61±0.07mm/s (n=20, p<0.01, ANOVA). Expression of *hSOD1* doesn't change crawling speed, 1.1±0.07mm/s (n=10, p<<0.05, ANOVA), and expression of *hSOD1* in *sod1* does not significantly rescue crawling speed 0.63±0.06mm/s (n=19) (p>>0.05, ANOVA).

bouton number and reduction in muscle surface area caused by mutations in *sod1*. This suggests that the physiological deficit incurred requires greater levels of *hSOD1* than is required to rescue the changes in form caused by these mutations (Fig. 6.4). Other studies in the Sweeney lab have shown that expression of UAS*hSOD1* by the promoter *spin*GAL4 only rescue viability by 80% (Radhika Sreedhar-Ashwin, Sweeney lab, personal communication). Another possibility is that because *sod1* mutants are semi-viable there is a chance that homozygous *sod1* mutants have mated in the stock. These flies have high levels of DNA damage due to increased ROS and therefore the

possibility of a second site mutation is high. However it must not be overlooked that sod1 is highly expressed therefore *spin*GAL4 might not provide high enough expression to combat the reduction caused by the mutation.

The observation that the reduction in crawling speed seen in *spinster*, *highwire* and *sod1* mutants is not rescued by expression of antioxidants suggests that it is not oxidative stress causing this phenotype. However this phenotype is so consistent between the mutants analysed that it is likely to be an effect induced by oxidative stress such as mitochondrial dysfunction which can be caused by oxidative stress and go on to cause further oxidative stress as a vicious cycle ensues.

6.2.5. The effects of *sod1*, *sod2* and *spinster* on synaptic transmission

As discussed earlier crawling is, physiologically, a complex process, involving complex nerve circuit pathways and muscle contraction. To establish how synaptic transmission itself is affected by mutations in *spinster* and *sod* to determine if impaired crawling correlates with impaired synaptic transmission at the neuromuscular junction, electrophysiological recordings were carried out. Previous data has shown that *spinster* has impaired synaptic transmission, with normal response to neurotransmitter from a single vesicle but with a reduced number of vesicles released in response to an elicited action potential. The *Drosophila* larval neuromuscular junction is a highly useful and well-established model for studying synaptic transmission and thus can be used effectively to study the effects of oxidative stress on synaptic transmission. By inserting microelectrodes into *Drosophila* muscle a lot can be learnt about the functioning of the neuromuscular junction in different conditions to allow deficits in synaptic transmission to be pinpointed. *sod* and *spinster* mutants were examined for synaptic transmission deficits. The first electrophysiological aspect investigated was resting membrane potential. Resting membrane potential is determined by

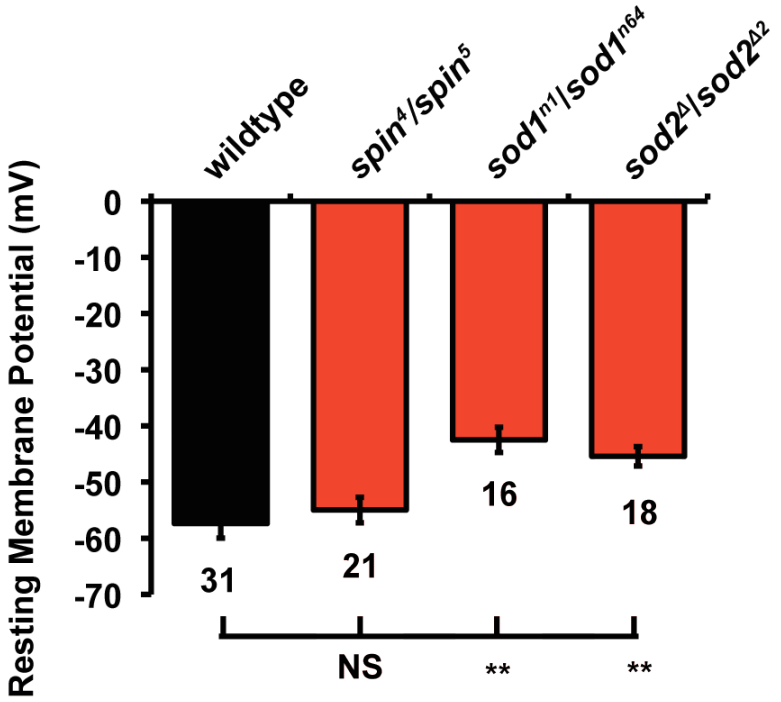

Figure 6.5: *spinster* has a normal resting membrane potential, *sod1* and *sod2* have increased resting membrane potentials. Wildtype muscles have a resting membrane potential of -57.39±2.59mV (n=31). The resting membrane potential in *spinster* is not significantly different -54.98±2.26mV (n=21). *sod1* and *sod2* have significantly increased resting membrane potentials of -41.32±1.64mV (n=16) and -45.42±1.73mV (n=18) respectively ($p<0.01$, ANOVA).

the difference between intracellular and extracellular ion concentrations. The Nernst and Goldman equations are used to calculate the potential difference between these components, this takes into account the relative concentrations of the different ions present. If the resting membrane potential is perturbed this suggests that ionic balance is impaired and thus normal excitability might be compromised. In agreement with previously published data *spinster* mutants show no change in resting membrane potential (Sweeney and Davies, 2002). *sod1* and *sod2* mutants both show increased resting membrane potentials suggesting abnormal electrochemical gradients between the intracellular and

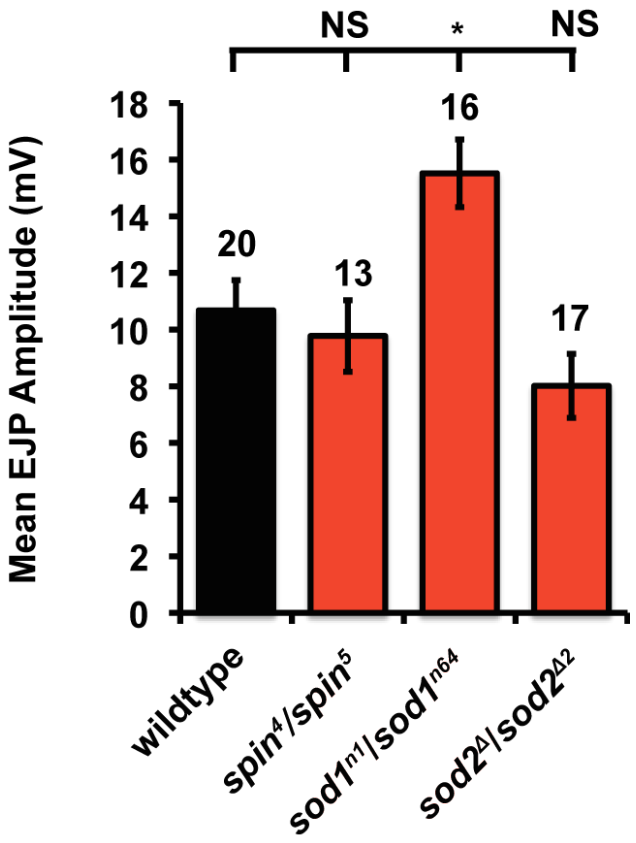

Figure 6.6 *spinster* and *sod2* have normal EJPs whereas *sod1* have increased EJP amplitude. The amplitude of wildtype EJPs is 10.67±1.06mV (n=20). *spinster* and *sod2* have statistically similar EJP amplitudes of 9.77±1.26mV (n=13) and 8.01±1.13mV (n=17) (p>>0.05, ANOVA). *sod1* muscles show increased EJP amplitudes of 15.52±1.19mV (n=16, p<0.05, ANOVA).

extracellular components (Fig. 6.5). The activity of the Na^+/K^+ pump could be impaired due to reduced levels of ATP, resulting in less sodium being pumped out leading to an increased resting membrane potential. An alternative reason for this could be that K+ leak out of the cell through non-gated channels leading to less K^+ in the cell, increasing the resting membrane potential. As discussed earlier the EJP is the response of the muscle to an action potential in the nerve resulting in neurotransmitter being released from the nerve terminal. Changes in EJP result in impaired synaptic transmission and hence measuring EJPs can give insight into neuronal functioning. Spontaneous EJPs in wildtype *spinster*, *sod1* and *sod2* were measured and the mean amplitude was only shown to be

different in *sod1* mutants (Fig. 6.6), where it was shown to be increased suggesting that either more neurotransmitter is released in response to an action potential in the nerve or the muscle is eliciting increased response to the normal level of neurotransmitter released. This suggests that *spinster* and *sod2* mutants are showing a normal response to neurotransmitter release from the pre-synaptic terminal. This is at odds with previous *spinster* data (Sweeney and Davies, 2002), which showed a 50% reduction in EJP amplitude. However the methods of electrophysiological analysis were different, and the method used here might be less sensitive and therefore overlook changes in EJP detected in the published data, as here spontaneous EJPs rather than evoked EJPs were recorded.

The amplitude of EJPs is dependent on the resting membrane potential (RMP). Generally speaking, the higher the RMP the smaller the EJP. Therefore, to take into account the changes in RMP seen in *sod* mutants the residual was calculated, based on what the EJP would be expected to be in wildtype for any given RMP. The difference between expected and actual EJPs is not significantly different to wildtype in *spinster* and *sod2* suggesting that EJPs are only altered in *sod1* (Fig. 6.7).

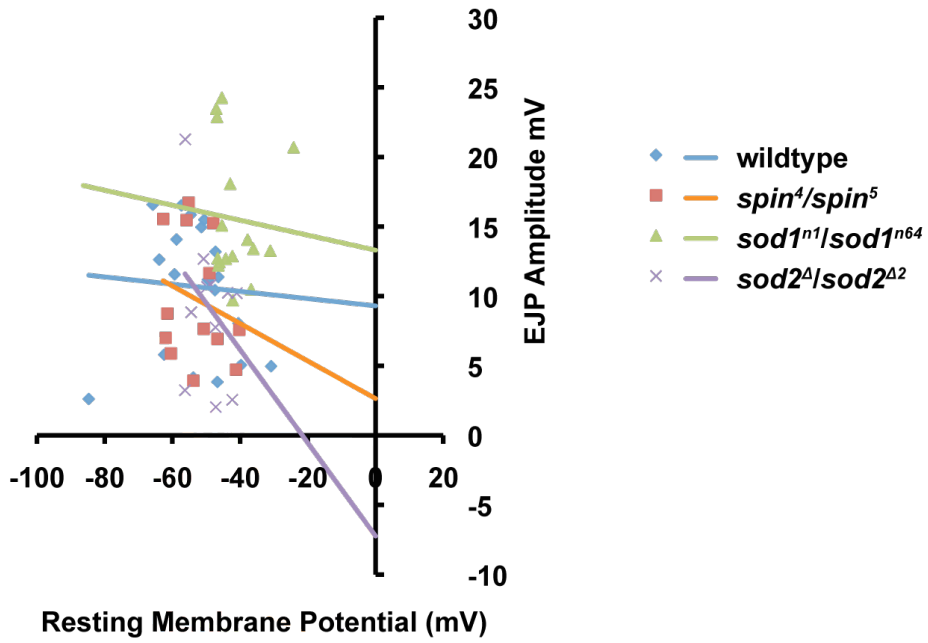

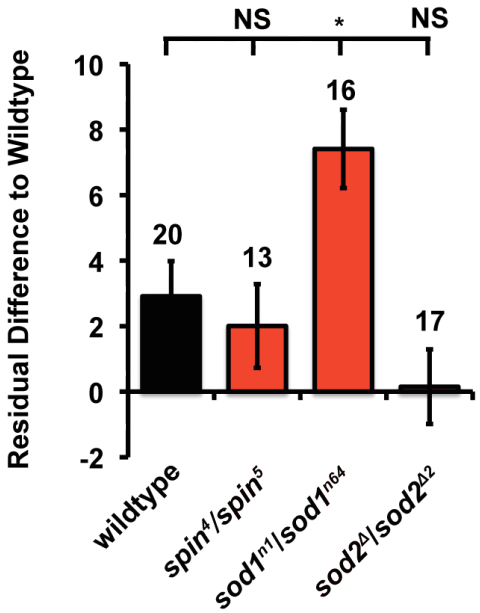

Figure 6.7: *spinster* and *sod2* have normal EJPs for the resting membrane potential, whereas *sod1* have a higher EJP amplitude than expected. (A) EJP amplitude is shown plotted against resting membrane potential, showing that EJP amplitude declines as the resting membrane potential decreases (B) When compared to the trend line for wildtype and calculating the residual only *sod1* has a significantly different EJP to expected based on resting membrane potential.

6.2.6. Normal and aberrant mitochondria are seen to be present in the *spinster* mutant.

We performed transmission electron microscopy (TEM) on the laminar area behind the optic lobe in 5-day-old adult flies. This area was chosen as it is neuronal and has a high level of mitochondria present. Normal mitochondria can be seen in both wildtype and *spinster* (Fig. 6.8 A -F). Normal mitochondrial morphology can be seen both in wildtype and *spinster* with regular outer and inner membrane morphology. However, there are also a number of damaged mitochondria only seen in *spinster* (Fig. 6.8 G-I). Multiple aberrant mitochondria were seen in every animal of *spinster* and none were seen in wildtype. In this damaged mitochondria the inner membrane is irregular and denser. In addition a mitochondrion that was unable to undergo mitophagy and became surrounded by many layers of membrane was also seen in *spinster*. This suggests that in addition to the build up of endosomes and lysosomes seen in *spinster* (Sweeney and Davis, 2002; Dermaut *et al.*, 2005) that were present, mitochondrial recycling may be impaired. Mitochondrial impairment suggests that there could be an energy deficit in *spinster*, as mitochondrial respiration is impaired so energy is not produced efficiently leading to increased ROS generation. To test whether *spinster* is incurring an energy deficit HPLC was used to test the ratio of AMP:ADP:ATP, however the results of this were inconclusive. A mitochondrial function assay by investigating oxygen consumption using a Clarke electrode was carried out. However, it was not possible to optimise this technique within the time available, although this experiment would be highly informative and would elucidate the status of mitochondrial function and metabolism in *spinster*.

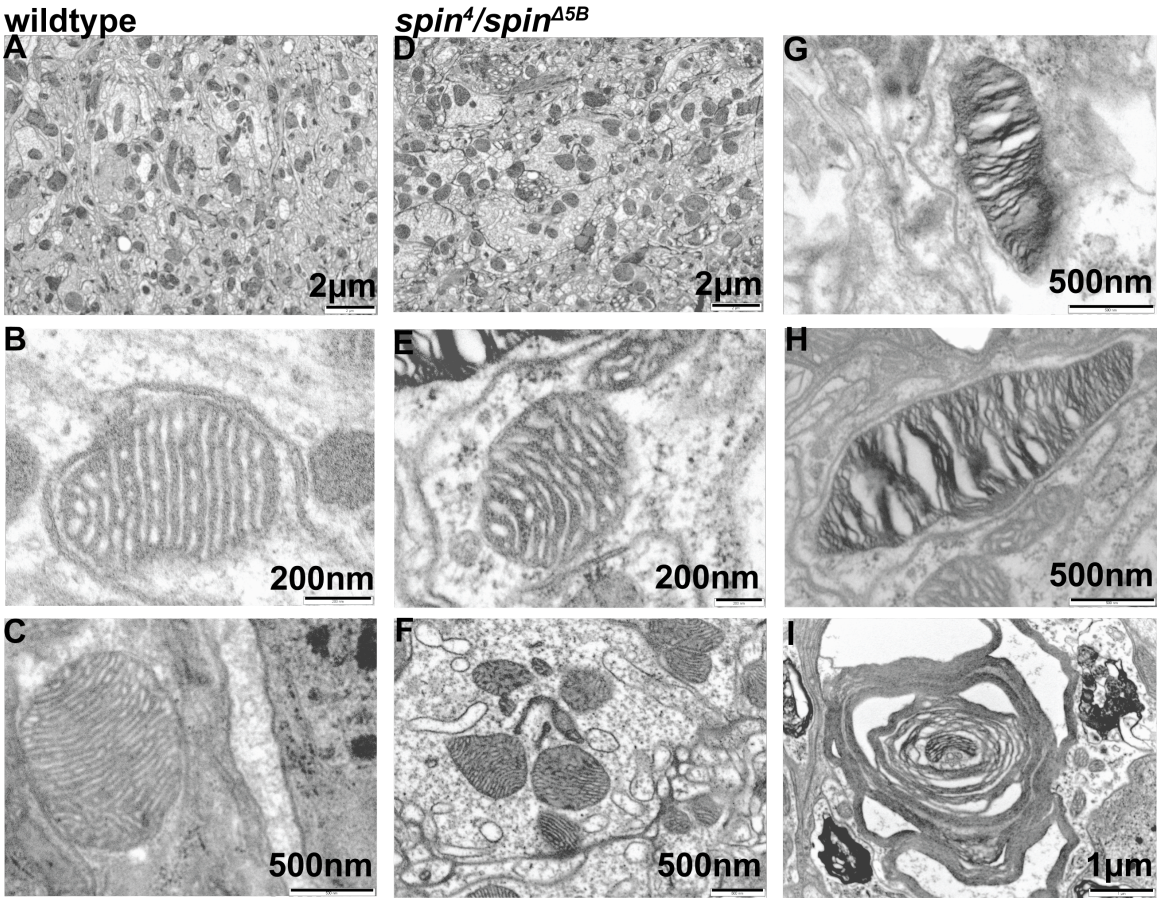

Figure 6.8: Aberrant mitochondria are present in *spinster*. Most mitochondria present in *spinster* show normal morphology. However there are also a number of diseased mitochondria (G and H) and examples of impaired mitophagy (I) that are not seen in wildtype.

6.2.7. AMPK is required for *spinster* induced overgrowth

Previous work has shown that mutations in subunit γ of AMPK prevent *spinster*-induced overgrowth (Sean Sweeney, personal communication). This is one of the regulatory subunits of AMPK. Therefore it was examined whether AMPK is involved in synapse development and confirm its role in *spinster*. To do this RNAi transgenes to AMPK subunit α, the catalytic subunit of AMPK were expressed. Reducing AMPK activity pre- and post-synaptically using either of the RNAi transgenes causes a reduction in bouton number in a wildtype background with one transgene (106200) but not the other (1827). In a *spinster* mutant background expression of either transgene reduces synaptic overgrowth. Reducing AMPK levels did cause a significant reduction in muscle surface area in with 106200 but not 1827. Nonetheless, reduction of AMPK function in a spinster mutant background reduced synapse growth significantly prior to any normalisation procedure. When these trangenes are expressed in *spinster,* muscle surface area is the same as wildtype, hence normalised bouton number shows the same reduction in overgrowth as prior to normalisation. This suggests that AMPK may be partly responsible for the reduction in muscle surface area.

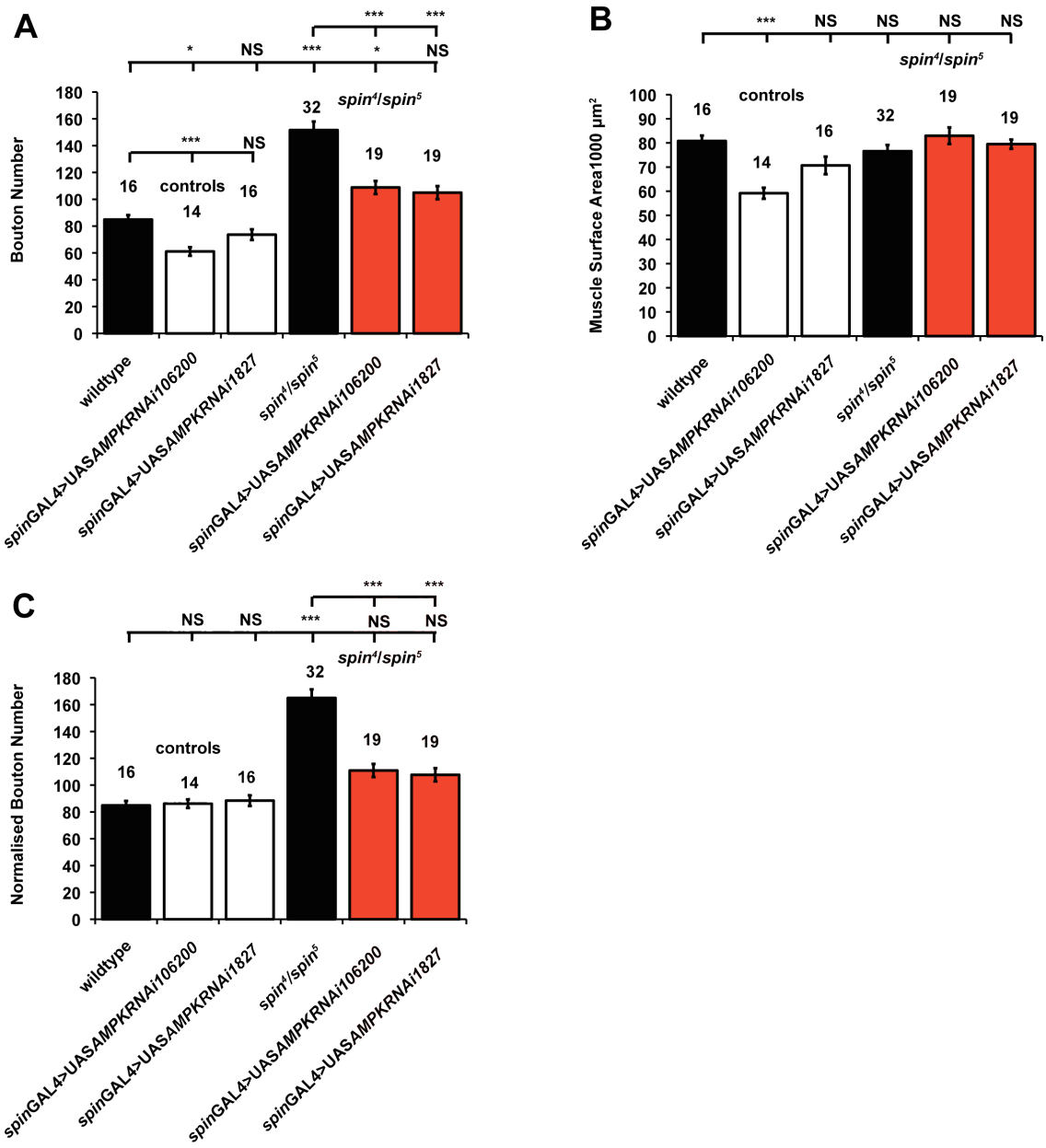

Figure 6.9: *Spinster* induced overgrowth requires AMPK. (A) Expression of *AMPK-RNAi106200* in a wildtype background causes a significant reduction in bouton number 61±4.0 (n=14) ($p<0.001$, when compared to wildtype and other transgene control and $p<0.05$, when compared to all means in the graph, ANOVA) no significant change in bouton number is seen with *AMPK-RNAi1827* 74±4.6 (n=16). *spinster* induced overgrowth is significantly reduced from 152±4.74 (n=32) to 109±6.2 (n=19) and 105±6.52 (n=19) ($p<0.001$, ANOVA). (B) Only UAS*AMPKRNAi106200* causes a significant change in muscle surface area, reducing it to 59153±2289, *AMPKRNAi1827* has a MSA of 706687μm^2. In *spinster* these transgenes cause MSAs of

82971±3443μm^2 and 79495±1919μm^2 ($p>0.05$, ANOVA) (C) Following normalisation to muscle surface area UAS*AMPKRNAi* significantly rescues *spinster* induced overgrowth from 165±7.5 (n=32) to 111±10(n=19) and 108±6.8 (n=19). The transgene controls have normlised bouton numbers of 86±7.45 (n=14) and 88±8.8 (n=16) ($p>0.05$, ANOVA).

6.2.8. Increased activation of AMPK is required pre- and post-synaptically to drive synapse growth

Having shown that AMPK is required for *spinster*-induced it was postulated that AMPK activity could drive synapse overgrowth. To determine the role of AMPK in synapse development a pseudo-phosphorylated AMPK transgene, UAS*AMPK*$^{T184D-}$, which simulates activated AMPK (Mirouse *et al.*, 2007) was expressed. When this is expressed pre-synaptically with *elaV*GAL4 there is no change in bouton number compared to wildtype, nor is there any statistically significant change in bouton number when AMPK activity is increased in the muscle (Fig. 6.10A). However it must be noted that when expression in only the nerve or the muscle is compared to wildtype using ANOVA, bouton number is significantly reduced compared to wildtype with neuronal expression of AMPK-P. Conversely, increased activity of AMPK in the muscle causes a significant increase in bouton number. The increased bouton number seen with *spin*GAL4 obscures these significances when included in statistical analysis. When expressed

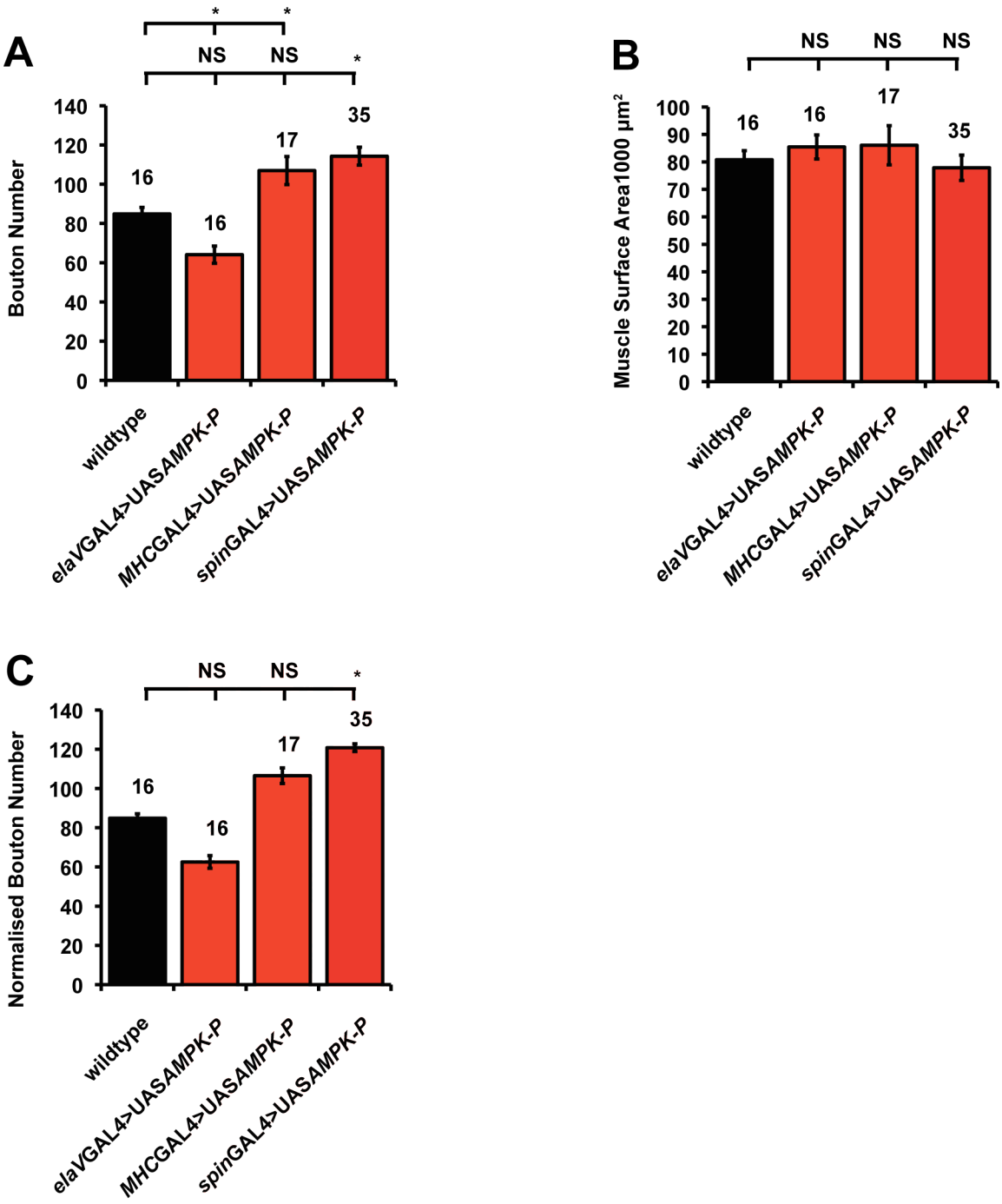

Figure 6.10: Increased AMPK activity pre- and post- synaptically results in synaptic overgrowth. (A) Driving psuedo-phosphorylated AMPK in either the nerve or the muscle does not significantly change bouton number with means of 64±4.4. (n=16) and 107±7.1 (n=17). Concurrent expression with *spin*GAL4 causes a significant increase in bouton number to 114±4.6 (n=35) ($p<0.05$, ANOVA). (B) Expression of this transgene in either the nerve muscle or both does not significantly affect muscle surface

area with mean muscle surface areas of 85443±2265μm^2 (n=16), 86061±3989μm^2 (n=17) and 77872±1933μm^2. (C) When normalised to muscle surface area expression in either the nerve or the muscle does not significantly alter normalised bouton number with bouton numbers of 63±5.4 and 107±9.9 respectively ($p>0.05$, ANOVA). Concurrent expression under the control of *spin*GAL4 results in significantly increased bouton number 121±5.6 ($p<0.001$, ANOVA).

simultaneously in the nerve and the muscle using spinGAL4, there is a significant increase in bouton number, when all conditions are compared by ANOVA. Expression of this transgene, pre- or post synaptically or simultaneously does not change muscle surface area, consequently when normalised, there is only a significant change in bouton number when AMPK-P is expressed simultaneously pre- and post- synaptically (Fig. 6.10C). The change caused by only neuronal or muscular expression is still not significant when normalised even when compared in the absence of simultaneous expression.

6.2.9. AMPK activity is required for crawling

Using *löe* mutations and the RNAi and pseudo-phosphorylated AMPK transgenes, the effects of AMPK activity levels on crawling speed were investigated (Fig. 6.11). Mutations in *löe* cause no change in larval crawling speed; the crawling speed is not statistically different to wildtype. *löe* is a mutation that causes neurodegeneration (Tschäpe *et al.*, 2002). It is a mutation in one isoform of the γ-subunit of AMPK, one of the regulatory subunits of AMPK. Reducing AMPK levels through expression of AMPK RNAi to the α-subunit of AMPK, which is the catalytic subunit causes a significant reduction in crawling speed. This suggests that under normal conditions activity of AMPK is required for normal physiological output. Expression of pseudo-phosphorylated AMPK causes no change in crawling speed.

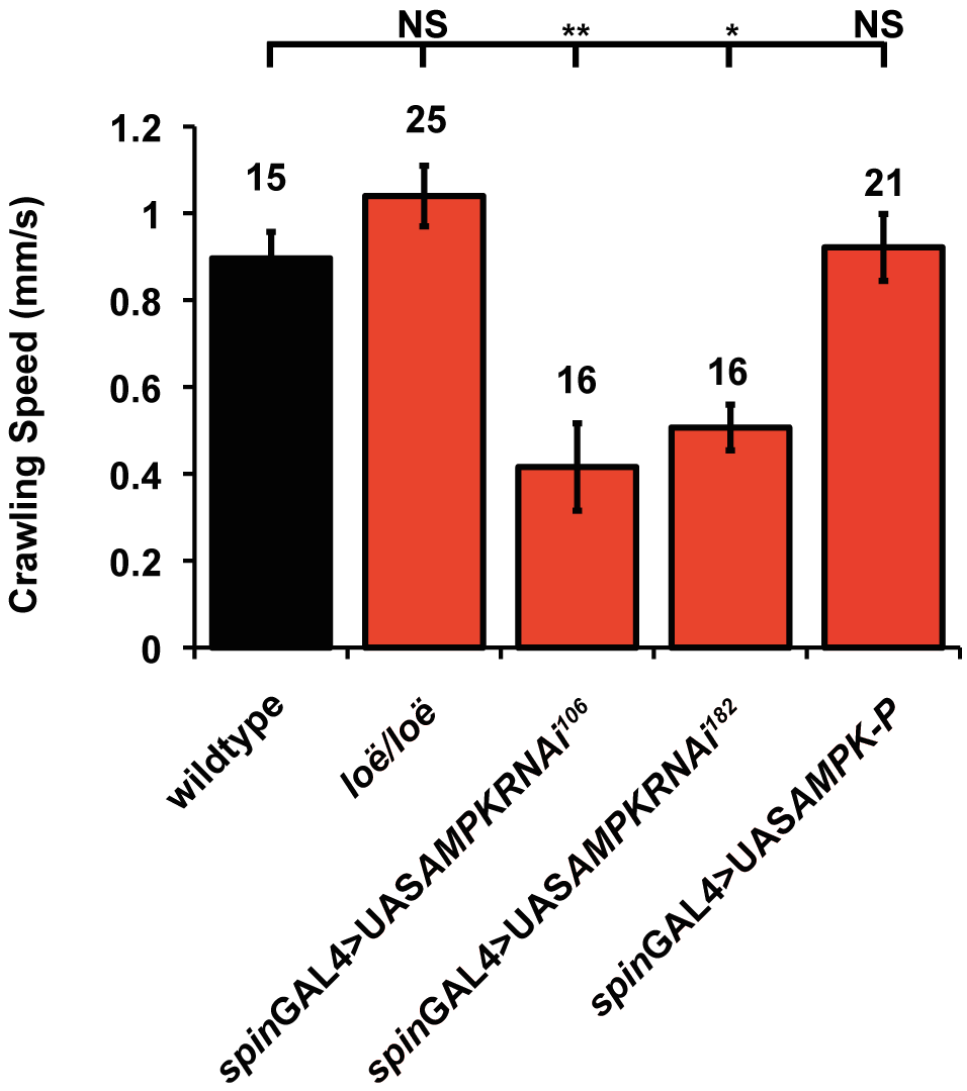

Figure 6.11: AMPK is involved in determining crawling speed. Mutations in loë do not affect crawling speed, 1.03±0.07 (n=25). Depleting AMPK through expression of AMPK RNAi results in a significant reduction in crawling speed to 0.42±0.1 (n=16, $p<0.01$, ANOVA) and 0.51±0.05 (n=16, $p<0.05$, ANOVA) for the two different transgenes. Pseudo-active AMPK causes no change in crawling speed relative to wildtype 0.92±0.08 (n=21, $p>>0.05$, ANOVA).

6.3. Discussion

6.3.1. Mutations causing oxidative stress can impair motor function

All the mutations investigated in this study, *spinster*, *hiw*, *sod1* and *sod2* have impaired crawling speed compared to wildtype. It was postulated that if oxidative stress were causing this deficit expression of anti-oxidant transgenes would rescue this phenotype. However, reducing oxidative stress in any of these mutants did not rescue the reduction in crawling speed. Expression of these transgenes did however rescue synaptic overgrowth. This suggests that the mechanisms through which these mutations cause synaptic overgrowth are distinct from those that cause impaired motor function. It could be that function is more sensitive to oxidative stress than form, in so far as relieving oxidative stress enough to prevent overgrowth still leaves a high enough level of ROS to impair motor function. The driver used, *spin*GAL4, expresses pre- and post-synaptically as well as in the central nervous system, but at relatively low levels compared to other global drivers such as *actin*GAL4 and *tubulin*GAL4, therefore using these drivers might still afford a rescue of the reduction of crawling speed seen in these mutants.

It is worth noting that *tub*GAL4 does not afford any greater rescue of bouton number in *spinster* than *spin*GAL4. This suggests that although reducing oxidative stress with *spin*GAL4>UAS*hSOD1* provides the maximum level of rescue seen with any driver in *spinster* bouton number there is still a significant reduction in motor function. In *hiw* mutants *spin*GAL4>UAS*hSOD1* does not rescue the crawling speed even though it significantly rescues the increase in bouton number seen in *hiw* mutants, in a similar fashion to that seen in *spinster* mutants. This supports the theory that function might be more sensitive to oxidative stress than synaptic morphology, or there is a defect other than oxidative stress present in *spinster* and *highwire* that is leading to the decline in

motor output seen. Based on the observation that *spin*GAL4>UAS*hSOD1* in *sod1* mutants fully rescues synaptic overgrowth yet does not rescue the deficit in motor function, it seems more likely that oxidative stress is not reduced enough to rescue synaptic function and thus supports the hypothesis that crawling speed is more sensitive to oxidative stress than synaptic function, rather than being caused by something else present in *spinster*, *highwire* and *sod1*. It is however, possible that build up of protein in these mutants, causing something other than oxidative stress, is the cause of the reduction seen in crawling speed, as mutations in *sod1* have been postulated to cause disease through aggregation of mutant *sod1* rather than reduction in antioxidant capacity (Vijayvergiya *et al.*, 2005). This remains to be investigated through using stronger drivers and a variety of anti-oxidants, and investigating other mutations that cause oxidative stress. It can however be seen that level of overgrowth is not directly correlated with reduction in crawling speed. It is also interesting to note that overgrowth does not necessarily result in impaired crawling, as *spin*GAL4>UAS*AMPK*^{T184D} has significantly increased bouton number yet normal crawling speed. This is also supported by studies into overgrowth mutants that show hyperactivity and overgrowth (Budnik *et al.*, 1990). The data here suggest that mutations that have oxidative stress induced changes in synaptic morphology show the general phenotype of impaired crawling speed, indicative of impaired synaptic function. This is supported by the electrophysiological data in *sod1* and *sod2*. Although, rescues have not been performed to determine whether the changes in synaptic transmission phenotypes seen in these mutants are caused by oxidative stress. Synaptic transmission does not seem to be significantly impaired in *spinster*, at odds with previously published data, but this is likely to be due to differences between spontaneous EJPs investigated here and evoked EJPs in the published data. Studies carried out in collaboration with the Sweeney lab by the Robinson Lab in Plymouth have shown that *spinster* has normal EJPs, similar to the data shown in this study, but they have also found fatigue phenotype during repeated

stimulation, potentially due to an inability to recycle synaptic vesicles at a rate suitable to sustain normal synaptic transmission (Iain Robinson, personal communication; Milton *et al.*, 2011), this phenotype was rescued by relieving oxidative stress through expression of *hSOD1* with the promoter *spin*GAL4. This 'fatigue phenotype' is consistent with other studies on mutants defective for endocytosis (Koh *et al.*, 2004; Marie *et al.*, 2004). A *drosophila* model of Parkinson's disease, caused by mutations in *pink1* also fails to maintain normal synaptic transmission during intense activity (Morais *et al.*, 2009). This does not explain why both *sod1* and *sod2* mutants show different phenotypes to *spinster*. Consequently, it is hard to determine which physiological phenotypes are caused by oxidative stress in *spinster* as *sod* mutations causes a significant increase in RMP that is not seen in *spinster*. This suggests that oxidative stress in *sod* mutations causes effects that are not seen in *spinster*, suggesting that something in *spinster* allows it to maintain its resting membrane potential despite the presence of oxidative stress. The other phenotypes seen in *spinster*, such as lipid peroxidation and increase in bouton number are rescued by expressing *hSOD1* suggesting that superoxide is contributing to these phenotypes. Therefore it may seem counterintuitive that mutations in *sod1* do not recapitulate this phenotype. However, there are other cellular defects in *spinster* that are unlikely to be present in either of the *sod* mutants. The decreased lysosomal degradation seen in *spinster* could lead to the prolonged and increased presence of cellular components that would otherwise be broken down during the cellular stress response to protect the cell from oxidative stress. This could also be the reason that *spinster* does not show a decrease in muscle surface area seen in all other cases of oxidative stress investigated.

Mutations in both *sod1* and *sod2* could directly affect mitochondrial function and the impaired mitochondria in *spinster* could be responsible for impaired crawling speed. Mitochondrial morphology in *sod* mutants would be an interesting avenue for future research. *sod2* mutations cause mitochondrial damage in muscles

(Godenschwege *et al.*, 2009). Defective mitochondria could result in reduced ATP production, leading to increased AMP:ATP activating AMPK.

6.3.2. Increased AMPK activity can cause synaptic overgrowth and is required for *spinster* induced overgrowth

Due to the potential metabolic deficit in *sod* mutants and *spinster*, a signalling pathway likely to be activated by defective ATP production was investigated. AMPK has not as yet been directly implicated in synaptic growth and in this study it is shown that AMPK positively regulates bouton number and furthermore that it is required for *spinster* induced overgrowth. Previous data surrounding the role of upstream regulators of autophagy have been somewhat contradictory. However, it is clearly shown that the regulatory subunits of AMPK are required for *spinster*-induced overgrowth in addition to the catalytic subunits. This is somewhat at odds with the findings that Rheb drives synapse growth as increased AMPK would increase tuberous sclerosis complex activity and therefore increase the inhibition of Rheb. Therefore the data displayed here support more the findings of Shen and Ganetzky (2009) as increased inhibition could lead to increased autophagy, which they find to produce an overgrowth. However AMPK has a number of potential effectors and therefore any phenotype caused by increased AMPK does not necessarily depend on autophagy. Nonetheless, for the first time, AMPK has been implicated in regulation of synaptic growth response, suggesting that energetic status is important for correct synaptic growth responses.

7. Discussion and Future Research

7.1. Introduction

The aims this investigation were to answer the following:

1. Do mutations in *spinster* cause oxidative stress and is oxidative stress contributing to the synaptic overgrowth phenotype?
2. Can oxidative stress cause synaptic overgrowth independently of lysosomal dysfunction?
3. Are ASK/JNK/AP-1 activation and autophagy required for synaptic growth observed under conditions of oxidative stress?
4. Oxidative stress is known to impair mitochondrial function. Does oxidative stress/ *spinster* cause an energy deficit resulting in impaired physiological output? If this is the case, are compensatory metabolic pathways induced in spinster?

The purpose of this chapter is to establish which of these aims have been fulfilled giving an overarching view of the data generated in this thesis and suggest future research questions that have arisen as a result of this study.

7.2. *spinster* as a model of a lysosomal storage disorder

Lysosomal storage disorders are characterised by impaired lysosomal degradation of cellular components, leading to accumulation of undegraded material in the lysosomal system (For review see Futerman and van Meer, 2004). A number of LSDs have been shown to have oxidative stress (Deganuto *et al.*, 2007; Fu *et al.*, 2010; Fillipon *et al.*, 2011), potentially due to the build up of lipofuscin. Lipofuscin is undegraded material that builds up during aging and pathological impairment of degradative pathways, as in lysosomal storage disorders. Lipofuscin potentiates the generation of ROS, thus further increasing

oxidative stress. Lysosomes are rich in transition metals in a low pH and dysregulation in LSD produces an environment conducive for Fenton reactions generating ROS (Kurz *et al.*, 2007, Kurz *et al*. 2008a and b). Oxidative stress induces autophagy (Higgins *et al.*, 2011; Chen *et al.*, 2009; Wu *et al.*, 2009) contributing further to lysosomal build-up of undegraded material. A positively reinforcing cycle ensues: impaired lysosomal degradation increases oxidative stress and induces autophagy coupled with impaired autophagic clearance this results in build up of autophagosomes and autophagolysosomes. Oxidative stress, presence of lipofuscin and dysregulated autophagy (Settembre *et al.*, 2009; Fu *et al.*, 2010) and mitochondrial aberrations are identified cellular hallmarks of LSD; excessive dendritogenesis and synaptogenesis are also observed (Walkley *et al.*, 1985 and 1988a and b; March *et al.*, 1995). Here *spinster* is confirmed as a model of LSD, as suggested by Dermaut *et al.*, 2005; Sweeney and Davis, 2002; Nakano *et al.*, 2001, as spinster is a late endosomal/lyososomal protein and mutations in *spinster* result in enlarged late endosomes/lysosomes, increased oxidative damage and activation of the oxidative stress response, increased synaptogenesis and mitochondrial aberrations.

7.2.1. Oxidative stress causes synaptic overgrowth

The data shown in the previous chapters show that oxidative stress causes growth of the *Drosophila* neuromuscular junction and is a contributory factor in the overgrowth seen in *spinster* loss of function mutants, a model of a neurodegenerative LSD. This suggests *spinster* lysosomal dysfunction generates oxidative stress as seen in known LSDs (Fu *et al.*, 2010). Oxidative stress is common in LSDs due to the pathological presence of undegraded material. Synapses are areas of high energy demand; hence they are rich in mitochondria, the greatest generators of ROS, making them susceptible to oxidative stress. Moreover, nerves are generally postmitotic and do not readily regenerate, thus they are predisposed to the accumulation of lipofuscin. The

majority of the synaptic overgrowth in *spinster* is rescued by reducing the oxidative stress burden. The data in this study are supported by the observation that oxidative stress generated independently of lysosomal dysfunction promotes synapse growth. A number of mutations identified by hyperexcitabilty phenotypes, due to mutations in potassium channels involved in terminating release from the presynaptic terminal, also cause synaptic overgrowth: *shaker* (*sh*), *ether a go-go (eag)* and *hyperkinetic (hk)* (Budnik *et al.*, 1990). These, and another hyperexcitable mutant, *quiver*, were subsequently found to be hypersensitive to oxidative stress (Wang *et al.*, 2000). It would be interesting to see if this overgrowth is rescued by expressing antioxidants. Excitability determines neuronal morphology as electrical activity regulates plasticity, but how this happens in these mutants is unknown; it could be that increased synaptic activity leads to oxidative stress leading to overgrowth. It would be interesting to differentiate between function and morphology in these mutants to determine if oxidative stress is causing the overgrowth, secondary to the primary cause of hyperexcitability. Another known cause of overgrowth is impaired downregulation of signalling molecules due to defective degradation pathways as seen in *spinster* and *ema* (Sweeney and Davies, 2002; Kim *et al.*, 2010). As shown in this study, *spinster* overgrowth is also caused by oxidative stress as well as increased TGFβ signalling. It is possible that mutations in *ema* cause oxidative stress as a result of enlarged endosomal compartments, resulting in oxidative stress derived overgrowth. It is interesting to note that in this study the level of increase in raw bouton number seen in *spinster* and *ema* cannot be obtained purely through induction of oxidative stress, in the absence of lysosomal dysfunction. This suggests that defective endosomal downregulation of TGFβ signalling and oxidative stress contribute to overgrowth in *spinster* whereas in *sod* mutants and paraquat fed animals TGFβ downregulation by the endosomal system is unimpeded thereby limiting the level of overgrowth.

Even though the general trend of the data in this study is that oxidative stress contributes to synaptic growth, this is clearly not always the case. Rotenone is also thought to generate elevated levels of superoxide, through inhibition of complex I of the mitochondrial respiratory chain. However, rotenone can impair microtubule formation (Brinkley *et al.*, 1974; Srivastava and Panda, 2007), which could impede autophagy, which is shown to be required for synaptic growth or overgrowth. This could be determined by looking at microtubule morophology in rotenone-fed animals compared to controls. It would also be interesting to determine the level of oxidative stress incurred by rotenone exposure for example using a lipid peroxidation assay or looking at expression of *gst-D*-GFP. Furthermore *sdhB* mutants do not show synaptic overgrowth, even though increased ROS generation has been demonstrated (Walker *et al.*, 2006). Interestingly though mutations in *sdhA,* which also cause oxidative stress, result in oxidative stress dependent synapse loss in the *Drosophila* eye. Taken together these findings suggest that oxidative stress can contribute to synaptic overgrowth at the *Drosophila* neuromuscular junction, but can also lead to the generation of other phenotypes, depending on the source and level of ROS.

7.2.1.1. Is oxidative stress induced synaptic morphology ROS specific or source specific?

In terms of bouton number it is hard to determine any clear conclusions about the role of different ROS in the generation of overgrowth phenotypes. With respect to *spinster* the same level of rescue was achieved regardless of the type of antioxidant present. This suggests that it does not matter whether it is superoxide anions or hydrogen peroxide or other ROS that specifically cause synaptic overgrowth. However, mutations in catalase, which would decrease the breakdown of hydrogen peroxide, did not result in overgrowth whereas mutations in *sod1* and *sod2* and paraquat exposure, which increase levels of superoxide, did cause overgrowth. This might suggest that superoxide potentiates synaptic growth. However when the vast overgrowth in *sod* is

removed from statistical analysis *cat* overgrowth is significant. *sod* is the only enzyme that can catalyse the conversion of superoxide anions to hydrogen peroxide whereas with catalase other enzymes could be compensating for the loss of *cat*. It was attempted to investigate the importance of different ROS using mutations in other proteins involved in the conversion of superoxide ions to hydrogen peroxide, such as thioredoxin reductase (TrxR), however these are not viable to 3rd instar as homozygotes or transheterozygotes in the conditions used in this study, even using apple juice agar plates and yeast mix. It might be possible to use animals lacking one copy of catalase and one copy of TrxR. Another alternative is to feed larvae hydrogen peroxide; this is currently being investigated in the Sweeney lab. It is hard to determine the proportionate levels of different ROS in living tissue with the current reporters available and therefore difficult at present to dissect which ROS are responsible for the generation of overgrowth phenotypes.

Mutations in *sod1* and *sod2* have differential effects on branching and bouton size, this could suggest that the source of ROS is important in determining these phenotypes. Superoxide anions are short lived molecules, so these phenotypes could reflect the differential effects of ROS damage leading to diverse phenotypes. *spinster*, *sod1* and paraquat all cause an increase in small boutons compared to wildtype whereas *sod2* results in increased medium sized boutons. It can also be seen that *sod2* is the only condition of oxidative stress that results in a decrease in branching, suggesting that something is different in this condition that is common to the other three, although it remains to be investigated what this might be, as it is probably not as simple as mitochondrial vs. cytoplasmic oxidative stress as paraquat causes predominantly mitochondrial generation of ROS.

Another observation from this study is that *sod2* and paraquat induced reductions in muscle surface area are not rescued by expression of *hSOD1* and *trx*^{CYTO} respectively. This could be due to mitochondrial dysfunction still being

impaired as both these antioxidants are cytoplasmic. Further tests need to be carried out with other antioxidants to confirm the specific effects of oxidative stress on bouton number and muscle surface area. *sod1* reduction in muscle surface area is partially rescued by *cat* expression, suggesting that it is not a type of ROS that cause a decrease in muscle surface area but the general presence of oxidative stress.

7.3. ASK/JNK/AP-1 signalling is required for oxidative stress induced synaptic overgrowth

The synergistic effect on bouton number seen in heterozygotes of *spin* and *sod1* are indicative of a threshold at which overgrowth is induced indicating these mutations affect a common pathway generating overgrowth. An important suggestion that can be made as a result is that trafficking defects previously suggested to cause overgrowth through continued expression/disinhibition of signalling pathways of growth signals (Sweeney and Davis, 2002; Kim *et al.*, 2010; Korolchuk *et al.*, 2007; Wang *et al.*, 2007) may not be the only mechanism through which lysosomal dysfunction causes synapse overgrowth; oxidative stress may contribute to the activation of synaptic growth pathways. The 'pathogenic signalling cascade' driving synapse growth in LSD has yet to be identified. The data here support the proposal that oxidative stress and the activation of JNK/AP-1, in *spin* mutants and other cases of oxidative stress, promotes the generation of synaptic overgrowth.

7.3.1. AP-1 activity is differentially required for oxidative stress induced growth

The requirement for Fos and Jun activity for oxidative stress induced synaptic growth is found to be different among *spin*, paraquat-fed, *sod1* and *sod2* mutants treated animals. This suggests differential activation of components of AP-1 in each condition. In *Drosophila*, Fos can homodimerise and is known to

act independently of Jun in synapse overgrowth in *hiw* mutants and conditions of cytoskeletal disruption (Collins *et al.*, 2006; Masaro *et al.*, 2009). In *sod2* mutants and paraquat treatment oxidative stress is generated predominantly in mitochondria, and under these conditions a role for Jun in synapse growth is identified. Jun is not implicated in synapse overgrowth in *spinster* and in *sod1* depleting Jun signalling affords only a partial rescue. This potentially suggests a context dependent role for Jun in the regulation of synaptic growth, which may indicate divergent responses to different cellular sources of oxidative stress. That is to say Jun has a greater role when mitochondrial oxidative stress (Fig. 7.1) is implicated which could suggest than Jun has a role in signalling an energy deficit arising from mitochondrial dysfunction.

7.3.2. Fos is required both in the nerve and the muscle for synaptic overgrowth in *spinster* and *sod2*

AP-1 signalling has previously only been studied acting pre-synaptically at the *Drosophila* neuromuscular junction, as its role in *highwire* is presynaptic as highwire is only expressed in the nerve (Collins *et al.*, 2000), and Sanyal (2003) only investigated AP-1 activity in the nerve. Here a novel role has been identified for Fos acting in the muscle during synaptic development.

7.3.2.1. AP-1 and muscle surface area

Expression of ASK/JNK/AP-1 dominant negative in paraquat fed animals did not alter the reduction in muscle surface area caused by paraquat. Expression of jun^{DN} and fos^{DN} in *sod1* rescue muscle surface area, however jun^{DN} in *sod2* does not rescue muscle surface area whereas fos^{DN} fully rescues muscle surface area. This could suggest a role for AP-1 signalling in determining muscle size.

7.4. Autophagy is required for synaptic overgrowth

7.4.1. Autophagy is required for synaptic overgrowth

Oxidative stress is a potent activator of autophagy. Furthermore, autophagy genes are required for *spinster* and paraquat-induced synaptic overgrowth, suggesting that autophagy promotes synaptic overgrowth in these phenotypes. However, the cellular process of autophagy at the neuromuscular junction during development has not been confirmed in this study, but genetically removing or reducing autophagy function implicates autophagy in overgrowth. The levels of autophagy in *spinster* were also investigated through the use of GFP-tagged atg constructs. Again however, the expression was not high enough to detect in the larvae even with *tub*GAL4 and α-GFP antibodies to amplify the signal. What might be possible in future studies is to analyse autophagy levels looking at these transgenes in the eye, or salivary glands where they have been used previously as a proxy for neuronal tissue.

Activation of autophagy has been shown to promote synapse growth in *Drosophila* via degradation of an upstream inhibitor of the JNK signaling pathway (Collins *et al.*, 2006). Autophagic downregulation of hiw protein has been proposed as a mechanism to regulate synaptic growth (Shen and Ganetzky, 2009). The major identified transcriptional output of the JNK/AP-1 pathway is anti-oxidant and autophagic responses (Wu *et al.*, 2009; Jegga *et al.*, 2011). Autophagy and oxidative stress may directly contribute to the regulation of synapse growth mechanisms. The function of the cell adhesion protein DE-cadherin is sensitive to oxidative stress (DeGennaro *et al.*, 2011) though the generality of this finding has yet to be defined. Autophagy has been observed to selectively phagocytose receptor proteins from an identified synapse (Rowland *et al.*, 2006; Bamber and Rowland, 2006) suggesting a mechanism where autophagy can directly regulate the function and growth of the synapse independently of highwire degradation.

7.4.2. Autophagy is required in the muscle for *spinster* overgrowth

This is a novel finding as previously autophagy has only been implicated in synapse development in the presynaptic compartment. The hiw protein and its target wallenda (wnd) are both found presynaptically (Collins *et al.*, 2006) while in *spinster* autophagy activity contributes to synapse overgrowth in both the muscle and nerve (Fig. 7.1). This observation suggests a novel muscle derived JNK/AP-1/autophagy signal contributing to synapse growth that is likely to be independent of direct *hiw*/*wnd* regulation. A future line of investigation would be to look at the role of TOR in synaptic development.

7.4.3. It is not known whether JNK is upstream of or downstream of autophagy in *spinster* and paraquat induced overgrowth

As discussed above JNK can act upstream of autophagy, whereby activation of JNK transcriptionally activates autophagy (Wu *et al.*, 2009). In addition autophagy was shown to be upstream of JNK signalling in *highwire* mutants, as *highwire* mutants still show synaptic overgrowth with impaired autophagy. However *spin* induced overgrowth is dependent on autophagy. It is hard to determine whether JNK is upstream of downstream of autophagy in *spinster* as qPCR comparing atg1 and atg18 transcripts in *spinster* with and without JNK activity were not informative, as the levels varied greatly even in wildtype. Investigating TOR in these contexts might elucidate the signalling involved in the regulation of autophagy. However many of these signalling cascades are cyclical, for example ROS activated Foxo and JNK are activated by TOR-induced accumulation of ROS, this then leads to upregulation of sestrin, which acts as a negative feedback inhibitor to TOR (Lee *et al.*, 2010). As shown in figure 7.1 JNK signalling is activated by ROS and is required for increases in bouton number but JNK can act both upstream (Wu *et al.*, 2009) or downstream

of autophagy (Shen and Ganetzky, 2009) and where it is acting in *spinster* and oxidative stress to cause synaptic overgrowth remains to be seen. This means that genetic and biochemical analysis in tandem could identify the mechanisms involved.

7.5. AMPK is implicated in synaptic growth

7.5.1. AMPK can drive synaptic overgrowth

Increased AMPK activity is required both in the nerve and the muscle to create a significant overgrowth, relative to muscle surface area. However it is likely that most of this overgrowth is due to activity in the muscle as expression in the muscle causes a significant overgrowth prior to normalisation. This suggests that the role of the muscle in synaptic overgrowth has been somewhat overlooked and requires further investigation. In addition AMPK was also required for overgrowth in *spinster*. It is as yet unknown whether AMPK derived overgrowth is dependent on autophagy as although AMPK activity is known to activate autophagy, it also has many other downstream effectors. To analyse the effectors of AMPK it is necessary to analyse AMPK induced overgrowth when genetically reducing autophagy, through mutations or expression of RNAi transgenes.

7.5.2. AMPK is required for *spinster* induced overgrowth

Given that the overgrowth caused by increased activation of AMPK requires activation both in the nerve and the muscle for significant overgrowth, though in all likelihood a great proportion of this overgrowth is caused by the muscle, and that autophagy is also required both pre- and post- synaptically for *spinster* overgrowth, it will be important to establish where at the synapse AMPK is required in for growth in *spinster*. This could be done through expression of RNAi transgenes, not only to knock down the regulatory subunits but also the catalytic subunit, pre and post-synaptically. The level of activation of AMPK in

spinster was investigated using an antibody specific to phosphorylated AMPK (P-AMPK); unfortunately the affinity of the antibody to *Drosophila* P-AMPK was not sufficient to allow analysis. However the involvement of AMPK in *spinster* overgrowth is indicative of AMPK activation in *spinster*. Although it is not known whether this is through regulation of autophagy or through other mechanisms (Fig. 7.1)

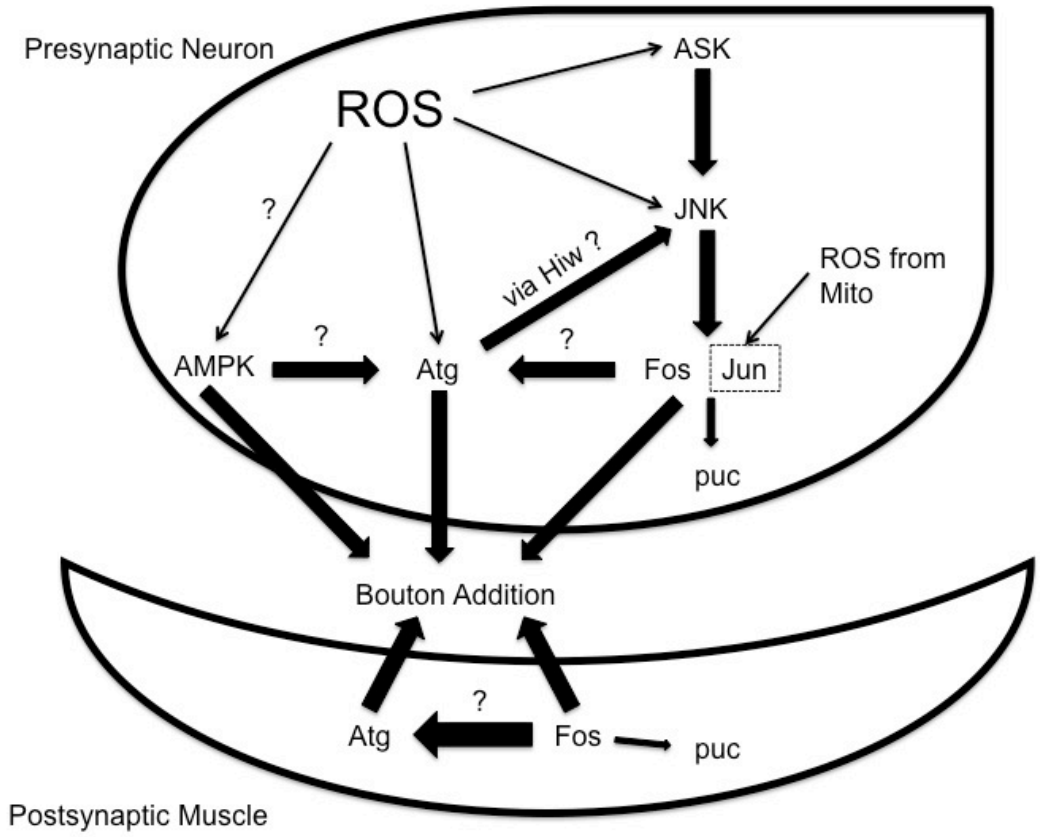

Fig. 7.1: Summary diagram of regulation of bouton number: ASK/JNK/Fos signalling is activated by ROS and leads to increased bouton numbers. Jun is also involved when ROS are a result of paraquat or mutations in *sod2* suggesting mitochondrial ROS generations. AMPK and autophagy are also required in for synaptic overgrowth. Autophagy genes and Fos are required both pre- and post-synaptically for overgrowth.

7.5.3. Mitochondrial defects in *spinster*

A large number of neurodegenerative disorders have been shown to have mitochondrial aberrations. For example, some genetic forms of Parkinson's disease are caused by mutations affecting mitochondrial networks, such as Pink1 and parkin (Clark *et al.*, 2006, Morais *et al.*, 2009). In addition to this some LSDs have mitochondrial aberrations. G_{M1}-gangliosidosis leads to decreased levels of the mitochondrial enzyme cytochrome c-oxidase and morphologically abnormal mitochondria (Takamura *et al.*, 2008). Furthermore, astrocytes extracted from mice with this defect showed increased sensitivity to oxidative stress that was reversed by increasing ATP, suggestive of an energy deficit. Another LSD, mucolipidosis type IV, results in mitochondrial fragmentation, putatively due to impaired recycling of mitochondria through the autophagolysosomal pathway as the mitochondrial defect was recapitulated through inhibition of autophagy (Jennings *et al.*, 2006). The role of AMPK and oxidative stress in *spinster* suggests that *spinster* might be metabolically impaired, due to oxidative stress-mediated disruption of energy metabolism, resulting in reduced ATP. *spinster* appears to have impaired autophagosomal degradation of mitochondria, and previous studies have shown that *spinster* has increased levels of autophagolysosomes following starvation (Rong *et al.*, 2011). The presence of morphologically abnormal mitochondria in *spinster* could suggest defective recycling of mitochondria, common to a number of LSDs and other neurodegenerative diseases. It is necessary to establish when during development mitochondrial aberrations become apparent as the mitochondria shown here are from adult flies. It is also necessary to determine whether these morphologically abnormal mitochondria result in defective mitochondrial function leading to an energy deficit as seen in the mouse model of G_{M1}-gangliosidosis (Takamura *et al.*, 2008).

7.6. Physiological output is more sensitive to oxidative stress than morphology of the neuromuscular junction

Generally increased activity is believed to promote synapse growth. This is seen in mutants with heightened neuronal activity such as *shaker,* a voltage-gated potassium channel. Mutations in *shaker* combined with other mutations that cause enhanced neuronal activity, such as *ether-a-go-go* (*eag*) and *hyperkinetic* (*Hk*) have an increase in bouton number (Budnik *et al.*, 1990). Reducing neuronal excitability in animals expressing these mutations, by introducing mutations in *no action potential* (*nap,* a sodium channel defect) rescues these phenotypes. Increased levels of cAMP cause synaptic overgrowth in *dunce* mutants; mutations in *dunce* reduce the breakdown of cAMP. This increase in synaptic growth is reduced by the mutant *rutabaga*, which is a mutation in adenylate cyclase, and hence impedes the production of cAMP (Zhong and Wu 1991a and b; Zhong *et al.*, 1992). Taken together these data suggest that hyperexcitablity or increased synaptic activity positively correlates with increased bouton number. However, *spinster* has been shown to impair synaptic function (Sweeney and Davies, 2002; Dermaut *et al.*, 2005), with reduced quantal content and normal quantal size. Conversely, *highwire* mutants have both decreased quantal content and decreased quantal size (Wan *et al.*, 2000). Other overgrowth mutants such as *hangover* show no change in electrophysiology showing that the relationship between bouton number and synapse strength is a complex one. It is interesting to note that hyperexcitability mutants show increased sensitivity to oxidative stress (Humphreys *et al.*, 1996, Wang *et al.*, 2000). While this does not conclusively show that they have oxidative stress the relationship is an interesting one and may hinge upon energetic demand and resultant mitochondrial stress.

The impaired crawling speed seen in *spinster* is not rescued through the expression of anti-oxidant transgenes suggesting that either oxidative stress is still at a high enough level to cause physiological dysfunction or the cause of

physiological impairment is distinct from oxidative stress. It must be noted that reducing oxidative stress does not afford a full rescue of overgrowth in *spinster.* However, other mutants investigated whose morphology was completely rescued by expression of antioxidants also showed impaired physiological output, shown by decreased crawling speed and this was not rescued by expression of antioxidants. This suggests that physiological output is more sensitive to oxidative stress than bouton number.

7.7. Summary

The key results and conclusions from this study can be summarised as follows:

1. *spinster* is carrying an oxidative stress burden that contributes to synaptic overgrowth.
2. Oxidative stress, independent of lysosomal dysfunction can cause overgrowth of the neuromuscular junction.
3. ASK/JNK/AP-1 signalling is required for spinster and oxidative stress induced overgrowth.
4. Autophagy genes are required for *spinster* and oxidative stress induced overgrowth.
5. Fos and autophagy are required both in the muscle and the nerve in *spinster* overgrowth.
6. *spinster* and oxidative stress result in physiological impairment.
7. *spinster* have aberrant mitochondria.
8. AMPK is required for *spinster* overgrowth suggestive of an energy deficit and AMPK can drive synapse growth.

Appendix 1: Bouton Numbers and MSA

Genotype and Conditions	Raw Bouton No±SEM	MSA±SEM (μm^2)	Normalised Bouton Number	N
atg18^{KG}/Df	54±3.9	67737±2439	68±6.3	28
atg1^{PZ}/atg1^{DG}	60±3.2	86857±3659	59±5.8	19
atg1^{PZ}/atg1^{DG} (10mM paraquat)	35±1.8	46302±2580	54±1.4	19
*elaV*GAL4> UAS*AMPK^{T184D}*	64±3.3	85443±3989	63±5.4	16
*elav*GAL4> UAS*atg5RNAi*	81±4.7	84374±1453	81±5.5	17
*elav*GAL4> UAS*fos^{DN}*	68±3.3			20
*elaV*GAL4>UAS*AP-1*	84±5.9	80069±2277	94±9.3	15
*elaV*GAL4>UAS*ATG1^{68}*	60±3.0	92288±4110	51±4.3	17
*elaV*GAL4>UAS*ATG1^{CG}*	81±4.7	82515±2447	81±5.6	17
*elaV*GAL4>UAS*cat* (male)				
*elaV*GAL4>UAS*FOS*	78±5.7	78603±3610	83±7.0	15
*elav*GAL4>UAS*hSOD1*	79±4.0			16
*elaV*GAL4>UAS*hSOD1* (male)	71±2.6			25
*elaV*GAL4>UAS*JUN*	98±6.8	84382±4108	98±9.0	12
hiw with *elaV*GAL4> UAS*cat* (male)	134±6.5			16
hiw with *elaV*GAL4> UAS*hSOD1* (male)	75±9.5			15
hiw with *MHC*GAL4> UAS*cat* (male)	162±24.1			16
hiw with *MHC*GAL4> UAS*hSOD1* (male)	108±7.0			21
hiw with *spin*GAL4> UAS*cat* (male)	125±4.7			16
hiw with *spin*GAL4> UAS*hSOD1* (male)	108±5.9			25
hiw (male)	146±5.7			20
*MHC*GAL4> UAS*atg5RNAi*	98±5.7	92440±3104	87±6.6	16
*MHC*GAL4> UAS*fos^{DN}*	79±3.7			22
*MHC*GAL4>UAS*AMPK^{T184D}*	107±7.1	85443±3231	107±5.6	17
*MHC*GAL4>UAS*AP-1*	86±6.7	84034±1800	83±6.5	19

Genotype and Conditions	Raw Bouton No±SEM	MSA±SEM (μm^2)	Normalised Bouton Number	N
*MHC*GAL4>UAS*ATG1*^{68}	72±4.7	80151±3015	74±5.9	14
*MHC*GAL4>UAS*ATG1*^{CG}	70±4.4	89057±3623	67±5.0	18
*MHC*GAL4>UAS*cat* (male)				
*MHC*GAL4>UAS*FOS*	98±5.2	85714±3490	95±7.6	14
*MHC*GAL4>UAS*hSOD1*	83±6.4			15
*MHC*GAL4>UAS*hSOD1* (male)	72±3.6			12
*MHC*GAL4>UAS*JUN*	107±10.2	76584±3738	114±10.0	14
sdhB/sdhB	59±4.4	67668±3238	76±8.2	16
sesB/sesB	109±4.0	63699±2222	139±4.0	13
sod1^{n1}/+	100±3.2	78550±3655	103±4.42	18
sod1^{n1}/*sod1*^{n64}	107±4.8	60421±4218	147±6.31	21
sod1^{n1}/*sod1*^{n64} with *spin*GAL4> UAS*cat*	66±2.1	74703±1805	72±1.8	16
sod1^{n1}/*sod1*^{n64} with *spin*GAL4> UAS*fos*^{DN}	59±3.70	71978±2063	67±4.62	21
sod1^{n1}/*sod1*^{n64} with *spin*GAL4> UAS*hSOD1*	75±5.0	79112±3990	79±5.6	17
sod1^{n1}/*sod1*^{n64} with *spin*GAL4> UAS*jun*^{DN}	104±3.69	69466±2060	122±3.88	18
sod1^{n64}/+	87±5.72	76112±2544	92±4.31	25
sod2^{delta}/*sod2*^{delta02}	107±4.9	62477±3136	146±10.3	22
sod2^{delta}/*sod2*^{delta02} *spin*^{5} with *spin*GAL4> UAS*fos*^{DN}	65±4.25	76877±2881	70±5.98	23
sod2^{delta}/*sod2*^{delta02} *spin*^{5} with *spin*GAL4> UAS*jnk*^{DN}	84±4.28	73878±2423	94±6.30	19
sod2^{delta}/*sod2*^{delta02} *spin*^{5} with *spin*GAL4> UAS*jun*^{DN}	72±3.77	59037±3609	102±5.51	20
sod2^{delta}/*sod2*^{delta02} with *elaV*GAL4>UAS*fos*^{DN}	73±4.2	79692±2919	77±4.9	27
sod2^{delta}/*sod2*^{delta02} with *MHC*GAL4>UAS*fos*^{DN}	78±4.5	81371±3621	81±6.4	20
sod2^{delta}/*sod2*^{delta02} with *spin*GAL4>UAS*trx*^{CYTO}	82±5.3	69273±2378	97±6.4	24
spin^{4}/+	93±4.00	80008±2321	94±4.10	31

Genotype and Conditions	Raw Bouton No±SEM	MSA±SEM (μm^2)	Normalised Bouton Number	N
spin^{4}/+; *sod1*^{n1}/+	114±4.39	72512±4565	127±5.47	19
spin^{4}/+; *sod1*^{n64}/+	116±7.3	71662±6982	131±8.03	21
spin^{4}/*spin*$^{\Delta 58}$	117±7.7	74129±1635	129±9.5	21
spin^{4}/*spin*^{5}	152±4.33	76580±2716	165±10.3	32
spin^{4}/*spin*^{5} with *atg18*^{KG}/*atg1*^{DG}	76±5.83			16
spin^{4}/*spin*^{5} with *atg18*^{KG}/*Df*	75±6.74			16
spin^{4}/*spin*^{5} with *atg1*^{PZ}/*atg1*^{DG}	72±4.90			28
spin^{4}/*spin*^{5} with *elav*GAL4> UAS*atg5RNAi*	127±5.57			16
spin^{4}/*spin*^{5} with *elav*GAL4> UAS*hSOD1*	106±7.99			14
spin^{4}/*spin*^{5} with *elav*GAL4>UAS*fos*^{DN}	113±9.49			9
spin^{4}/*spin*^{5} with *MHC*GAL4> UAS*atg5RNAi*	126±6.51			16
spin^{4}/*spin*^{5} with *MHC*GAL4> UAS*fos*^{DN}	120±8.42			11
spin^{4}/*spin*^{5} with *MHC*GAL4> UAS*hSOD1*	103±3.166			14
spin^{4}/*spin*^{5} with *spin*GAL4> UAS*AMPK-RNAi*^{1062}	109±6.2	82971±3443	111	19
spin^{4}/*spin*^{5} with *spin*GAL4> UAS*AMPK-RNAi*^{1827}	105±6.52	79595±1919	108	19
spin^{4}/*spin*^{5} with *spin*GAL4> UAS*ask*^{DN}	128±6.37			16
spin^{4}/*spin*^{5} with *spin*GAL4> UAS*cat*	103±5.9			17
spin^{4}/*spin*^{5} with *spin*GAL4> UAS*fos*^{DN}	74±1.92			19
spin^{4}/*spin*^{5} with *spin*GAL4> UAS*fos*^{RNAi}	119±3.81			16
spin^{4}/*spin*^{5} with *spin*GAL4> UAS*hSOD1*	110±3.7			46

Genotype and Conditions	Raw Bouton No±SEM	MSA±SEM (μm^2)	Normalised Bouton Number	N
spin^4/*spin*^{5} with *spin*GAL4> UAS*jnk*^{DN}	117±5.79			16
spin^4/*spin*^{5} with *spin*GAL4> UAS*jnk*^{RNAi}	121±3.45			19
spin^4/*spin*^{5} with *spin*GAL4> UAS*jun*^{DN}	148±7.19			22
spin^4/*spin*^{5} with *spin*GAL4>UAS*trx*^{CYTO}	113±8.3			10
spin^4/*spin*^{5} with *spin*GAL4>UAS*trx*^{MITO}	103±6.8			15
spin^4/*spin*^{5} with *tub*GAL4>UAS*hSOD1*	115±6.0			22
spin^5/+	85±3.66	75229±2665	91±6.49	12
spin^5/+; *sod1*^{n1}/+	121±3.89	75440±2355	130±6.29	24
spin^5/+; *sod1*^{n64}/+	137±3.87	78594±2157	141±6.14	28
spin^5/*spin*$^{\Delta 58}$	124±9.0	82067±4538	126±13.3	8
*spin*GAL4->UAS*hSOD1* (10mM paraquat)	57±2.64	59332±1937	72±4.07	41
*spin*GAL4->UAS*hSOD1* (instant food)	76±5.56	75308±3996	74±4.13	21
*spin*GAL4> UAS*AMPK-RNAi*^{1062}	61±4.0	70669±3618	86±7.5	14
*spin*GAL4> UAS*AMPK-RNAi*^{1827}	74±4.6	76581±2552	88±8.8	16
*spin*GAL4> UAS*AMPK*^{T184D}	114±4.6	77872±1933	121±5.6	35
*spin*GAL4> UAS*fos*^{RNAi}	82±4.24			17
*spin*GAL4> UAS*jnk*^{RNAi}	65±3.44			22
*spin*GAL4> UAS*jnk*^{RNAi} (10mM paraquat)	64±3.7	49061±1688	94±5.5	19
*spin*GAL4> UAS*jnk*^{RNAi} (instant food)	70±3.2	78429±2319	66±4.2	16
*spin*GAL4>UAS*AP-1*				
*spin*GAL4>UAS*ask*^{DN}	60±4.18	79476±4102	61±4.66	15
*spin*GAL4>UAS*ask*^{DN} (10mM paraquat)	86±7.80	59207±5602	86±7.81	19

Genotype and Conditions	Raw Bouton No±SEM	MSA±SEM (μm^2)	Normalised Bouton Number	N
*spin*GAL4>UAS*ask*^{DN} (instant food)	54±3.64	81124±2338	63±4.45	16
*spin*GAL4>UAS*cat*	76±4.6	75369±4901	88±8.7	18
*spin*GAL4>UAS*cat* (male)	67±4.3			19
*spin*GAL4>UAS*FOS*	69±2.9	82460±2595	68±3.4	21
*spin*GAL4>UAS*fos*^{DN}	56±2.29	75297±3820	65±6.25	18
*spin*GAL4>UAS*fos*^{DN} (10mM paraquat)	58±2.23	57525±2346	75±5.26	19
*spin*GAL4>UAS*fos*^{DN} (instant food)	55±2.70	62919±4115	56±5.77	13

Appendix 2: Branch Number and Normalisation

Genotype	Branch No±SEM	Branch No Normalised to Bouton No±SEM	Branch No Normalised To MSA±SEM	N
*spin*GAL4>UAS*hSOD1*	4.86±0.44			16
*spin*GAL4>UAS*cat*	4.47±0.38			15
$sod1^{n1}/sod1^{n64}$	7.19±0.64	5.66±0.50	3.92±1.74	16
$sod2^{delta}/sod2^{delta02}$	3.47±0.32	2.76±0.26	2.01±1.35	17
$spin^{4}/spin^{5}$	10.82±1.33	6.05±0.75	5.54±1.96	11
Wildtype	5.31±0.44	5.31±0.44	5.31±0.44	16
Wildtype (Instant Food)	4.38±1.19	4.38±1.19	4.38±1.19	8
Wildtype 10mM Paraquat	6.17±0.60	6.01±0.59	4.22±0.41	6
*spin*GAL4>UAStrx^{CYTO}	4.08±0.29			13
$sod1^{n1}/sod1^{n64}$ with *spin*GAL4>UAS*hSOD1*	5.00±0.49			12
$sod1^{n1}/sod1^{n64}$ with *spin*GAL4>UAS*cat*	4.75±0.31			16
$sod2^{delta}/sod2^{delta02}$ with *spin*GAL4> UAStrx^{CYTO}	4.55±0.37			19
$spin^{4}/spin^{5}$ with *spin*GAL4> UAStrx^{CYTO}	4.41±0.36			12

Appendix 3: Bouton Width

Genotype	Mean Bouton Width (μm)	N	No NMJs
$sod1^{n1}/sod1^{n64}$	2.202±0.042	610	6
$sod2^{delta}/sod2^{delta02}$	2.646±0.053	551	5
$spin^{4}/spin^{5}$	2.350±0.040	873	5
Wildtype	2.616±0.064	468	6
Wildtype (Instant Food)	2.82±0.068	557	7
Wildtype 10mM paraquat	2.41±0.052	607	7

Abbreviations:

Acetyl CoA	Acetyl coenzyme A
AD	Alzheimer's Disease
ADP	Adenosine Disphosphate
AEL	After Egg Laying
ALS	Amyotrophic Lateral Sclerosis (Lou Gehrig's Disease)
AMPA	Alpha-Amino-3-Hydroxy-5-Methyl-4-Isoxazole Propionic Acid
AMPK	Adenosise Monophosphate- Activated Protein Kinase
AP	Action Potential
AP-1	Activator Protein-1
APE-1	Apurinic/apyramidic endonuclease-1
ASK	Apoptosis Signal Regulating Kinase
ATG	Autophagy Related Gene
ATP	Adenosine Triphosphate
Aβ	Beta-amyloid
Bcl-2	B-cell lymphoma 2
BRP	Bruchpilot
bZIP	Basic Leucine Zipper Domain
cAMP	Cyclic Adenosine Monophosphate
Cat	Catalase
CLIC1	Chloride Intracellular Channel Protein 1
CLN	Ceroid Lipofuscinosis, Neuronal
CREB	cAMP Responsive Element Binding (protein)
cvt	Cytoplasm to Vacuole Transport
CyO	CurlyO
CYTO	Cytoplasmic
DFz2	DFrizzled2
Dlg	Discs-large
DNA	Deoxyribose Nucleic Acid
ELAV	Embyronic Lethal Abnormal Vision
EM	Electron Microscopy
EMS	Ethyl Methane Sulfonate
EPP	Excitatory Post-synaptic Potential
ER	Endoplasmic Reticulum

ERK	Extracellular Signal Regulated Kinase
ETC	Electron Transport Chain
EtOH	Ethanol
$FADH_2$	flavin adenine dinucleotide (hydroquinone form)
FasII	Fasciclin II
FM6	First Chromosome Marker (6)
Gbb	Glass Bottom Boat
GFP	Green Fluorescent Protein
GluR	Glutamate Receptor
GPx	Glutathione Peroxidase
GSH	Glutathione (monomeric)
GSSG	Glutathione Disulphide
GST	Glutathione Transferase
GTP	Guanosine-5'-triphosphate
GTPases	small guanosine triphosphatases
H_2O_2	Hydrogen Peroxide
hep	Hemipterous (MKK7)
Hiw	Highwire
HL3	Hemolymph-like Buffer 3
HNE	4-hydroxy-2,3-nonenal
HO-1	Heme-oxygenase-1
HOPS	homotypic fusion and protein sorting
HRP	Horseradish Peroxidase
ISN	Intersegmental Nerve
JNK	c-Jun N-terminal Kinase
Kb	kilo base pairs
KEAP-1	Kelch-like ECH-associated protein 1
LAMP	Lysosomal-associated Membrane Protein
LGIC	Ligand Gated Ion Channels
Loe	Lochrig
LRRK2	Leucine Rich Repeat Kinase
LSD	Lysosomal Storage Disorder
LTP	Long Term Potentiation
MAPK	Mitogen-Activated Protein Kinase
MBF1	Multiprotein Bridging Factor

MDA	malondialdehyde
MED	Medea
Mef2	Myocyte Enhancer Factor-2
mEPP	Mini Excitatory Post-synaptic Potential
MHC	Myosin Heavy Chain
MITO	Mitochondrial
MKK	Mitogen-Activated Protein Kinase Kinase
MKRS	Stubble Marker
MSA	Muscle Surface Area
NADH	Nicotinamide adenine dinucleotide
NADPH	Nicotinamide adenine dinucleotide phosphate
NCL	Neuronal Ceroid Lipofuscinosis
NMDA	N-Methyl-D-Aspartate
NMJ	Neuromuscular Junction
NO	Nitric Oxide
NOS	Nitric Oxide Synthase
NPC	Niemann Pick Type C
Nrf2	Nuclear factor (erythroid-derived 2)-like 2
$O_2^{-\cdot}$	Superoxide Anions
$OH^{\cdot}$	Hydroxyl Radicais
$OH^{\cdot -}$	Hydroxyl Anions
$ONOO^-$	peroxynitrite
PBS	Phosphate Buffered Saline
PBS-T	Phosphate Buffered Saline-Triton
PCD	Programmed Cell Death
PCR	Polymerase Chain Reaction
PD	Parkinson's Disease
PI3K	Phosphoinositide 3-kinase
PKA	Protein Kinase A
PKC	Protein Kinase C
PMA	phorbol 12-myristate 13- acetate (PKC Activator)
Puc	Puckered
Ref-1	Redox Factor-1
RNA(i)	(Interfering) Ribose Nucleic Acid
RNS	Reactive Nitrogen Species

ROS	Reactive Oxygen Species
RSK	Ribosomal S6 Kinase
S6K	S6 Kinase
SAPK	Stress Activated Protein Kinase
Sax	Saxophone
Sbh	Succinate Dehydrogenase
Sco	Scutella
SesB	Stress Sensitive B
SN	Segmental Nerve
SNAP25	N-ethylmaleimide-sensitive factor attachment protein-25
SNARE	NAP (Soluble NSF Attachment Protein) Receptor
SOD	Superoxide Dismutase
spin	Spinster
SSB	Subsynaptic Reticulum
TGFβ	Transforming Growth Factor β
Tkv	Thick Veins
TM6	Third Chromosome Marker
TMOP	1,1,3,3-tetramethoxypropane
TN	Transverse Nerve
TOR	Target of Rapamycin
TORC	Target of Rapamycin Complex
Trx	Thioredoxin
TrxR	Thioredoxin Reductase
TSC	Tuberous Sclerosis Complex
TUB	Tubulin
UAS	Upstream Activating Sequence
Unc-51	Uncoordinated-51
VGIC	Voltage Gated Ion Channels
VPS	Vacuolar Protein Sorting
Wnd	Wallenda
XO	Xanthine Oxidase

References:

ADAMS, M. D., CELNIKER, S. E., HOLT, R. A., EVANS, C. A., GOCAYNE, J. D., AMANATIDES, P. G., SCHERER, S. E., LI, P. W., HOSKINS, R. A., GALLE, R. F., GEORGE, R. A., LEWIS, S. E., RICHARDS, S., ASHBURNER, M., HENDERSON, S. N., SUTTON, G. G., WORTMAN, J. R., YANDELL, M. D., ZHANG, Q., CHEN, L. X., BRANDON, R. C., ROGERS, Y. H., BLAZEJ, R. G., CHAMPE, M., PFEIFFER, B. D., WAN, K. H., DOYLE, C., BAXTER, E. G., HELT, G., NELSON, C. R., GABOR, G. L., ABRIL, J. F., AGBAYANI, A., AN, H. J., ANDREWS-PFANNKOCH, C., BALDWIN, D., BALLEW, R. M., BASU, A., BAXENDALE, J., BAYRAKTAROGLU, L., BEASLEY, E. M., BEESON, K. Y., BENOS, P. V., BERMAN, B. P., BHANDARI, D., BOLSHAKOV, S., BORKOVA, D., BOTCHAN, M. R., BOUCK, J., BROKSTEIN, P., BROTTIER, P., BURTIS, K. C., BUSAM, D. A., BUTLER, H., CADIEU, E., CENTER, A., CHANDRA, I., CHERRY, J. M., CAWLEY, S., DAHLKE, C., DAVENPORT, L. B., DAVIES, P., DE PABLOS, B., DELCHER, A., DENG, Z., MAYS, A. D., DEW, I., DIETZ, S. M., DODSON, K., DOUP, L. E., DOWNES, M., DUGAN-ROCHA, S., DUNKOV, B. C., DUNN, P., DURBIN, K. J., EVANGELISTA, C. C., FERRAZ, C., FERRIERA, S., FLEISCHMANN, W., FOSLER, C., GABRIELIAN, A. E., GARG, N. S., GELBART, W. M., GLASSER, K., GLODEK, A., GONG, F., GORRELL, J. H., GU, Z., GUAN, P., HARRIS, M., HARRIS, N. L., HARVEY, D., HEIMAN, T. J., HERNANDEZ, J. R., HOUCK, J., HOSTIN, D., HOUSTON, K. A., HOWLAND, T. J., WEI, M. H., IBEGWAM, C., et al. 2000. The genome sequence of Drosophila melanogaster. *Science,* 287**,** 2185-95.

ADLER, V., YIN, Z., FUCHS, S. Y., BENEZRA, M., ROSARIO, L., TEW, K. D., PINCUS, M. R., SARDANA, M., HENDERSON, C. J., WOLF, C. R., DAVIS, R. J. & RONAI, Z. 1999. Regulation of JNK signaling by GSTp. *The EMBO journal,* 18**,** 1321-34.

ALBERT L. LEHNINGER, D. L. N., MICHAEL M. COX 2008. Chapter 19: Oxidative Phosphorylation and Photophosphorylation. *Lehninger principles of biochemistry.* W.H. Freeman.

ALBERTS B, J. A., LEWIS J, ET AL 2002. Chapter 12: Intracellular Compartments and Protein Sorting. *Molecular Biology of the Cell.* 4th ed.: Garland Science.

AMENDOLA, J., VERRIER, B., ROUBERTOUX, P. & DURAND, J. 2004. Altered sensorimotor development in a transgenic mouse model of amyotrophic lateral sclerosis. *The European journal of neuroscience,* 20**,** 2822-6.

ANDO, K., HIRAO, S., KABE, Y., OGURA, Y., SATO, I., YAMAGUCHI, Y., WADA, T. & HANDA, H. 2008. A new APE1/Ref-1-dependent pathway leading to reduction of NF-kappaB and AP-1, and activation of their DNA-binding activity. *Nucleic acids research,* 36**,** 4327-36.

ANDREYEV, A. Y., KUSHNAREVA, Y. E. & STARKOV, A. A. 2005. Mitochondrial metabolism of reactive oxygen species. *Biochemistry. Biokhimiia,* 70**,** 200-14.

ARLT, S., KONTUSH, A., ZERR, I., BUHMANN, C., JACOBI, C., SCHRÖTER, A., POSER, S. & BEISIEGEL, U. 2002. Increased Lipid Peroxidation in Cerebrospinal Fluid and Plasma from Patients with Creutzfeldt–Jakob Disease. *Neurobiology of Disease,* 10**,** 150-156.

ARSHAM, A. M. & NEUFELD, T. P. 2009. A genetic screen in Drosophila reveals novel cytoprotective functions of the autophagy-lysosome pathway. *PloS one,* 4**,** e6068.

ATKINS, P. C., NORMAN, M., ZWEIMAN, B. & ROSENBLUM, F. 1979. Further characterization and biologic activity of ragweed antigen--induced neutrophil chemotactic activity in man. *The Journal of allergy and clinical immunology,* 64**,** 251-8.

ATWOOD, H. L., GOVIND, C. K. & WU, C. F. 1993. Differential ultrastructure of synaptic terminals on ventral longitudinal abdominal muscles in Drosophila larvae. *Journal of neurobiology,* 24**,** 1008-24.

AUERBACH, J. M. & SEGAL, M. 1997. Peroxide modulation of slow onset potentiation in rat hippocampus. *The Journal of neuroscience : the official journal of the Society for Neuroscience,* 17**,** 8695-701.

AVRAHAM, K. B., SCHICKLER, M., SAPOZNIKOV, D., YAROM, R. & GRONER, Y. 1988. Down's syndrome: abnormal neuromuscular junction in tongue of transgenic mice with elevated levels of human Cu/Zn-superoxide dismutase. *Cell,* 54**,** 823-9.

AXE, E. L., WALKER, S. A., MANIFAVA, M., CHANDRA, P., RODERICK, H. L., HABERMANN, A., GRIFFITHS, G. & KTISTAKIS, N. T. 2008. Autophagosome formation from membrane compartments enriched in phosphatidylinositol 3-phosphate and dynamically connected to the endoplasmic reticulum. *The Journal of cell biology,* 182**,** 685-701.

BAILLET, A., CHANTEPERDRIX, V., TROCME, C., CASEZ, P., GARREL, C. & BESSON, G. 2010. The role of oxidative stress in amyotrophic lateral sclerosis and Parkinson's disease. *Neurochemical research,* 35**,** 1530-7.

BAMBER, B. A. & ROWLAND, A. M. 2006. Shaping cellular form and function by autophagy. *Autophagy,* 2**,** 247-9.

BARNHAM, K. J., MASTERS, C. L. & BUSH, A. I. 2004. Neurodegenerative diseases and oxidative stress. *Nature reviews. Drug discovery,* 3**,** 205-14.

BEDARD, K. & KRAUSE, K. H. 2007. The NOX family of ROS-generating NADPH oxidases: physiology and pathophysiology. *Physiological reviews,* 87**,** 245-313.

BELLEN, H. J., LEVIS, R. W., LIAO, G., HE, Y., CARLSON, J. W., TSANG, G., EVANS-HOLM, M., HIESINGER, P. R., SCHULZE, K. L., RUBIN, G. M., HOSKINS, R. A. & SPRADLING, A. C. 2004. The BDGP gene disruption project: single transposon insertions associated with 40% of Drosophila genes. *Genetics,* 167**,** 761-81.

BERLETT, B. S. & STADTMAN, E. R. 1997. Protein oxidation in aging, disease, and oxidative stress. *The Journal of biological chemistry,* 272**,** 20313-6.

BETARBET, R., SHERER, T. B., MACKENZIE, G., GARCIA-OSUNA, M., PANOV, A. V. & GREENAMYRE, J. T. 2000. Chronic systemic pesticide exposure reproduces features of Parkinson's disease. *Nature neuroscience,* 3**,** 1301-6.

BINDOKAS, V. P., JORDAN, J., LEE, C. C. & MILLER, R. J. 1996. Superoxide production in rat hippocampal neurons: selective imaging with hydroethidine. *The Journal of neuroscience : the official journal of the Society for Neuroscience,* 16**,** 1324-36.

BISHOP, T., ST-PIERRE, J. & BRAND, M. D. 2002. Primary causes of decreased mitochondrial oxygen consumption during metabolic depression in snail cells. *American journal of physiology. Regulatory, integrative and comparative physiology,* 282**,** R372-82.

BLISS, T. V. & LOMO, T. 1973. Long-lasting potentiation of synaptic transmission in the dentate area of the anaesthetized rabbit following stimulation of the perforant path. *The Journal of physiology,* 232**,** 331-56.

BOHMANN, D., ELLIS, M. C., STASZEWSKI, L. M. & MLODZIK, M. 1994. Drosophila Jun mediates Ras-dependent photoreceptor determination. *Cell,* 78**,** 973-86.

BOKOCH, G. M. & KNAUS, U. G. 2003. NADPH oxidases: not just for leukocytes anymore! *Trends in biochemical sciences,* 28**,** 502-8.

BONDY, S. C. & NADERI, S. 1994. Contribution of hepatic cytochrome P450 systems to the generation of reactive oxygen species. *Biochemical pharmacology,* 48**,** 155-9.

BOVERIS, A. & CHANCE, B. 1973. The mitochondrial generation of hydrogen peroxide. General properties and effect of hyperbaric oxygen. *The Biochemical journal,* 134**,** 707-16.

BOVERIS, A., OSHINO, N. & CHANCE, B. 1972. The cellular production of hydrogen peroxide. *The Biochemical journal,* 128**,** 617-30.

BRAND, A. H. & PERRIMON, N. 1993. Targeted gene expression as a means of altering cell fates and generating dominant phenotypes. *Development,* 118**,** 401-15.

BRIGELIUS-FLOHE, R. & TRABER, M. G. 1999. Vitamin E: function and metabolism. *The FASEB journal : official publication of the Federation of American Societies for Experimental Biology,* 13**,** 1145-55.

BRINKLEY, B. R., BARHAM, S. S., BARRANCO, S. C. & FULLER, G. M. 1974. Rotenone inhibition of spindle microtubule assembly in mammalian cells. *Experimental cell research,* 85**,** 41-6.

BROADIE, K. S. & BATE, M. 1993. Development of the embryonic neuromuscular synapse of Drosophila melanogaster. *The Journal of neuroscience : the official journal of the Society for Neuroscience,* 13**,** 144-66.

BROWN, G. C. & BORUTAITE, V. 2011. There is no evidence that mitochondria are the main source of reactive oxygen species in mammalian cells. *Mitochondrion*.

BUDNIK, V. 1996. Synapse maturation and structural plasticity at Drosophila neuromuscular junctions. *Current opinion in neurobiology,* 6**,** 858-67.

BUDNIK, V., ZHONG, Y. & WU, C. F. 1990. Morphological plasticity of motor axons in Drosophila mutants with altered excitability. *The Journal of neuroscience : the official journal of the Society for Neuroscience,* 10**,** 3754-68.

BUETTNER, G. R., NG, C. F., WANG, M., RODGERS, V. G. & SCHAFER, F. Q. 2006. A new paradigm: manganese superoxide dismutase influences the production of H2O2 in cells and thereby their biological state. *Free radical biology & medicine,* 41**,** 1338-50.

BUHMANN, C., ARLT, S., KONTUSH, A., MÖLLER-BERTRAM, T., SPERBER, S., OECHSNER, M., STUERENBURG, H.-J. & BEISIEGEL, U. 2004. Plasma and CSF markers of oxidative stress are increased in Parkinson's disease and influenced by antiparkinsonian medication. *Neurobiology of Disease,* 15**,** 160-170.

BUS, J. S., AUST, S. D. & GIBSON, J. E. 1976a. Paraquat toxicity: proposed mechanism of action involving lipid peroxidation. *Environmental health perspectives,* 16**,** 139-46.

BUS, J. S., CAGEN, S. Z., OLGAARD, M. & GIBSON, J. E. 1976b. A mechanism of paraquat toxicity in mice and rats. *Toxicology and applied pharmacology,* 35**,** 501-13.

CADENAS, E., BOVERIS, A., RAGAN, C. I. & STOPPANI, A. O. 1977. Production of superoxide radicals and hydrogen peroxide by NADH-ubiquinone reductase and ubiquinol-cytochrome c reductase from beef-heart mitochondria. *Archives of biochemistry and biophysics,* 180**,** 248-57.

CAPDEVILA, J., CHACOS, N., WERRINGLOER, J., PROUGH, R. A. & ESTABROOK, R. W. 1981. Liver microsomal cytochrome P-450 and the oxidative metabolism of arachidonic acid. *Proceedings of the National Academy of Sciences of the United States of America,* 78**,** 5362-6.

CARPENTER, J. M. 1950. A new semisynthetic food medium for Drosophila. *Drosophila Inform. Serv.***,** 96-97.

CASTELLANI, R., SMITH, M. A., RICHEY, P. L. & PERRY, G. 1996. Glycoxidation and oxidative stress in Parkinson disease and diffuse Lewy body disease. *Brain research,* 737**,** 195-200.

CHA, G. H., KIM, S., PARK, J., LEE, E., KIM, M., LEE, S. B., KIM, J. M., CHUNG, J. & CHO, K. S. 2005. Parkin negatively regulates JNK pathway in the dopaminergic neurons of Drosophila. *Proceedings of the National Academy of Sciences of the United States of America,* 102**,** 10345-50.

CHAI, A., WITHERS, J., KOH, Y. H., PARRY, K., BAO, H., ZHANG, B., BUDNIK, V. & PENNETTA, G. 2008. hVAPB, the causative gene of a heterogeneous group of motor neuron diseases in humans, is functionally

interchangeable with its Drosophila homologue DVAP-33A at the neuromuscular junction. *Human molecular genetics,* 17**,** 266-80.

CHEN, K. & FEATHERSTONE, D. E. 2005. Discs-large (DLG) is clustered by presynaptic innervation and regulates postsynaptic glutamate receptor subunit composition in Drosophila. *BMC biology,* 3**,** 1.

CHEN, W., WHITE, M. A. & COBB, M. H. 2002. Stimulus-specific requirements for MAP3 kinases in activating the JNK pathway. *The Journal of biological chemistry,* 277**,** 49105-10.

CHEN, Y. & KLIONSKY, D. J. 2011. The regulation of autophagy - unanswered questions. *Journal of cell science,* 124**,** 161-70.

CHEN, Y., MCMILLAN-WARD, E., KONG, J., ISRAELS, S. J. & GIBSON, S. B. 2008. Oxidative stress induces autophagic cell death independent of apoptosis in transformed and cancer cells. *Cell death and differentiation,* 15**,** 171-82.

CHENG, W. T., GUO, Z. X., LIN, C. A., LIN, M. Y., TUNG, L. C. & FANG, K. 2009. Oxidative stress promotes autophagic cell death in human neuroblastoma cells with ectopic transfer of mitochondrial PPP2R2B (Bbeta2). *BMC cell biology,* 10**,** 91.

CHERRA, S. J., 3RD, KULICH, S. M., UECHI, G., BALASUBRAMANI, M., MOUNTZOURIS, J., DAY, B. W. & CHU, C. T. 2010. Regulation of the autophagy protein LC3 by phosphorylation. *The Journal of cell biology,* 190**,** 533-9.

CLARK, I. E., DODSON, M. W., JIANG, C., CAO, J. H., HUH, J. R., SEOL, J. H., YOO, S. J., HAY, B. A. & GUO, M. 2006. Drosophila pink1 is required for mitochondrial function and interacts genetically with parkin. *Nature,* 441**,** 1162-6.

COLLINS, C. A. & DIANTONIO, A. 2007. Synaptic development: insights from Drosophila. *Current opinion in neurobiology,* 17**,** 35-42.

COLLINS, C. A., WAIRKAR, Y. P., JOHNSON, S. L. & DIANTONIO, A. 2006. Highwire restrains synaptic growth by attenuating a MAP kinase signal. *Neuron,* 51**,** 57-69.

COOK, C. I. & YU, B. P. 1998. Iron accumulation in aging: modulation by dietary restriction. *Mechanisms of ageing and development,* 102**,** 1-13.

COUTEAUX, R. & PECOT-DECHAVASSINE, M. 1970. [Synaptic vesicles and pouches at the level of "active zones" of the neuromuscular junction]. *Comptes rendus hebdomadaires des seances de l'Academie des sciences. Serie D: Sciences naturelles,* 271**,** 2346-9.

COWAN W. M., K. E. R. 2003. Chapter 1: A Brief History of Synaptic Transmission. *In:* COWAN W.M., S. T. C., STEVENS C.F. (ed.) *Synapses.* 1st ed.: JHU Press.

COYLE, I. P., KOH, Y. H., LEE, W. C., SLIND, J., FERGESTAD, T., LITTLETON, J. T. & GANETZKY, B. 2004. Nervous wreck, an SH3 adaptor protein that interacts with Wsp, regulates synaptic growth in Drosophila. *Neuron,* 41**,** 521-34.

DARSOW, T., RIEDER, S. E. & EMR, S. D. 1997. A multispecificity syntaxin homologue, Vam3p, essential for autophagic and biosynthetic protein transport to the vacuole. *The Journal of cell biology,* 138**,** 517-29.

DAVIS, G. W., SCHUSTER, C. M. & GOODMAN, C. S. 1996. Genetic dissection of structural and functional components of synaptic plasticity. III. CREB is necessary for presynaptic functional plasticity. *Neuron,* 17**,** 669-79.

DAVIS, R. J. 2000. Signal transduction by the JNK group of MAP kinases. *Cell,* 103**,** 239-52.

DE ROBERTIS, E. D. & BENNETT, H. S. 1955. Some features of the submicroscopic morphology of synapses in frog and earthworm. *The Journal of biophysical and biochemical cytology,* 1**,** 47-58.

DEAK, P., OMAR, M. M., SAUNDERS, R. D., PAL, M., KOMONYI, O., SZIDONYA, J., MAROY, P., ZHANG, Y., ASHBURNER, M., BENOS, P., SAVAKIS, C., SIDEN-KIAMOS, I., LOUIS, C., BOLSHAKOV, V. N., KAFATOS, F. C., MADUENO, E., MODOLELL, J. & GLOVER, D. M. 1997. P-element insertion alleles of essential genes on the third chromosome of Drosophila melanogaster: correlation of physical and cytogenetic maps in chromosomal region 86E-87F. *Genetics,* 147**,** 1697-722.

DEGANUTO, M., PITTIS, M. G., PINES, A., DOMINISSINI, S., KELLEY, M. R., GARCIA, R., QUADRIFOGLIO, F., BEMBI, B. & TELL, G. 2007. Altered intracellular redox status in Gaucher disease fibroblasts and impairment of adaptive response against oxidative stress. *Journal of cellular physiology,* 212**,** 223-35.

DEGENNARO, M., HURD, T. R., SIEKHAUS, D. E., BITEAU, B., JASPER, H. & LEHMANN, R. 2011. Peroxiredoxin stabilization of DE-cadherin promotes primordial germ cell adhesion. *Developmental cell,* 20**,** 233-43.

DERIJARD, B., HIBI, M., WU, I. H., BARRETT, T., SU, B., DENG, T., KARIN, M. & DAVIS, R. J. 1994. JNK1: a protein kinase stimulated by UV light and Ha-Ras that binds and phosphorylates the c-Jun activation domain. *Cell,* 76**,** 1025-37.

DERIJARD, B., RAINGEAUD, J., BARRETT, T., WU, I. H., HAN, J., ULEVITCH, R. J. & DAVIS, R. J. 1995. Independent human MAP-kinase signal transduction pathways defined by MEK and MKK isoforms. *Science,* 267**,** 682-5.

DERMAUT, B., NORGA, K. K., KANIA, A., VERSTREKEN, P., PAN, H., ZHOU, Y., CALLAERTS, P. & BELLEN, H. J. 2005. Aberrant lysosomal carbohydrate storage accompanies endocytic defects and neurodegeneration in Drosophila benchwarmer. *The Journal of cell biology,* 170**,** 127-39.

DETER, R. L., BAUDHUIN, P. & DE DUVE, C. 1967. Participation of lysosomes in cellular autophagy induced in rat liver by glucagon. *The Journal of cell biology,* 35**,** C11-6.

DIETZL, G., CHEN, D., SCHNORRER, F., SU, K. C., BARINOVA, Y., FELLNER, M., GASSER, B., KINSEY, K., OPPEL, S., SCHEIBLAUER,

S., COUTO, A., MARRA, V., KELEMAN, K. & DICKSON, B. J. 2007. A genome-wide transgenic RNAi library for conditional gene inactivation in Drosophila. *Nature,* 448**,** 151-6.

DONAHUE, C. P., KOSIK, K. S. & SHORS, T. J. 2006. Growth hormone is produced within the hippocampus where it responds to age, sex, and stress. *Proceedings of the National Academy of Sciences of the United States of America,* 103**,** 6031-6.

DORLING, P. R., HUXTABLE, C. R. & COLEGATE, S. M. 1980. Inhibition of lysosomal alpha-mannosidase by swainsonine, an indolizidine alkaloid isolated from Swainsona canescens. *The Biochemical journal,* 191**,** 649-51.

DROGE, W. & SCHIPPER, H. M. 2007. Oxidative stress and aberrant signaling in aging and cognitive decline. *Aging cell,* 6**,** 361-70.

DUDU, V., BITTIG, T., ENTCHEV, E., KICHEVA, A., JULICHER, F. & GONZALEZ-GAITAN, M. 2006. Postsynaptic mad signaling at the Drosophila neuromuscular junction. *Current biology : CB,* 16**,** 625-35.

DURAND, J., AMENDOLA, J., BORIES, C. & LAMOTTE D'INCAMPS, B. 2006. Early abnormalities in transgenic mouse models of amyotrophic lateral sclerosis. *Journal of physiology, Paris,* 99**,** 211-20.

DUTTAROY, A., MEIDINGER, R., KIRBY, K., CARMICHAEL, S., HILLIKER, A. & PHILLIPS, J. 1994. A manganese superoxide dismutase-encoding cDNA from Drosophila melanogaster. *Gene,* 143**,** 223-5.

DUTTAROY, A., PARKES, T., EMTAGE, P., KIRBY, K., BOULIANNE, G. L., WANG, X., HILLIKER, A. J. & PHILLIPS, J. P. 1997. The manganese superoxide dismutase gene of Drosophila: structure, expression, and evidence for regulation by MAP kinase. *DNA and cell biology,* 16**,** 391-9.

ELROY-STEIN, O., BERNSTEIN, Y. & GRONER, Y. 1986. Overproduction of human Cu/Zn-superoxide dismutase in transfected cells: extenuation of paraquat-mediated cytotoxicity and enhancement of lipid peroxidation. *The EMBO journal,* 5**,** 615-22.

ELROY-STEIN, O. & GRONER, Y. 1988. Impaired neurotransmitter uptake in PC12 cells overexpressing human Cu/Zn-superoxide dismutase--implication for gene dosage effects in Down syndrome. *Cell,* 52**,** 259-67.

EMERIT, J., EDEAS, M. & BRICAIRE, F. 2004. Neurodegenerative diseases and oxidative stress. *Biomedicine & pharmacotherapy = Biomedecine & pharmacotherapie,* 58**,** 39-46.

ERESH, S., RIESE, J., JACKSON, D. B., BOHMANN, D. & BIENZ, M. 1997. A CREB-binding site as a target for decapentaplegic signalling during Drosophila endoderm induction. *The EMBO journal,* 16**,** 2014-22.

FATT, P. & KATZ, B. 1951. An analysis of the end-plate potential recorded with an intracellular electrode. *The Journal of physiology,* 115**,** 320-70.

FATTMAN, C. L., SCHAEFER, L. M. & OURY, T. D. 2003. Extracellular superoxide dismutase in biology and medicine. *Free radical biology & medicine,* 35**,** 236-56.

FEATHERSTONE, D. E. & BROADIE, K. 2000. Surprises from Drosophila: genetic mechanisms of synaptic development and plasticity. *Brain research bulletin,* 53**,** 501-11.

FEATHERSTONE, D. E., RUSHTON, E., ROHRBOUGH, J., LIEBL, F., KARR, J., SHENG, Q., RODESCH, C. K. & BROADIE, K. 2005. An essential Drosophila glutamate receptor subunit that functions in both central neuropil and neuromuscular junction. *The Journal of neuroscience : the official journal of the Society for Neuroscience,* 25**,** 3199-208.

FERRANTE, R. J., GUTEKUNST, C. A., PERSICHETTI, F., MCNEIL, S. M., KOWALL, N. W., GUSELLA, J. F., MACDONALD, M. E., BEAL, M. F. & HERSCH, S. M. 1997. Heterogeneous topographic and cellular distribution of huntingtin expression in the normal human neostriatum. *The Journal of neuroscience : the official journal of the Society for Neuroscience,* 17**,** 3052-63.

FILIPPON, L., VANZIN, C. S., BIANCINI, G. B., PEREIRA, I. N., MANFREDINI, V., SITTA, A., PERALBA MDO, C., SCHWARTZ, I. V., GIUGLIANI, R. & VARGAS, C. R. 2011. Oxidative stress in patients with mucopolysaccharidosis type II before and during enzyme replacement therapy. *Molecular genetics and metabolism,* 103**,** 121-7.

FISCHER, M., RAABE, T., HEISENBERG, M. & SENDTNER, M. 2009. Drosophila RSK negatively regulates bouton number at the neuromuscular junction. *Developmental neurobiology,* 69**,** 212-20.

FORMAN, H. J. & AZZI, A. 1997. On the virtual existence of superoxide anions in mitochondria: thoughts regarding its role in pathophysiology. *The FASEB journal : official publication of the Federation of American Societies for Experimental Biology,* 11**,** 374-5.

FRANCISCOVICH, A. L., MORTIMER, A. D., FREEMAN, A. A., GU, J. & SANYAL, S. 2008. Overexpression screen in Drosophila identifies neuronal roles of GSK-3 beta/shaggy as a regulator of AP-1-dependent developmental plasticity. *Genetics,* 180**,** 2057-71.

FU, R., YANJANIN, N. M., BIANCONI, S., PAVAN, W. J. & PORTER, F. D. 2010. Oxidative stress in Niemann-Pick disease, type C. *Molecular genetics and metabolism,* 101**,** 214-8.

FUKUSHIMA, T., TANAKA, K., LIM, H. & MORIYAMA, M. 2002. Mechanism of cytotoxicity of paraquat. *Environmental health and preventive medicine,* 7**,** 89-94.

FUKUSHIMA, T., YAMADA, K., HOJO, N., ISOBE, A., SHIWAKU, K. & YAMANE, Y. 1994. Mechanism of cytotoxicity of paraquat. III. The effects of acute paraquat exposure on the electron transport system in rat mitochondria. *Experimental and toxicologic pathology : official journal of the Gesellschaft fur Toxikologische Pathologie,* 46**,** 437-41.

FUTERMAN, A. H. & VAN MEER, G. 2004. The cell biology of lysosomal storage disorders. *Nature reviews. Molecular cell biology,* 5**,** 554-65.

GAHTAN, E., AUERBACH, J. M., GRONER, Y. & SEGAL, M. 1998. Reversible impairment of long-term potentiation in transgenic Cu/Zn-SOD mice. *The European journal of neuroscience,* 10**,** 538-44.

GANETZKY, B. & WU, C. F. 1983. Neurogenetic analysis of potassium currents in Drosophila: synergistic effects on neuromuscular transmission in double mutants. *Journal of neurogenetics,* 1**,** 17-28.

GARDNER, P. R. & FRIDOVICH, I. 1991a. Superoxide sensitivity of the Escherichia coli 6-phosphogluconate dehydratase. *The Journal of biological chemistry,* 266**,** 1478-83.

GARDNER, P. R. & FRIDOVICH, I. 1991b. Superoxide sensitivity of the Escherichia coli aconitase. *The Journal of biological chemistry,* 266**,** 19328-33.

GARG, T. K. & CHANG, J. Y. 2003. Oxidative stress causes ERK phosphorylation and cell death in cultured retinal pigment epithelium: prevention of cell death by AG126 and 15-deoxy-delta 12, 14-PGJ2. *BMC ophthalmology,* 3**,** 5.

GAUT, J. R. & HENDERSHOT, L. M. 1993. The modification and assembly of proteins in the endoplasmic reticulum. *Current opinion in cell biology,* 5**,** 589-95.

GEUKING, P., NARASIMAMURTHY, R., LEMAITRE, B., BASLER, K. & LEULIER, F. 2009. A non-redundant role for Drosophila Mkk4 and hemipterous/Mkk7 in TAK1-mediated activation of JNK. *PloS one,* 4**,** e7709.

GINIATULLIN, A. R., DARIOS, F., SHAKIRZYANOVA, A., DAVLETOV, B. & GINIATULLIN, R. 2006. SNAP25 is a pre-synaptic target for the depressant action of reactive oxygen species on transmitter release. *Journal of neurochemistry,* 98**,** 1789-97.

GINIATULLIN, A. R. & GINIATULLIN, R. A. 2003. Dual action of hydrogen peroxide on synaptic transmission at the frog neuromuscular junction. *The Journal of physiology,* 552**,** 283-93.

GINIATULLIN, A. R., GRISHIN, S. N., SHARIFULLINA, E. R., PETROV, A. M., ZEFIROV, A. L. & GINIATULLIN, R. A. 2005. Reactive oxygen species contribute to the presynaptic action of extracellular ATP at the frog neuromuscular junction. *The Journal of physiology,* 565**,** 229-42.

GINSBORG, B. L. 1973. Electrical changes in the membrane in junctional transmission. *Biochimica et biophysica acta,* 300**,** 289-317.

GLAUM, S. R., HARA, M., BINDOKAS, V. P., LEE, C. C., POLONSKY, K. S., BELL, G. I. & MILLER, R. J. 1996. Leptin, the obese gene product, rapidly modulates synaptic transmission in the hypothalamus. *Molecular pharmacology,* 50**,** 230-5.

GLICK, D., BARTH, S. & MACLEOD, K. F. 2010. Autophagy: cellular and molecular mechanisms. *The Journal of pathology,* 221**,** 3-12.

GODENSCHWEGE, T., FORDE, R., DAVIS, C. P., PAUL, A., BECKWITH, K. & DUTTAROY, A. 2009. Mitochondrial superoxide radicals differentially affect muscle activity and neural function. *Genetics,* 183**,** 175-84.

GONZALEZ-MATEOS, A., CAMELLO, P. J., SALIDO, G. M. & PARIENTE, J. A. 2001. Effect of xanthine oxidase-catalyzed reactive oxygen species generation on secretagogue-evoked calcium mobilization in mouse pancreatic acinar cells. *Biochemical pharmacology,* 62**,** 1621-7.

GONZALEZ-POLO, R. A., BOYA, P., PAULEAU, A. L., JALIL, A., LAROCHETTE, N., SOUQUERE, S., ESKELINEN, E. L., PIERRON, G., SAFTIG, P. & KROEMER, G. 2005. The apoptosis/autophagy paradox: autophagic vacuolization before apoptotic death. *Journal of cell science,* 118**,** 3091-102.

GORCZYCA, M., AUGART, C. & BUDNIK, V. 1993. Insulin-like receptor and insulin-like peptide are localized at neuromuscular junctions in Drosophila. *The Journal of neuroscience : the official journal of the Society for Neuroscience,* 13**,** 3692-704.

GROSS, E., SEVIER, C. S., HELDMAN, N., VITU, E., BENTZUR, M., KAISER, C. A., THORPE, C. & FASS, D. 2006. Generating disulfides enzymatically: reaction products and electron acceptors of the endoplasmic reticulum thiol oxidase Ero1p. *Proceedings of the National Academy of Sciences of the United States of America,* 103**,** 299-304.

GUIDI, I., GALIMBERTI, D., LONATI, S., NOVEMBRINO, C., BAMONTI, F., TIRITICCO, M., FENOGLIO, C., VENTURELLI, E., BARON, P., BRESOLIN, N. & SCARPINI, E. 2006. Oxidative imbalance in patients with mild cognitive impairment and Alzheimer's disease. *Neurobiology of aging,* 27**,** 262-9.

GUTTERIDGE, J. M. 1982. The role of superoxide and hydroxyl radicals in phospholipid peroxidation catalysed by iron salts. *FEBS letters,* 150**,** 454-8.

GWINN, D. M., SHACKELFORD, D. B., EGAN, D. F., MIHAYLOVA, M. M., MERY, A., VASQUEZ, D. S., TURK, B. E. & SHAW, R. J. 2008. AMPK phosphorylation of raptor mediates a metabolic checkpoint. *Molecular cell,* 30**,** 214-26.

HALLIWELL, B. 1976. An attempt to demonstrate a reaction between superoxide and hydrogen peroxide. *FEBS letters,* 72**,** 8-10.

HALLIWELL, B. 1978a. Superoxide-dependent formation of hydroxyl radicals in the presence of iron chelates: is it a mechanism for hydroxyl radical production in biochemical systems? *FEBS letters,* 92**,** 321-6.

HALLIWELL, B. 1978b. Superoxide-dependent formation of hydroxyl radicals in the presence of iron salts. Its role in degradation of hyaluronic acid by a superoxide-generating system. *FEBS letters,* 96**,** 238-42.

HALLIWELL, B. 1989. Free radicals, reactive oxygen species and human disease: a critical evaluation with special reference to atherosclerosis. *British journal of experimental pathology,* 70**,** 737-57.

HALLIWELL, B. 1992a. Oxygen radicals as key mediators in neurological disease: fact or fiction? *Annals of neurology,* 32 Suppl**,** S10-5.

HALLIWELL, B. 1992b. Reactive oxygen species and the central nervous system. *Journal of neurochemistry,* 59**,** 1609-23.

HALLIWELL, B. 2006. Oxidative stress and neurodegeneration: where are we now? *Journal of neurochemistry,* 97**,** 1634-58.

HALLIWELL, B. & WHITEMAN, M. 2004. Measuring reactive species and oxidative damage in vivo and in cell culture: how should you do it and what do the results mean? *British journal of pharmacology,* 142**,** 231-55.

HAN, Y., WANG, Q., SONG, P., ZHU, Y. & ZOU, M. H. 2010. Redox regulation of the AMP-activated protein kinase. *PloS one,* 5**,** e15420.

HARDIE, D. G. & CARLING, D. 1997. The AMP-activated protein kinase--fuel gauge of the mammalian cell? *European journal of biochemistry / FEBS,* 246**,** 259-73.

HARDING, T. M., HEFNER-GRAVINK, A., THUMM, M. & KLIONSKY, D. J. 1996. Genetic and phenotypic overlap between autophagy and the cytoplasm to vacuole protein targeting pathway. *The Journal of biological chemistry,* 271**,** 17621-4.

HARMAN, D. 1956. Aging: a theory based on free radical and radiation chemistry. *Journal of gerontology,* 11**,** 298-300.

HARRISON, R. 2004. Physiological roles of xanthine oxidoreductase. *Drug metabolism reviews,* 36**,** 363-75.

HARTLEY, W. J. 1971. Some observations on the pathology of Swainsona SPP poisoning in farm livestock in Eastern Australia. *Acta neuropathologica,* 18**,** 342-55.

HAYES, J. D., CHANAS, S. A., HENDERSON, C. J., MCMAHON, M., SUN, C., MOFFAT, G. J., WOLF, C. R. & YAMAMOTO, M. 2000. The Nrf2 transcription factor contributes both to the basal expression of glutathione S-transferases in mouse liver and to their induction by the chemopreventive synthetic antioxidants, butylated hydroxyanisole and ethoxyquin. *Biochemical Society transactions,* 28**,** 33-41.

HIBI, M., LIN, A., SMEAL, T., MINDEN, A. & KARIN, M. 1993. Identification of an oncoprotein- and UV-responsive protein kinase that binds and potentiates the c-Jun activation domain. *Genes & development,* 7**,** 2135-48.

HIGGINS, G. C., DEVENISH, R. J., BEART, P. M. & NAGLEY, P. 2011. Autophagic activity in cortical neurons under acute oxidative stress directly contributes to cell death. *Cellular and molecular life sciences : CMLS*.

HOLMGREN, A. 1989. Thioredoxin and glutaredoxin systems. *The Journal of biological chemistry,* 264**,** 13963-6.

HOPPER, R. A. & GARTHWAITE, J. 2006. Tonic and phasic nitric oxide signals in hippocampal long-term potentiation. *The Journal of neuroscience : the official journal of the Society for Neuroscience,* 26**,** 11513-21.

HUANG, X., SUYAMA, K., BUCHANAN, J., ZHU, A. J. & SCOTT, M. P. 2005. A Drosophila model of the Niemann-Pick type C lysosome storage disease: dnpc1a is required for molting and sterol homeostasis. *Development,* 132**,** 5115-24.

HUDDLESTON, A. T., TANG, W., TAKESHIMA, H., HAMILTON, S. L. & KLANN, E. 2008. Superoxide-induced potentiation in the hippocampus requires activation of ryanodine receptor type 3 and ERK. *Journal of neurophysiology,* 99**,** 1565-71.

HUMPHREYS, J. M., DUYF, B., JOINER, M. L., PHILLIPS, J. P. & HILLIKER, A. J. 1996. Genetic analysis of oxygen defense mechanisms in Drosophila melanogaster and identification of a novel behavioural mutant with a Shaker phenotype. *Genome / National Research Council Canada = Genome / Conseil national de recherches Canada,* 39**,** 749-57.

HWANG, C., SINSKEY, A. J. & LODISH, H. F. 1992. Oxidized redox state of glutathione in the endoplasmic reticulum. *Science,* 257**,** 1496-502.

IGAKI, T., KANDA, H., YAMAMOTO-GOTO, Y., KANUKA, H., KURANAGA, E., AIGAKI, T. & MIURA, M. 2002. Eiger, a TNF superfamily ligand that triggers the Drosophila JNK pathway. *The EMBO journal,* 21**,** 3009-18.

INOKI, K., ZHU, T. & GUAN, K. L. 2003. TSC2 mediates cellular energy response to control cell growth and survival. *Cell,* 115**,** 577-90.

ISHII, T., ITOH, K., TAKAHASHI, S., SATO, H., YANAGAWA, T., KATOH, Y., BANNAI, S. & YAMAMOTO, M. 2000. Transcription factor Nrf2 coordinately regulates a group of oxidative stress-inducible genes in macrophages. *The Journal of biological chemistry,* 275**,** 16023-9.

JAGER, S., BUCCI, C., TANIDA, I., UENO, T., KOMINAMI, E., SAFTIG, P. & ESKELINEN, E. L. 2004. Role for Rab7 in maturation of late autophagic vacuoles. *Journal of cell science,* 117**,** 4837-48.

JAN, Y. N., JAN, L. Y. & DENNIS, M. J. 1977. Two mutations of synaptic transmission in Drosophila. *Proceedings of the Royal Society of London. Series B, Containing papers of a Biological character. Royal Society,* 198**,** 87-108.

JANCA, F. C., WOLOSHYN, E. P. & NASH, D. 1986. Heterogeneity of lethals in a "simple" lethal complementation group. *Genetics,* 112**,** 43-64.

JANSEN, M., TEN KLOOSTER, J. P., OFFERHAUS, G. J. & CLEVERS, H. 2009. LKB1 and AMPK family signaling: the intimate link between cell polarity and energy metabolism. *Physiological reviews,* 89**,** 777-98.

JEGGA, A. G., SCHNEIDER, L., OUYANG, X. & ZHANG, J. 2011. Systems biology of the autophagy-lysosomal pathway. *Autophagy,* 7**,** 477-89.

JENNINGS, J. J., JR., ZHU, J. H., RBAIBI, Y., LUO, X., CHU, C. T. & KISELYOV, K. 2006. Mitochondrial aberrations in mucolipidosis Type IV. *The Journal of biological chemistry,* 281**,** 39041-50.

JEYAPAUL, J. & JAISWAL, A. K. 2000. Nrf2 and c-Jun regulation of antioxidant response element (ARE)-mediated expression and induction of gamma-glutamylcysteine synthetase heavy subunit gene. *Biochemical pharmacology,* 59**,** 1433-9.

JINDRA, M., GAZIOVA, I., UHLIROVA, M., OKABE, M., HIROMI, Y. & HIROSE, S. 2004. Coactivator MBF1 preserves the redox-dependent AP-1 activity during oxidative stress in Drosophila. *The EMBO journal,* 23**,** 3538-47.

JONES, S. A., O'DONNELL, V. B., WOOD, J. D., BROUGHTON, J. P., HUGHES, E. J. & JONES, O. T. 1996. Expression of phagocyte NADPH oxidase components in human endothelial cells. *The American journal of physiology,* 271**,** H1626-34.

KAMADA, Y., FUNAKOSHI, T., SHINTANI, T., NAGANO, K., OHSUMI, M. & OHSUMI, Y. 2000. Tor-mediated induction of autophagy via an Apg1 protein kinase complex. *The Journal of cell biology,* 150**,** 1507-13.

KATZ, B. & MILEDI, R. 1965. The Effect of Calcium on Acetylcholine Release from Motor Nerve Terminals. *Proceedings of the Royal Society of London. Series B, Containing papers of a Biological character. Royal Society,* 161**,** 496-503.

KESHISHIAN, H., BROADIE, K., CHIBA, A. & BATE, M. 1996. The drosophila neuromuscular junction: a model system for studying synaptic development and function. *Annual review of neuroscience,* 19**,** 545-75.

KESHISHIAN, H. & CHIBA, A. 1993. Neuromuscular development in Drosophila: insights from single neurons and single genes. *Trends in neurosciences,* 16**,** 278-83.

KESHISHIAN, H., CHIBA, A., CHANG, T. N., HALFON, M. S., HARKINS, E. W., JARECKI, J., WANG, L., ANDERSON, M., CASH, S., HALPERN, M. E. & ET AL. 1993. Cellular mechanisms governing synaptic development in Drosophila melanogaster. *Journal of neurobiology,* 24**,** 757-87.

KIM, S., WAIRKAR, Y. P., DANIELS, R. W. & DIANTONIO, A. 2010. The novel endosomal membrane protein Ema interacts with the class C Vps-HOPS complex to promote endosomal maturation. *The Journal of cell biology,* 188**,** 717-34.

KINA, S., NAKASONE, T., TAKEMOTO, H., MATAYOSHI, A., MAKISHI, S., SUNAGAWA, N., LIANG, F., PHONAPHONH, T. & SUNAKAWA, H. 2009. Regulation of chemokine production via oxidative pathway in HeLa cells. *Mediators of inflammation,* 2009**,** 183760.

KIRKLAND, K. C. & PHILLIPS, J. P. 1987. Isolation and chromosomal localization of genomic DNA sequences coding for cytoplasmic superoxide dismutase from Drosophila melanogaster. *Gene,* 61**,** 415-9.

KITTEL, R. J., HALLERMANN, S., THOMSEN, S., WICHMANN, C., SIGRIST, S. J. & HECKMANN, M. 2006a. Active zone assembly and synaptic release. *Biochemical Society transactions,* 34**,** 939-41.

KITTEL, R. J., WICHMANN, C., RASSE, T. M., FOUQUET, W., SCHMIDT, M., SCHMID, A., WAGH, D. A., PAWLU, C., KELLNER, R. R., WILLIG, K. I., HELL, S. W., BUCHNER, E., HECKMANN, M. & SIGRIST, S. J. 2006b. Bruchpilot promotes active zone assembly, Ca2+ channel clustering, and vesicle release. *Science,* 312**,** 1051-4.

KLANN, E. 1998. Cell-permeable scavengers of superoxide prevent long-term potentiation in hippocampal area CA1. *Journal of neurophysiology,* 80**,** 452-7.

KLANN, E., ROBERSON, E. D., KNAPP, L. T. & SWEATT, J. D. 1998. A role for superoxide in protein kinase C activation and induction of long-term potentiation. *The Journal of biological chemistry,* 273**,** 4516-22.

KLINTWORTH, H., NEWHOUSE, K., LI, T., CHOI, W. S., FAIGLE, R. & XIA, Z. 2007. Activation of c-Jun N-terminal protein kinase is a common mechanism underlying paraquat- and rotenone-induced dopaminergic cell apoptosis. *Toxicological sciences : an official journal of the Society of Toxicology,* 97**,** 149-62.

KLIONSKY, D. J. 2005. The molecular machinery of autophagy: unanswered questions. *Journal of cell science,* 118**,** 7-18.

KLIONSKY, D. J., CREGG, J. M., DUNN, W. A., JR., EMR, S. D., SAKAI, Y., SANDOVAL, I. V., SIBIRNY, A., SUBRAMANI, S., THUMM, M., VEENHUIS, M. & OHSUMI, Y. 2003. A unified nomenclature for yeast autophagy-related genes. *Developmental cell,* 5**,** 539-45.

KNAPP, L. T. & KLANN, E. 2002a. Potentiation of hippocampal synaptic transmission by superoxide requires the oxidative activation of protein kinase C. *The Journal of neuroscience : the official journal of the Society for Neuroscience,* 22**,** 674-83.

KNAPP, L. T. & KLANN, E. 2002b. Role of reactive oxygen species in hippocampal long-term potentiation: contributory or inhibitory? *Journal of neuroscience research,* 70**,** 1-7.

KNOTT, A. B. & BOSSY-WETZEL, E. 2009. Nitric oxide in health and disease of the nervous system. *Antioxidants & redox signaling,* 11**,** 541-54.

KNOX, S., GE, H., DIMITROFF, B. D., REN, Y., HOWE, K. A., ARSHAM, A. M., EASTERDAY, M. C., NEUFELD, T. P., O'CONNOR, M. B. & SELLECK, S. B. 2007. Mechanisms of TSC-mediated control of synapse assembly and axon guidance. *PloS one,* 2**,** e375.

KOCH, I., SCHWARZ, H., BEUCHLE, D., GOELLNER, B., LANGEGGER, M. & ABERLE, H. 2008. Drosophila ankyrin 2 is required for synaptic stability. *Neuron,* 58**,** 210-22.

KOH, T. W., VERSTREKEN, P. & BELLEN, H. J. 2004. DAP-160/intersectin acts as a stabilizing scaffold required for synaptic development and vesicle endocytosis. *Neuron,* 43**,** 193-205.

KOH, Y. H., RUIZ-CANADA, C., GORCZYCA, M. & BUDNIK, V. 2002. The Ras1-mitogen-activated protein kinase signal transduction pathway regulates synaptic plasticity through fasciclin II-mediated cell adhesion. *The Journal of neuroscience : the official journal of the Society for Neuroscience,* 22**,** 2496-504.

KOROLCHUK, V. I., SCHUTZ, M. M., GOMEZ-LLORENTE, C., ROCHA, J., LANSU, N. R., COLLINS, S. M., WAIRKAR, Y. P., ROBINSON, I. M. & O'KANE, C. J. 2007. Drosophila Vps35 function is necessary for normal endocytic trafficking and actin cytoskeleton organisation. *Journal of cell science,* 120**,** 4367-76.

KUBOTA, C., TORII, S., HOU, N., SAITO, N., YOSHIMOTO, Y., IMAI, H. & TAKEUCHI, T. 2010. Constitutive reactive oxygen species generation

from autophagosome/lysosome in neuronal oxidative toxicity. *The Journal of biological chemistry,* 285**,** 667-74.

KURANAGA, E., KANUKA, H., IGAKI, T., SAWAMOTO, K., ICHIJO, H., OKANO, H. & MIURA, M. 2002. Reaper-mediated inhibition of DIAP-1-induced DTRAF1 degradation results in activation of JNK in Drosophila. *Nature cell biology,* 4**,** 705-10.

KURANAGA, E. & MIURA, M. 2002. Molecular genetic control of caspases and JNK-mediated neural cell death. *Archives of histology and cytology,* 65**,** 291-300.

KURZ, T., TERMAN, A. & BRUNK, U. T. 2007. Autophagy, ageing and apoptosis: the role of oxidative stress and lysosomal iron. *Arch Biochem Biophys,* 462**,** 220-30.

KURZ, T., TERMAN, A., GUSTAFSSON, B. & BRUNK, U. T. 2008a. Lysosomes and oxidative stress in aging and apoptosis. *Biochim Biophys Acta,* 1780**,** 1291-303.

KURZ, T., TERMAN, A., GUSTAFSSON, B. & BRUNK, U. T. 2008b. Lysosomes in iron metabolism, ageing and apoptosis. *Histochemistry and cell biology,* 129**,** 389-406.

KUTHAN, H. & ULLRICH, V. 1982. Oxidase and oxygenase function of the microsomal cytochrome P450 monooxygenase system. *European journal of biochemistry / FEBS,* 126**,** 583-8.

LAHEY, T., GORCZYCA, M., JIA, X. X. & BUDNIK, V. 1994. The Drosophila tumor suppressor gene dlg is required for normal synaptic bouton structure. *Neuron,* 13**,** 823-35.

LE BELLE, J. E., OROZCO, N. M., PAUCAR, A. A., SAXE, J. P., MOTTAHEDEH, J., PYLE, A. D., WU, H. & KORNBLUM, H. I. 2011. Proliferative neural stem cells have high endogenous ROS levels that regulate self-renewal and neurogenesis in a PI3K/Akt-dependant manner. *Cell stem cell,* 8**,** 59-71.

LEE, J. A. & GAO, F. B. 2009. Inhibition of autophagy induction delays neuronal cell loss caused by dysfunctional ESCRT-III in frontotemporal dementia. *The Journal of neuroscience : the official journal of the Society for Neuroscience,* 29**,** 8506-11.

LEE, K. Y., CHUNG, K. & CHUNG, J. M. 2010a. Involvement of reactive oxygen species in long-term potentiation in the spinal cord dorsal horn. *Journal of neurophysiology,* 103**,** 382-91.

LEE, S., LIU, H. P., LIN, W. Y., GUO, H. & LU, B. 2010b. LRRK2 kinase regulates synaptic morphology through distinct substrates at the presynaptic and postsynaptic compartments of the Drosophila neuromuscular junction. *The Journal of neuroscience : the official journal of the Society for Neuroscience,* 30**,** 16959-69.

LEE, S. B., KIM, S., LEE, J., PARK, J., LEE, G., KIM, Y., KIM, J. M. & CHUNG, J. 2007. ATG1, an autophagy regulator, inhibits cell growth by negatively regulating S6 kinase. *EMBO reports,* 8**,** 360-5.

LEE, T. & LUO, L. 2001. Mosaic analysis with a repressible cell marker (MARCM) for Drosophila neural development. *Trends in neurosciences,* 24**,** 251-4.

LEIPER, K., CAMPBELL, B. J., JENKINSON, M. D., MILTON, J., YU, L. G., DEMOCRATIS, J. & RHODES, J. M. 2001. Interaction between bacterial peptides, neutrophils and goblet cells: a possible mechanism for neutrophil recruitment and goblet cell depletion in colitis. *Clinical science,* 101**,** 395-402.

LI, C., CAPAN, E., ZHAO, Y., ZHAO, J., STOLZ, D., WATKINS, S. C., JIN, S. & LU, B. 2006. Autophagy is induced in CD4+ T cells and important for the growth factor-withdrawal cell death. *Journal of immunology,* 177**,** 5163-8.

LIANG, J., SHAO, S. H., XU, Z. X., HENNESSY, B., DING, Z., LARREA, M., KONDO, S., DUMONT, D. J., GUTTERMAN, J. U., WALKER, C. L., SLINGERLAND, J. M. & MILLS, G. B. 2007. The energy sensing LKB1-AMPK pathway regulates p27(kip1) phosphorylation mediating the decision to enter autophagy or apoptosis. *Nature cell biology,* 9**,** 218-24.

LIBERATI, N. T., DATTO, M. B., FREDERICK, J. P., SHEN, X., WONG, C., ROUGIER-CHAPMAN, E. M. & WANG, X. F. 1999. Smads bind directly to the Jun family of AP-1 transcription factors. *Proceedings of the National Academy of Sciences of the United States of America,* 96**,** 4844-9.

LIEBL, F. L., WU, Y., FEATHERSTONE, D. E., NOORDERMEER, J. N., FRADKIN, L. & HING, H. 2008. Derailed regulates development of the Drosophila neuromuscular junction. *Developmental neurobiology,* 68**,** 152-65.

LINDMO, K., SIMONSEN, A., BRECH, A., FINLEY, K., RUSTEN, T. E. & STENMARK, H. 2006. A dual function for Deep orange in programmed autophagy in the Drosophila melanogaster fat body. *Experimental cell research,* 312**,** 2018-27.

LIPPAI, M., CSIKOS, G., MAROY, P., LUKACSOVICH, T., JUHASZ, G. & SASS, M. 2008. SNF4Agamma, the Drosophila AMPK gamma subunit is required for regulation of developmental and stress-induced autophagy. *Autophagy,* 4**,** 476-86.

LIPTON, S. A., CHOI, Y. B., PAN, Z. H., LEI, S. Z., CHEN, H. S., SUCHER, N. J., LOSCALZO, J., SINGEL, D. J. & STAMLER, J. S. 1993. A redox-based mechanism for the neuroprotective and neurodestructive effects of nitric oxide and related nitroso-compounds. *Nature,* 364**,** 626-32.

LIU, Q., BERCHNER-PFANNSCHMIDT, U., MOLLER, U., BRECHT, M., WOTZLAW, C., ACKER, H., JUNGERMANN, K. & KIETZMANN, T. 2004. A Fenton reaction at the endoplasmic reticulum is involved in the redox control of hypoxia-inducible gene expression. *Proceedings of the National Academy of Sciences of the United States of America,* 101**,** 4302-7.

LIU, Y., FISKUM, G. & SCHUBERT, D. 2002. Generation of reactive oxygen species by the mitochondrial electron transport chain. *Journal of neurochemistry,* 80**,** 780-7.

LNENICKA, G. A. & KESHISHIAN, H. 2000. Identified motor terminals in Drosophila larvae show distinct differences in morphology and physiology. *Journal of neurobiology,* 43**,** 186-97.

LOSCHEN, G., AZZI, A., RICHTER, C. & FLOHE, L. 1974. Superoxide radicals as precursors of mitochondrial hydrogen peroxide. *FEBS letters,* 42**,** 68-72.

LOSCHEN, G., FLOHE, L. & CHANCE, B. 1971. Respiratory chain linked H(2)O(2) production in pigeon heart mitochondria. *FEBS letters,* 18**,** 261-264.

MACKAY, W. J. & BEWLEY, G. C. 1989. The genetics of catalase in Drosophila melanogaster: isolation and characterization of acatalasemic mutants. *Genetics,* 122**,** 643-52.

MADHANI, H. D. 1997. Genetic abnormalities in Friedreich's ataxia. *The New England journal of medicine,* 336**,** 1022; author reply 1022-3.

MADHANI, H. D. & FINK, G. R. 1997. Combinatorial control required for the specificity of yeast MAPK signaling. *Science,* 275**,** 1314-7.

MADHANI, H. D., STYLES, C. A. & FINK, G. R. 1997. MAP kinases with distinct inhibitory functions impart signaling specificity during yeast differentiation. *Cell,* 91**,** 673-84.

MAFFEI, A., PRESTORI, F., SHIBUKI, K., ROSSI, P., TAGLIETTI, V. & D'ANGELO, E. 2003. NO enhances presynaptic currents during cerebellar mossy fiber-granule cell LTP. *Journal of neurophysiology,* 90**,** 2478-83.

MARCH, P. A., WURZELMANN, S. & WALKLEY, S. U. 1995. Morphological alterations in neocortical and cerebellar GABAergic neurons in a canine model of juvenile Batten disease. *American journal of medical genetics,* 57**,** 204-12.

MARIE, B., SWEENEY, S. T., POSKANZER, K. E., ROOS, J., KELLY, R. B. & DAVIS, G. W. 2004. DAP-160/intersectin scaffolds the periactive zone to achieve high-fidelity endocytosis and normal synaptic growth. *Neuron,* 43**,** 207-19.

MARNETT, L. J. 1999. Lipid peroxidation-DNA damage by malondialdehyde. *Mutation research,* 424**,** 83-95.

MARQUES, G. 2005. Morphogens and synaptogenesis in Drosophila. *Journal of neurobiology,* 64**,** 417-34.

MARRIOTT, H. M., JACKSON, L. E., WILKINSON, T. S., SIMPSON, A. J., MITCHELL, T. J., BUTTLE, D. J., CROSS, S. S., INCE, P. G., HELLEWELL, P. G., WHYTE, M. K. & DOCKRELL, D. H. 2008. Reactive oxygen species regulate neutrophil recruitment and survival in pneumococcal pneumonia. *American journal of respiratory and critical care medicine,* 177**,** 887-95.

MARRUS, S. B. & DIANTONIO, A. 2004. Preferential localization of glutamate receptors opposite sites of high presynaptic release. *Current biology : CB,* 14**,** 924-31.

MARRUS, S. B. & DIANTONIO, A. 2005. Investigating the safety factor at an invertebrate neuromuscular junction. *Journal of neurobiology,* 63**,** 62-9.

MARRUS, S. B., PORTMAN, S. L., ALLEN, M. J., MOFFAT, K. G. & DIANTONIO, A. 2004. Differential localization of glutamate receptor subunits at the Drosophila neuromuscular junction. *The Journal of neuroscience : the official journal of the Society for Neuroscience,* 24**,** 1406-15.

MARTIN-BLANCO, E., GAMPEL, A., RING, J., VIRDEE, K., KIROV, N., TOLKOVSKY, A. M. & MARTINEZ-ARIAS, A. 1998. puckered encodes a phosphatase that mediates a feedback loop regulating JNK activity during dorsal closure in Drosophila. *Genes & development,* 12**,** 557-70.

MASSARO, C. M., PIELAGE, J. & DAVIS, G. W. 2009. Molecular mechanisms that enhance synapse stability despite persistent disruption of the spectrin/ankyrin/microtubule cytoskeleton. *The Journal of cell biology,* 187**,** 101-17.

MAST, J. D., TOMALTY, K. M., VOGEL, H. & CLANDININ, T. R. 2008. Reactive oxygen species act remotely to cause synapse loss in a Drosophila model of developmental mitochondrial encephalopathy. *Development,* 135**,** 2669-79.

MATHEW, D., ATAMAN, B., CHEN, J., ZHANG, Y., CUMBERLEDGE, S. & BUDNIK, V. 2005. Wingless signaling at synapses is through cleavage and nuclear import of receptor DFrizzled2. *Science,* 310**,** 1344-7.

MAVRAKIS, M., LIPPINCOTT-SCHWARTZ, J., STRATAKIS, C. A. & BOSSIS, I. 2006. Depletion of type IA regulatory subunit (RIalpha) of protein kinase A (PKA) in mammalian cells and tissues activates mTOR and causes autophagic deficiency. *Human molecular genetics,* 15**,** 2962-71.

MAY, D. W. 1901. Catalase, a New Enzym of General Occurrence. *Science,* 14**,** 815-6.

MCCABE, B. D., HOM, S., ABERLE, H., FETTER, R. D., MARQUES, G., HAERRY, T. E., WAN, H., O'CONNOR, M. B., GOODMAN, C. S. & HAGHIGHI, A. P. 2004. Highwire regulates presynaptic BMP signaling essential for synaptic growth. *Neuron,* 41**,** 891-905.

MCCABE, B. D., MARQUES, G., HAGHIGHI, A. P., FETTER, R. D., CROTTY, M. L., HAERRY, T. E., GOODMAN, C. S. & O'CONNOR, M. B. 2003. The BMP homolog Gbb provides a retrograde signal that regulates synaptic growth at the Drosophila neuromuscular junction. *Neuron,* 39**,** 241-54.

MCCORD, J. M. & FRIDOVICH, I. 1968. The reduction of cytochrome c by milk xanthine oxidase. *The Journal of biological chemistry,* 243**,** 5753-60.

MCCORD, J. M. & FRIDOVICH, I. 1969a. Superoxide dismutase. An enzymic function for erythrocuprein (hemocuprein). *The Journal of biological chemistry,* 244**,** 6049-55.

MCCORD, J. M. & FRIDOVICH, I. 1969b. The utility of superoxide dismutase in studying free radical reactions. I. Radicals generated by the interaction of sulfite, dimethyl sulfoxide, and oxygen. *The Journal of biological chemistry,* 244**,** 6056-63.

MCDONALD, D. R., BRUNDEN, K. R. & LANDRETH, G. E. 1997. Amyloid fibrils activate tyrosine kinase-dependent signaling and superoxide production in microglia. *The Journal of neuroscience : the official journal of the Society for Neuroscience,* 17**,** 2284-94.

MCNALLY, J. S., DAVIS, M. E., GIDDENS, D. P., SAHA, A., HWANG, J., DIKALOV, S., JO, H. & HARRISON, D. G. 2003. Role of xanthine oxidoreductase and NAD(P)H oxidase in endothelial superoxide production in response to oscillatory shear stress. *American journal of physiology. Heart and circulatory physiology,* 285**,** H2290-7.

MEIKLE, P. J., HOPWOOD, J. J., CLAGUE, A. E. & CAREY, W. F. 1999. Prevalence of lysosomal storage disorders. *JAMA : the journal of the American Medical Association,* 281**,** 249-54.

MIGLIACCIO, E., GIORGIO, M., MELE, S., PELICCI, G., REBOLDI, P., PANDOLFI, P. P., LANFRANCONE, L. & PELICCI, P. G. 1999. The p66shc adaptor protein controls oxidative stress response and life span in mammals. *Nature,* 402**,** 309-13.

MILLS, G. C. 1957. Hemoglobin catabolism. I. Glutathione peroxidase, an erythrocyte enzyme which protects hemoglobin from oxidative breakdown. *The Journal of biological chemistry,* 229**,** 189-97.

MILTON, N. G. 1999. Amyloid-beta binds catalase with high affinity and inhibits hydrogen peroxide breakdown. *The Biochemical journal,* 344 Pt 2**,** 293-6.

MILTON, N. G. 2001. Inhibition of catalase activity with 3-amino-triazole enhances the cytotoxicity of the Alzheimer's amyloid-beta peptide. *Neurotoxicology,* 22**,** 767-74.

MILTON, R. H., ABETI, R., AVERAIMO, S., DEBIASI, S., VITELLARO, L., JIANG, L., CURMI, P. M., BREIT, S. N., DUCHEN, M. R. & MAZZANTI, M. 2008. CLIC1 function is required for beta-amyloid-induced generation of reactive oxygen species by microglia. *The Journal of neuroscience : the official journal of the Society for Neuroscience,* 28**,** 11488-99.

MILTON, V. J., JARRETT, H. E., GOWERS, K., CHALAK, S., BRIGGS, L., ROBINSON, I. M. & SWEENEY, S. T. 2011. Oxidative stress induces overgrowth of the Drosophila neuromuscular junction. *Proceedings of the National Academy of Sciences of the United States of America,* 108**,** 17521-6.

MINAMINO, T., YUJIRI, T., PAPST, P. J., CHAN, E. D., JOHNSON, G. L. & TERADA, N. 1999. MEKK1 suppresses oxidative stress-induced apoptosis of embryonic stem cell-derived cardiac myocytes. *Proceedings of the National Academy of Sciences of the United States of America,* 96**,** 15127-32.

MIROUSE, V., SWICK, L. L., KAZGAN, N., ST JOHNSTON, D. & BRENMAN, J. E. 2007. LKB1 and AMPK maintain epithelial cell polarity under energetic stress. *The Journal of cell biology,* 177**,** 387-92.

MISSIRLIS, F., HU, J., KIRBY, K., HILLIKER, A. J., ROUAULT, T. A. & PHILLIPS, J. P. 2003. Compartment-specific protection of iron-sulfur

proteins by superoxide dismutase. *The Journal of biological chemistry,* 278**,** 47365-9.

MISSIRLIS, F., ULSCHMID, J. K., HIROSAWA-TAKAMORI, M., GRONKE, S., SCHAFER, U., BECKER, K., PHILLIPS, J. P. & JACKLE, H. 2002. Mitochondrial and cytoplasmic thioredoxin reductase variants encoded by a single Drosophila gene are both essential for viability. *The Journal of biological chemistry,* 277**,** 11521-6.

MOJSILOVIC-PETROVIC, J., NEDELSKY, N., BOCCITTO, M., MANO, I., GEORGIADES, S. N., ZHOU, W., LIU, Y., NEVE, R. L., TAYLOR, J. P., DRISCOLL, M., CLARDY, J., MERRY, D. & KALB, R. G. 2009. FOXO3a is broadly neuroprotective in vitro and in vivo against insults implicated in motor neuron diseases. *The Journal of neuroscience : the official journal of the Society for Neuroscience,* 29**,** 8236-47.

MORAIS, V. A., VERSTREKEN, P., ROETHIG, A., SMET, J., SNELLINX, A., VANBRABANT, M., HADDAD, D., FREZZA, C., MANDEMAKERS, W., VOGT-WEISENHORN, D., VAN COSTER, R., WURST, W., SCORRANO, L. & DE STROOPER, B. 2009. Parkinson's disease mutations in PINK1 result in decreased Complex I activity and deficient synaptic function. *EMBO molecular medicine,* 1**,** 99-111.

MOTOHASHI, H., O'CONNOR, T., KATSUOKA, F., ENGEL, J. D. & YAMAMOTO, M. 2002. Integration and diversity of the regulatory network composed of Maf and CNC families of transcription factors. *Gene,* 294**,** 1-12.

MOTOHASHI, H. & YAMAMOTO, M. 2004. Nrf2-KeAP-1 defines a physiologically important stress response mechanism. *Trends in molecular medicine,* 10**,** 549-57.

MUELLER, L. D., FOLK, D. G., NGUYEN, N., NGUYEN, P., LAM, P., ROSE, M. R. & BRADLEY, T. 2005. Evolution of larval foraging behaviour in Drosophila and its effects on growth and metabolic rates. *Physiological Entomology,* 30**,** 262-269.

MURRAY, C. A. & LYNCH, M. A. 1998. Dietary supplementation with vitamin E reverses the age-related deficit in long term potentiation in dentate gyrus. *The Journal of biological chemistry,* 273**,** 12161-8.

NACHMANSOHN, D. 1971. Chemical events in conducting and synaptic membranes during electrical activity. *Proceedings of the National Academy of Sciences of the United States of America,* 68**,** 3170-4.

NAKANO, Y., FUJITANI, K., KURIHARA, J., RAGAN, J., USUI-AOKI, K., SHIMODA, L., LUKACSOVICH, T., SUZUKI, K., SEZAKI, M., SANO, Y., UEDA, R., AWANO, W., KANEDA, M., UMEDA, M. & YAMAMOTO, D. 2001. Mutations in the novel membrane protein spinster interfere with programmed cell death and cause neural degeneration in Drosophila melanogaster. *Molecular and cellular biology,* 21**,** 3775-88.

NELSON, E. J., CONNOLLY, J. & MCARTHUR, P. 2003. Nitric oxide and S-nitrosylation: excitotoxic and cell signaling mechanism. *Biology of the cell / under the auspices of the European Cell Biology Organization,* 95**,** 3-8.

NEMOTO, S. & FINKEL, T. 2002. Redox regulation of forkhead proteins through a p66shc-dependent signaling pathway. *Science,* 295**,** 2450-2.

NYLANDSTED, J., GYRD-HANSEN, M., DANIELEWICZ, A., FEHRENBACHER, N., LADEMANN, U., HOYER-HANSEN, M., WEBER, E., MULTHOFF, G., ROHDE, M. & JAATTELA, M. 2004. Heat shock protein 70 promotes cell survival by inhibiting lysosomal membrane permeabilization. *The Journal of experimental medicine,* 200**,** 425-35.

O'SHEA, E. K., RUTKOWSKI, R. & KIM, P. S. 1992. Mechanism of specificity in the Fos-Jun oncoprotein heterodimer. *Cell,* 68**,** 699-708.

OBARA, K., SEKITO, T., NIIMI, K. & OHSUMI, Y. 2008. The Atg18-Atg2 complex is recruited to autophagic membranes via phosphatidylinositol 3-phosphate and exerts an essential function. *The Journal of biological chemistry,* 283**,** 23972-80.

OGATA, M., HINO, S., SAITO, A., MORIKAWA, K., KONDO, S., KANEMOTO, S., MURAKAMI, T., TANIGUCHI, M., TANII, I., YOSHINAGA, K., SHIOSAKA, S., HAMMARBACK, J. A., URANO, F. & IMAIZUMI, K. 2006. Autophagy is activated for cell survival after endoplasmic reticulum stress. *Molecular and cellular biology,* 26**,** 9220-31.

OWUSU-ANSAH, E., YAVARI, A., MANDAL, S. & BANERJEE, U. 2008. Distinct mitochondrial retrograde signals control the G1-S cell cycle checkpoint. *Nature genetics,* 40**,** 356-61.

PACKARD, M., KOO, E. S., GORCZYCA, M., SHARPE, J., CUMBERLEDGE, S. & BUDNIK, V. 2002. The Drosophila Wnt, wingless, provides an essential signal for pre- and postsynaptic differentiation. *Cell,* 111**,** 319-30.

PADAYATTY, S. J., KATZ, A., WANG, Y., ECK, P., KWON, O., LEE, J. H., CHEN, S., CORPE, C., DUTTA, A., DUTTA, S. K. & LEVINE, M. 2003. Vitamin C as an antioxidant: evaluation of its role in disease prevention. *Journal of the American College of Nutrition,* 22**,** 18-35.

PADDISON, P. J., CAUDY, A. A., BERNSTEIN, E., HANNON, G. J. & CONKLIN, D. S. 2002a. Short hairpin RNAs (shRNAs) induce sequence-specific silencing in mammalian cells. *Genes & development,* 16**,** 948-58.

PADDISON, P. J., CAUDY, A. A. & HANNON, G. J. 2002b. Stable suppression of gene expression by RNAi in mammalian cells. *Proceedings of the National Academy of Sciences of the United States of America,* 99**,** 1443-8.

PALADE, G. E. 1953. An electron microscope study of the mitochondrial structure. *The journal of histochemistry and cytochemistry : official journal of the Histochemistry Society,* 1**,** 188-211.

PALAY, S. L. & PALADE, G. E. 1955. The fine structure of neurons. *The Journal of biophysical and biochemical cytology,* 1**,** 69-88.

PALMER, L. A. & JOHNS, R. A. 1998. Hypoxia upregulates inducible (Type II) nitric oxide synthase in an HIF-1 dependent manner in rat pulmonary microvascular but not aortic smooth muscle cells. *Chest,* 114**,** 33S-34S.

PAN, D. A. & HARDIE, D. G. 2002. A homologue of AMP-activated protein kinase in Drosophila melanogaster is sensitive to AMP and is activated by ATP depletion. *The Biochemical journal,* 367**,** 179-86.

PANCHENKO, M. V., FARBER, H. W. & KORN, J. H. 2000. Induction of heme oxygenase-1 by hypoxia and free radicals in human dermal fibroblasts. *American journal of physiology. Cell physiology,* 278**,** C92-C101.

PAPADIA, S., SORIANO, F. X., LEVEILLE, F., MARTEL, M. A., DAKIN, K. A., HANSEN, H. H., KAINDL, A., SIFRINGER, M., FOWLER, J., STEFOVSKA, V., MCKENZIE, G., CRAIGON, M., CORRIVEAU, R., GHAZAL, P., HORSBURGH, K., YANKNER, B. A., WYLLIE, D. J., IKONOMIDOU, C. & HARDINGHAM, G. E. 2008. Synaptic NMDA receptor activity boosts intrinsic antioxidant defenses. *Nature neuroscience,* 11**,** 476-87.

PAPPOLLA, M. A., OMAR, R. A., KIM, K. S. & ROBAKIS, N. K. 1992. Immunohistochemical evidence of oxidative [corrected] stress in Alzheimer's disease. *The American journal of pathology,* 140**,** 621-8.

PARK, G. B., KIM, Y. S., LEE, H. K., SONG, H., CHO, D. H., LEE, W. J. & HUR, D. Y. 2010. Endoplasmic reticulum stress-mediated apoptosis of EBV-transformed B cells by cross-linking of CD70 is dependent upon generation of reactive oxygen species and activation of p38 MAPK and JNK pathway. *Journal of immunology,* 185**,** 7274-84.

PARK, K. J., LEE, S. H., LEE, C. H., JANG, J. Y., CHUNG, J., KWON, M. H. & KIM, Y. S. 2009. Upregulation of Beclin-1 expression and phosphorylation of Bcl-2 and p53 are involved in the JNK-mediated autophagic cell death. *Biochemical and biophysical research communications,* 382**,** 726-9.

PARK, K. W., BAIK, H. H. & JIN, B. K. 2008. Interleukin-4-induced oxidative stress via microglial NADPH oxidase contributes to the death of hippocampal neurons in vivo. *Current aging science,* 1**,** 192-201.

PARKES, T. L., ELIA, A. J., DICKINSON, D., HILLIKER, A. J., PHILLIPS, J. P. & BOULIANNE, G. L. 1998. Extension of Drosophila lifespan by overexpression of human SOD1 in motorneurons. *Nature genetics,* 19**,** 171-4.

PATEL, P. H., THAPAR, N., GUO, L., MARTINEZ, M., MARIS, J., GAU, C. L., LENGYEL, J. A. & TAMANOI, F. 2003. Drosophila Rheb GTPase is required for cell cycle progression and cell growth. *Journal of cell science,* 116**,** 3601-10.

PATTEN, D. A., GERMAIN, M., KELLY, M. A. & SLACK, R. S. 2010. Reactive oxygen species: stuck in the middle of neurodegeneration. *Journal of Alzheimer's disease : JAD,* 20 Suppl 2**,** S357-67.

PATTINGRE, S., BAUVY, C. & CODOGNO, P. 2003. Amino acids interfere with the ERK1/2-dependent control of macroautophagy by controlling the activation of Raf-1 in human colon cancer HT-29 cells. *The Journal of biological chemistry,* 278**,** 16667-74.

PATTINGRE, S. & LEVINE, B. 2006. Bcl-2 inhibition of autophagy: a new route to cancer? *Cancer research,* 66**,** 2885-8.

PAUL, A., WILSON, S., BELHAM, C. M., ROBINSON, C. J., SCOTT, P. H., GOULD, G. W. & PLEVIN, R. 1997. Stress-activated protein kinases: activation, regulation and function. *Cellular signalling,* 9**,** 403-10.

PELLMAR, T. C., HOLLINDEN, G. E. & SARVEY, J. M. 1991. Free radicals accelerate the decay of long-term potentiation in field CA1 of guinea-pig hippocampus. *Neuroscience,* 44**,** 353-9.

PERKINS, K. K., ADMON, A., PATEL, N. & TJIAN, R. 1990. The Drosophila Fos-related AP-1 protein is a developmentally regulated transcription factor. *Genes & development,* 4**,** 822-34.

POTTER, C. J., PEDRAZA, L. G., HUANG, H. & XU, T. 2003. The tuberous sclerosis complex (TSC) pathway and mechanism of size control. *Biochemical Society transactions,* 31**,** 584-6.

PREHN, J. H., BINDOKAS, V. P., JORDAN, J., GALINDO, M. F., GHADGE, G. D., ROOS, R. P., BOISE, L. H., THOMPSON, C. B., KRAJEWSKI, S., REED, J. C. & MILLER, R. J. 1996. Protective effect of transforming growth factor-beta 1 on beta-amyloid neurotoxicity in rat hippocampal neurons. *Molecular pharmacology,* 49**,** 319-28.

PROKOP, A., LANDGRAF, M., RUSHTON, E., BROADIE, K. & BATE, M. 1996. Presynaptic development at the Drosophila neuromuscular junction: assembly and localization of presynaptic active zones. *Neuron,* 17**,** 617-26.

PULIPPARACHARUVIL, S., AKBAR, M. A., RAY, S., SEVRIOUKOV, E. A., HABERMAN, A. S., ROHRER, J. & KRAMER, H. 2005. Drosophila Vps16A is required for trafficking to lysosomes and biogenesis of pigment granules. *Journal of cell science,* 118**,** 3663-73.

PUNTARULO, S. 2005. Iron, oxidative stress and human health. *Molecular aspects of medicine,* 26**,** 299-312.

PURPURA, D. P. & SUZUKI, K. 1976. Distortion of neuronal geometry and formation of aberrant synapses in neuronal storage disease. *Brain research,* 116**,** 1-21.

RAMACHANDIRAN, S., HANSEN, J. M., JONES, D. P., RICHARDSON, J. R. & MILLER, G. W. 2007. Divergent mechanisms of paraquat, MPP+, and rotenone toxicity: oxidation of thioredoxin and caspase-3 activation. *Toxicological sciences : an official journal of the Society of Toxicology,* 95**,** 163-71.

RAWSON, J. M., LEE, M., KENNEDY, E. L. & SELLECK, S. B. 2003. Drosophila neuromuscular synapse assembly and function require the TGF-beta type I receptor saxophone and the transcription factor Mad. *Journal of neurobiology,* 55**,** 134-50.

RETH, M. 2002. Hydrogen peroxide as second messenger in lymphocyte activation. *Nature immunology,* 3**,** 1129-34.

RICHARDSON, J. R., QUAN, Y., SHERER, T. B., GREENAMYRE, J. T. & MILLER, G. W. 2005. Paraquat neurotoxicity is distinct from that of MPTP and rotenone. *Toxicological sciences : an official journal of the Society of Toxicology,* 88**,** 193-201.

RING, J. M. & MARTINEZ ARIAS, A. 1993. puckered, a gene involved in position-specific cell differentiation in the dorsal epidermis of the Drosophila larva. *Development*, 251-9.

RONG, Y., MCPHEE, C. K., DENG, S., HUANG, L., CHEN, L., LIU, M., TRACY, K., BAEHRECKE, E. H., YU, L. & LENARDO, M. J. 2011. Spinster is required for autophagic lysosome reformation and mTOR reactivation following starvation. *Proceedings of the National Academy of Sciences of the United States of America,* 108, 7826-31.

ROWLAND, A. M., RICHMOND, J. E., OLSEN, J. G., HALL, D. H. & BAMBER, B. A. 2006. Presynaptic terminals independently regulate synaptic clustering and autophagy of GABAA receptors in Caenorhabditis elegans. *The Journal of neuroscience : the official journal of the Society for Neuroscience,* 26, 1711-20.

RUBIN, G. M. & LEWIS, E. B. 2000. A brief history of Drosophila's contributions to genome research. *Science,* 287, 2216-8.

SAITOH, M., NISHITOH, H., FUJII, M., TAKEDA, K., TOBIUME, K., SAWADA, Y., KAWABATA, M., MIYAZONO, K. & ICHIJO, H. 1998. Mammalian thioredoxin is a direct inhibitor of apoptosis signal-regulating kinase (ASK) 1. *The EMBO journal,* 17, 2596-606.

SANYAL, S., NARAYANAN, R., CONSOULAS, C. & RAMASWAMI, M. 2003. Evidence for cell autonomous AP-1 function in regulation of Drosophila motor-neuron plasticity. *BMC neuroscience,* 4, 20.

SANYAL, S., SANDSTROM, D. J., HOEFFER, C. A. & RAMASWAMI, M. 2002. AP-1 functions upstream of CREB to control synaptic plasticity in Drosophila. *Nature,* 416, 870-4.

SARKAR, S., RAVIKUMAR, B., FLOTO, R. A. & RUBINSZTEIN, D. C. 2009. Rapamycin and mTOR-independent autophagy inducers ameliorate toxicity of polyglutamine-expanded huntingtin and related proteinopathies. *Cell death and differentiation,* 16, 46-56.

SCHIPPER, H. M. 2004a. Brain iron deposition and the free radical-mitochondrial theory of ageing. *Ageing research reviews,* 3, 265-301.

SCHIPPER, H. M. 2004b. Heme oxygenase-1: transducer of pathological brain iron sequestration under oxidative stress. *Annals of the New York Academy of Sciences,* 1012, 84-93.

SCHUSTER, C. M., DAVIS, G. W., FETTER, R. D. & GOODMAN, C. S. 1996a. Genetic dissection of structural and functional components of synaptic plasticity. I. Fasciclin II controls synaptic stabilization and growth. *Neuron,* 17, 641-54.

SCHUSTER, C. M., DAVIS, G. W., FETTER, R. D. & GOODMAN, C. S. 1996b. Genetic dissection of structural and functional components of synaptic plasticity. II. Fasciclin II controls presynaptic structural plasticity. *Neuron,* 17, 655-67.

SCHWENKERT, I., ELTROP, R., FUNK, N., STEINERT, J. R., SCHUSTER, C. M. & SCHOLZ, H. 2008. The hangover gene negatively regulates bouton

addition at the Drosophila neuromuscular junction. *Mechanisms of development,* 125**,** 700-11.

SCOTT, R. C., JUHASZ, G. & NEUFELD, T. P. 2007. Direct induction of autophagy by Atg1 inhibits cell growth and induces apoptotic cell death. *Current biology : CB,* 17**,** 1-11.

SCOTT, S. V., HEFNER-GRAVINK, A., MORANO, K. A., NODA, T., OHSUMI, Y. & KLIONSKY, D. J. 1996. Cytoplasm-to-vacuole targeting and autophagy employ the same machinery to deliver proteins to the yeast vacuole. *Proceedings of the National Academy of Sciences of the United States of America,* 93**,** 12304-8.

SCOTT, S. V., NICE, D. C., 3RD, NAU, J. J., WEISMAN, L. S., KAMADA, Y., KEIZER-GUNNINK, I., FUNAKOSHI, T., VEENHUIS, M., OHSUMI, Y. & KLIONSKY, D. J. 2000. Apg13p and Vac8p are part of a complex of phosphoproteins that are required for cytoplasm to vacuole targeting. *The Journal of biological chemistry,* 275**,** 25840-9.

SEEHAFER, S. S. & PEARCE, D. A. 2006. You say lipofuscin, we say ceroid: defining autofluorescent storage material. *Neurobiology of aging,* 27**,** 576-88.

SETTEMBRE, C., ARTEAGA-SOLIS, E., BALLABIO, A. & KARSENTY, G. 2009. Self-eating in skeletal development: implications for lysosomal storage disorders. *Autophagy,* 5**,** 228-9.

SHEEHAN, D., MEADE, G., FOLEY, V. M. & DOWD, C. A. 2001. Structure, function and evolution of glutathione transferases: implications for classification of non-mammalian members of an ancient enzyme superfamily. *The Biochemical journal,* 360**,** 1-16.

SHEN, W. & GANETZKY, B. 2009. Autophagy promotes synapse development in Drosophila. *The Journal of cell biology,* 187**,** 71-9.

SHERER, T. B., BETARBET, R., TESTA, C. M., SEO, B. B., RICHARDSON, J. R., KIM, J. H., MILLER, G. W., YAGI, T., MATSUNO-YAGI, A. & GREENAMYRE, J. T. 2003. Mechanism of toxicity in rotenone models of Parkinson's disease. *The Journal of neuroscience : the official journal of the Society for Neuroscience,* 23**,** 10756-64.

SIES, H. 1997. Oxidative stress: oxidants and antioxidants. *Experimental physiology,* 82**,** 291-5.

SIMONSEN, A., CUMMING, R. C., BRECH, A., ISAKSON, P., SCHUBERT, D. R. & FINLEY, K. D. 2008. Promoting basal levels of autophagy in the nervous system enhances longevity and oxidant resistance in adult Drosophila. *Autophagy,* 4**,** 176-84.

SMITH, M. E. & FORD, W. L. 1983. The recirculating lymphocyte pool of the rat: a systematic description of the migratory behaviour of recirculating lymphocytes. *Immunology,* 49**,** 83-94.

SOHAL, R. S., WENNBERG-KIRCH, E., JAISWAL, K., KWONG, L. K. & FORSTER, M. J. 1999. Effect of age and caloric restriction on bleomycin-chelatable and nonheme iron in different tissues of C57BL/6 mice. *Free radical biology & medicine,* 27**,** 287-93.

SONG, W., ONISHI, M., JAN, L. Y. & JAN, Y. N. 2007. Peripheral multidendritic sensory neurons are necessary for rhythmic locomotion behavior in Drosophila larvae. *Proceedings of the National Academy of Sciences of the United States of America,* 104**,** 5199-204.

SPASIC, M. R., CALLAERTS, P. & NORGA, K. K. 2008. Drosophila alicorn is a neuronal maintenance factor protecting against activity-induced retinal degeneration. *The Journal of neuroscience : the official journal of the Society for Neuroscience,* 28**,** 6419-29.

SRIVASTAVA, P. & PANDA, D. 2007. Rotenone inhibits mammalian cell proliferation by inhibiting microtubule assembly through tubulin binding. *The FEBS journal,* 274**,** 4788-801.

ST-PIERRE, J., BUCKINGHAM, J. A., ROEBUCK, S. J. & BRAND, M. D. 2002. Topology of superoxide production from different sites in the mitochondrial electron transport chain. *The Journal of biological chemistry,* 277**,** 44784-90.

STATHOPOULOU, P. G., BENAKANAKERE, M. R., GALICIA, J. C. & KINANE, D. F. 2009. The host cytokine response to Porphyromonas gingivalis is modified by gingipains. *Oral microbiology and immunology,* 24**,** 11-7.

STROMHAUG, P. E., REGGIORI, F., GUAN, J., WANG, C. W. & KLIONSKY, D. J. 2004. Atg21 is a phosphoinositide binding protein required for efficient lipidation and localization of Atg8 during uptake of aminopeptidase I by selective autophagy. *Molecular biology of the cell,* 15**,** 3553-66.

STURTZ, L. A., DIEKERT, K., JENSEN, L. T., LILL, R. & CULOTTA, V. C. 2001. A fraction of yeast Cu,Zn-superoxide dismutase and its metallochaperone, CCS, localize to the intermembrane space of mitochondria. A physiological role for SOD1 in guarding against mitochondrial oxidative damage. *The Journal of biological chemistry,* 276**,** 38084-9.

SUZUKI, K., KIRISAKO, T., KAMADA, Y., MIZUSHIMA, N., NODA, T. & OHSUMI, Y. 2001. The pre-autophagosomal structure organized by concerted functions of APG genes is essential for autophagosome formation. *The EMBO journal,* 20**,** 5971-81.

SWEATT, J. D., ATKINS, C. M., JOHNSON, J., ENGLISH, J. D., ROBERSON, E. D., CHEN, S. J., NEWTON, A. & KLANN, E. 1998. Protected-site phosphorylation of protein kinase C in hippocampal long-term potentiation. *Journal of neurochemistry,* 71**,** 1075-85.

SWEENEY, S. T. & DAVIS, G. W. 2002. Unrestricted synaptic growth in spinster-a late endosomal protein implicated in TGF-beta-mediated synaptic growth regulation. *Neuron,* 36**,** 403-16.

SYKIOTIS, G. P. & BOHMANN, D. 2008. KeAP-1/Nrf2 signaling regulates oxidative stress tolerance and lifespan in Drosophila. *Developmental cell,* 14**,** 76-85.

TAKAMURA, A., HIGAKI, K., KAJIMAKI, K., OTSUKA, S., NINOMIYA, H., MATSUDA, J., OHNO, K., SUZUKI, Y. & NANBA, E. 2008. Enhanced

autophagy and mitochondrial aberrations in murine G(M1)-gangliosidosis. *Biochemical and biophysical research communications,* 367**,** 616-22.

TAKEUCHI, H., GEORGIEV, O., FETCHKO, M., KAPPELER, M., SCHAFFNER, W. & EGLI, D. 2007. In vivo construction of transgenes in Drosophila. *Genetics,* 175**,** 2019-28.

TANNER, C. M., KAMEL, F., ROSS, G. W., HOPPIN, J. A., GOLDMAN, S. M., KORELL, M., MARRAS, C., BHUDHIKANOK, G. S., KASTEN, M., CHADE, A. R., COMYNS, K., RICHARDS, M. B., MENG, C., PRIESTLEY, B., FERNANDEZ, H. H., CAMBI, F., UMBACH, D. M., BLAIR, A., SANDLER, D. P. & LANGSTON, J. W. 2011. Rotenone, paraquat, and Parkinson's disease. *Environmental health perspectives,* 119**,** 866-72.

TEJEDOR, F. J., BOKHARI, A., ROGERO, O., GORCZYCA, M., ZHANG, J., KIM, E., SHENG, M. & BUDNIK, V. 1997. Essential role for dlg in synaptic clustering of Shaker K+ channels in vivo. *The Journal of neuroscience : the official journal of the Society for Neuroscience,* 17**,** 152-9.

TENNENBERG, S. D., FEY, D. E. & LIESER, M. J. 1993. Oxidative priming of neutrophils by interferon-gamma. *Journal of leukocyte biology,* 53**,** 301-8.

TERMAN, A. & BRUNK, U. T. 2006. Oxidative stress, accumulation of biological 'garbage', and aging. *Antioxidants & redox signaling,* 8**,** 197-204.

THIELS, E., URBAN, N. N., GONZALEZ-BURGOS, G. R., KANTEREWICZ, B. I., BARRIONUEVO, G., CHU, C. T., OURY, T. D. & KLANN, E. 2000. Impairment of long-term potentiation and associative memory in mice that overexpress extracellular superoxide dismutase. *The Journal of neuroscience : the official journal of the Society for Neuroscience,* 20**,** 7631-9.

THOMAS, U., KIM, E., KUHLENDAHL, S., KOH, Y. H., GUNDELFINGER, E. D., SHENG, M., GARNER, C. C. & BUDNIK, V. 1997. Synaptic clustering of the cell adhesion molecule fasciclin II by discs-large and its role in the regulation of presynaptic structure. *Neuron,* 19**,** 787-99.

THUMM, M., EGNER, R., KOCH, B., SCHLUMPBERGER, M., STRAUB, M., VEENHUIS, M. & WOLF, D. H. 1994. Isolation of autophagocytosis mutants of Saccharomyces cerevisiae. *FEBS letters,* 349**,** 275-80.

TOURNIER, C., HESS, P., YANG, D. D., XU, J., TURNER, T. K., NIMNUAL, A., BAR-SAGI, D., JONES, S. N., FLAVELL, R. A. & DAVIS, R. J. 2000. Requirement of JNK for stress-induced activation of the cytochrome c-mediated death pathway. *Science,* 288**,** 870-4.

TOURNIER, C., WHITMARSH, A. J., CAVANAGH, J., BARRETT, T. & DAVIS, R. J. 1999. The MKK7 gene encodes a group of c-Jun NH2-terminal kinase kinases. *Molecular and cellular biology,* 19**,** 1569-81.

TROTTA, N., RODESCH, C. K., FERGESTAD, T. & BROADIE, K. 2004. Cellular bases of activity-dependent paralysis in Drosophila stress-sensitive mutants. *Journal of neurobiology,* 60**,** 328-47.

TSAI, P. I., KAO, H. H., GRABBE, C., LEE, Y. T., GHOSE, A., LAI, T. T., PENG, K. P., VAN VACTOR, D., PALMER, R. H., CHEN, R. H., YEH, S. R. & CHIEN, C. T. 2008. Fak56 functions downstream of integrin alphaPS3betanu and suppresses MAPK activation in neuromuscular junction growth. *Neural development,* 3**,** 26.

TSCHAPE, J. A., HAMMERSCHMIED, C., MUHLIG-VERSEN, M., ATHENSTAEDT, K., DAUM, G. & KRETZSCHMAR, D. 2002. The neurodegeneration mutant lochrig interferes with cholesterol homeostasis and Appl processing. *The EMBO journal,* 21**,** 6367-76.

TSUKADA, M. & OHSUMI, Y. 1993. Isolation and characterization of autophagy-defective mutants of Saccharomyces cerevisiae. *FEBS letters,* 333**,** 169-74.

TU, B. P. & WEISSMAN, J. S. 2002. The FAD- and O(2)-dependent reaction cycle of Ero1-mediated oxidative protein folding in the endoplasmic reticulum. *Molecular cell,* 10**,** 983-94.

TURRENS, J. F., ALEXANDRE, A. & LEHNINGER, A. L. 1985. Ubisemiquinone is the electron donor for superoxide formation by complex III of heart mitochondria. *Archives of biochemistry and biophysics,* 237**,** 408-14.

TURRENS, J. F. & BOVERIS, A. 1980. Generation of superoxide anion by the NADH dehydrogenase of bovine heart mitochondria. *The Biochemical journal,* 191**,** 421-7.

TUXWORTH, R. I., CHEN, H., VIVANCOS, V., CARVAJAL, N., HUANG, X. & TEAR, G. 2011. The Batten disease gene CLN3 is required for the response to oxidative stress. *Human molecular genetics,* 20**,** 2037-47.

TUXWORTH, R. I., VIVANCOS, V., O'HARE, M. B. & TEAR, G. 2009. Interactions between the juvenile Batten disease gene, CLN3, and the Notch and JNK signalling pathways. *Human molecular genetics,* 18**,** 667-78.

TYLKI-SZYMANSKA, A., CZARTORYSKA, B., VANIER, M. T., POORTHUIS, B. J., GROENER, J. A., LUGOWSKA, A., MILLAT, G., VACCARO, A. M. & JURKIEWICZ, E. 2007. Non-neuronopathic Gaucher disease due to saposin C deficiency. *Clinical genetics,* 72**,** 538-42.

UEDA, A. & WU, C. F. 2008. Effects of hyperkinetic, a beta subunit of Shaker voltage-dependent K+ channels, on the oxidation state of presynaptic nerve terminals. *Journal of neurogenetics,* 22**,** 1-13.

VENKATACHALAM, K., LONG, A. A., ELSAESSER, R., NIKOLAEVA, D., BROADIE, K. & MONTELL, C. 2008. Motor deficit in a Drosophila model of mucolipidosis type IV due to defective clearance of apoptotic cells. *Cell,* 135**,** 838-51.

VENUGOPAL, R. & JAISWAL, A. K. 1996. Nrf1 and Nrf2 positively and c-Fos and Fra1 negatively regulate the human antioxidant response element-mediated expression of NAD(P)H:quinone oxidoreductase1 gene. *Proceedings of the National Academy of Sciences of the United States of America,* 93**,** 14960-5.

VENUGOPAL, R. & JAISWAL, A. K. 1998. Nrf2 and Nrf1 in association with Jun proteins regulate antioxidant response element-mediated expression and coordinated induction of genes encoding detoxifying enzymes. *Oncogene,* 17**,** 3145-56.

VIEIRA, H. L., ALVES, P. M. & VERCELLI, A. 2011. Modulation of neuronal stem cell differentiation by hypoxia and reactive oxygen species. *Progress in neurobiology,* 93**,** 444-55.

VIJAYVERGIYA, C., BEAL, M. F., BUCK, J. & MANFREDI, G. 2005. Mutant superoxide dismutase 1 forms aggregates in the brain mitochondrial matrix of amyotrophic lateral sclerosis mice. *The Journal of neuroscience : the official journal of the Society for Neuroscience,* 25**,** 2463-70.

VINCENT, A., BRIGGS, L., CHATWIN, G. F., EMERY, E., TOMLINS, R., OSWALD, M., MIDDLETON, C. A., EVANS, G. J., SWEENEY, S. T. & ELLIOTT, C. J. 2012. parkin-induced defects in neurophysiology and locomotion are generated by metabolic dysfunction and not oxidative stress. *Human molecular genetics*.

WAGH, D. A., RASSE, T. M., ASAN, E., HOFBAUER, A., SCHWENKERT, I., DURRBECK, H., BUCHNER, S., DABAUVALLE, M. C., SCHMIDT, M., QIN, G., WICHMANN, C., KITTEL, R., SIGRIST, S. J. & BUCHNER, E. 2006. Bruchpilot, a protein with homology to ELKS/CAST, is required for structural integrity and function of synaptic active zones in Drosophila. *Neuron,* 49**,** 833-44.

WAIRKAR, Y. P., TODA, H., MOCHIZUKI, H., FURUKUBO-TOKUNAGA, K., TOMODA, T. & DIANTONIO, A. 2009. Unc-51 controls active zone density and protein composition by downregulating ERK signaling. *The Journal of neuroscience : the official journal of the Society for Neuroscience,* 29**,** 517-28.

WALKER, D. W., HAJEK, P., MUFFAT, J., KNOEPFLE, D., CORNELISON, S., ATTARDI, G. & BENZER, S. 2006. Hypersensitivity to oxygen and shortened lifespan in a Drosophila mitochondrial complex II mutant. *Proceedings of the National Academy of Sciences of the United States of America,* 103**,** 16382-7.

WALKER, L. J., ROBSON, C. N., BLACK, E., GILLESPIE, D. & HICKSON, I. D. 1993. Identification of residues in the human DNA repair enzyme HAP-1 (Ref-1) that are essential for redox regulation of Jun DNA binding. *Molecular and cellular biology,* 13**,** 5370-6.

WALKLEY, S. U., HASKINS, M. E. & SHULL, R. M. 1988a. Alterations in neuron morphology in mucopolysaccharidosis type I. A Golgi study. *Acta neuropathologica,* 75**,** 611-20.

WALKLEY, S. U. & SIEGEL, D. A. 1985. Ectopic dendritogenesis occurs on cortical pyramidal neurons in swainsonine-induced feline alpha-mannosidosis. *Brain research,* 352**,** 143-8.

WALKLEY, S. U., SIEGEL, D. A. & WURZELMANN, S. 1988b. Ectopic dendritogenesis and associated synapse formation in swainsonine-

induced neuronal storage disease. *The Journal of neuroscience : the official journal of the Society for Neuroscience,* 8**,** 445-57.

WAN, H. I., DIANTONIO, A., FETTER, R. D., BERGSTROM, K., STRAUSS, R. & GOODMAN, C. S. 2000. Highwire regulates synaptic growth in Drosophila. *Neuron,* 26**,** 313-29.

WANG, J., WHITEMAN, M. W., LIAN, H., WANG, G., SINGH, A., HUANG, D. & DENMARK, T. 2009. A non-canonical MEK/ERK signaling pathway regulates autophagy via regulating Beclin 1. *The Journal of biological chemistry,* 284**,** 21412-24.

WANG, J. W., HUMPHREYS, J. M., PHILLIPS, J. P., HILLIKER, A. J. & WU, C. F. 2000. A novel leg-shaking Drosophila mutant defective in a voltage-gated K(+)current and hypersensitive to reactive oxygen species. *The Journal of neuroscience : the official journal of the Society for Neuroscience,* 20**,** 5958-64.

WANG, J. W., SYLWESTER, A. W., REED, D., WU, D. A., SOLL, D. R. & WU, C. F. 1997. Morphometric description of the wandering behavior in Drosophila larvae: aberrant locomotion in Na+ and K+ channel mutants revealed by computer-assisted motion analysis. *Journal of neurogenetics,* 11**,** 231-54.

WANG, M. C., BOHMANN, D. & JASPER, H. 2003. JNK signaling confers tolerance to oxidative stress and extends lifespan in Drosophila. *Developmental cell,* 5**,** 811-6.

WANG, X., SHAW, W. R., TSANG, H. T., REID, E. & O'KANE, C. J. 2007. Drosophila spichthyin inhibits BMP signaling and regulates synaptic growth and axonal microtubules. *Nature neuroscience,* 10**,** 177-85.

WASSARMAN, D. A., SOLOMON, N. M. & RUBIN, G. M. 1996. Pk92B: a Drosophila melanogaster protein kinase that belongs to the MEKK family. *Gene,* 169**,** 283-4.

WEBER, U., PARICIO, N. & MLODZIK, M. 2000. Jun mediates Frizzled-induced R3/R4 cell fate distinction and planar polarity determination in the Drosophila eye. *Development,* 127**,** 3619-29.

WEI, H., KIM, S. J., ZHANG, Z., TSAI, P. C., WISNIEWSKI, K. E. & MUKHERJEE, A. B. 2008a. ER and oxidative stresses are common mediators of apoptosis in both neurodegenerative and non-neurodegenerative lysosomal storage disorders and are alleviated by chemical chaperones. *Human molecular genetics,* 17**,** 469-77.

WEI, Q., JIANG, H., MATTHEWS, C. P. & COLBURN, N. H. 2008b. Sulfiredoxin is an AP-1 target gene that is required for transformation and shows elevated expression in human skin malignancies. *Proceedings of the National Academy of Sciences of the United States of America,* 105**,** 19738-43.

WEI, Y., PATTINGRE, S., SINHA, S., BASSIK, M. & LEVINE, B. 2008c. JNK1-mediated phosphorylation of Bcl-2 regulates starvation-induced autophagy. *Molecular cell,* 30**,** 678-88.

WEITZMAN, S. A., TURK, P. W., MILKOWSKI, D. H. & KOZLOWSKI, K. 1994. Free radical adducts induce alterations in DNA cytosine methylation. *Proceedings of the National Academy of Sciences of the United States of America,* 91**,** 1261-4.

WHITWORTH, A. J., THEODORE, D. A., GREENE, J. C., BENES, H., WES, P. D. & PALLANCK, L. J. 2005. Increased glutathione S-transferase activity rescues dopaminergic neuron loss in a Drosophila model of Parkinson's disease. *Proceedings of the National Academy of Sciences of the United States of America,* 102**,** 8024-9.

WILLIAMSON, T. L. & CLEVELAND, D. W. 1999. Slowing of axonal transport is a very early event in the toxicity of ALS-linked SOD1 mutants to motor neurons. *Nature neuroscience,* 2**,** 50-6.

WONG, C., ROUGIER-CHAPMAN, E. M., FREDERICK, J. P., DATTO, M. B., LIBERATI, N. T., LI, J. M. & WANG, X. F. 1999. Smad3-Smad4 and AP-1 complexes synergize in transcriptional activation of the c-Jun promoter by transforming growth factor beta. *Molecular and cellular biology,* 19**,** 1821-30.

WU, C., DANIELS, R. W. & DIANTONIO, A. 2007. DFsn collaborates with Highwire to down-regulate the Wallenda/DLK kinase and restrain synaptic terminal growth. *Neural development,* 2**,** 16.

WU, C. F., GANETZKY, B., HAUGLAND, F. N. & LIU, A. X. 1983. Potassium currents in Drosophila: different components affected by mutations of two genes. *Science,* 220**,** 1076-8.

WU, H., WANG, M. C. & BOHMANN, D. 2009. JNK protects Drosophila from oxidative stress by trancriptionally activating autophagy. *Mechanisms of development,* 126**,** 624-37.

XIE, Z., NAIR, U. & KLIONSKY, D. J. 2008. Atg8 controls phagophore expansion during autophagosome formation. *Molecular biology of the cell,* 19**,** 3290-8.

XIONG, X., WANG, X., EWANEK, R., BHAT, P., DIANTONIO, A. & COLLINS, C. A. 2010. Protein turnover of the Wallenda/DLK kinase regulates a retrograde response to axonal injury. *The Journal of cell biology,* 191**,** 211-23.

XU, P., DAS, M., REILLY, J. & DAVIS, R. J. 2011. JNK regulates FoxO-dependent autophagy in neurons. *Genes & development,* 25**,** 310-22.

YAMAMOTO, A., MORISAWA, Y., VERLOES, A., MURAKAMI, N., HIRANO, M., NONAKA, I. & NISHINO, I. 2001. Infantile autophagic vacuolar myopathy is distinct from Danon disease. *Neurology,* 57**,** 903-5.

YAMAMOTO, D. & NAKANO, Y. 1999. Sexual behavior mutants revisited: molecular and cellular basis of Drosophila mating. *Cellular and molecular life sciences : CMLS,* 56**,** 634-46.

YAMANE, D., ZAHOOR, M. A., MOHAMED, Y. M., AZAB, W., KATO, K., TOHYA, Y. & AKASHI, H. 2009. Activation of extracellular signal-regulated kinase in MDBK cells infected with bovine viral diarrhea virus. *Archives of virology,* 154**,** 1499-503.

YANG, D., TOURNIER, C., WYSK, M., LU, H. T., XU, J., DAVIS, R. J. & FLAVELL, R. A. 1997. Targeted disruption of the MKK4 gene causes embryonic death, inhibition of c-Jun NH2-terminal kinase activation, and defects in AP-1 transcriptional activity. *Proceedings of the National Academy of Sciences of the United States of America,* 94**,** 3004-9.

YANG, S., MISNER, B. J., CHIU, R. J. & MEYSKENS, F. L., JR. 2007. Redox effector factor-1, combined with reactive oxygen species, plays an important role in the transformation of JB6 cells. *Carcinogenesis,* 28**,** 2382-90.

YOGEV, O., GOLDBERG, R., ANZI, S. & SHAULIAN, E. 2010. Jun proteins are starvation-regulated inhibitors of autophagy. *Cancer research,* 70**,** 2318-27.

YOGEV, O. & SHAULIAN, E. 2010. Jun proteins inhibit autophagy and induce cell death. *Autophagy,* 6.

YORIMITSU, T. & KLIONSKY, D. J. 2005. Autophagy: molecular machinery for self-eating. *Cell death and differentiation,* 12 Suppl 2**,** 1542-52.

ZAMPIERI, S., MELLON, S. H., BUTTERS, T. D., NEVYJEL, M., COVEY, D. F., BEMBI, B. & DARDIS, A. 2009. Oxidative stress in NPC1 deficient cells: protective effect of allopregnanolone. *Journal of cellular and molecular medicine,* 13**,** 3786-96.

ZANGAR, R. C., DAVYDOV, D. R. & VERMA, S. 2004. Mechanisms that regulate production of reactive oxygen species by cytochrome P450. *Toxicology and applied pharmacology,* 199**,** 316-31.

ZANGER, U. M., RAIMUNDO, S. & EICHELBAUM, M. 2004. Cytochrome P450 2D6: overview and update on pharmacology, genetics, biochemistry. *Naunyn-Schmiedeberg's archives of pharmacology,* 369**,** 23-37.

ZHANG, K., CHAILLET, J. R., PERKINS, L. A., HALAZONETIS, T. D. & PERRIMON, N. 1990. Drosophila homolog of the mammalian jun oncogene is expressed during embryonic development and activates transcription in mammalian cells. *Proceedings of the National Academy of Sciences of the United States of America,* 87**,** 6281-5.

ZHANG, Y., FENG, X. H. & DERYNCK, R. 1998. Smad3 and Smad4 cooperate with c-Jun/c-Fos to mediate TGF-beta-induced transcription. *Nature,* 394**,** 909-13.

ZHENG, X., KOH, K., SOWCIK, M., SMITH, C. J., CHEN, D., WU, M. N. & SEHGAL, A. 2009. An isoform-specific mutant reveals a role of PDP1 epsilon in the circadian oscillator. *The Journal of neuroscience : the official journal of the Society for Neuroscience,* 29**,** 10920-7.

ZHONG, Y., BUDNIK, V. & WU, C. F. 1992. Synaptic plasticity in Drosophila memory and hyperexcitable mutants: role of cAMP cascade. *The Journal of neuroscience : the official journal of the Society for Neuroscience,* 12**,** 644-51.

ZHONG, Y. & WU, C. F. 1991a. Alteration of four identified K+ currents in Drosophila muscle by mutations in eag. *Science,* 252**,** 1562-4.

ZHONG, Y. & WU, C. F. 1991b. Altered synaptic plasticity in Drosophila memory mutants with a defective cyclic AMP cascade. *Science,* 251**,** 198-201.